



ALASKA DEPARTMENT OF TRANSPORTATION

Ductility of Welded Steel Column to Steel Cap Beam Connections

Prepared by: Mr. Steven Fulmer, Graduate Research Assistant
Dr. Mervyn Kowalsky, Principle Investigator
Dr. James Nau, Co-Principle Investigator
Dr. Tasnim Hassan, Co-Principle Investigator

February 1, 2010

Prepared for:
Alaska Department of Transportation
Statewide Research Office
3132 Channel Drive
Juneau, AK 99801-7898

FHWA-AK-RD-10-04

Alaska Department of Transportation & Public Facilities
Research & Technology Transfer

Notice

This document is disseminated under the sponsorship of the U.S. Department of Transportation in the interest of information exchange. The U.S. Government assumes no liability for the use of the information contained in this document.

The U.S. Government does not endorse products or manufacturers. Trademarks or manufacturers' names appear in this report only because they are considered essential to the objective of the document.

Quality Assurance Statement

The Federal Highway Administration (FHWA) provides high-quality information to serve Government, industry, and the public in a manner that promotes public understanding. Standards and policies are used to ensure and maximize the quality, objectivity, utility, and integrity of its information. FHWA periodically reviews quality issues and adjusts its programs and processes to ensure continuous quality improvement.

Author's Disclaimer

Opinions and conclusions expressed or implied in the report are those of the author. They are not necessarily those of the Alaska DOT&PF or funding agencies.

REPORT DOCUMENTATION PAGE

Form approved OMB No.

Public reporting for this collection of information is estimated to average 1 hour per response, including the time for reviewing instructions, searching existing data sources, gathering and maintaining the data needed, and completing and reviewing the collection of information. Send comments regarding this burden estimate or any other aspect of this collection of information, including suggestion for reducing this burden to Washington Headquarters Services, Directorate for Information Operations and Reports, 1215 Jefferson Davis Highway, Suite 1204, Arlington, VA 22202-4302, and to the Office of Management and Budget, Paperwork Reduction Project (0704-1833), Washington, DC 20503

1. AGENCY USE ONLY (LEAVE BLANK) FHWA-AK-RD-10-04		2. REPORT DATE February 2010	3. REPORT TYPE AND DATES COVERED	
4. TITLE AND SUBTITLE Ductility of Welded Steel Column to Steel Cap Beam Connections			5. FUNDING NUMBERS DOT & PF AKSAS #76985 FEDERAL #HPR-4000(59) /T2-07-03	
6. AUTHOR(S) Steven J. Fulmer, Graduate Research Assistant Dr. Mervyn J. Kowalsky, Principle Investigator Dr. James M. Nau, Co-Principle Investigator Dr. Tasnim Hassan, Co-Principle Investigator				
7. PERFORMING ORGANIZATION NAME(S) AND ADDRESS(ES) North Carolina State University Constructed Facilities Laboratory 2414 Campus Shore Drive Raleigh, NC 27695-7533			8. PERFORMING ORGANIZATION REPORT NUMBER	
9. SPONSORING/MONITORING AGENCY NAME(S) AND ADDRESS(ES) State of Alaska, Alaska Dept. of Transportation and Public Facilities Research and Technology Transfer 2301 Peger Rd Fairbanks, AK 99709-5399			10. SPONSORING/MONITORING AGENCY REPORT NUMBER FHWA-AK-RD-10-04	
11. SUPPLEMENTARY NOTES Performed in cooperation with the U.S. Department of Transportation, Federal Highway Administration.				
12a. DISTRIBUTION / AVAILABILITY STATEMENT No restrictions. This document is available to the public through the National Technical Information Service, Springfield, VA 22161			12b. DISTRIBUTION CODE	
13. ABSTRACT (Maximum 200 words) This report discusses the seismic behavior of a bridge bent systems that consist of round HSS piles, welded to a steel HP section cap beam. Past practice has typically utilized a simple fillet weld to complete the connection between the pile and cap beam. The results of this research indicate that the ductility capacity of this system is controlled by the configuration of the welded connection between the piles and cap beam. Six full scale bridge bent tests have been conducted at North Carolina State University to evaluate the performance of the system when subjected to simulated seismic loading. The two main goals of the research were to first evaluate the behavior of the system with a simple fillet weld connection and secondly to improve performance by investigating alternative weld configurations and connection details. The results indicate that the use of a simple fillet weld led to premature connection failure. Subsequent tests showed that the use of other weld configurations improved the capabilities of the system but were still inadequate for higher seismic regions. However, promising results were obtained from a connection in which the flexural hinge region was relocated away from the pile to cap beam connection weld.				
14- KEYWORDS : bridge, pier, bent, steel, connection, seismic, ductility, weld			15. NUMBER OF PAGES 290	
			16. PRICE CODE N/A	
17. SECURITY CLASSIFICATION OF REPORT Unclassified	18. SECURITY CLASSIFICATION OF THIS PAGE Unclassified	19. SECURITY CLASSIFICATION OF ABSTRACT Unclassified	20. LIMITATION OF ABSTRACT N/A	

SI* (MODERN METRIC) CONVERSION FACTORS

APPROXIMATE CONVERSIONS TO SI UNITS

Symbol	When You Know	Multiply By	To Find	Symbol
LENGTH				
in	inches	25.4	millimeters	mm
ft	feet	0.305	meters	m
yd	yards	0.914	meters	m
mi	miles	1.61	kilometers	km
AREA				
in ²	square inches	645.2	square millimeters	mm ²
ft ²	square feet	0.093	square meters	m ²
yd ²	square yard	0.836	square meters	m ²
ac	acres	0.405	hectares	ha
mi ²	square miles	2.59	square kilometers	km ²
VOLUME				
fl oz	fluid ounces	29.57	milliliters	mL
gal	gallons	3.785	liters	L
ft ³	cubic feet	0.028	cubic meters	m ³
yd ³	cubic yards	0.765	cubic meters	m ³
NOTE: volumes greater than 1000 L shall be shown in m ³				
MASS				
oz	ounces	28.35	grams	g
lb	pounds	0.454	kilograms	kg
T	short tons (2000 lb)	0.907	megagrams (or "metric ton")	Mg (or "t")
TEMPERATURE (exact degrees)				
°F	Fahrenheit	5 (F-32)/9 or (F-32)/1.8	Celsius	°C
ILLUMINATION				
fc	foot-candles	10.76	lux	lx
fl	foot-Lamberts	3.426	candela/m ²	cd/m ²
FORCE and PRESSURE or STRESS				
lbf	poundforce	4.45	newtons	N
lbf/in ²	poundforce per square inch	6.89	kilopascals	kPa
APPROXIMATE CONVERSIONS FROM SI UNITS				
Symbol	When You Know	Multiply By	To Find	Symbol
LENGTH				
mm	millimeters	0.039	inches	in
m	meters	3.28	feet	ft
m	meters	1.09	yards	yd
km	kilometers	0.621	miles	mi
AREA				
mm ²	square millimeters	0.0016	square inches	in ²
m ²	square meters	10.764	square feet	ft ²
m ²	square meters	1.195	square yards	yd ²
ha	hectares	2.47	acres	ac
km ²	square kilometers	0.386	square miles	mi ²
VOLUME				
mL	milliliters	0.034	fluid ounces	fl oz
L	liters	0.264	gallons	gal
m ³	cubic meters	35.314	cubic feet	ft ³
m ³	cubic meters	1.307	cubic yards	yd ³
MASS				
g	grams	0.035	ounces	oz
kg	kilograms	2.202	pounds	lb
Mg (or "t")	megagrams (or "metric ton")	1.103	short tons (2000 lb)	T
TEMPERATURE (exact degrees)				
°C	Celsius	1.8C+32	Fahrenheit	°F
ILLUMINATION				
lx	lux	0.0929	foot-candles	fc
cd/m ²	candela/m ²	0.2919	foot-Lamberts	fl
FORCE and PRESSURE or STRESS				
N	newtons	0.225	poundforce	lbf
kPa	kilopascals	0.145	poundforce per square inch	lbf/in ²

*SI is the symbol for the International System of Units. Appropriate rounding should be made to comply with Section 4 of ASTM E380.
(Revised March 2003)

ABSTRACT

This report discusses the seismic behavior of a bridge bent systems that consist of round HSS piles, welded to a steel HP section cap beam. Past practice has typically utilized a simple fillet weld to complete the connection between the pile and cap beam. The results of the research indicate that the overall ductility capacity of this system is controlled by the configuration of the welded connection between the piles and cap beam.

In response to a lack of current knowledge concerning this type of connection, six full scale bridge bent tests have been conducted at North Carolina State University's Constructed Facilities Laboratory to evaluate the performance of the system when subjected to incremental simulated seismic loading. The two main goals of the research were to first evaluate the behavior of the system with a fillet weld which mimics the current typical design practice, and secondly to improve performance by investigating alternative weld configurations and connection details.

The results indicate that the use of a simple fillet weld led to connection failure at a low ductility level rendering the detail inadequate for even moderate seismic regions. Subsequent tests showed that the use of other weld configurations, such as full joint penetration welds, improved the capabilities of the system but were still inadequate for higher seismic regions. However, promising results were obtained from a connection in which the flexural hinge region was relocated away from the pile to cap beam connection weld. This connection system remained essentially elastic at the pile to cap beam interface, which allowed for a more ductile base metal failure away from the connection.

ACKNOWLEDGMENTS

The research discussed in this report has been funded the Alaska Department of Transportation which deserves top acknowledgement. The significant involvement of Mr. Elmer Marx as well as the entire technical review committee of the AKDOT is much appreciated by the research team at NCSU. The general success of this research is largely due the input received from the AKDOT.

Appreciation should also be given to members of the Constructed Facilities Laboratory staff and other graduate students at North Carolina State University. In particular, Mr. Jerry Atkinson, Mr. Greg Lucier, and Mr. Bill Dunleavy are thanked for their support in regards to testing set up and design. Graduate students Mr. Lennie Gonzalez, Mr. Chad Goodnight, and Mr. Yuhao Feng were instrumental in general support of the project. Special appreciation should be given to Ms. Kendra Cookson for her support of test 1-4.

The NCSU research team would lastly like to thank Mr. Don Sherrill of Steel Fab for their support providing necessary specimen materials and Mr. Randy Dempsey of NCDOT for volunteering his weld inspection skills.

TABLE OF CONTENTS

LIST OF FIGURES	ix
LIST OF TABLES	xx
Chapter 1 Introduction to the Research Program	1
1.1 General Background Information	1
1.2 Motivation for Research	4
1.2.1 Alaskan Seismic Hazard	4
1.2.2 Welded Steel Connection Issues	4
1.3 General Research Plan	6
1.4 Literature Review.....	7
1.4.1 Introduction.....	7
1.4.2 “Seismic Behavior of Steel Pile to Precast Concrete Cap Beam Connections”	7
1.4.3 “Retrofitting for seismic upgrading of steel bridge columns”	9
Chapter 2 The Experimental Program	11
2.1 Specimen and Testing Frame Design	11
2.1.1 Introduction.....	11
2.1.2 Specimen Design.....	11
2.1.3 Test Frame Design	15
2.2 Instrumentation Overview	19

2.2.1 General Instrumentation Discussion	19
2.2.2 Optotrak Overview	19
2.2.3 Calculation of Strains and Curvatures with the Optotrak System.....	21
2.2.4 Advantages of the Optotrak System.....	21
2.3 Loading Protocol: Traditional Three Cycle Sets	22
2.3.1 Background of the Load History.....	22
2.3.2 Application of Lateral Load	25
Chapter 3 Experimental Observations	27
3.1 Introduction.....	27
3.2 Test 1 Purpose, Observations, and Conclusions	27
3.2.1 Purpose: Evaluate the Capacity of the Current Design.....	27
3.2.2 Test 1 Observations.....	30
3.3 Test 2 Purpose, Observations, and Conclusions	34
3.3.1 Purpose: Improve Connection Ductility with New Weld Configuration.....	34
3.3.2 Test 2 Observations.....	37
3.3.3 Test 2 Conclusion.....	40
3.4 Test 3 Purpose, Observations, and Conclusions	42
3.4.1 Purpose: Evaluate Ductility of Full Penetration Weld without a Reinforcing Fillet	42
3.4.2 Test 3 Observations.....	44
3.4.3 Test 3 Conclusion.....	49
3.5 Test 4 Purpose, Observations, and Conclusions	50
3.5.1 Purpose: Validate Results of Test 2	50

3.5.2 Test 4 Observations.....	51
3.5.3 Test 4 Conclusion.....	56
3.6 Test 5 Purpose, Observations, and Conclusions	56
3.6.1 Purpose: Attempt to Control Joint Deformation Utilizing an Inside Reinforcing Fillet Weld.....	56
3.6.2 Test 5 Observations.....	59
3.6.3 Test 5 Conclusion.....	62
3.7 Test 6 Purpose, Observations, and Conclusions	63
3.7.1 Test 6 Purpose: Relocation of Flexural Plastic Hinging	63
3.7.2 Test 6 Observations.....	68
3.7.3 Test 6 Conclusions	73
Chapter 4 Response Considerations and Comparisons	76
4.1 Review of the Testing Series	76
4.2 Force Displacement Response Envelopes	81
4.3 Equivalent Viscous Damping Comparison.....	83
4.4 Selected Strain Topics.....	87
4.4.1 General Introduction to Strain Considerations.....	87
4.4.2 Validation of Optotrak Capabilities	88
4.4.3 Strain Issues Relating to Local Buckling.....	91
4.4.4 Curvature and Plastic Hinge Length	94
Chapter 5 DDBD Analysis and Drift Considerations.....	97
5.1 Introduction to DDBD Analysis of Hollow Steel Pile Bents.....	97

5.2 Development of DDBD Analysis Tools	99
5.2.1 Minimum Hazard to Require Explicit Lateral Strength Design.....	99
5.2.2 Required Hazard to Develop the Full Lateral Strength of the System.....	103
5.3 Application of DDBD Analysis Tools	109
5.4 Displacement Considerations: Ductility vs. Drift.....	112
5.4.1 Ductility Considerations	112
5.4.2 Alternate Deformation Modes	113
5.4.3 Conclusions Regarding Displacement Issues.....	114
Chapter 6 Detailed Analysis of Test 6.....	116
6.1 Introduction.....	116
6.2 Local Buckling Considerations.....	117
6.3 Performance of the Flared Column Capital	141
6.4 Effects of Joint Panel Zone Shear	154
6.5 Development of a Finite Element Model.....	158
Chapter 7 General Conclusions and Design Recommendations	159
7.1 General Conclusions of the Research Program	159
7.2 Design Recommendations for Hollow Steel Pipe Pile to Cap Beam Connections	160
7.3 Consideration of Pipe Buckling Under Pure Bending	161
7.4 Future Considerations	163
7.4.1 General Issues Related to Future Research.....	163
7.4.2 New Design Options	164
7.4.3 Retrofit Options.....	165

7.4.4 Future Research Conclusions.....	167
7.5 Final Conclusions.....	167
REFERENCES	169
Appendix 1: Specimen and Set Up Design Drawings	170
Appendix 2: Flared Column Capital Details.....	181
Appendix 3: Material Certification.....	183
Appendix 4: Construction Inspection and Weld Certification Details	187
A4.1 Welder Certifications	187
A4.2 Inspector Certifications	191
A4.3 Test 1 Details	199
A4.4 Test 2 Details	200
A4.5 Test 3 Details	217
A4.6 Test 4 Details	238
A4.7 Test 5 Details	251
A4.8 Test 6 Details	261

LIST OF FIGURES

Figure 1.1 76 th Ave. Underpass	2
Figure 1.2 Bird Creek Pedestrian Bridge.....	3
Figure 1.3 Cruise Ship Mooring Dock – Juneau, AK.....	3
Figure 1.4 Excerpt from Lowell Creek Bridge As-Builts.....	5
Figure 1.5 Excerpt from Bodenbug Creek Drawings (Note: Pile Thickness 0.375”).....	6
Figure 1.6 Testing Force Displacement Hysteresis	8
Figure 1.7 Test Specimen Detail	9
Figure 1.8 Test Specimen Detail	10
Figure 2.1 Pile Bending Moment Schematic	12
Figure 2.2 Bent Elevation	14
Figure 2.3 Double HP Cap Beam Detail	14
Figure 2.4 Front Elevation of Pinned Base Assembly.....	15
Figure 2.5 Side Elevation of Pinned Base Assembly	16
Figure 2.6 Plan View of Pinned Base Assembly.....	16
Figure 2.7 Picture of Pinned Base Assembly	17
Figure 2.8 Elevated Steel Frame.....	18
Figure 2.9 Specimen and Testing Frame	18
Figure 2.10 Optotrak Motion Capturing Camera	20
Figure 2.11 Grid Application of Optotrak Markers.....	20
Figure 2.12 Optotrak 3D Grid Snapshots	21

Figure 2.13 Example Three Cycle Sets Load History	24
Figure 2.14 Example Three Cycle Sets Displacement History	24
Figure 2.15 Lateral Loading System	25
Figure 2.16 220 kip MTS Actuator.....	26
Figure 2.17 Loading Assembly Connection	26
Figure 3.1 Test 1 Connection Detail Section.....	28
Figure 3.2 Test 1 Fillet Weld Connection	29
Figure 3.3 Test 1 Strain Gauge Map.....	29
Figure 3.4 Test 1 LED Grid.....	30
Figure 3.5 Cracking of South Coumn in Test 1.....	31
Figure 3.6 Test 1 Force Displacement Hysteresis	32
Figure 3.7 Test 1 Load History	33
Figure 3.8 Test 1 – Base Displacement vs Cap Beam Displacement.....	33
Figure 3.9 Test 2 Connection Detail Section.....	35
Figure 3.10 Completed Test 2 Connection Weld	36
Figure 3.11 Test 2 Strain Gauge Map.....	36
Figure 3.12 Test 2 – Base Displacement vs. Cap Beam Displacement.....	37
Figure 3.13 Test 2 Force Displacement Hysteresis	38
Figure 3.14 Test 2 Load History	38
Figure 3.15 Test 2- Cracking at Weld Toe North Column South Face	39
Figure 3.16 Test 2 – Local Buckling of North Column.....	39
Figure 3.17 Test 2- Base Material Fracture on South Column.....	40

Figure 3.18 Displaced Test 2 Specimen	42
Figure 3.19 Test 3 Connection Detail Section.....	43
Figure 3.20 Test 3 Connection.....	44
Figure 3.21 Test 3 Force Displacement Hysteresis	45
Figure 3.22 Test 3 Load History	45
Figure 3.23 North Column Crack During Overload Cycle.....	46
Figure 3.24 South Column Cracking – Ductility 1.5 Second Pull cycle	46
Figure 3.25 South Column Propagation of Cracking through the Weld	47
Figure 3.26 North Column Propagation of Cracking through the Weld	47
Figure 3.27 Cap Beam Distortion.....	47
Figure 3.28 Test 4 Weld Detail Section.....	50
Figure 3.29 Microphone Layout	51
Figure 3.30 Recording at Mic 3 – Ductility 2 Cycle -3.....	52
Figure 3.31 Recording at Mic 3 – Ductility 3 cycle -1	52
Figure 3.32 Typical Pin Slip Recording	52
Figure 3.33 Cracking on South Column	53
Figure 3.34 Cracking on South Column – Post Test	54
Figure 3.35 Test 4 Force Displacement Hysteresis	54
Figure 3.36 Test 4 Load History	55
Figure 3.37 Minor Local Buckling on the South Column	55
Figure 3.38 Connection Detail Section.....	57
Figure 3.39 Test 5 – Inside Reinforcing Fillet Weld	58

Figure 3.40 Completed Stub Column Weld	58
Figure 3.41 Sound Emission Possibly Related to Interior Cracking	59
Figure 3.42 Failure Crack – Ductility 3 Cycle 3	60
Figure 3.43 Test 5 Force Displacement Hysteresis	61
Figure 3.44 Test 5 Load History	61
Figure 3.45 Double Buckling of North Column	62
Figure 3.46 Test 5 Response – Ductility 3	63
Figure 3.47 Test 6 – Flared Column Capital	64
Figure 3.48 Moment Demand Relationship.....	65
Figure 3.49 Test 6 Connection Detail Section.....	66
Figure 3.50 Detail of Column Capital Assembly	66
Figure 3.51 Construction Sequence of Test 6.....	67
Figure 3.52 Location of PI Gauges.....	68
Figure 3.53 Propagation of Local Buckling – Ductility 3 Cycle 1.....	69
Figure 3.54 Test 6 Rupture – South Column North Face – Ductility 4 Cycle -3	69
Figure 3.55 Test 6 Force Displacement Hysteresis	70
Figure 3.56 Test 6 Load History	70
Figure 3.57 Vertical Strain Profile – South Column South Face	72
Figure 3.58 Test 6 – Ductility 4.....	73
Figure 3.59 Typical PI Gauge Recording	74
Figure 3.60 North Column Joint Rotation	75
Figure 4.1 Test 1 Force Displacement Hysteresis	77

Figure 4.2 Test 2 Force Displacement Hysteresis	77
Figure 4.3 Test 3 Force Displacement Hysteresis	78
Figure 4.4 Test 4 Force Displacement Hysteresis	78
Figure 4.5 Test 5 Force Displacement Hysteresis	79
Figure 4.6 Test 6 Force Displacement Hysteresis	79
Figure 4.7 Cycle 1 Force Displacement Envelopes.....	81
Figure 4.8 Cycle 2 Force Displacement Envelopes.....	82
Figure 4.9 Cycle 3 Force Displacement Envelopes.....	82
Figure 4.10 Relationship Between Hysteretic and Plastic Response	84
Figure 4.11 Damping Comparison	86
Figure 4.12 Yield Cycle Comparison	87
Figure 4.13 Example Optotrak Marker Grid	89
Figure 4.14 Strain Comparison (S-S-3", Test 6)	89
Figure 4.15 Strain Comparison (S-S-19", Test 6)	90
Figure 4.16 Strain Comparison (S-S-25", Test 6)	90
Figure 4.17 Example Strain Cross Section Prior to Local Buckling	92
Figure 4.18 Example Strain Cross Section Following Local Buckling.....	92
Figure 4.19 Strain Hysteresis Test 6 at S-S-29.....	93
Figure 4.20 Plastic Hinge Idealization of Non-Linear Curvature Distribution	95
Figure 5.1 Actual vs. Assumed Pile Moment Pattern.....	98
Figure 5.2 Minimum S_{D1} to Require Explicit Lateral Strength Design ($T_c=12s$).....	101
Figure 5.3 Minimum S_{D1} to Require Explicit Lateral Strength Design ($T_c=6s$).....	102

Figure 5.4 Required S_{D1} to Develop Pile Flexural Strength (W=360k, 2 Piles, D/t =32)	107
Figure 5.5 Required S_{D1} to Develop Pile Flexural Strength (W=180k, 4 Piles, D/t=32)	108
Figure 6.1 Test 1/Test6 Force Displacement Comparison	116
Figure 6.2 Test 6 Force Displacement Hysteresis	117
Figure 6.3 Severe Local Buckling in Test 6 – Ductility 4	118
Figure 6.4 Strain Cross Section 7 inches Below the Cap Beam – Push Direction	120
Figure 6.5 Strain Cross Section 7 inches Below the Cap Beam – Pull Direction	121
Figure 6.6 Strain Cross Section 25 inches Below the Cap Beam – Push Direction	122
Figure 6.7 Strain Cross Section 25 inches Below the Cap Beam – Pull Direction	123
Figure 6.8 Strain Cross Section 25” Down - Ductility 1 Cycle 1	124
Figure 6.9 Strain Cross Section 25” Down - Ductility 1 Cycle -1	125
Figure 6.10 Strain Cross Section 25” Down - Ductility 1 Cycle 2	125
Figure 6.11 Strain Cross Section 25” Down - Ductility 1 Cycle -2	126
Figure 6.12 Strain Cross Section 25” Down - Ductility 1 Cycle 3	126
Figure 6.13 Strain Cross Section 25” Down - Ductility 1 Cycle -3	127
Figure 6.14 Strain Cross Section 25” Down - Ductility 1.5 Cycle 1	127
Figure 6.15 Strain Cross Section 25” Down - Ductility 1.5 Cycle -1	128
Figure 6.16 Strain Cross Section 25” Down - Ductility 1.5 Cycle 2	128
Figure 6.17 Strain Cross Section 25” Down - Ductility 1.5 Cycle -2	129
Figure 6.18 Strain Cross Section 25” Down - Ductility 1.5 Cycle 3	129
Figure 6.19 Strain Cross Section 25” Down - Ductility 1.5 Cycle -3	130
Figure 6.20 Strain Cross Section 25” Down - Ductility 2 Cycle 1	130

Figure 6.21 Strain Cross Section 25” Down - Ductility 2 Cycle -1	131
Figure 6.22 Strain Cross Section 25” Down - Ductility 2 Cycle 2.....	131
Figure 6.23 Strain Cross Section 25” Down - Ductility 2 Cycle -2	132
Figure 6.24 Strain Cross Section 25” Down - Ductility 2 Cycle 3.....	132
Figure 6.25 Strain Cross Section 25” Down - Ductility 2 Cycle -3	133
Figure 6.26 Strain Cross Section 25” Down - Ductility 3 Cycle 1.....	133
Figure 6.27 Strain Cross Section 25” Down - Ductility 3 Cycle -1	134
Figure 6.28 Strain Cross Section 25” Down - Ductility 3 Cycle 2.....	134
Figure 6.29 Strain Cross Section 25” Down - Ductility 3 Cycle -2	135
Figure 6.30 Strain Cross Section 25” Down - Ductility 3 Cycle 3.....	135
Figure 6.31 Strain Cross Section 25” Down - Ductility 3 Cycle -3	136
Figure 6.32 Strain Cross Section 25” Down - Ductility 4 Cycle 1.....	136
Figure 6.33 Force – Displacement/Buckling Comparison – Cycle 1	138
Figure 6.34 Force – Displacement/Buckling Comparison – Cycle 2	139
Figure 6.35 Force – Displacement/Buckling Comparison – Cycle 3	140
Figure 6.36 Flared Column Capital Prior to Testing	141
Figure 6.37 Observed Local Buckling in Test 6.....	142
Figure 6.38 Optotrak Vertical Strain Profile – South Column South Face Push Direction	144
Figure 6.39 Optotrak Vertical Strain Profile – South Column South Face Pull Direction	145
Figure 6.40 Optotrak Vertical Strain Profile – South Column North Face Push Direction	146

Figure 6.41 Optotrak Vertical Strain Profile – South Column North Face Pull Direction	147
Figure 6.42 Strain Gauge Vertical Strain Profile – North Column South Face Push Direction	148
Figure 6.43 Strain Gauge Vertical Strain Profile – South Column South Face Pull Direction	149
Figure 6.44 Strain Gauge Vertical Strain Profile – North Column North Face Push Direction	150
Figure 6.45 Strain Guage Vertical Strain Profile – North Column North Face Pull Direction	151
Figure 6.46 Strain Cross Section Diagram–19” Down the South Pile–Push Direction ...	152
Figure 6.47 Strain Cross Section Diagram–19” Down the South Pile – Pull Direction...	153
Figure 6.48 Location of Inclinometers	154
Figure 6.49 Test 6 – North Joint Rotation Hysteresis	155
Figure 6.50 Test 6 - South Joint Rotation Hysteresis	155
Figure 6.51 Strain Gauge Hysteresis - Bottom Flange of Cap Beam at South Column...	156
Figure 6.52 Test 5 – South Joint Rotation	157
Figure 7.1 Example of Local Buckling of a Pile Subjected to Pure Bedding	162
Figure 7.2 Example of Strength Loss Due to Rapid Buckling	162
Figure 7.3 Possible New Design Conections.....	165
Figure 7.4 Non-Welded Stiffened Collar Option	166
Figure 7.5 Plane Stiffener Option.....	166
Figure 7.6 Reduced Section Option.....	166

Figure 7.7 Heat Treatment Option.....	167
Figure A 1.1 Pin Base Construction	170
Figure A 1.2 Lower Base Support Detail	171
Figure A 1.3 Lower Base Support Detail Continued.....	172
Figure A 1.4 Upper Base Support Detail.....	173
Figure A 1.5 Upper Base Support Detail Continued	174
Figure A 1.6 Pin Sleeve Support Details	175
Figure A 1.7 Pin Sleeve Construction Details	176
Figure A 1.8 Restraining Angle Detail	177
Figure A 1.9 Steel Pin Detail	178
Figure A 1.10 Pin Sleeve Detail	179
Figure A 1.11 Actuator Connection Details	180
Figure A 2.1 Column Capital Design Drawing	181
Figure A 2.2 Column Capital Design Calculations	182
Figure A 3.1 HSS Pile Material Certification.....	183
Figure A 3.2 HSS Pile Certification Continued.....	184
Figure A 3.3 HSS Pile Material Certification Continued	185
Figure A 3.4 Column Capital Material Certification.....	186
Figure A 4.1 Justin Green Welding Certification (Test 1-6).....	187
Figure A 4.2 Moises Sanchez Welding Certification (Test 2).....	188
Figure A 4.3 Ralph Quick Weld Certification (Test 5)	189
Figure A 4.4 Ralph Quick Weld Certification Continued (Test 5).....	190

Figure A 4.5 Randy Dempsey Certification (Test 1-4)	191
Figure A 4.6 Randy Dempsey Certification (Test 1-4)	192
Figure A 4.7 Randy Dempsey Certification (Test 1-4)	193
Figure A 4.8 Randy Dempsey Certification (Test 1-4)	194
Figure A 4.9 Randy Dempsey Certification (Test 1-4)	195
Figure A 4.10 Randy Dempsey Certification (Test 1-4)	196
Figure A 4.11 Russell Ogden Certification (Test 5).....	197
Figure A 4.12 Rhonda Rogers Certification (Test 5)	198
Figure A 4.13 Test 1 Connection Detail.....	199
Figure A 4.14 Test 2 Connection Detail.....	200
Figure A 4.15 Test 2 WPS.....	201
Figure A 4.16 Test 2 UT Report.....	216
Figure A 4.17 Test 3 Connection Detail.....	217
Figure A 4.18 Test 3 WPS.....	218
Figure A 4.19 Test 3 UT Report.....	237
Figure A 4.20 Test 4 Connection Detail.....	238
Figure A 4.21 Test 4 WPS.....	239
Figure A 4.22 Test 4 UT Report.....	250
Figure A 4.23 Test 5 Connection Detail.....	251
Figure A 4.24 Test 5 WPS.....	252
Figure A 4.25 Test 5 QC Report.....	253
Figure A 4.26 Test 5 QC Report Continued.....	254

Figure A 4.27 Test 5 QC Report Continued.....	255
Figure A 4.28 Test 5 QC Report Continued.....	256
Figure A 4.29 Test 5 QC Report Continued.....	257
Figure A 4.30 Test 5 QC Report Continued.....	258
Figure A 4.31 Test 5 UT Report.....	259
Figure A 4.32 Test 6 WPS.....	262
Figure A 4.33 Test 6 WPS Continued.....	263
Figure A 4.34 Test 6 WPS Continued.....	264
Figure A 4.35 Test 6 UT Report.....	265

LIST OF TABLES

Table 2.1 Sampling of AKDOT Steel Bridge Inventory	12
Table 3.1 Overview of Test 1 Cracking.....	32
Table 3.2 Test 2 Failure Mechanism Summary.....	41
Table 3.3 Test 3 Summary.....	48
Table 4.1 Testing Results Summary	80
Table 4.2 Detailed Test 6 Lp Calculations	96
Table 4.3 Selected Lp Results	96
Table 5.1 Minimum S_{D1} to Require Explicit Lateral Strength Design	101
Table 5.2 Required SD1 to Develop Column Flexural Strength.....	105
Table 5.3 Modified Analyses of Test Structures	115
Table A 4.1 Test 2 QC Report.....	202
Table A 4.2 Test 3 QC Report.....	219
Table A 4.3 Test 4 QC Report.....	240

Introduction to the Research Program

1.1 General Background Information

Although the bridge construction industry is historically dominated by the use of reinforced concrete, the use of steel as a bridge pier construction material has its place in history as well as the future. The benefits of the use of steel for the construction of bridge piers or bents includes but is not limited to speed and ease of construction, as well as the utilization of what is inherently a very ductile material. For these reasons the Alaska Department of Transportation and Public facilities desires to maintain the use of steel bridge piers as an option for future designs. In addition, the Department of Transportation is responsible for existing structures of this type that have been inherited into their inventory of bridges to maintain.

The typical design of these existing structures includes driven hollow steel pipe piles extending above grade to the cap beam where a welded connection exists between the two elements. This system of two or more driven pile columns welded to the cap beam, which typically consist of double HP steel sections, comprises the lateral force resisting system for the structure. Although the superstructure of the bridge system may vary between construction materials such as steel or concrete, this is of little consequence to the behavior of the bent system when subjected to seismically induced forces and displacements. Examples of this type of bridge bent construction can be seen in Figure 1.1 and Figure 1.2.

Although from the perspective of the Alaska Department of Transportation, these structures are typically used as road and highway overpasses, they have actually been

found to be useful in a number of other applications. In particular, similar driven pile steel moment frames have been commonly utilized as pier and wharf-type marine structures. For example, as can be seen in Figure 1.3, mooring docks located in the city of Juneau, AK utilized by the cruise ship industry contain this type of system.



Figure 1.1 76th Ave. Underpass
Compliments of AKDOT



Figure 1.2 Bird Creek Pedestrian Bridge
 Compliments of AKDOT



Figure 1.3 Cruise Ship Mooring Dock – Juneau, AK

1.2 Motivation for Research

1.2.1 Alaskan Seismic Hazard

Many areas of the state of Alaska are susceptible to high seismic hazard. This is mainly due its geographic location near the North American and Pacific tectonic plate boundary. The circum-Pacific belt, one of the world's most active seismic regions, brushes along Alaska's Aleutian Islands which extend from central Alaska for approximately 2500 miles. This region is arguably the most active seismic area in the world as "more than 80 percent of the planet's tremors" (usgs.gov) occur here. In addition more earthquakes take place in this area than "in the other 49 States combined" (usgs.gov). However, this is not the only highly active seismic zone of the state. Another zone "begins north of Yakutat Bay in southeastern Alaska and extends southeastward to the west coast of the Vancouver island" (usgs.gov) encompassing portions of the Denali and Fairweather fault systems. The state is also home to the most powerful earthquake ever recorded by modern equipment in North America and second largest in the world. This event took place on March 27th, 1964 occurring in the Anchorage area and measuring a moment magnitude of 9.2. Clearly a significant concern would exist within the Alaska Department of Transportation as to the performance of their bridge structure in such a highly active seismic region.

1.2.2 Welded Steel Connection Issues

When subjected to design level seismic events, structures are expected to perform in the non-linear range and sustain damage. This damage must however be controllable, prevent collapse, and in the case of demands less than the design seismic event, be repairable. Although as a base metal steel is very desirable due to its ductile characteristics, welded steel connections, if not detailed properly, can be problematic when subjected to large inelastic deformations. In accordance with the principals of capacity design, undesirable modes of failure such as brittle connection failures must be avoided in order to develop plastic hinges at the intended location. Should undesirable modes of failure develop prior to the formation of pile plastic hinges, issues such as structural collapse, irreparable damage, or lack of member ductility will occur.

Concern has existed amongst the Alaska DOT as to the capabilities of the existing steel bent bridge inventory as well as of any future steel bridges subjected to earthquake

excitation. In particular, major concern exists regarding the capabilities of the welded column to cap beam connection. The typical connection utilized in existing bridges and the design of new bridges prior to this research project consisted of a simple field performed fillet weld. Many of the fillet welds in the existing structures are too small to develop the full flexural strength of the pile. Examples of existing connections can be seen in Figure 1.4 and Figure 1.5.

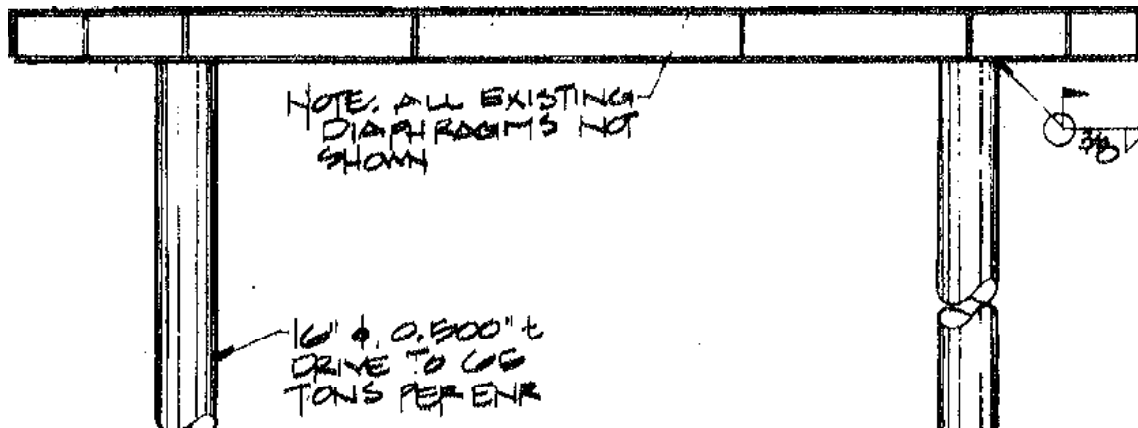


Figure 1.4 Excerpt from Lowell Creek Bridge As-Builts
Compliments of AKDOT

Regardless of whether the fillet weld is adequate to develop the strength of the pile, issues such as weld geometry, quality of the weld, and heat effects could lead to undesirable brittle connection failures. Taking into account this consideration paired with the high seismicity of Alaska as discussed in section 1.2.1 and the lack of research concerning hollow steel pipe connections, it is of interest to investigate the capability of the connection and more generally the entire steel bent.

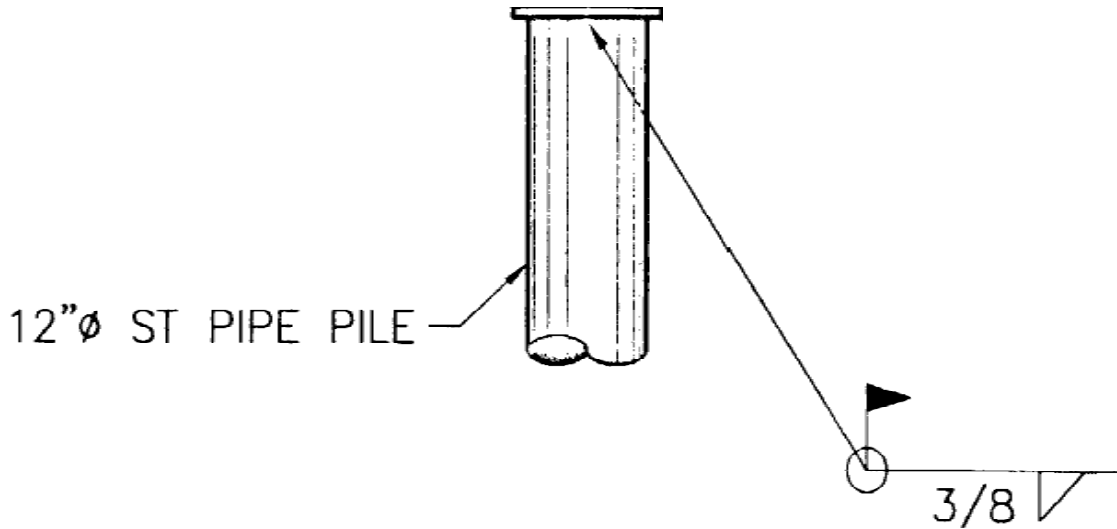


Figure 1.5 Excerpt from Bodenbug Creek Drawings (Note: Pile Thickness 0.375")
Compliments of AKDOT

1.3 General Research Plan

Six full scale tests, consisting of two pile bents, were conducted at North Carolina State University's (NCSU) Constructed Facilities Laboratory (CFL) in which the bents were subjected to increasing levels of reversed cyclic lateral displacement demand until failure. Emphasis was placed on the implementation of a flexible testing matrix in order to maximize the benefits of the research. The initial test was aimed at assessing the capabilities of the existing system (a plane field conducted overhead fillet welded connection). The result of this test dictated the course of action for the remaining tests.

Had the existing system been shown to perform well and allow for the proper flexural plastic hinges to form in the pile sections, the remaining tests would have incorporated construction tolerances such as cap-beam miss-alignment. Since the existing system proved inadequate, the remaining tests focused on development of an adequate connection that is capable of withstanding the demands of a capacity design

The tests were conducted utilizing reversed cyclic three cycle set loadings, typical of seismic testing. Data analysis was conducted that primarily focused on strain and

curvature interpretation to understand failure modes and assist in development of a better connection. Direct Displacement-Based Design calculations have also been conducted to create a generalized method of providing estimation of spectral acceleration necessary to fail a given bridge structure consisting of hollow steel pile bents. The ultimate goal of the testing series was to provide a relatively simple connection capable of meeting the inelastic demands necessary in high seismic regions.

1.4 Literature Review

1.4.1 Introduction

A search of multiple engineering focused bibliographic databases provided no prior studies with direct applicability to this research project. This affirms the research team's initial hypothesis that no prior testing of this unique structural system has been conducted. However, the literature review did produce two studies of interest that discuss projects of moderate similarity to this research. The first of these two studies, "Seismic Behavior of Steel Pile to Precast Concrete Cap Beam Connections" (Steunenberg, M., et. al., 1998), discusses testing of a single column hollow steel pile welded to a steel plate which was embedded in concrete. The second article, "Retrofitting for seismic upgrading of steel bridge columns" (Nishikawa, K., et. al., 1998), discusses research in which single column hollow piles sections were tested utilizing a pocketed style connection with outer reinforcing rings to control buckling. The details of these two projects are provided in the remainder of this section.

1.4.2 "Seismic Behavior of Steel Pile to Precast Concrete Cap Beam Connections"

The research discussed in this paper focuses on a single laboratory test that evaluated the performance of a steel pile welded to a steel plate that was embedded in concrete using anchor rods. The connection utilized a full joint penetrating weld which was conducted in an overhead position to simulate actual construction practice. The specimen was subjected to reverse cyclic lateral load and was ultimately able to achieve a displacement ductility of 8 after local buckling formed in the pile according to the researchers. Although this seems to be a positive response, a review of the testing results

indicates otherwise. The yield displacement reported in the article is 30 mm. However, as can be seen in Figure 1.6, this structure did not reach first yield at 30 mm much less full yield. From Figure 1.6, it is apparent that a ductility one displacement value would be approximately 50 mm indicating a maximum ductility of approximately four and a reliable ductility capacity of slightly over two.

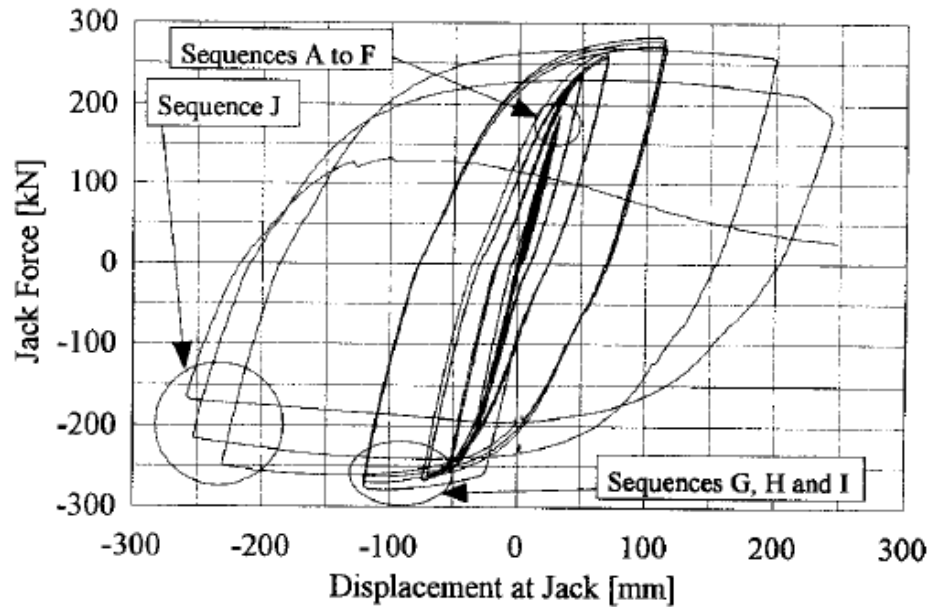


Figure 1.6 Testing Force Displacement Hysteresis

(Steunenberg, et. al., 2007)

Although the dimensions and diameter-to-thickness (D/t) ratio of the pile tested were similar to the dimensions used in this research project several differences in the test specimen exist. First, the steel plate will produce a more stiff connection face than will connecting to an actual flexible cap beam. As will be discussed later in this report, this effect is likely significant. Secondly, no axial load was applied during testing as would develop in a full scale bent test. This effect is likely less significant than the rigidity of the connection face but non-the-less does produce another difference. Although this specimen was able to develop base metal failure prior to connection cracking, the force displacement response indicates that these structures may be of limited ductility capacity.

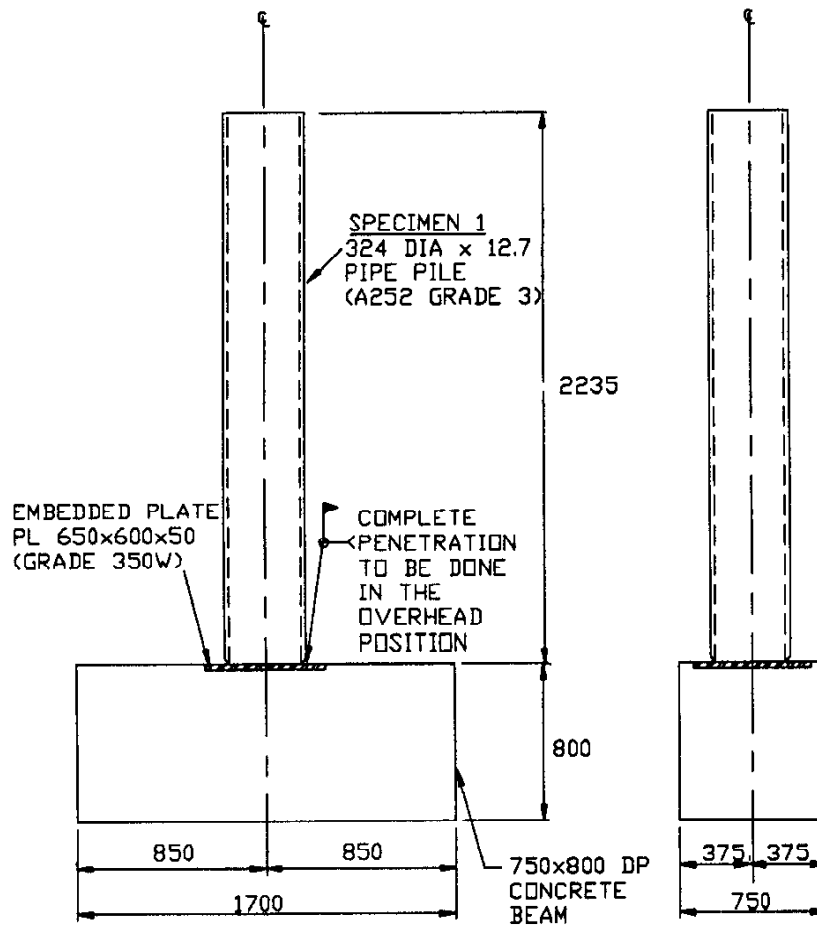


Figure 1.7 Test Specimen Detail

(Steunenberg, et. al., 2007)

1.4.3 “Retrofitting for seismic upgrading of steel bridge columns”

The research considered in this paper focused on retrofitting of existing columns as the title indicates. The study considered both square and circular sections. However, only the results of the circular specimens are presented here as the basis of this research project is to determine the performance capabilities of circular sections.

The study assumed that local buckling of pile would occur before connection cracking, as was reportedly experienced following the Kobe earthquake of 1995. The goal of the research was to prolong the life of the structure by controlling the growth of outward local buckling. This would be achieved by placing an outside reinforcing pipe

around the column with a specified tolerance. The lack of contact between the two elements indicates that the outer ring provides no strength or stiffness to the structure until buckling occurs. Following local buckling, the bulges that develop should come in contact with the outer ring which in turn will control the growth of these bulges and prolong the life of the structure.

Although the results of single column testing proved the method to be relatively successful, this conclusion is not of great importance to this research project. The fact that connection cracking did not occur prior to pile local buckling is of importance to this project. However, the connection utilized during this testing was a pocketed type connection where the pile was passed through an upper plate then welded to both a lower plate and the upper plate as shown in Figure 1.8. This significant difference indicates that direct comparison of these results to the results of this research project is not possible. Regardless, the study does provide what may be a viable connection alternative, the pocketed connection, to the simple welded connection considered in this research project.

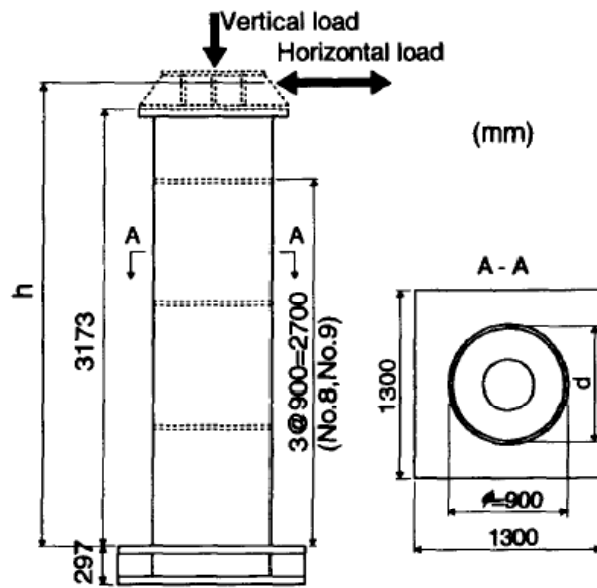


Figure 1.8 Test Specimen Detail

(Steunenberg, et. al., 2007)

The Experimental Program

2.1 Specimen and Testing Frame Design

2.1.1 Introduction

The main goal of the experimental program was to model as accurately as possible a typical steel bridge bent used in Alaska. The use of a full scale two pile bent ensured that the influence of axial forces and proper boundary conditions were captured. Although laboratory limitations were considered throughout the design, an attempt, as indicated in the following sections, was made to minimize the influence of these limitations in order to achieve the main goal of capturing the actual system response to lateral load.

2.1.2 Specimen Design

A very important aspect of the specimen design was coordination with Alaska DOT to ensure that the design was, in fact, representative of their existing bridge inventory. Table 2.1 provides a representative sampling of the steel bent bridge inventory provided by AKDOT. Note from Table 2.1, that the pile heights range from 10-20 feet and the pile diameters range from 12-30 inches. Taking into account the fact that pinned based supports would be used to model the point of inflection, which would exist under lateral loading as illustrated in Figure 2.1, the decision was made to set a target pile height at 10-14 feet which would correlate to a 20-28 foot pile in the field to the point of fixity. The decision was also made to use 16 inch diameter piles which are typical (although on the smaller side) piles used in the field. The thickness was chosen as 0.5 inches to create a D/t ratio of 32 which is within the typical range of AKDOT practice. ASTM A500 Grade B&C material was chosen for the pipe, with an anticipated yield stress of 50 ksi.

The design of the cap beam was controlled by capacity design principles. In order to ensure that flexural hinging occurred at the tops of the piles, other failure mechanisms

(beam hinging, joint failure) had to be capacity protected. An over-strength factor of 1.3 was assumed in the calculation of the ultimate pile strength as shown in Eq. 2.1. The selection of an HP section to comprise the double HP cap beam was then based on the evaluated moment demand at the column face as calculated in Eq. 2.3. From this value an HP14x89 section comprised of ASTM A572 Grade 50 material was chosen since it remains elastic at the over-strength column face moment demand as shown in Eq. 2.4. Note that Eqs. 2.1-2.4 are all based on final dimensions selected as is discussed in the next paragraph Full depth stiffeners of ¾ inch thickness were also included in order to protect the cap beam inside the joint region. These stiffeners were placed over the extreme fiber of the HSS pile.

Table 2.1 Sampling of AKDOT Steel Bridge Inventory
Compliments of AKDOT

Name	Weld Type	Weld Size [in]	Pile Diam.	Pile thickness [in]	Pile Height above ground [ft]	Number of Piles per bent	Cap Beam	# of Spans	Span Length [ft]	Location		Figure reference
										Latitude	Longitude	
208	Field Fillet	0.25	12"	N/A	10	4	HP14x73	3	75	57.618	-152.315	N/A
1196	Field Fillet	0.25	12"	0.833	14	4	HP14x73	3	33	59.478	-139.608	N/A
1754	Field Fillet	0.75	30"	N/A	16.5	4	2W36x280	3	50	61.150	-149.700	Figure 1.2 and Figure 1.6
1820	Field Fillet	0.375	16"	N/A	20	4	2HP10x57	3	35	60.178	-149.365	Figure 1.4
1136	Field Fillet	0.375	16"	0.5	10	2	2HP14x89	1	80	60.105	-149.448	Figure 1.7
1945	Field Fillet	0.3125	20"	0.625	20	3	2W18x36	23	30	54.852	-163.408	Figure 1.1
1714	Field Fillet	0.375	12"	0.375	N/A	2	W24x84	1	74	61.560	-149.038	Figure 1.3 and Figure 1.5

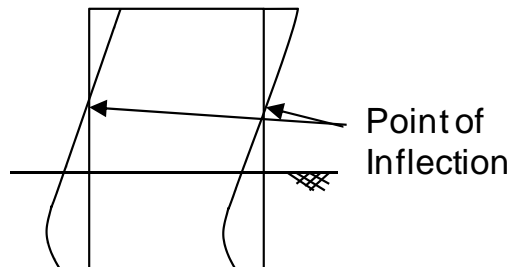


Figure 2.1 Pile Bending Moment Schematic

$$M_{p_pile} = Z_x \cdot f_y \cdot \phi_o = (112 \text{in}^3) \cdot (50 \text{ksi}) \cdot (1.3) = 607 \text{ kip}\cdot\text{ft} \quad \text{Eq. 2.1}$$

ϕ_o = "Over Strength Factor"

$$M_{beam_cl} = \frac{H_{cl}}{H_{clear}} \cdot M_{p_pile} = \frac{139 \text{in}}{132 \text{in}} \cdot (607 \text{ kip}\cdot\text{ft}) = 639 \text{ kip}\cdot\text{ft} \quad \text{Eq. 2.2}$$

M_{beam_cl} = "Moment Demand at Beam Center Line"

H_{cl} = "Height to Center Line of Cap Beam"

H_{clear} = "Column Clear Height"

$$M_{beam_cf} = \frac{0.5L_{clear}}{0.5L_{cl}} \cdot M_{beam_cl} = \frac{0.5 \cdot 124 \text{in}}{0.5 \cdot 140 \text{in}} \cdot (639 \text{ kip}\cdot\text{ft}) = 566 \text{ kip}\cdot\text{ft} \quad \text{Eq. 2.3}$$

M_{beam_cf} = "Moment Demand of Beam at Column Face"

L_{cl} = "Horizontal Distance from Center to Center of Piles"

L_{clear} = "Horizontal Distance from Inside Face to Inside Face of Piles"

$$M_{y_HP14x89} = S_x \cdot f_y = (13 \text{in}^3) \cdot 50 \text{ksi} = 546 \text{ kip}\cdot\text{ft} \quad \text{Eq. 2.4}$$

$M_{y_HP14x89}$ = "Elastic Moment Capacity of SINGLE HP14x89"

Although the desired sections comprising the test specimen had been chosen, the exact dimensions of the bent were ultimately dictated by laboratory restrictions. The CFL strong floor and strong wall each have restraining access holes at 3 feet on center. Taking this into account as well as the design of the testing frame, which will be discussed in the next section, it was decided that the clear distance from the point of inflection (pin base) to the bottom flange of the cap beam would be 10 feet 11-1/8 inches. Since the width of the bent was assumed to create no significant affects, a center to center of pile distance of 11 feet 8 inches was chosen to accommodate the layout of the strong floor. Design drawings of the entire bent are provided in Figure 2.2 and Figure 2.3.

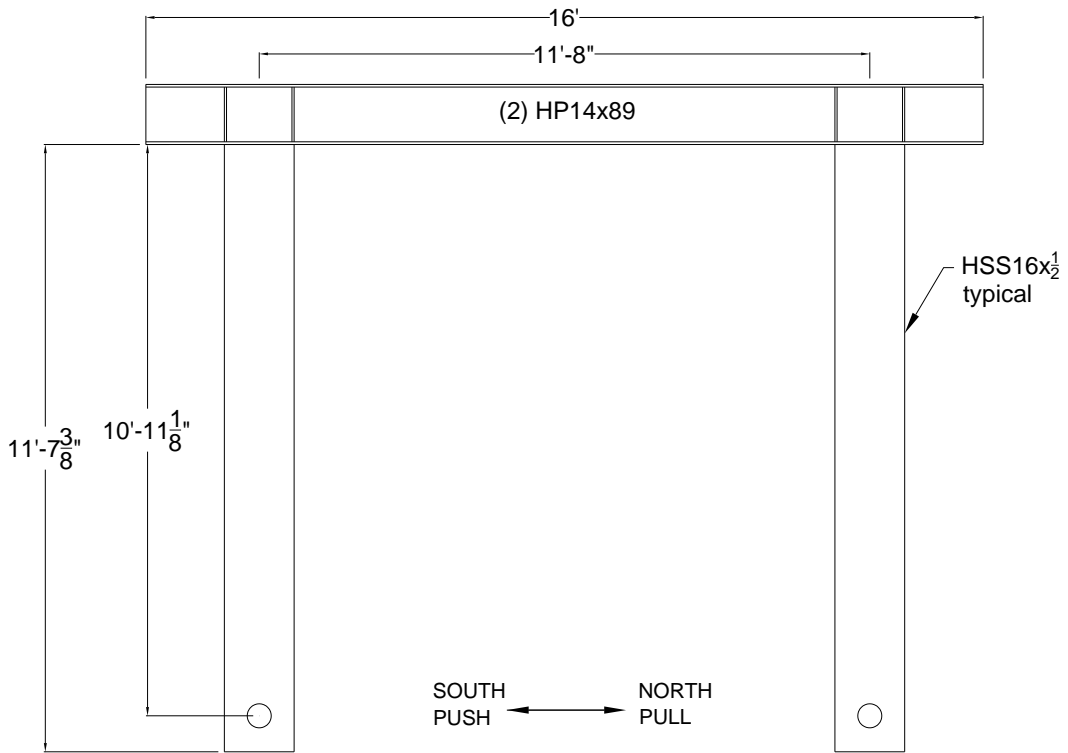


Figure 2.2 Bent Elevation

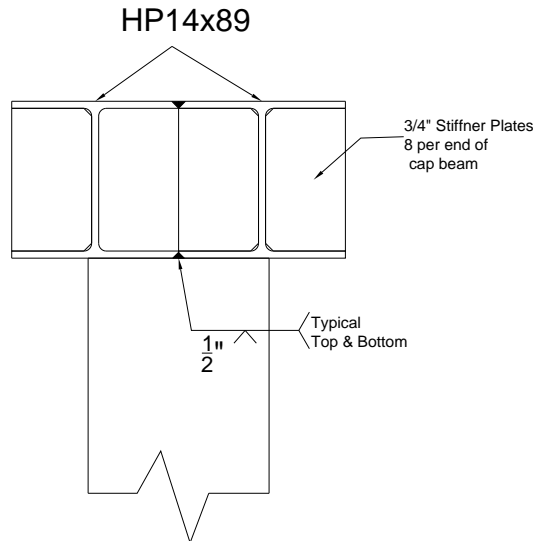


Figure 2.3 Double HP Cap Beam Detail

2.1.3 Test Frame Design

The testing frame design consisted of two main entities. The first and most crucial was the design of the pinned base supports. As described earlier the function of these supports was to model the point of inflection that would exist half way between the point of fixity created by the soil restraint and the bottom of the cap beam in an actual driven pile bent. The second entity of the testing frame design was the elevated lateral support frame. The purpose of the frame was to resist any out-of-plane motion that may occur during testing. Although no such motion was anticipated, this frame was utilized as a safety measure.

Each assembly, which can be seen in Figure 2.4 through Figure 2.7, consists of four short W14x159 sections, two shoes, two sleeves, four restraining angles, and one 5.5 inch diameter steel pin. The tolerance between the sleeves and pin was 0.002 inch. Each assembly was post tensioned to the CFL strong floor using four 1-3/8 inch Dywidag post tensioning bars, tensioned to approximately 50 kips. The assembly also utilized a 1 inch steel bearing plate beneath each shoe to replace rocker bearings which were used in the first two tests but proved to be problematic. Base displacement observed in the first two tests was found to be due to the rocker bearings and for this reason they were replaced during subsequent tests. Detailed shop drawings of the assembly are included in Appendix 1.

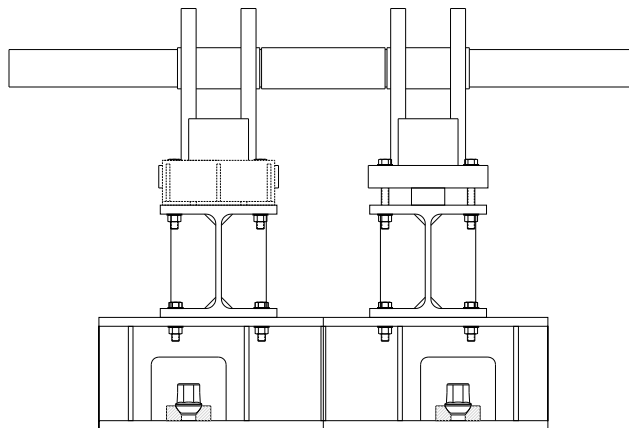


Figure 2.4 Front Elevation of Pinned Base Assembly

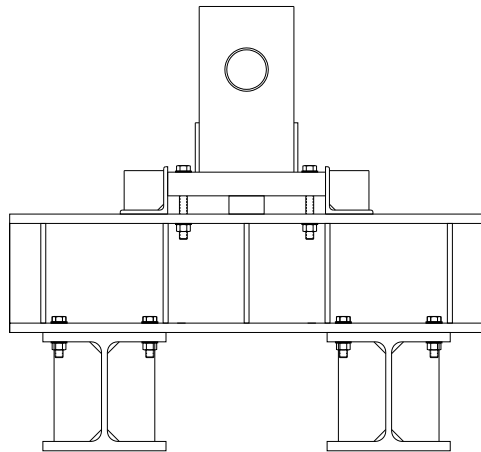


Figure 2.5 Side Elevation of Pinned Base Assembly

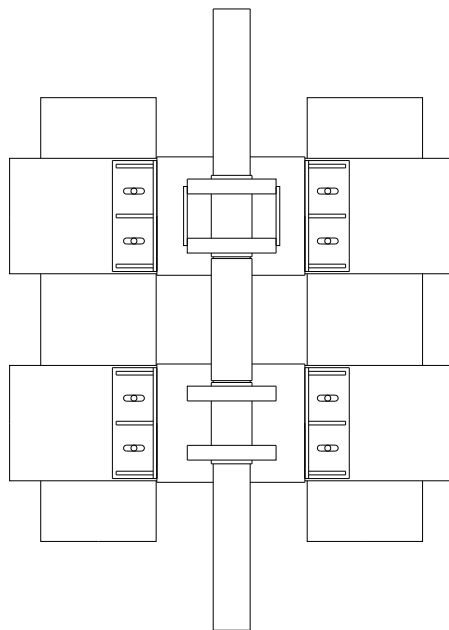


Figure 2.6 Plan View of Pinned Base Assembly



Figure 2.7 Picture of Pinned Base Assembly

As stated earlier, the main function of the elevated steel frame was to resist any incidental out of plane motion. This frame consisted of the three main elements. The first is the beams and columns forming the frame. Secondly, K bracing was used to provide the actual out of plane stiffness. Lastly, a caster (roller) system was used to guide the cap beam should they come in contact. This system can be seen in Figure 2.8 and the entire setup can be seen in Figure 2.9.



Figure 2.8 Elevated Steel Frame



Figure 2.9 Specimen and Testing Frame

2.2 Instrumentation Overview

2.2.1 General Instrumentation Discussion

Multiple systems of instrumentation were used during the testing series. These systems included traditional measurement devices such strain gauges, linear potentiometers, and inclinometers all of which conduct a particular type of measurement based on electric resistivity readings. There were also two types of non-traditional measurement equipment used throughout the testing series. The first of these two was an audio recording system consisting of ten microphones. The purpose of the audio recording device was to help the researchers identify possibly locations of cracking. The second type of non-traditional equipment and arguably the most valuable measurement device used during testing was the Optotrak system which is discussed in subsequent sections. Although for most tests the instrumentation layout was very similar, there were some alterations made between tests. For this reason, the instrumentation layout will be discussed on a per test basis in the remainder of this report.

2.2.2 Optotrak Overview

The Optotrak system is a motion capturing device that utilizes a combination of LED markers, strobers, a camera and a data acquisition station as shown in Figure 2.10 to record the relative motion associated with the markers throughout a test. The system captures X, Y, and Z location data at a prescribed frequency with accuracy to the hundredth of a millimeter for each marker. By applying a grid of markers to a specimen as is shown in Figure 2.11 and Figure 2.12, simple post processing of the recorded data allows for accurate calculations of strains and cross section curvatures.



Figure 2.10 Optotrak Motion Capturing Camera
Compliments of NDI



Figure 2.11 Grid Application of Optotrak Markers

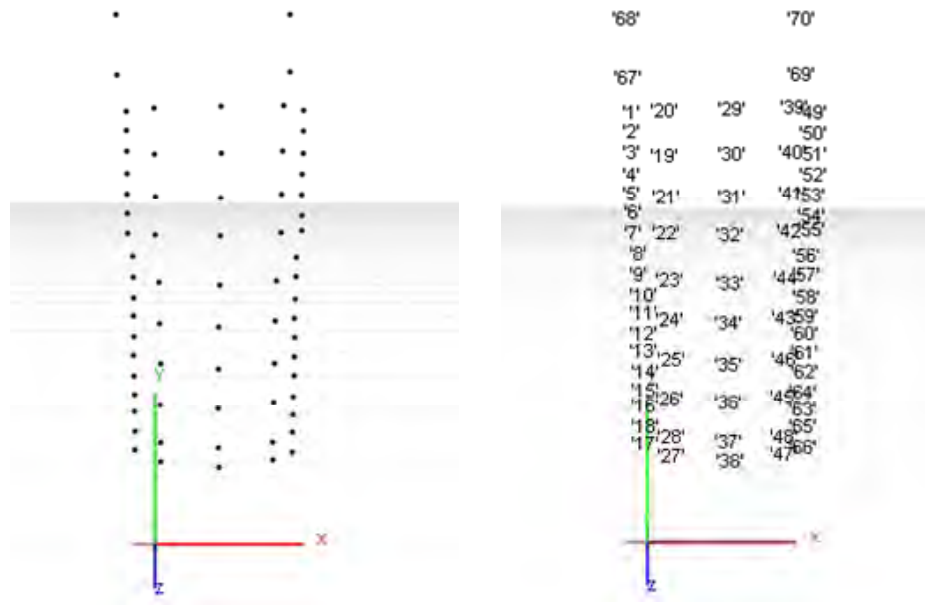


Figure 2.12 Optotrak 3D Grid Snapshots

2.2.3 Calculation of Strains and Curvatures with the Optotrak System

For these calculations, the initial gauge length between markers is simply taken as the distance between any two given markers recorded at time zero prior to the beginning of the test. The magnitude of strain can then be calculated for the remainder of the test by simply dividing the change in distance between the markers by the initial reading. This system allows for an average value of strain to be calculated between any two markers. Since the markers are attached in a grid system, the total of the absolute value of strain at either extreme fiber of a cross section divided by the diameter of the column provides the curvature of that cross section at that given time.

2.2.4 Advantages of the Optotrak System

In general, the system provides accurate data far beyond the capabilities of the traditional systems such as electric resistance strain gauges which typically cannot handle very high levels of inelastic strain. The markers are applied to the specimen using a hot glue system and accurate data is collected as long as the markers stay attached. It was typically seen that the Optotrak markers are able to remain adhered to the specimen for the duration of the test and provide reliable data beyond buckling or fracture. By employing the grid system it is also possible to capture the strain variance along the height of the

column or through a cross section of the column. It is important to note that although the primary use of the Optotrak system in this testing series was for the calculation of strains, any measurement related to the relative motion of points on the specimen can be derived from the raw data.

2.3 Loading Protocol: Traditional Three Cycle Sets

2.3.1 Background of the Load History

The lateral load history applied to the test specimens throughout this series consisted of traditional reverse cyclic three cycle sets. The main objective of this type of load history is to test the capabilities of the system for large inelastic reverse cyclic demands typical of seismic loadings. To establish this load history, material properties and member geometry must be known. Based upon mill certifications of the pile material, a material yield stress of 54 ksi was used for the development of the load history.

The first section of a typical three cycle set load history consists of load controlled cycles beginning at $1/4F_y$ as calculated in Eq. 2.5. After testing both the push and pull direction, the load is then increased to $1/2F_y$. Increasing increments of $1/4F_y$ are repeated until a full cycle of F_y has been conducted. During this cycle, the structural displacements recorded during testing at both $+F_y$ and $-F_y$ (+ indicates actuator pushing, - indicates actuator pulling) are averaged to establish an observed first yield displacement. This observed displacement is then extrapolated by a factor equal to M_p/M_y for the pile cross section to determine the displacement magnitude of ductility 1 as is shown in Eq. 2.6 to establish the equivalent first yield displacement. This equivalent first yield displacement is equal to the magnitude of the displacement ductility level 1 often indicated by μ_1 . The remainder of the test is then run in displacement control testing increments of ductility as indicated in Eq. 2.7. The typical sequence followed includes ductility 1, 1.5, 2, 3, 4, 6, and 8. Three complete cycles are conducted at each level until specimen failure occurs. A typical three cycle set load and displacement history is shown in Figure 2.13 and Figure 2.14 respectively.

$$F_y = 2 \left(\frac{S_x \cdot f_y}{H} \right) \quad \text{Eq. 2.5}$$

S_x = "Section Modulus of Pile"

H = "Moment Arm From Pinned Support to Bottom of Cap Beam"

$$\mu_1 = \Delta_y = \Delta'_y \cdot \frac{M_p}{M_y} \quad \text{Eq. 2.6}$$

μ_1 = "Ductility 1 Displacement"

Δ_y = "Calculated Equivalent Yield Displacement"

Δ'_y = "Observed Average First Yield Displacement"

M_p = "Calculated Plastic Moment Capacity of the Pile"

M_y = "Calculated First Yield Moment Capacity of the Pile"

$$\mu_i = i \cdot \mu_1 \quad \text{Eq. 2.7}$$

μ_i = "Ductility i Displacement"

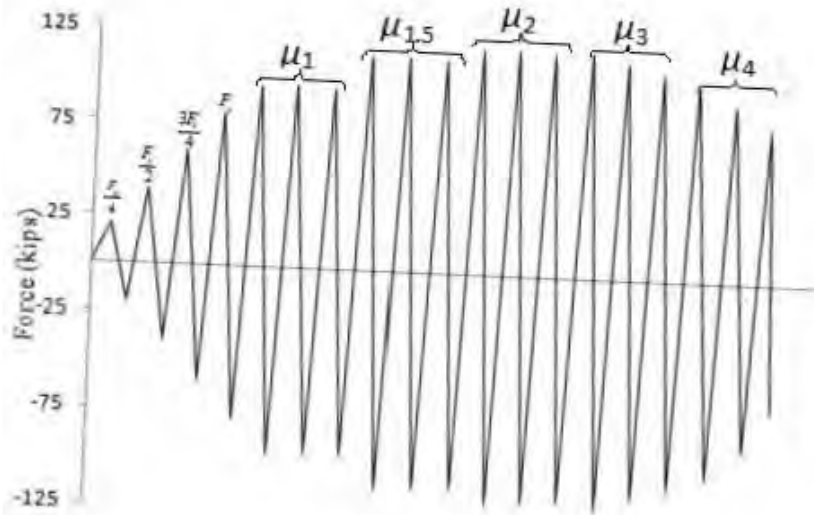


Figure 2.13 Example Three Cycle Sets Load History

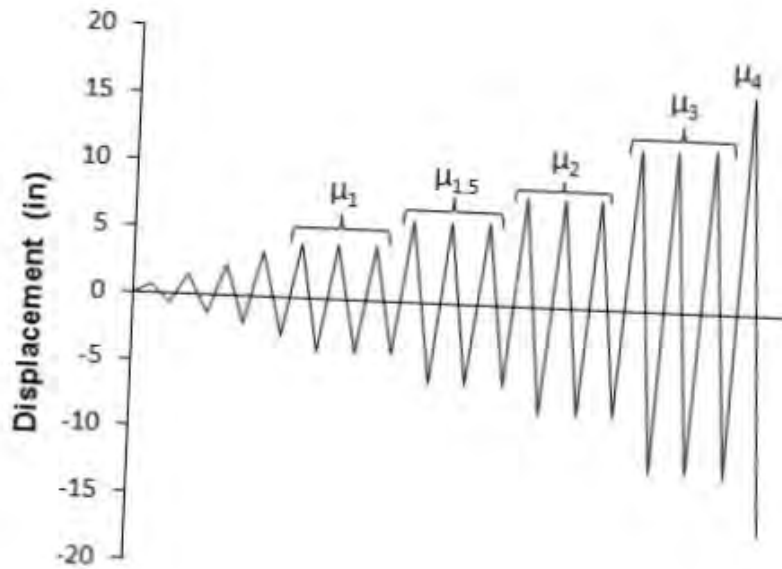


Figure 2.14 Example Three Cycle Sets Displacement History

2.3.2 Application of Lateral Load

Structural analysis was conducted with the known material properties of the piles to determine that a 220 kip MTS actuator (220 kip compression or push, 150 kip tension or pull capacity) would be adequate to test the specimen. The other major consideration when designing the lateral loading system was actuator stroke. The 220 kip MTS actuator has a total stroke capacity of 40in. For the purpose of reverse cyclic loading, the lateral loading system was designed to allow for a balanced set up that would provide plus or minus 20 inches of stroke. This would be enough stroke to test a ductility level of 8 based upon elastic column flexure calculations. The lateral loading system can be seen in Figure 2.15 and Figure 2.16. The connection system between the actuator and the cap beam is shown in Figure 2.17.

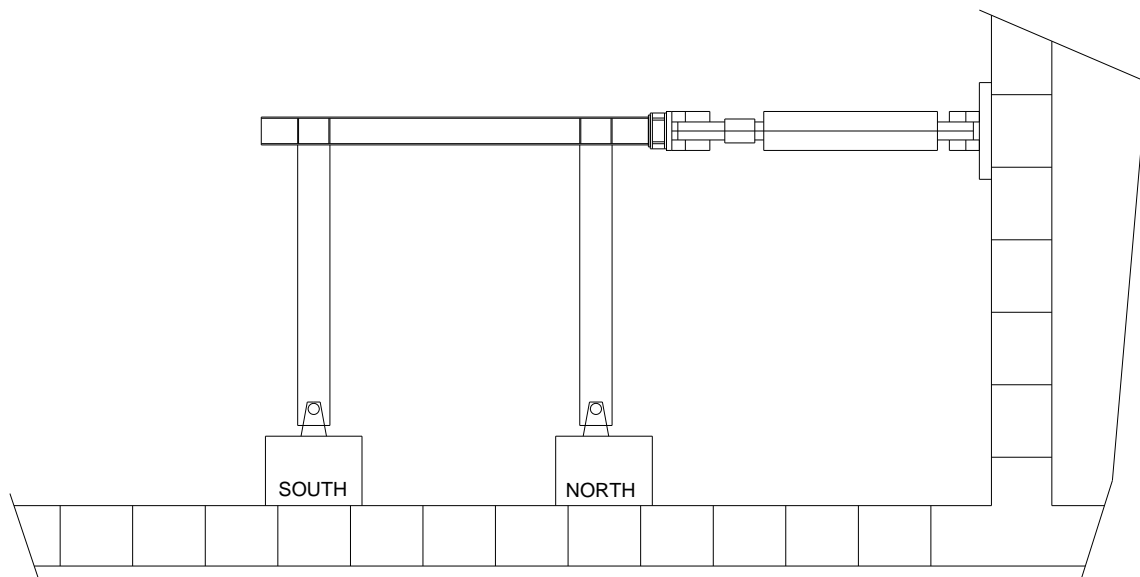


Figure 2.15 Lateral Loading System



Figure 2.16 220 kip MTS Actuator

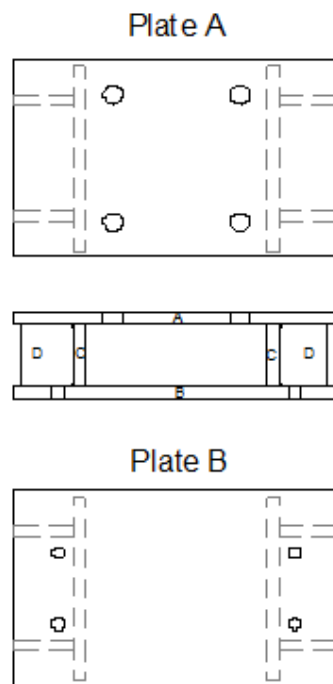


Figure 2.17 Loading Assembly Connection

Experimental Observations

3.1 Introduction

As discussed in Chapter 2, emphasis was placed on the use of a flexible testing matrix which would allow the outcome of a test to dictate the direction of the subsequent tests. For this reason it is of value to review the tests in chronological order. Issues regarding the connection design, instrumentation, and response of each test are included in this Chapter.

3.2 Test 1 Purpose, Observations, and Conclusions

3.2.1 Purpose: Evaluate the Capacity of the Current Design

As was discussed in Chapter 1, the typical detail utilized during construction of the existing bridge inventory consists of a simple field conducted fillet weld. The connection requires no backing bar and provides no root opening as can be seen in Figure 3.1 which depicts a section cut of the 1/2 inch pile wall and the bottom flange of the HP section cap beam. It is important to note that due to a construction error the actual weld used in test 1 was undersized by approximately 1/16 of an inch. Although this is an error, the situation is actually more indicative of the existing bridge inventory which possesses many undersized fillet welds with throat thicknesses less than the pile wall thickness.

During construction of the test specimen, care was taken to mimic construction practices as much as possible. Although for this initial test an optimal weld was desired with minimal defects and no construction tolerances considered, the methods used to construct the test specimen needed to be equitable to field procedures. For this reason all welding of the connection, which can be seen in Figure 3.2, was done from an overhead

position. The instrumentation utilized to monitor the response of the specimen included traditional equipment as well as the Optotrak system. The layout of this instrumentation is shown below in Figure 3.3 and Figure 3.4. Figure 3.3 provides the reference location and distance below the bottom flange of the cap beam in inches (i.e. North Column North Face 4 inches down) for all strain gauges used in the test. In addition to the instrumentation shown, four linear potentiometers were used. Two were placed at the centerline of the cap beam on the south end, one at mid height of the south column and one at the base. Four inclinometers were also utilized on the specimen. Two were located at the cap beam/column centerline intersection and two at the base of the columns.

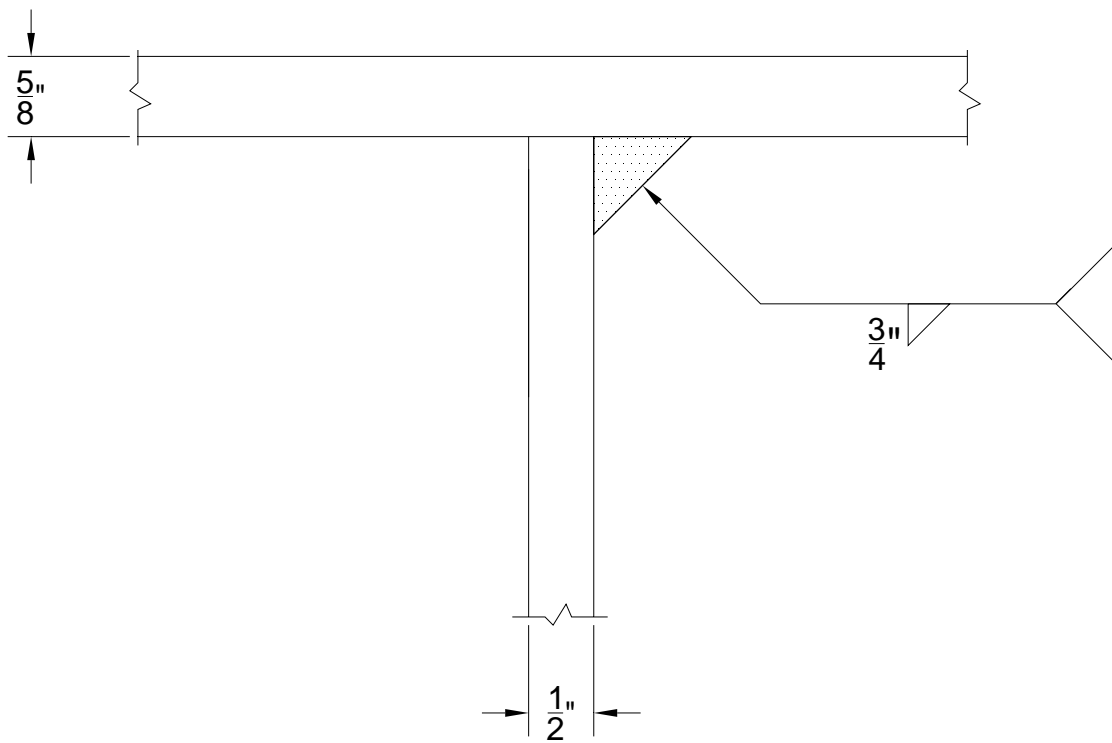


Figure 3.1 Test 1 Connection Detail Section



Figure 3.2 Test 1 Fillet Weld Connection

	CB N-Top		CB S-Top		
	North	CB N-Bottom	CB S-Bottom	South	
N-N-4-T	N-M-4	N-S-4-T	S-N-4-T	S-M-4	S-S-4-T
N-N-4		N-S-4	S-S-4		S-S-4
N-N-12	N-M-12	N-S-12	S-N-12	S-M-12	S-S-12
N-N-20	N-M-20	N-S-20	S-N-20	S-M-20	S-S-20
N-N-70	N-M-70	N-S-70	S-N-70	S-M-70	S-S-70

Figure 3.3 Test 1 Strain Gauge Map

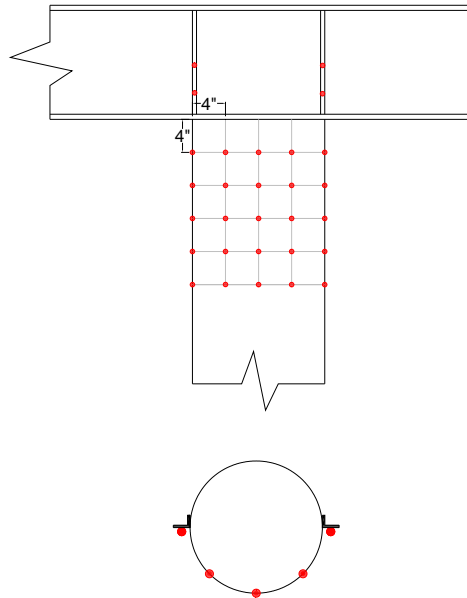


Figure 3.4 Test 1 LED Grid

3.2.2 Test 1 Observations

Structural analysis conducted prior to testing provided a system first yield force of 73 kips on which the initial portion of the loading history was based. The average first yield displacement of the system was observed to be 2.99 in which is considerably higher than the calculated estimate of 1.75 in. One reason for the higher than expected yield displacement is the effect of base displacement which can be attributed to the rocker bearings located in the base supports as mentioned in the description of the support design. However, larger than expected first yield displacements were observed throughout the testing series even after the removal of the rocker bearings. This issue will be discussed in later Chapters of this report. From the recorded first yield displacement of 2.99 in, the equivalent yield displacement or ductility 1 displacement was calculated as 3.89 in.

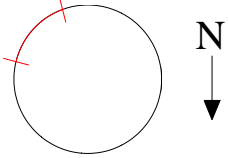
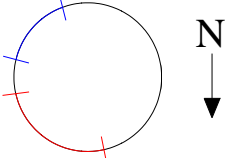
Regardless of the base displacement issue, the specimen was found to respond adequately within the elastic range. No signs of failure were observed during the load controlled portion of the load history prior to first yield nor were any observed during the ductility 1 and 1.5 levels. However, rapid degradation of the connection was observed during the first cycle of the second ductility level. During this cycle cracking was seen at

the toe of the fillet weld on the south column as can be seen in Figure 3.5 and described in Table 3.1. The effect of this cracking in regards to the strength of the specimen can be seen in Figure 3.6 and Figure 3.7 which provide the force displacement hysteresis and the load history respectively. It should be noted that the force displacement hysteresis appears to be shifted towards the positive direction due to the effects of base displacement which is plotted in Figure 3.8. As a result of the cracking in the first cycle of ductility 2, the specimen was assumed to be failed and the test was concluded.



Figure 3.5 Cracking of South Column in Test 1

Table 3.1 Overview of Test 1 Cracking

Ductility Cycle	Load [kips]	Displacement [inches]	Plan view*	Notes
μ_{2_1}	74	6.4	 <p>South column</p>	Crack appeared to originate at the bottom of weld
$\mu_{2_{-1}}$	59	7.1	 <p>South column</p>	Crack in heat affected zone below weld and opened up approx. 1/4 "

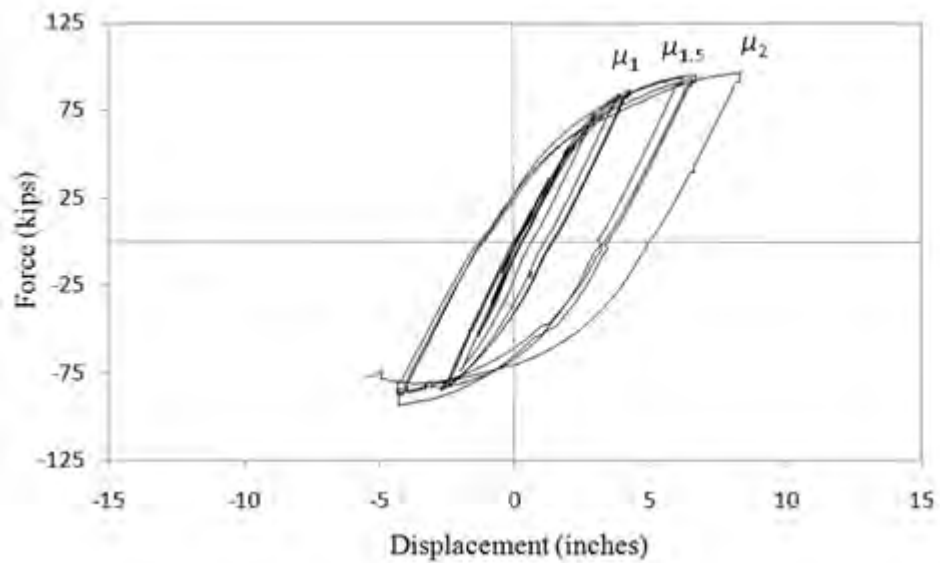


Figure 3.6 Test 1 Force Displacement Hysteresis

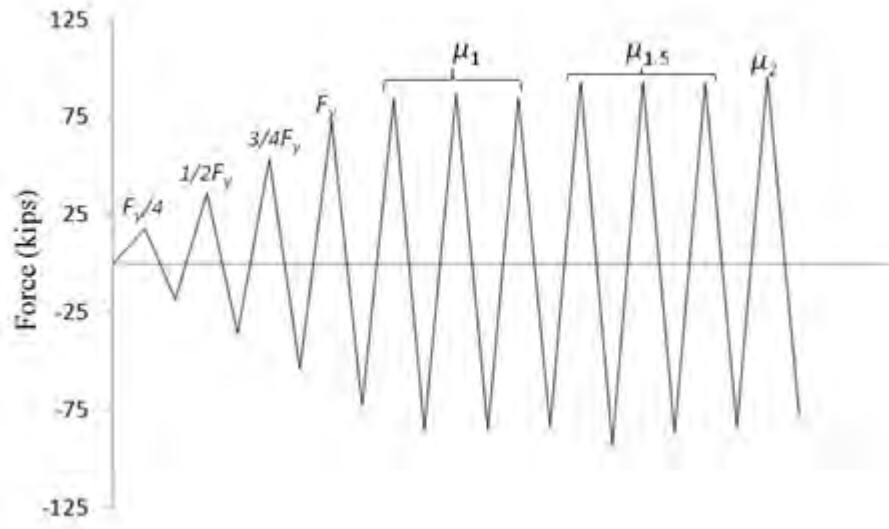


Figure 3.7 Test 1 Load History

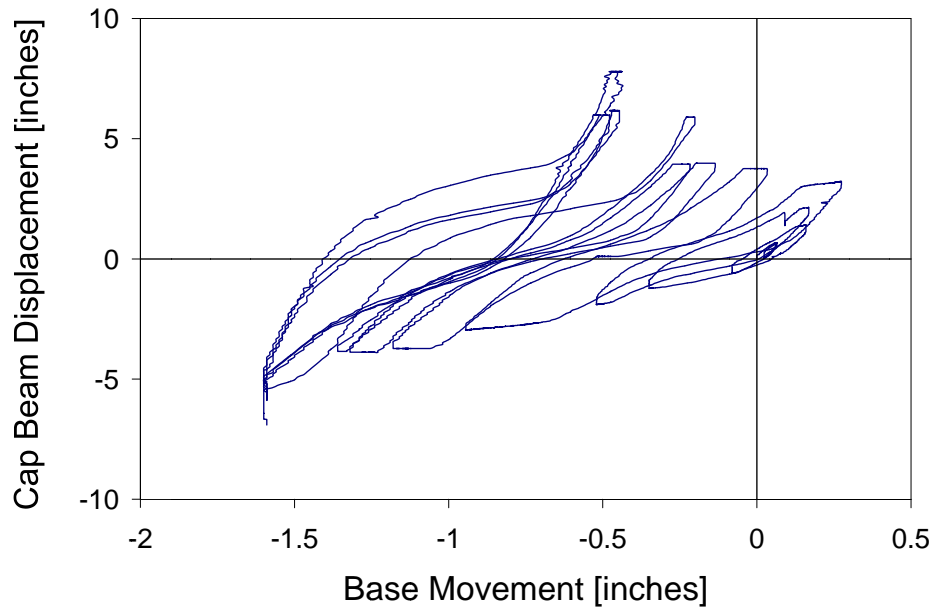


Figure 3.8 Test 1 – Base Displacement vs Cap Beam Displacement

3.2.3 Test 1 Conclusion

Reviewing the outcome of test 1 and considering that a target ductility of 8 was desired by AKDOT, it seems that the current connection design is inadequate. Given the failure which occurred early in the second ductility level the current design would likely be assigned a reliable ductility 1 or 1.5 by most designers. This is barely outside the elastic range and inadequate for even mild levels of seismic activity. For this reason AKDOT decided to put an immediate halt to the construction of any bridges involving this type of connection until a better system could be determined. It was decided in conjunction with AKDOT that no more tests would be used to evaluate the capacity of the current design and the research program would be redirected towards the goal of finding an adequate connection.

3.3 Test 2 Purpose, Observations, and Conclusions

3.3.1 Purpose: Improve Connection Ductility with New Weld Configuration

Realizing that the current fillet weld detail was inadequate, test 2 focused on improvement of the connection. The overall goal at this point in the testing series was to provide a detail that would allow for plastic hinging to form in the pile section without the connection becoming overly complex. Multiple options were considered such as the use of stiffeners and reduced sections. Ultimately it was decided that refinement of the weld geometry would be most sensible option for the first attempt at system improvement.

Possible options for weld geometry refinement included the use of a partial penetration weld, a full penetration weld, or a full penetration weld with a reinforcing fillet. In general it was felt that the cracks observed in test 1 were likely due to high stress concentrations around the sharp geometry of the fillet weld. For this reason it was decided that a full penetration weld with a full size reinforcing fillet as can be seen in Figure 3.9 would be used in order to induce smooth stress flow from the column to the beam flange. Although the use of such a large amount of weld material does induce more heat effect and provides for the possibility of more defects, it was still felt to be the best option.

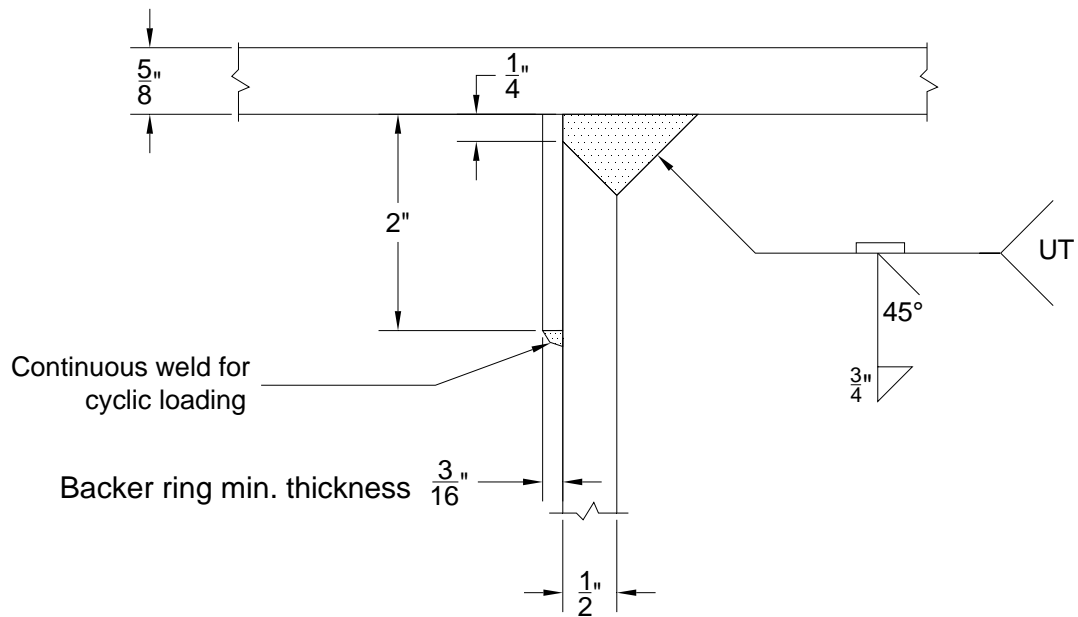


Figure 3.9 Test 2 Connection Detail Section

As was the case in test 1, care was taken during construction of the specimen to ensure that the construction practices were in fact realistic. For this reason, all welds were performed from an overhead position after the columns were erected in the lab. In addition, a welding procedure specification (WPS) as required by the American Welding Society (AWS) code was established and utilized in conjunction with visual and ultrasonic inspection, as appropriate for each type of weld. These measures were taken to ensure the weld tested would at least meet the minimum quality requirements of typical engineered welds. The credentials of the inspectors used and the results of the inspections can be found in Appendix 4. The completed weld is shown in Figure 3.10

The instrumentation plan for test 2 remained the same as for test 1 except for alterations to the strain gauge layout. For test 2 the strain gauge map was altered by excluding the transverse gauges, the radial quarter point gauges, and the top of cap beam gauges. The total number of longitudinal gauges used at the extreme fibers of the pile was increased. The revised strain gauge map for test 2 is provided in Figure 3.11 and again shows the reference location and distance below the cap beam for each strain gauge utilized.

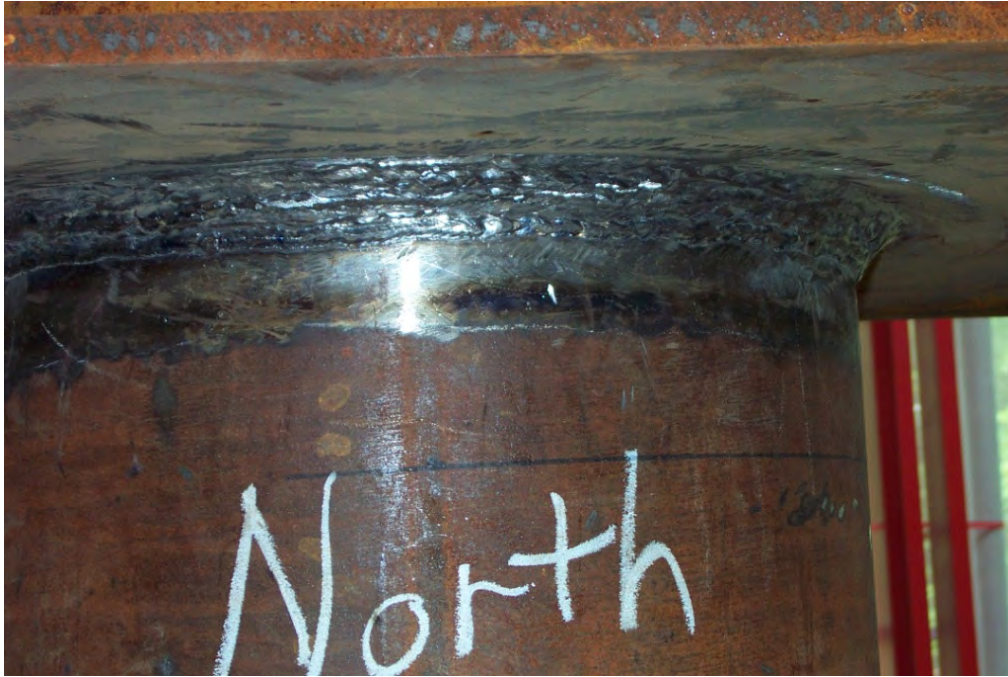


Figure 3.10 Completed Test 2 Connection Weld

	North	CB N	CB S	South	
N-N-3		N-S-3	S-S-3		S-S-3
N-N-11		N-S-11	S-N-11		S-S-11
N-N-19		N-S-19	S-N-19		S-S-19
N-N-26		N-S-26	S-N-26		S-S-26
N-N-34		N-S-36	S-N-34		S-S-34
N-N-70		N-S-70	S-N-70		S-S-70

Figure 3.11 Test 2 Strain Gauge Map

3.3.2 Test 2 Observations

Given that the only alteration to the system was the welding configuration, the global strength and stiffness were not affected. For this reason the first yield force remained at 73 kips as in test 1. The observed average first yield displacement in this test was found to be 2.49 inches and was used to establish a new displacement history for the remainder of the test. From the first yield displacement, the equivalent yield displacement or ductility 1 displacement was calculated as 3.24 inches from Eq. 2.6. Although the base displacement was much more controlled as can be seen in Figure 3.12, the observed first yield displacement was again higher than expected.

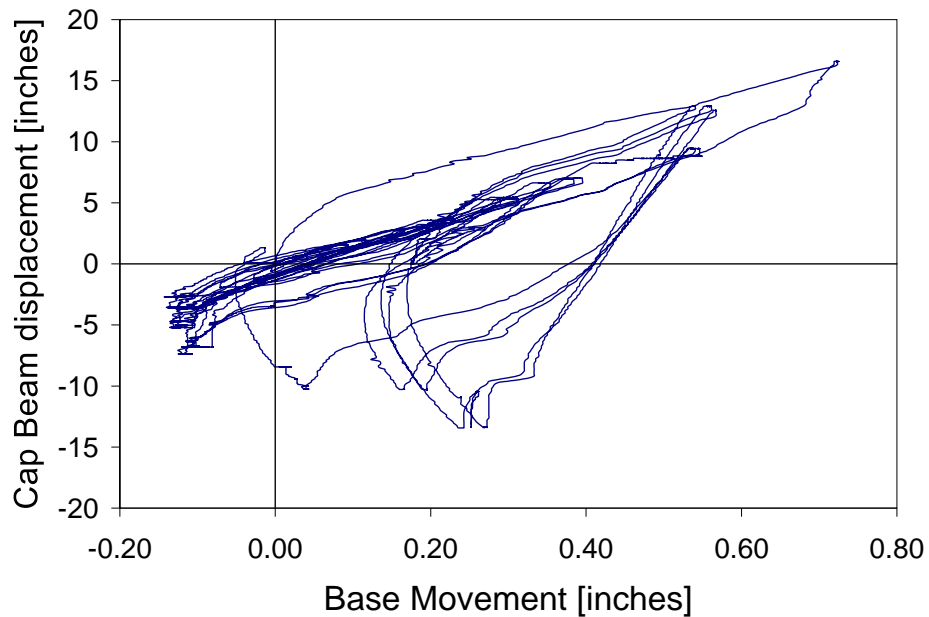


Figure 3.12 Test 2 – Base Displacement vs. Cap Beam Displacement

The test 2 specimen generally performed much better than the test 1 specimen. No signs of failure were observed through the displacement ductility 1, 1.5, and 2 levels. The specimen was accidentally subjected to an overload cycle corresponding to a displacement ductility of 5 during the transition from ductility 2 to 3 as can be seen in Figure 3.13. Although no damage was observed during this overloading, reversal to the negative or pull correct ductility 3 displacement led to a crack forming at the weld toe in the north

column. This crack extended from the extreme fiber of the south face to approximately the neutral axis as shown in Figure 3.15. It is possible that this crack was due to damage sustained during the overload cycle. For this reason and the fact that only minor strength loss had been experienced as is shown in Figure 3.14, the test was continued.

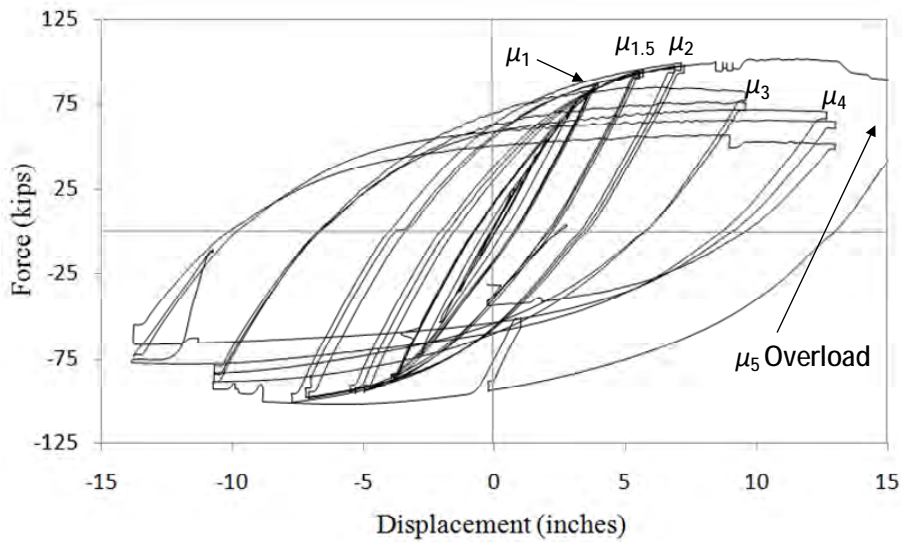


Figure 3.13 Test 2 Force Displacement Hysteresis

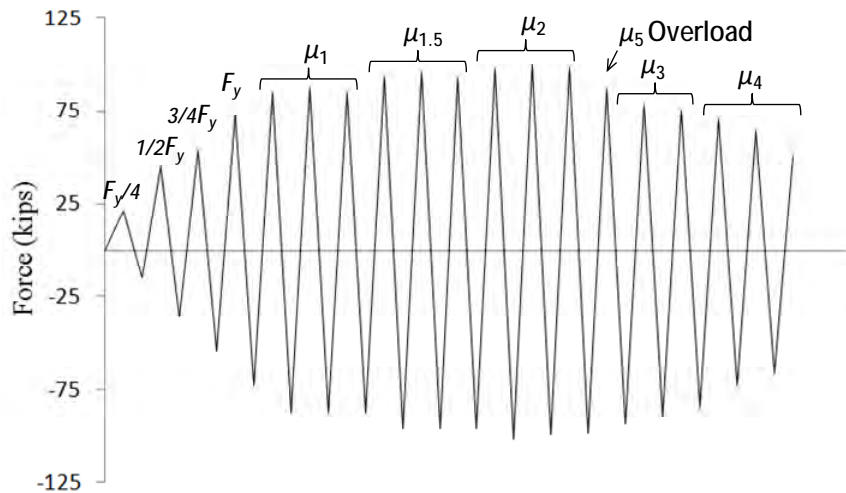


Figure 3.14 Test 2 Load History



Figure 3.15 Test 2- Cracking at Weld Toe North Column South Face

Ultimately the specimen was able to develop local buckling as is seen in Figure 3.16 when subjected to ductility 4 displacements. This buckling led to significant strength degradation and base material fracture at a location of local buckling on the south column shown in Figure 3.17. The failure mechanism of this specimen can be summarized as a combination of local buckling, strength loss, base material fracture, and weld to fracture possibly due to the overload cycle. A summary of these failure mechanisms has been provided in Table 3.2,



Figure 3.16 Test 2 – Local Buckling of North Column



Figure 3.17 Test 2- Base Material Fracture on South Column

3.3.3 Test 2 Conclusion

The overall performance of test 2 was significantly better than that of test 1. Taking into account the multiple failure mechanisms, the specimen would likely be assigned a reliable displacement ductility of 3 assuming that the crack at the weld toe was due to the errant overload cycle. Although this reliable ductility level is still far below the originally desired value of 8, it had become clear that a value of 8 was likely unattainable. Also, a reliable ductility value of 3 for this specimen corresponds to approximately 7% drift. This is a reasonably high allowable drift percentage.

It is clear that the value of displacement ductility should not be the only measure of capacity considered when evaluating the capabilities of the system. Since the measure of ductility is normalized to the yield displaced, the value of reliable ductility is sensitive the magnitude of the yield displacement. Considering that the test 2 specimen had an equivalent yield displacement 3.34 inches, a reliable ductility value of 3 would correspond to 10.02 inches of reliable displacement. This is a considerable amount of displacement capacity which may be adequate in some moderate seismic hazard regions. The displaced test 2 specimen can be seen in Figure 3.18.

Table 3.2 Test 2 Failure Mechanism Summary

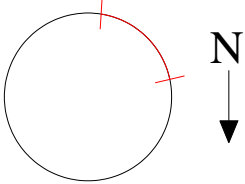
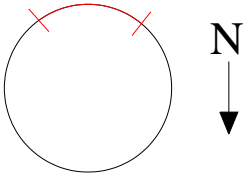
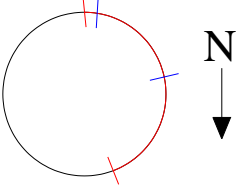
Ductility Cycle	Load [kips]	Displacement [inches]	Plan view*	Notes
μ_{3_1}				Loaded past ductility 3 to a displacement of 16", approx. μ_5
μ_{3-1}	-91	9.72	 <p style="text-align: center;">North Column</p>	
μ_{4_1}	71	12.96		Buckling on both columns
μ_{4_2}	62	12.96	 <p style="text-align: center;">South column</p>	Crack at the toe of the weld or a little below
μ_{4_2}	62	12.96	 <p style="text-align: center;">North Column</p>	Crack lengthen from μ_{3-1}
μ_{4-2}	-58	12.96		Crack in buckling region of south column



Figure 3.18 Displaced Test 2 Specimen

3.4 Test 3 Purpose, Observations, and Conclusions

3.4.1 Purpose: Evaluate Ductility of Full Penetration Weld without a Reinforcing Fillet

Given the relatively good results obtained in test 2, the research team desired to determine if an equitable response could be obtained with the exclusion of the full depth reinforcing fillet weld as seen in Figure 3.19. Should the results be repeatable without the reinforcing fillet, the benefits of the revised connection would be numerous. By removing the reinforcing fillet, a significant amount of weld material and welding time would be saved along with the benefits of reducing heat effects and the probability of weld defects.

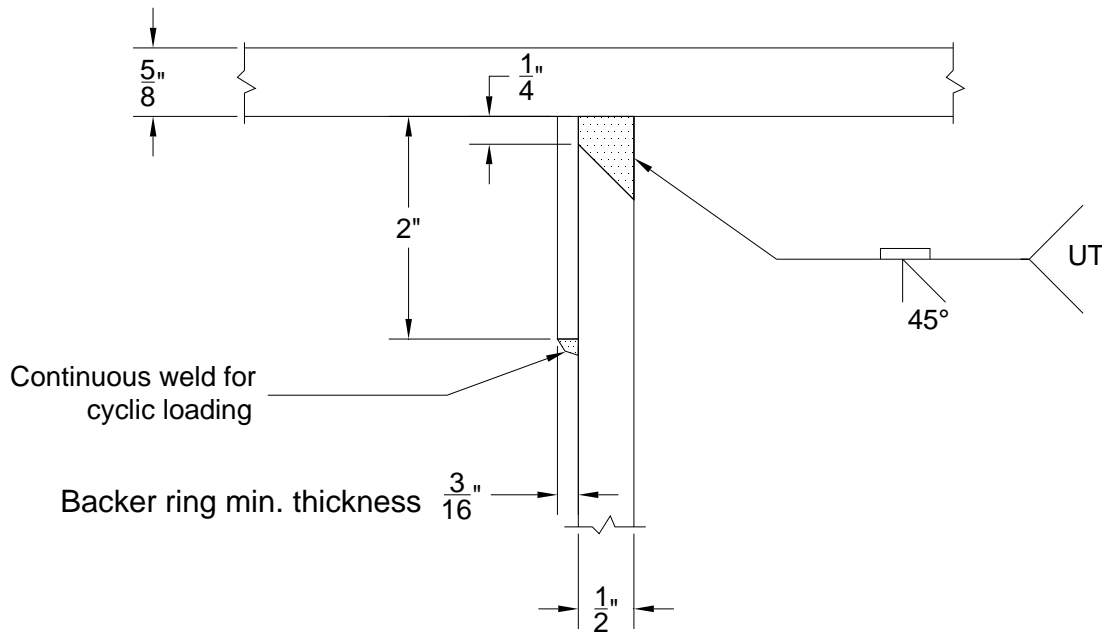


Figure 3.19 Test 3 Connection Detail Section

Given that the global system was still unaltered, the yield force remained at 73 kips. Although the base displacement had been reduced in test 2 the magnitude observed was still 5% of the yield displacement, an unacceptable amount. For this reason the rocker bearings were removed and replaced with a steel shim plate. The instrumentation layout remained the same except for the string potentiometers which were reduced in total number to two. One was located at the cap beam centerline and one at the base support.

As in test 2, significant quality control measures were implemented to ensure that the best possible weld, still constructed under realistic conditions, was achieved. Both visual and ultrasonic testing of the weld, which can be seen in Figure 3.20, was conducted and can be found in Appendix 4.



Figure 3.20 Test 3 Connection

3.4.2 Test 3 Observations

During the testing of the third specimen, a loading error occurred early in the test. Following the 50% F_y push. The specimen was significantly overloaded and data was lost during this time as is seen in Figure 3.21. As can be seen in Figure 3.22 estimates from extrapolation of the force displacement hysteresis indicate that the overload cycle reached approximately -100 kips (pull) and -15.74 inches of displacement. Unfortunately, due to the time during testing at which the overload cycle occurred, no first yield displacement could be established for this specimen. For this reason the average displacement value of 2.49 inches found in test 2 was utilized resulting in an equivalent yield or ductility one value of 3.24 inches.

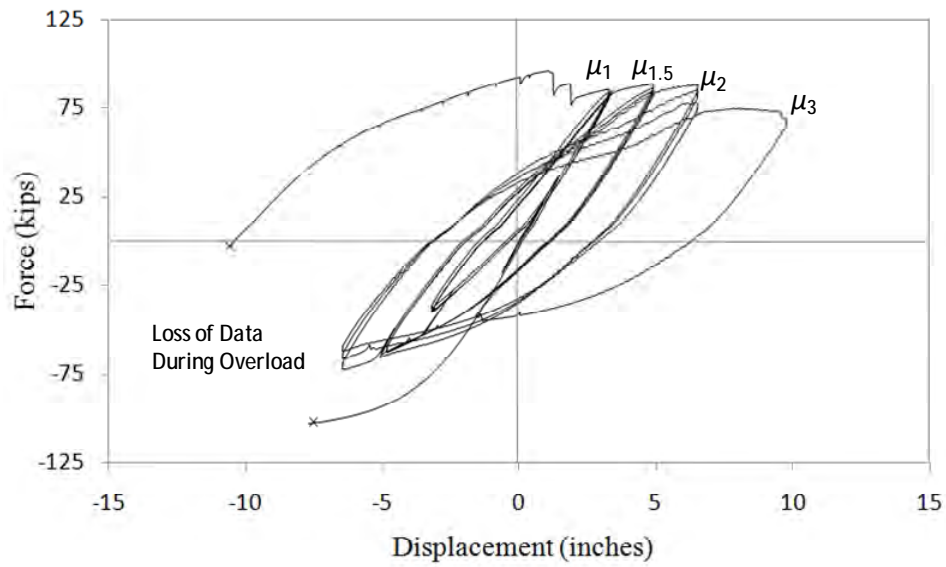


Figure 3.21 Test 3 Force Displacement Hysteresis

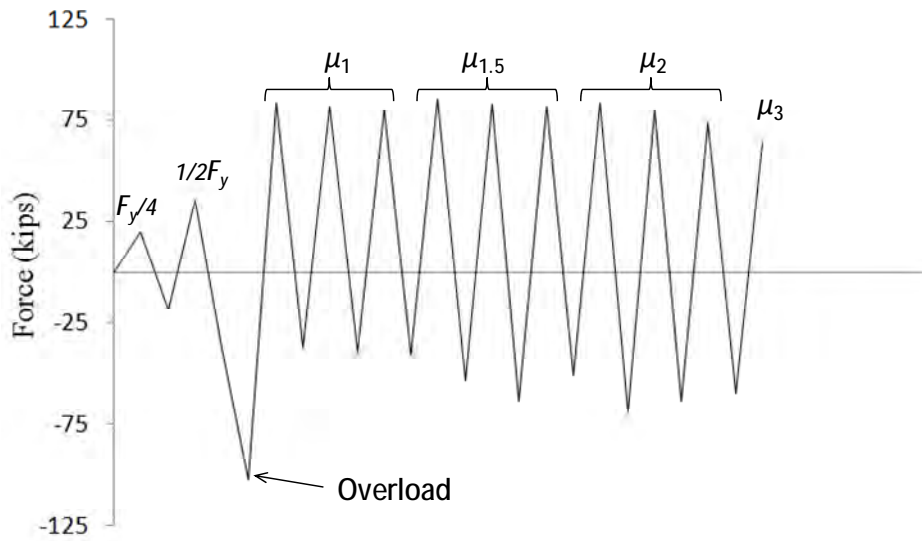


Figure 3.22 Test 3 Load History

During the overload cycle, a fracture developed at the weld toe at the beam flange in the north column as is seen in Figure 3.23. The next crack that formed was during

second pull cycle of ductility 1.5 on the south column in the northeastern quadrant at the cap beam weld toe as seen in Figure 3.24. Multiple small cracks also developed on the south side of the south column. The crack seen at the weld toe of the north column also grew in length during this cycle. The cracks already formed on both columns continued to grow both in length and width during the first cycle of the second ductility level and even propagated through the weld in the case of the cracking on the south column during the second cycle of ductility 2 as shown in Figure 3.25. The cracking observed on the north pile was also seen to propagate through the weld during the third cycle of ductility 2 as shown in Figure 3.26. The test was continued into ductility three even though the reduction in strength was clearly more than 20%. After the first cycle of ductility 3 the cap beam showed distortion near both columns, as seen in Figure 3.27, and a new crack had formed in the north column at the cap beam weld toe. At this point the test was stopped due the extent of damage and loss of strength of the test unit as has been summarized in Table 3.3.



Figure 3.23 North Column Crack During Overload Cycle



Figure 3.24 South Column Cracking – Ductility 1.5 Second Pull cycle



Figure 3.25 South Column Propagation of Cracking through the Weld



Figure 3.26 North Column Propagation of Cracking through the Weld



Figure 3.27 Cap Beam Distortion

Table 3.3 Test 3 Summary

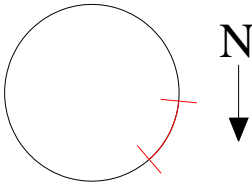
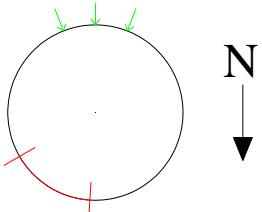
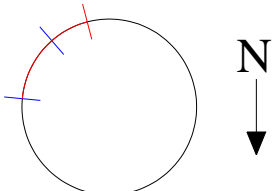
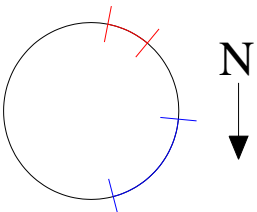
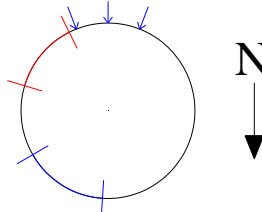
Ductility Cycle	Load [kips]	Displacement [inches]	Plan view	Notes
Over load	-100	Unknown		Specimen was loaded past 50%F _y to an unknown load and displacement
μ ₁	50	3.24	 <p>North column</p>	
μ _{1.5-2}	-61.5	4.86	 <p>South column</p>	Green arrows show area where small cracks were seen
μ _{1.5-2}	-61.5	4.86	 <p>North column</p>	Red line growth of crack and blue lines are old crack
μ ₂₋₁	85	12.96	 <p>North column</p>	Red lines are new crack that formed

Table 3.3 Test 3 Summary Continued

$\mu_{2.2}$	-70	12.96		South Column crack from $\mu_{1.5-2}$ propagated through weld in location shown previously
$\mu_{2.3}$	76			North column crack from $\mu_{2.1}$ propagated through weld in location shown previously
$\mu_{3.1}$	-58	9.72	 <p style="text-align: center;">South column</p>	New crack on south column shown in red.

3.4.3 Test 3 Conclusion

Regardless of the loading error, it is clear that the response of test 3 was inadequate. Although the test would likely be assigned a reliable ductility of 1.5 to 2 which is slightly better than that of test 1, the response was not comparable to that of test 2. The unreinforced complete joint penetration weld was therefore deemed inadequate and the connection would not be used in future tests.

3.5 Test 4 Purpose, Observations, and Conclusions

3.5.1 Purpose: Validate Results of Test 2

As test 3 had proven that a complete joint penetration weld without a reinforcing fillet was generally inadequate, test 4 aimed to validate the results of test 2. For this reason an identical weld detail to test 2, as shown in Figure 3.28, was conducted following the earlier practice of visual and ultrasonic testing to ensure the weld was as defect free as possible. Again, all welding was performed overhead in order to follow typical construction practices.

Although the traditional instrumentation and Optotrak system remained unchanged from test 3, test 4 also included audio monitoring equipment. The system consisted of ten microphones of which the layout can be seen in Figure 3.29 and a recording station. The main purpose of this equipment was to assist the research team in identifying locations of damage, cracking in particular, over random noises emitted by the setup such as pin rotations. The system was also successful in helping to identify when possible cracking inside the pile occurred as will be discussed in subsequent sections.

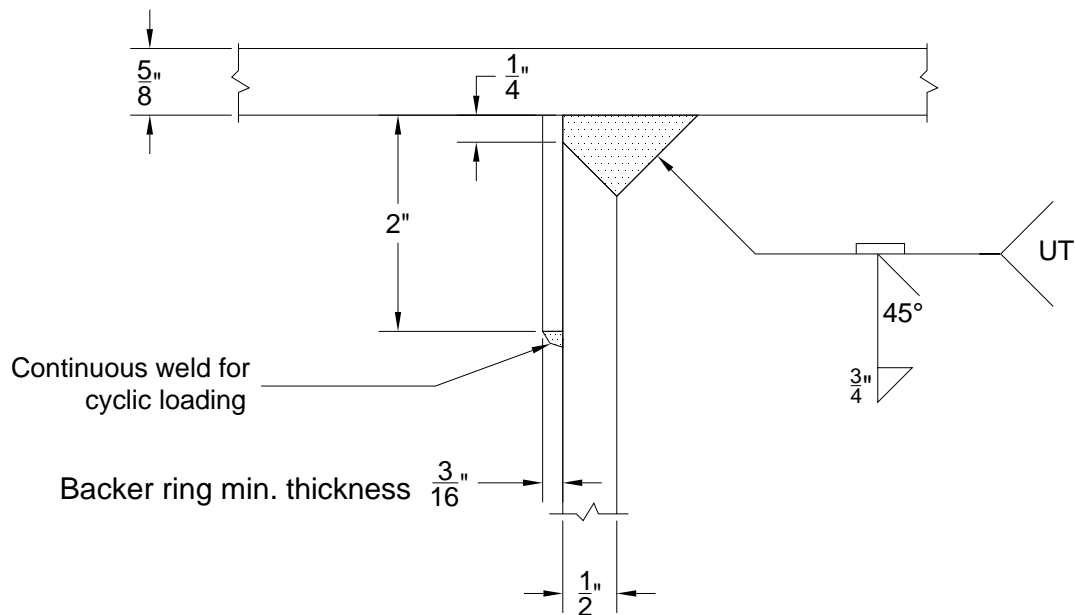


Figure 3.28 Test 4 Weld Detail Section



Figure 3.29 Microphone Layout

3.5.2 Test 4 Observations

Again since the global system remained unchanged, the first yield was maintained as 73 kips. In the case of test 4, the observed average first yield displacement was 2.54 inches resulting in an equivalent yield displacement of 3.30 inches. Although no visual signs of failure and no strength loss was observed prior to the third cycle of ductility 3, two audio emissions not attributable to support noise were recorded. The first of these occurred during the third pull cycle of ductility 2 and registered highest at microphone 3 as shown in Figure 3.30. The next omission occurred during the first pull cycle of ductility 3 and again was recorded with the highest amplitude at microphone 3 as shown in Figure 3.31. Both these records indicate a much sharper and shorter emission than that of a common pin slip emission which is shown in Figure 3.32. It is possible that these emissions were the result of cracking in the inside of the pile which may have been at the backing bar weld or the root of the complete joint penetration weld.

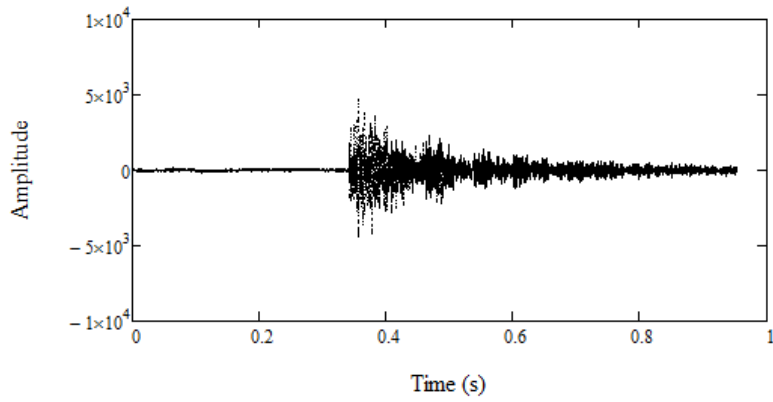


Figure 3.30 Recording at Mic 3 – Ductility 2 Cycle -3

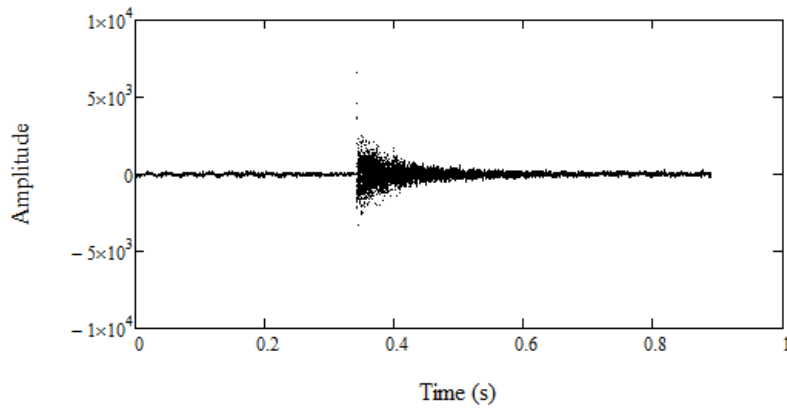


Figure 3.31 Recording at Mic 3 – Ductility 3 cycle -1

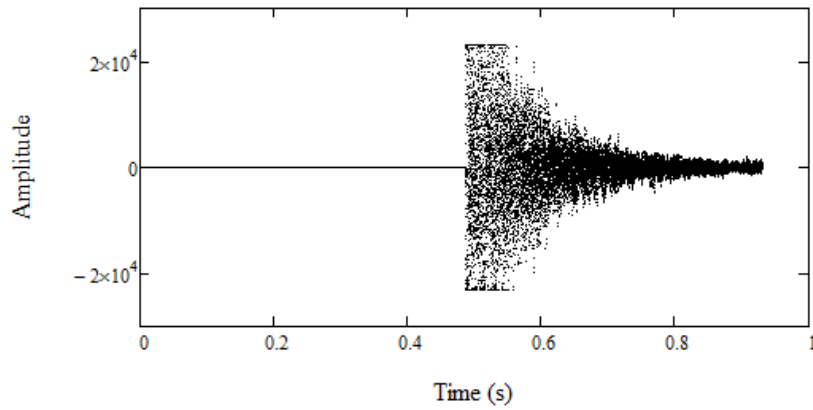


Figure 3.32 Typical Pin Slip Recording

Ultimate failure occurred rapidly during the third push cycle of ductility 3. A large crack quickly formed and propagated around a significant portion of the south face of the south column as seen in Figure 3.33 and Figure 3.34. This crack significantly affected the strength of the system as can be seen in both Figure 3.35 and Figure 3.36. The last pull cycle of ductility three was completed and the test was assumed to be completed given the significant cracking on the south column and approximately 30% strength loss.



Figure 3.33 Cracking on South Column



Figure 3.34 Cracking on South Column – Post Test

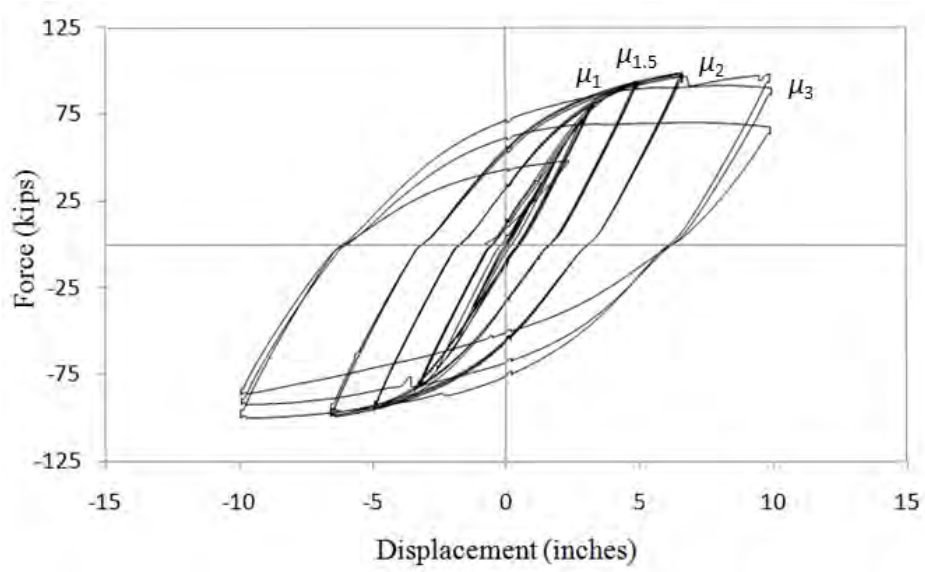


Figure 3.35 Test 4 Force Displacement Hysteresis

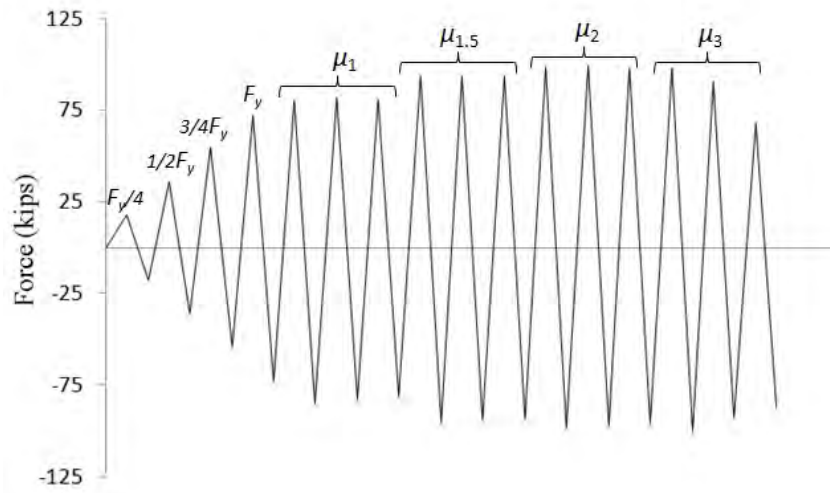


Figure 3.36 Test 4 Load History



Figure 3.37 Minor Local Buckling on the South Column

3.5.3 Test 4 Conclusion

The test 4 specimen generally responded in an adequate manner prior to ductility 3. The rapid onset of failure in the third push cycle of ductility 3 involving cracking at the weld toe is however a rather undesirable failure mode. The specimen was able to develop only a minor amount of local buckling as shown in Figure 3.37. In comparison to test 2 which was able to develop significant local buckling and eventual base material fracture, test 4 was not very successful. For this reason it was felt that the results of test 2 were not adequately validated by the given connection detail.

3.6 Test 5 Purpose, Observations, and Conclusions

3.6.1 Purpose: Attempt to Control Joint Deformation Utilizing an Inside Reinforcing Fillet Weld

Following the first four tests it had become clear that simple weld configuration changes were not going to produce a reliably adequate design. Taking this into account, the research team in conjunction with AKDOT decided that more drastic measures were going to be necessary. At this point in the testing series, it was still unclear whether the failures seen in test 1-4 were a strain controlled or stress controlled issue. Considering this, it was decided that the addition of an inside reinforcing fillet weld would provide a larger capacity and possibly prolong the life of the structure. The detail shown in Figure 3.38 was developed to incorporate this inside reinforcing fillet. Consideration was given to the fact that the detail develop would induce even more heat effects and introduce the possibility for more defects. The addition of the splice weld also adds to the negative effects of the detail. However, it was decided that regardless of these issues the connection still had good potential and was the next logical step.

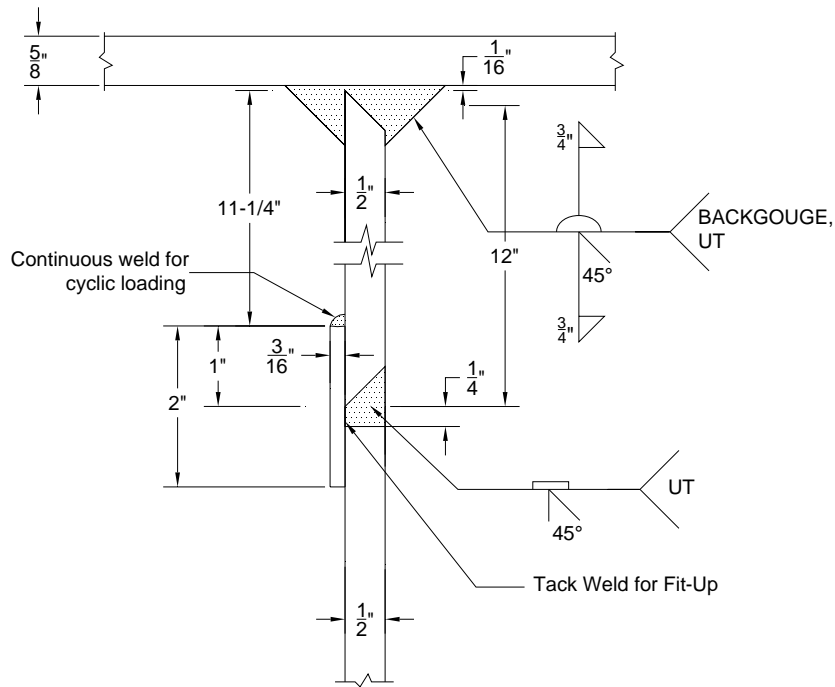


Figure 3.38 Connection Detail Section

Considerable effort was made to ensure that during the construction process each step taken could be realistically reproduced in the field. In order to incorporate the inside fillet weld as shown in Figure 3.39, it was necessary to use a 12 inch stub column which would first be welded to the cap beam in a sequence indicated by a WPS. Prior to the welding of the stub column to the cap beam, the proper location of the stub column on the cap beam was marked by placing the cap beam on the piles which had already been erected and marking their location. This step was utilized to ensure alignment of the stub column to the pile. The welding of the stub column to the cap beam as can be seen in Figure 3.40 was then conducted underhand on the ground prior to the placement of the cap beam as could be done in the field. Next, the cap beam was placed on the piles and the splice weld between the stub column and piles was completed. Again all three types of instrumentation were used in this test. The layout of each system remained the same as in test 4.



Figure 3.39 Test 5 – Inside Reinforcing Fillet Weld



Figure 3.40 Completed Stub Column Weld

3.6.2 Test 5 Observations

A first yield force of 73 kips was again used and the average first yield displacement for this test was found to be 2.84 inches resulting in an equivalent yield magnitude of 3.69 inches. The overall response of the test 5 specimen was very similar to that of test 4. No visual signs of failure or strength degradation were observed prior to a displacement ductility level of 3. Also similar to test 4, several audio emissions were noted prior to failure that were not attributable to set up noise as shown in Figure 3.41. However there were again no visual signs of failure associated with the noises. It is likely that these noises can be attributed to cracking taking place inside the column. This inside cracking could likely be taking place in the weld region of the backer ring.

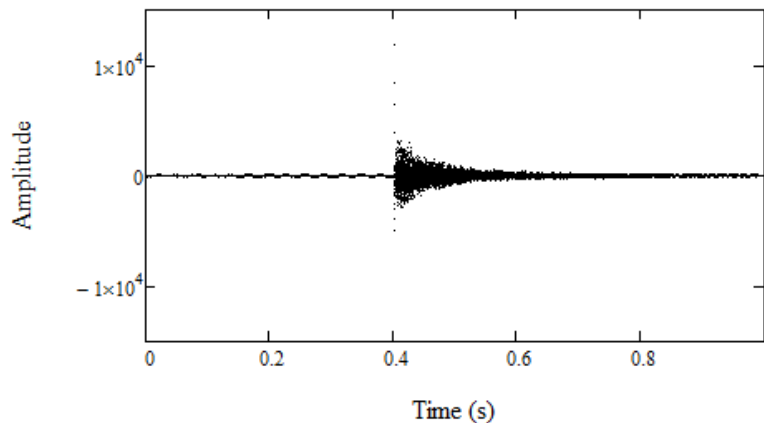


Figure 3.41 Sound Emission Possibly Related to Interior Cracking

The ultimate failure mechanism in test 5 again occurred in the third push cycle of ductility 3 and consisted of a large fracture at the weld toe on the south side of the south column as shown in Figure 3.42. The crack was associated with over 20% strength loss as shown in Figure 3.43 and Figure 3.44. Since the full cycle had not been completed, the research team attempted to continue pushing the specimen but the crack began to propagate very quickly. For this reason the test was concluded.

Unlike test 4, test 5 was able to develop a minor level of local buckling on both columns. The first signs of local buckling began to develop during the second push cycle

of ductility 3 at a location just above the splice weld on the north face of the south column and near the cap beam weld on the north face of the north column. The second pull cycle of ductility 3 led to slight local buckling developing near the cap beam weld on the south face of the south column and at both the cap beam weld and splice weld on the south face of the north column as can be seen in Figure 3.45. The buckling never had a chance to propagate and develop strength loss due to large the fracture that formed shortly after buckling had begun.



Figure 3.42 Failure Crack – Ductility 3 Cycle 3

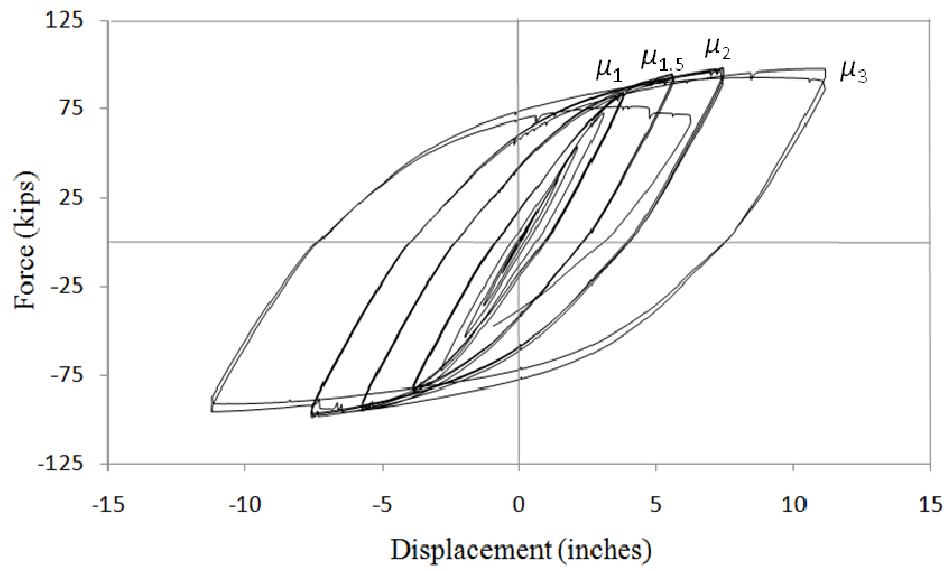


Figure 3.43 Test 5 Force Displacement Hysteresis

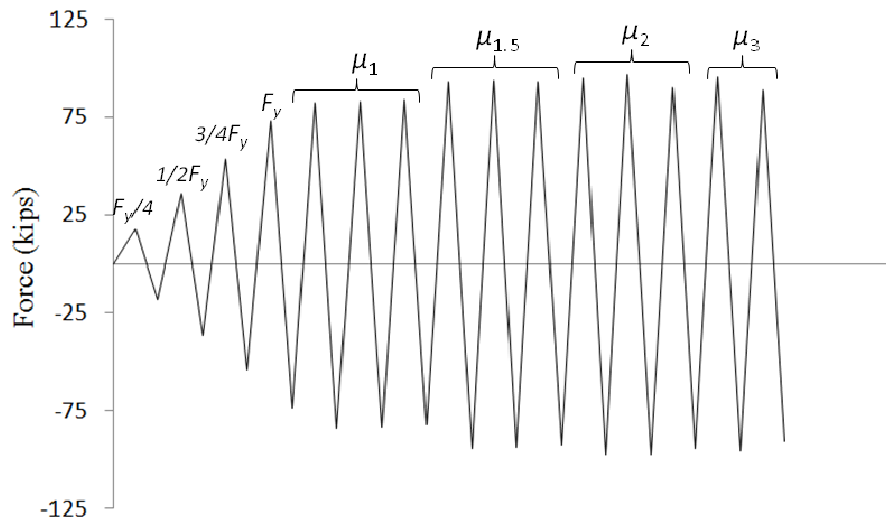


Figure 3.44 Test 5 Load History



Figure 3.45 Double Buckling of North Column

3.6.3 Test 5 Conclusion

Although the test 5 specimen was able to withstand most cycles of ductility 3 as is shown in Figure 3.46, the reliability of the design was no better than that of test 4. The test 5 detail did allow for minor local buckling to begin occurring, but ultimately the failure took place again at the weld toe. The detail was not capable of producing a base material failure and was therefore considered to be inadequate and unreliable. It was still felt following this test that the weld toe failures observed were likely strain related as opposed to stress related. Unfortunately the inside reinforcing fillet weld did not prolong the life of the structure leading to the conclusion that the failure may be strain controlled.

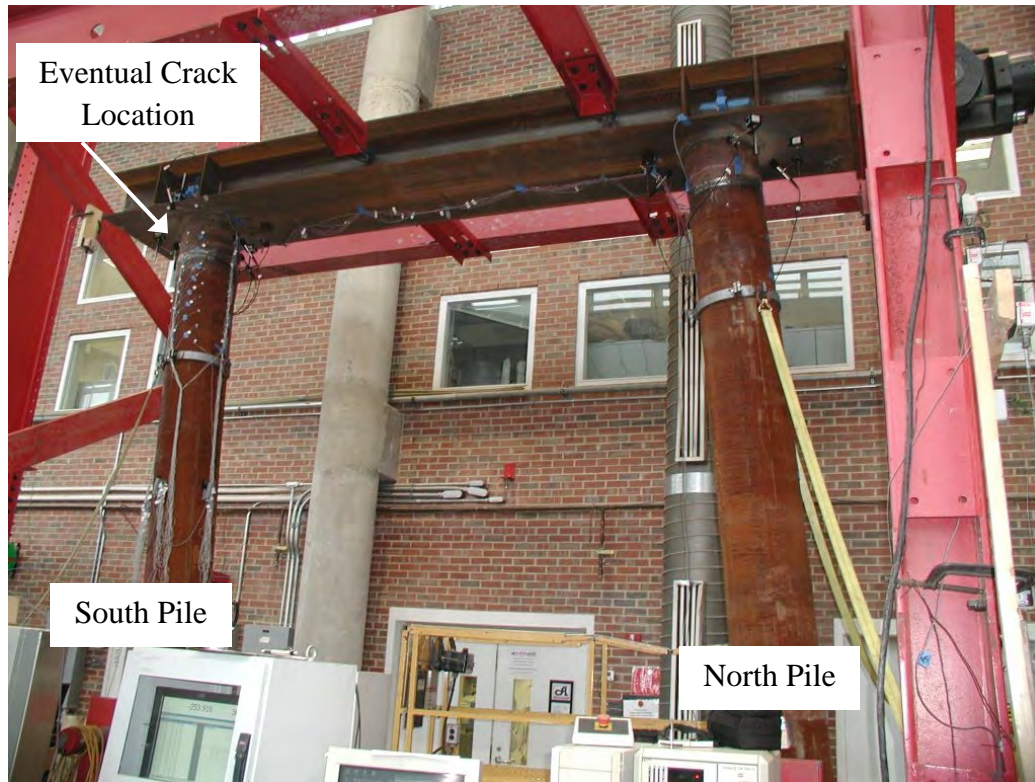


Figure 3.46 Test 5 Response – Ductility 3

3.7 Test 6 Purpose, Observations, and Conclusions

3.7.1 Test 6 Purpose: Relocation of Flexural Plastic Hinging

From tests 1-5 it had become apparent that manipulation of the weld joint alone would not produce a reliable connection. For this reason it was decided that an attempt would be made to relocate the plastic hinge region to force failure away from the complicated geometry of the cap beam/column connection. If the failure at the weld region is impacted by high strains, relocating the hinge away from the weld will improve behavior. However, if stress is the more important parameter, relocating the hinge does not help the situation since the stresses at the joint remain high (albeit in the elastic range). Multiple systems for relocating the location of hinging were considered including a reduced section, a heat treated section, and a strengthened column capital amongst others.

Ultimately it was decided that a flared column capital as shown in Figure 3.47 would be utilized. Although the system was more complicated than originally desired by AKDOT, it was considered a necessary effort should for an adequate connection to be achieved.



Figure 3.47 Test 6 – Flared Column Capital

The design of this system was based on the principle that the critical section of the flared column (adjacent to the cap beam flange) should remain elastic under full plastic flexural moment at the intended hinge region just below the flared section. Taking into account the demand relationship as shown in Figure 3.48 and the properties of ASTM A527 Gr. 50 material which was to be used in the fabrication of the column capital, the final design shown in Figure 3.49 was created. It is important to note that the connectivity of the smaller diameter portion of the column capital to the larger was not created by welding. The assembly is a single unit fabricated by the bending of plates into two 180 degree sections that were in turn seam welded down the longitudinal axis. The smaller diameter section was created by then milling down the section as specified. The intention of this process was to create an intended hinging region away from either weld. By designing the section for the top weld to remain elastic, it was hoped that the strains would remain low enough to preclude failure similar to that seen in the prior tests. An excerpt

from the shop drawings of the assembly can be seen in Figure 3.50. The full shop drawings are provided in Appendix 2.

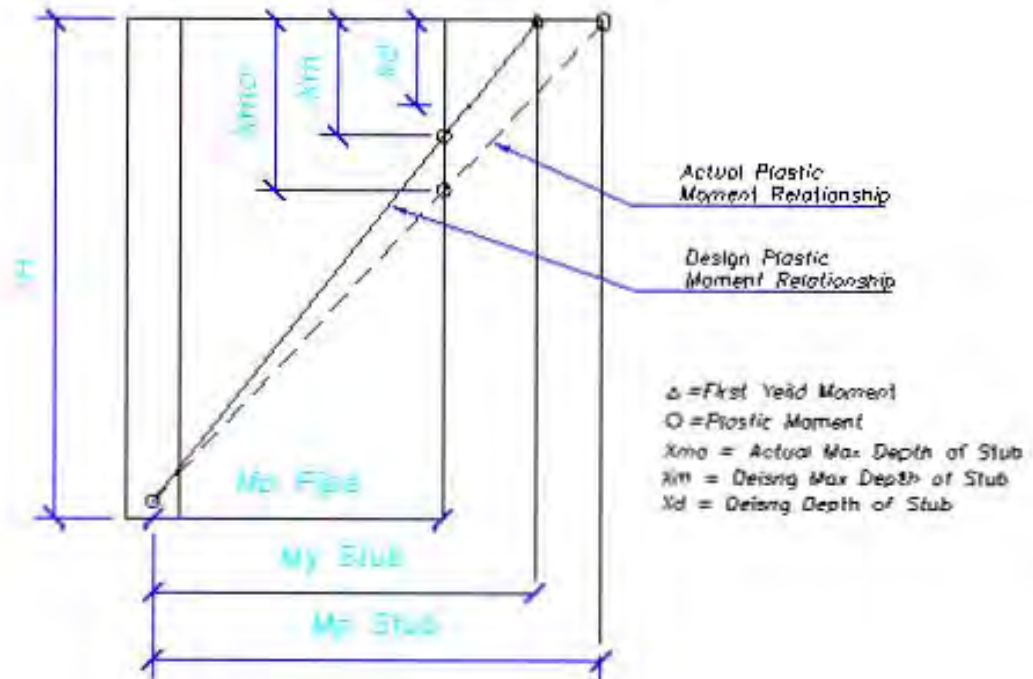


Figure 3.48 Moment Demand Relationship

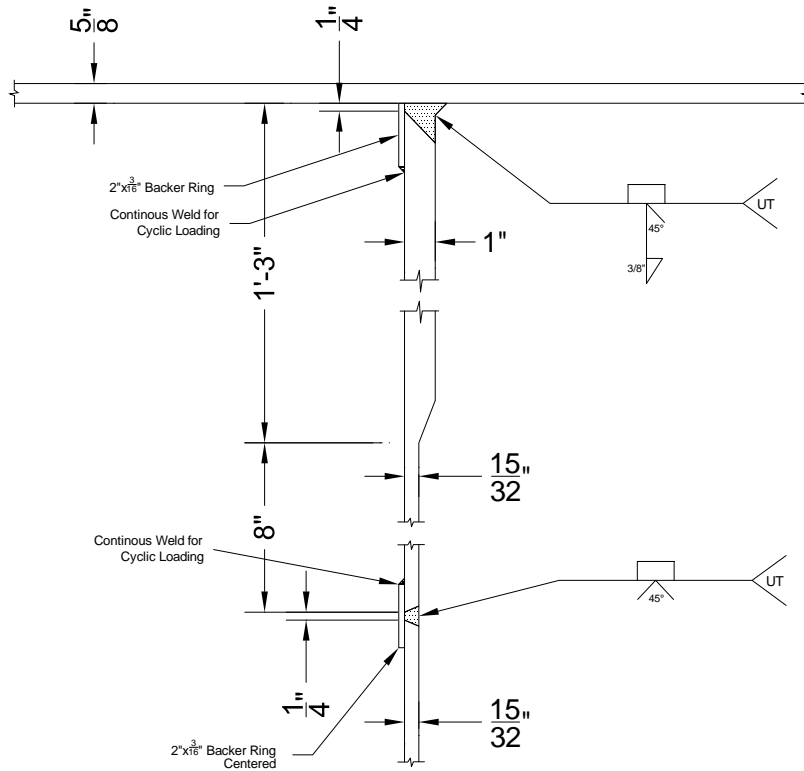


Figure 3.49 Test 6 Connection Detail Section

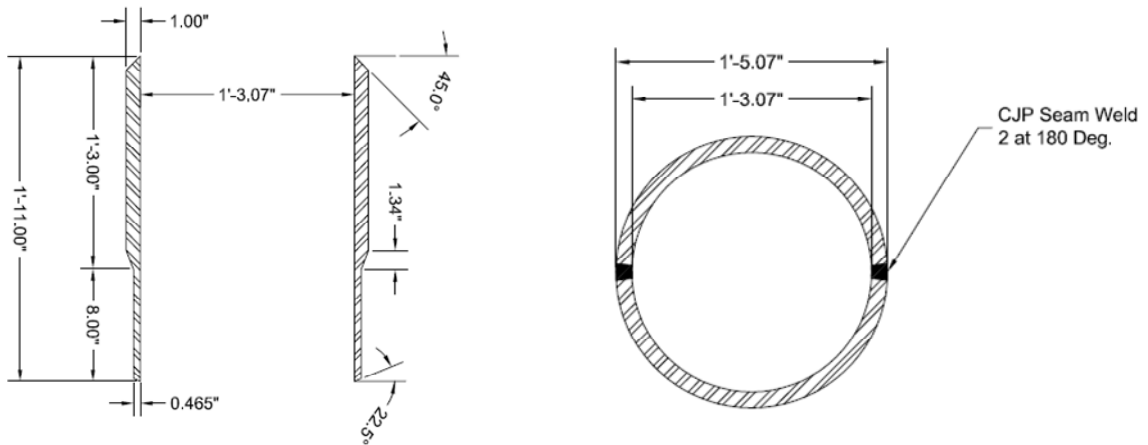


Figure 3.50 Detail of Column Capital Assembly

Similar to all prior tests, consideration was given to the repeatability and practicality of the bent construction process. A process similar to that of test 5 was used and has been described in Figure 3.51. Both the top connection and splice weld were inspected by visual and ultrasonic testing. It is also important to note that a 3/8 inch reinforcing fillet was used in the top weld of the assembly to the cap beam flange. Although this is likely unnecessary given the elastic design intention of the joint it was desired to help relieve the sharp geometry of a plane complete joint penetration weld.

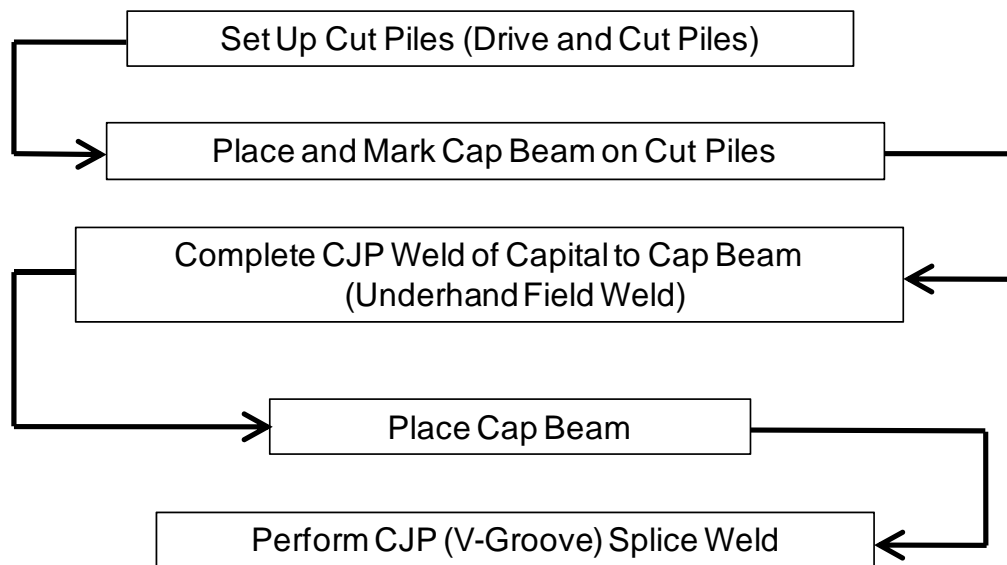


Figure 3.51 Construction Sequence of Test 6

In addition to the instrumentation used in test 5, a series of 4 PI gauges were used to measure base rotation due to bolt strain. Although the calculated estimates of these measurements were of no considerable magnitude, the gauges were used in hopes of determining a source of the consistently higher than anticipated first yield deflections. The layout of these gauges is shown in Figure 3.52.

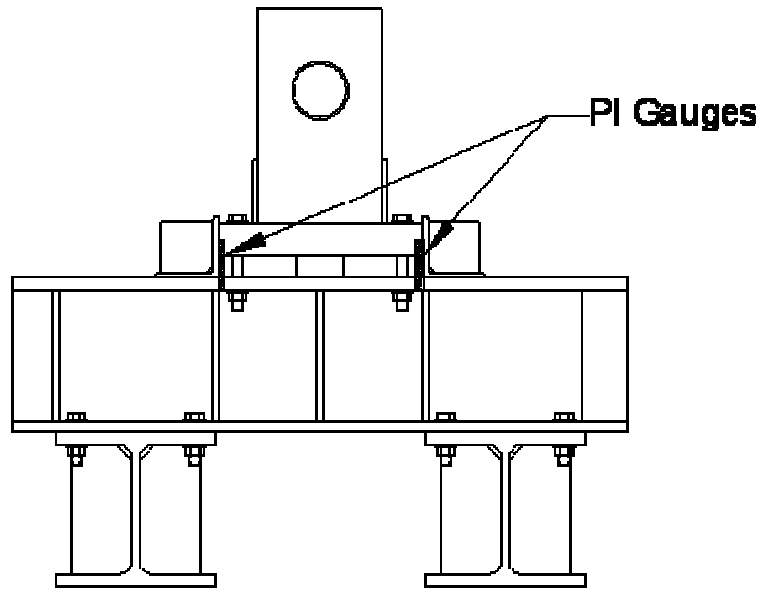


Figure 3.52 Location of PI Gauges

3.7.2 Test 6 Observations

Given that the global strength of the system had been altered due to the inclusion of the flared column capital, it was necessary to increase the system first yield force to 79.7 kips. The observed average first yield displacement was 2.33 inches resulting in an equivalent yield or ductility 1 value of 3.03 inches. As in prior tests, multiple audio emissions were noted well before failure but no visual signs of cracking existed nor was any strength degradation associated with these emissions. It is likely that the recordings are due to the cracking of the welding of the backing bars used in the connection details.

The test 6 specimen showed no signs of failure through ductility 1.5 and began to develop slight local buckling during ductility 2 as shown in Figure 3.53. This local buckling progressed throughout the cycles of ductility 2, 3, and 4. The slow propagation of the local buckling on both columns allowed for the degradation of the structures strength to also take place in a slow manner. Ultimately failure was dictated by base material rupture at a location of local buckling on the south column as shown in Figure 3.54. This rupture was not associated with a welded zone and occurred after approximately 30% strength loss as can be seen in Figure 3.55 and Figure 3.56.

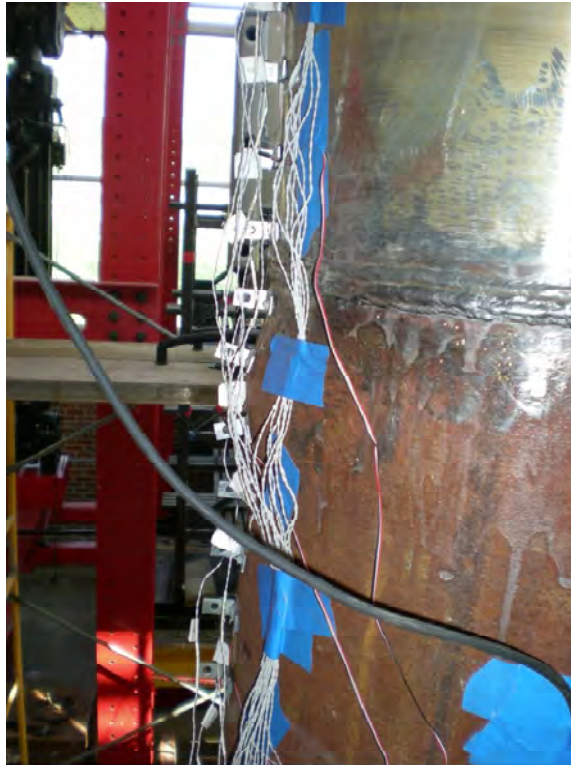


Figure 3.53 Propagation of Local Buckling – Ductility 3 Cycle 1



Figure 3.54 Test 6 Rupture – South Column North Face – Ductility 4 Cycle -3

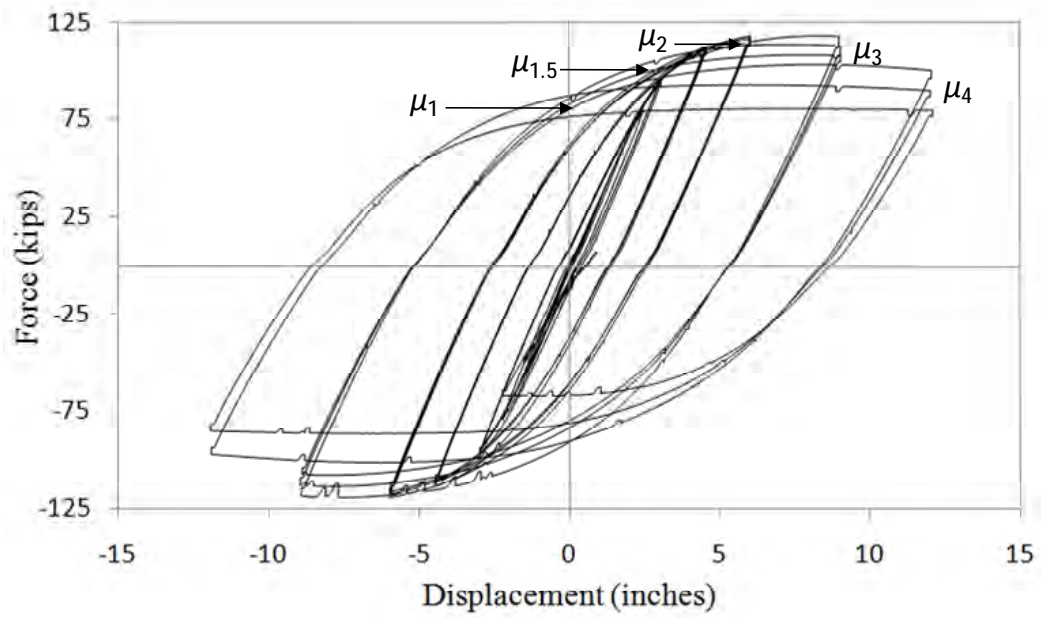


Figure 3.55 Test 6 Force Displacement Hysteresis

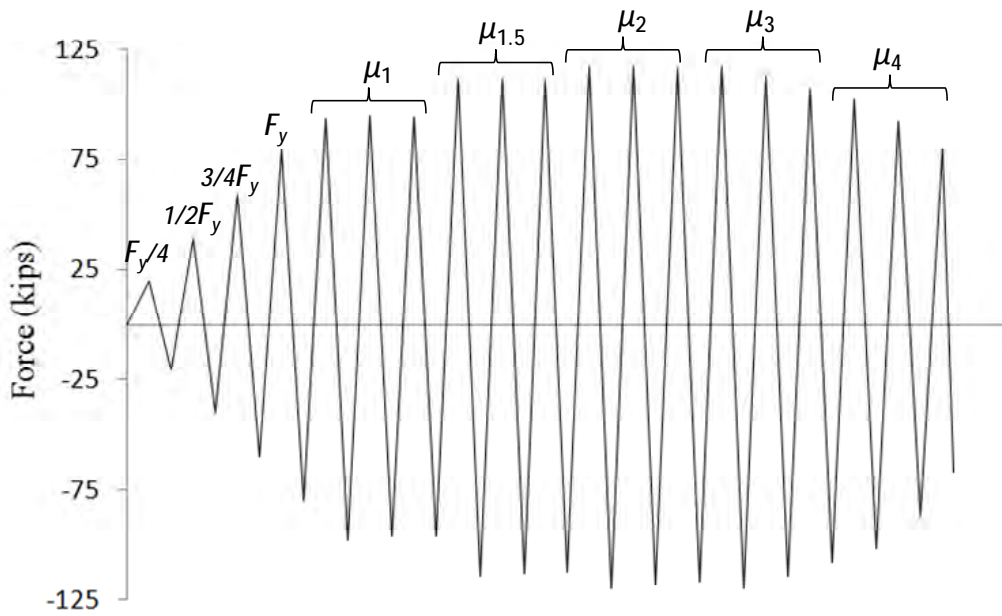


Figure 3.56 Test 6 Load History

As can be seen in the figures provided the buckling observed occurred below the intended hinging region of the flared column capital. Initial speculation for how this occurred included the possibility that the capital was acting as a rigid end more than a flexural member for an unknown reason. As seen in Figure 3.57 Vertical Strain Profile – South Column South Face, flexural strains were present in the capital and it was not acting as a rigid end block. However, the strains were marginally higher just below the intended region. Although no theoretical reasons exist for this since the intended hinge region and plane pile section have the same properties, it is likely due to stiffening effects created by the presence of the backer ring and splice weld. In future tests it would be possible to avoid this effect by lengthening the intended hinge region or weakening the material. A combination of both would also be possible. It should be noted that in this particular tests, no adverse affects were generated by the location of buckling being outside the intended region. It is however desired to be able to control the exact location of this buckling to ensure that it will not occur near the splice weld. More in depth analysis of test 6 as well as discussion of future considerations are both provided in subsequent Chapters of this report.

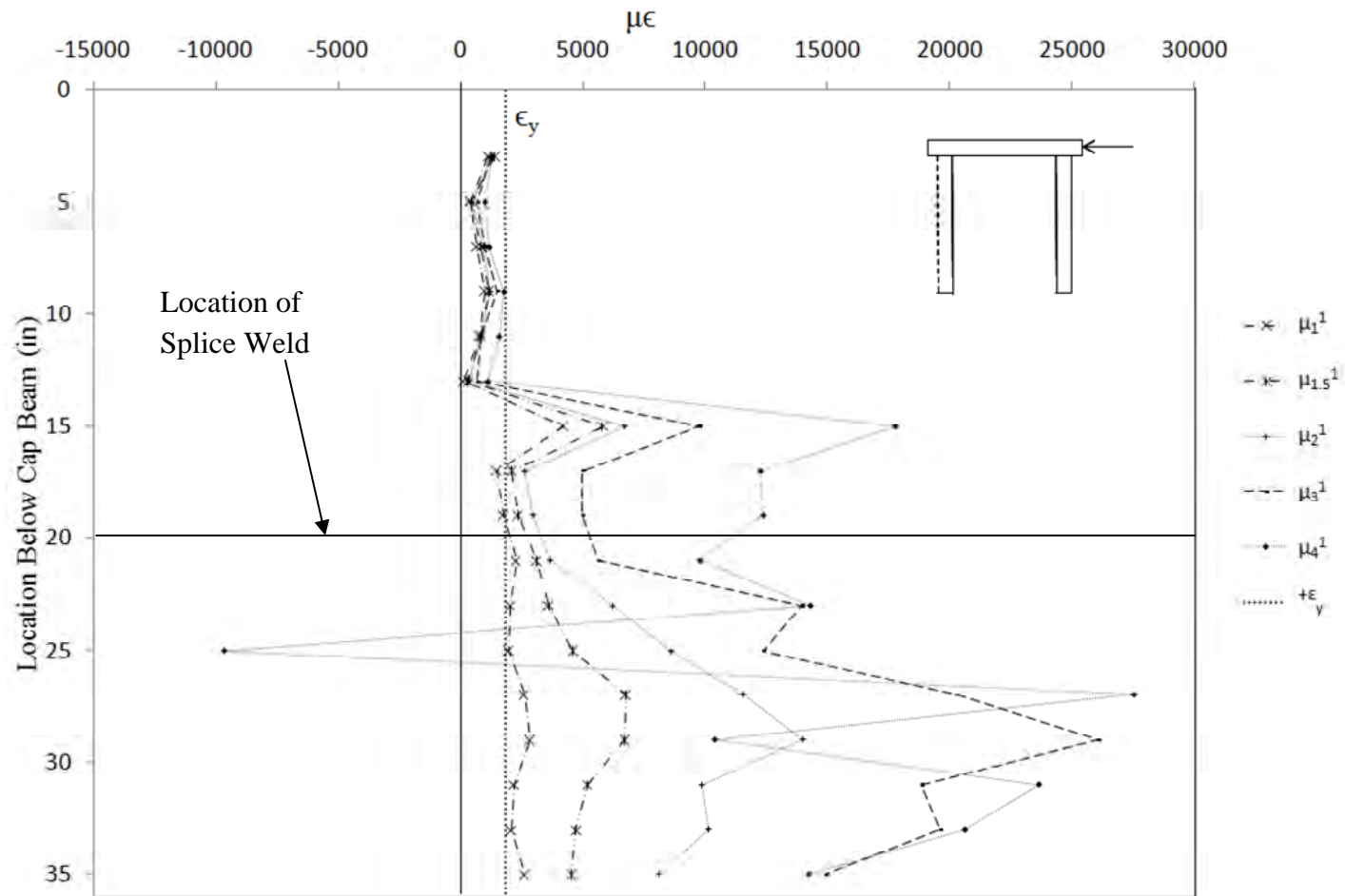


Figure 3.57 Vertical Strain Profile – South Column South Face

3.7.3 Test 6 Conclusions

In general, the test 6 specimen significantly outperformed that of any prior specimen as can be seen in Figure 3.58. The system would likely be assigned a reliable ductility of 3 or 4, at least one level greater than that of test 1-5. Not only was the ultimate displacement ductility capacity increased in this test, a more desirable and controllable failure mode was observed. By inducing local buckling and base material fracture prior to brittle rupture at a weld region the specimen has achieved its ultimate capability. Should greater displacement capacity be desired, it may be possible with a detail similar to that of test 6 to decrease the pile D/t ratio and achieve an even higher reliable ductility prior to base material fracture.



Figure 3.58 Test 6 – Ductility 4

It was also found during test 6, that the influence of base rotation due to elongation of the bolts in the base supports was insignificant as was suspected. As seen in Figure 3.59, the measurements of bolt elongation remained at extremely low values that would be

considered insignificant even when taking into account the extrapolation factor of about 12 that would exist when calculating the observed displacement at the cap beam level due to this elongation. This would indicate that bolt elongation does not contribute to the higher than expected first yield displacements.

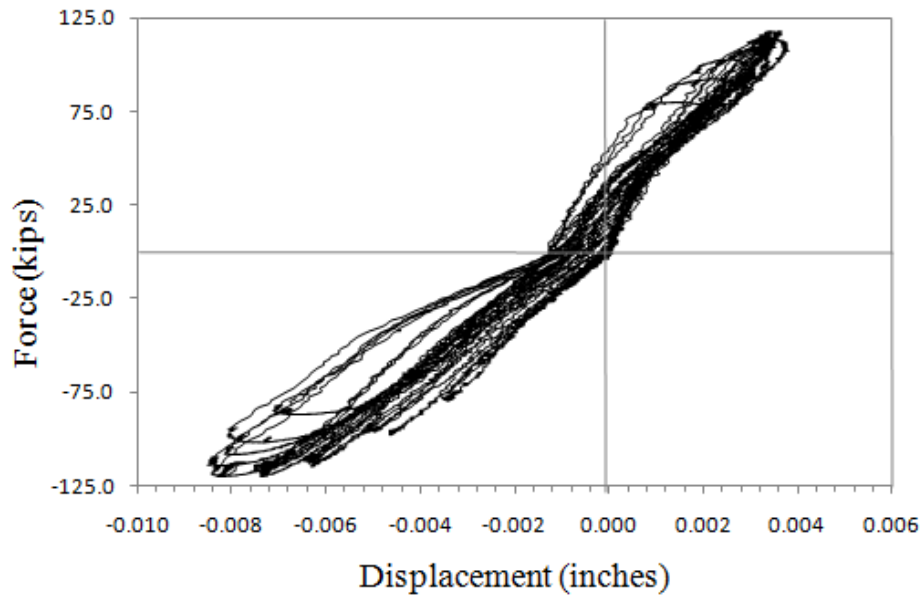


Figure 3.59 Typical PI Gauge Recording

During the testing of specimen 6 it was noted that both inclinometers located at the intersections of the cap beam and pile centerlines fell off at an early ductility level. This prompted the research team to investigate the data recorded by the gauges prior to them falling off. It was found that the joint rotations of this intersection were much higher than expected at first yield. It also appears that inelastic panel shear strain was experienced in the joint as is seen in Figure 3.60. This apparently weak joint could be the source of some or all of the first yield displacement discrepancy that had been experienced. These issues will also be discussed in more detail in the following Chapters.

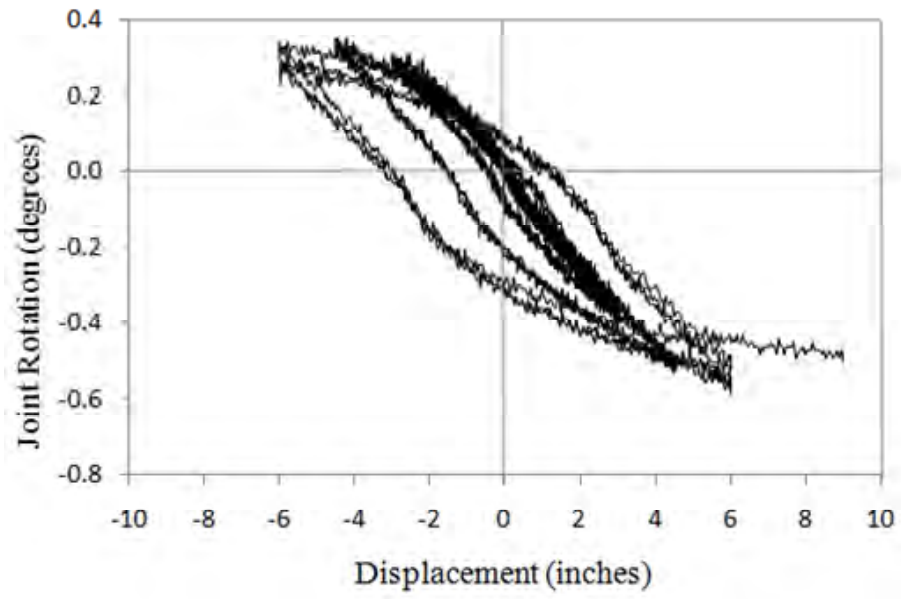


Figure 3.60 North Column Joint Rotation

Response Considerations and Comparisons

4.1 Review of the Testing Series

To summarize Chapter 3, the specimens of tests 1-5 consisted of matching global systems with varying connection details while test 6 consisted of a specimen with a slightly altered global system in order to relocate the plastic hinge. With exception of loading errors, the force deformation response of the matching specimens remained relatively similar as would be anticipated. However the failure ductility and reliable displacement ductility capacities were highly variable. For convenience the six tests conducted have been summarized in Table 4.1 Testing Results Summary and the force displacement hysteresees from the six tests are provided in successive order within this section.

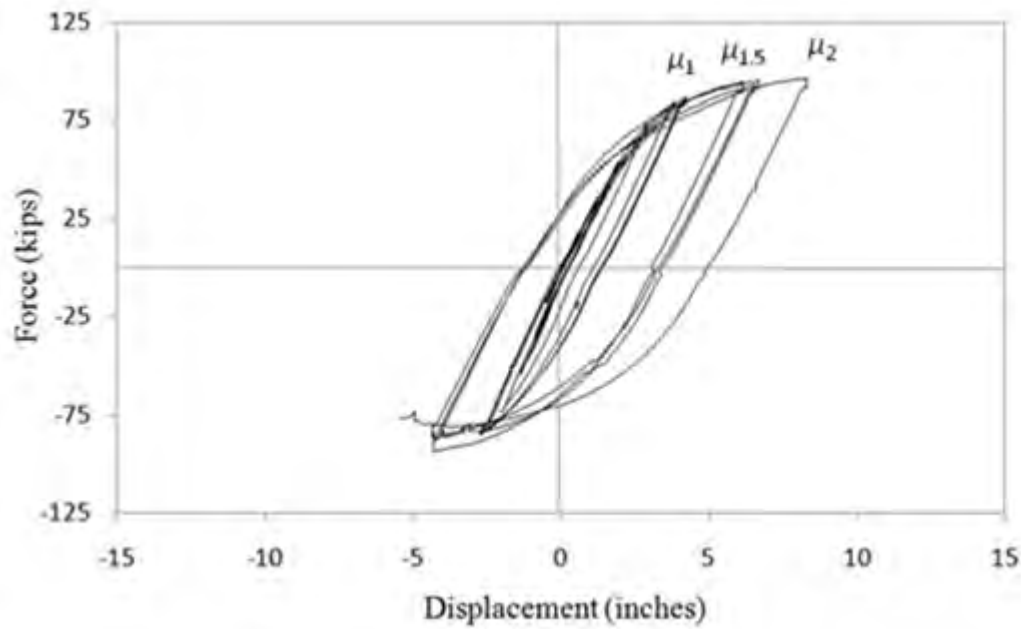


Figure 4.1 Test 1 Force Displacement Hysteresis

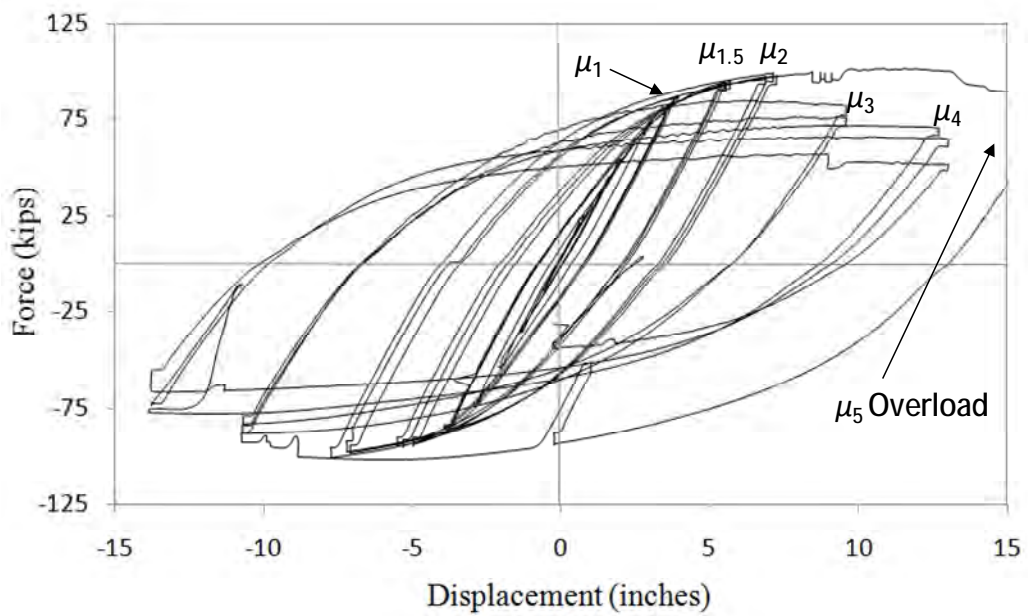


Figure 4.2 Test 2 Force Displacement Hysteresis

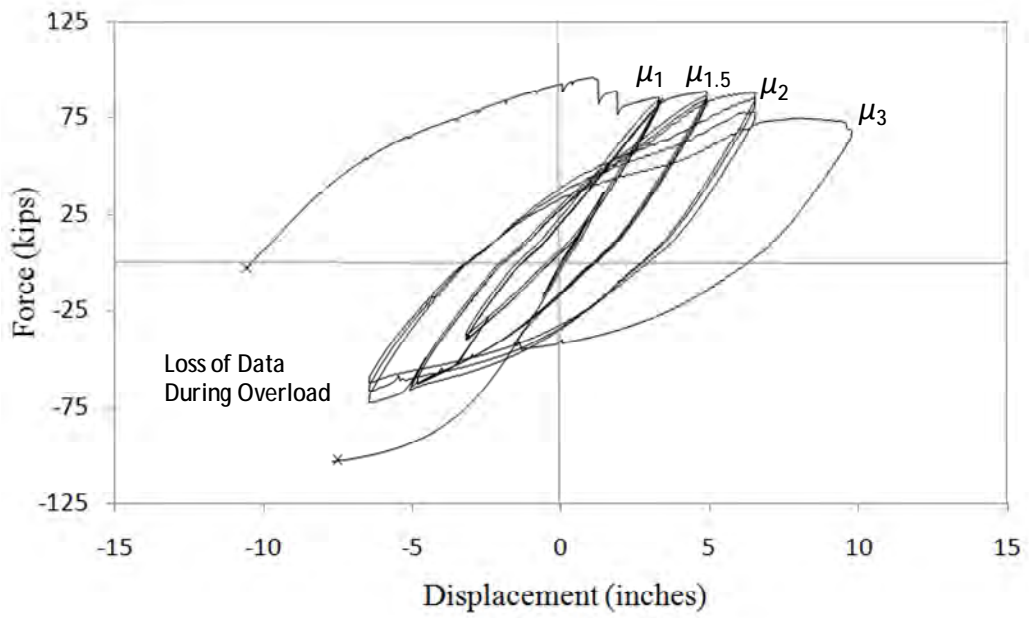


Figure 4.3 Test 3 Force Displacement Hysteresis

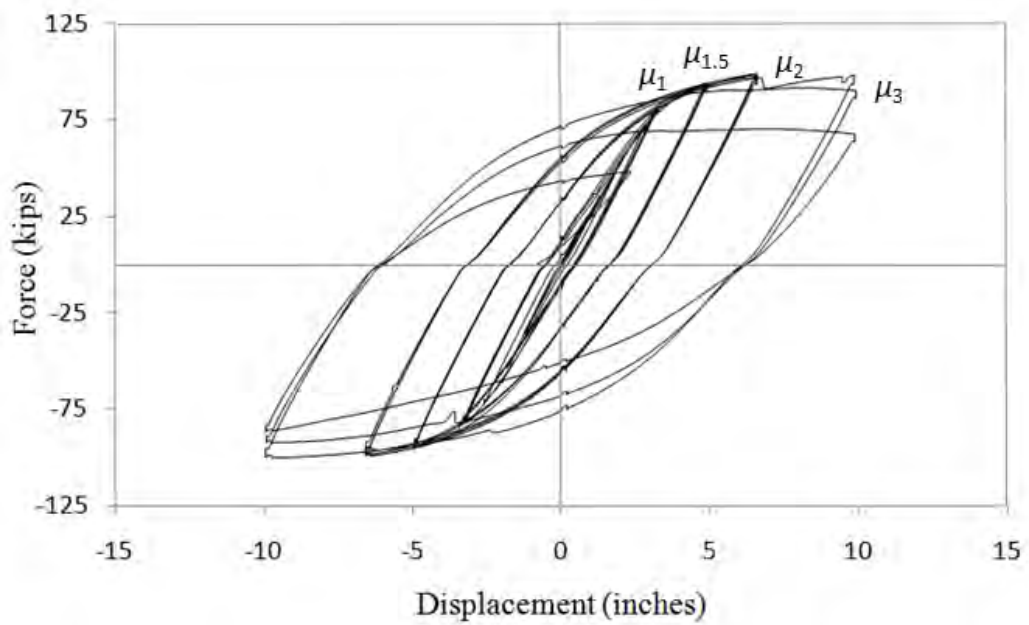


Figure 4.4 Test 4 Force Displacement Hysteresis

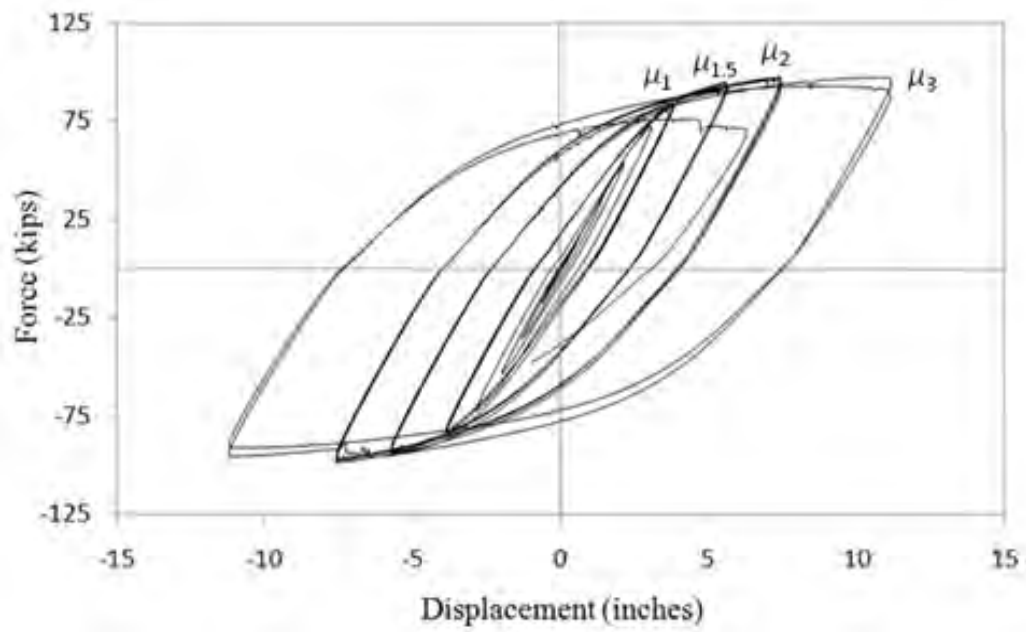


Figure 4.5 Test 5 Force Displacement Hysteresis

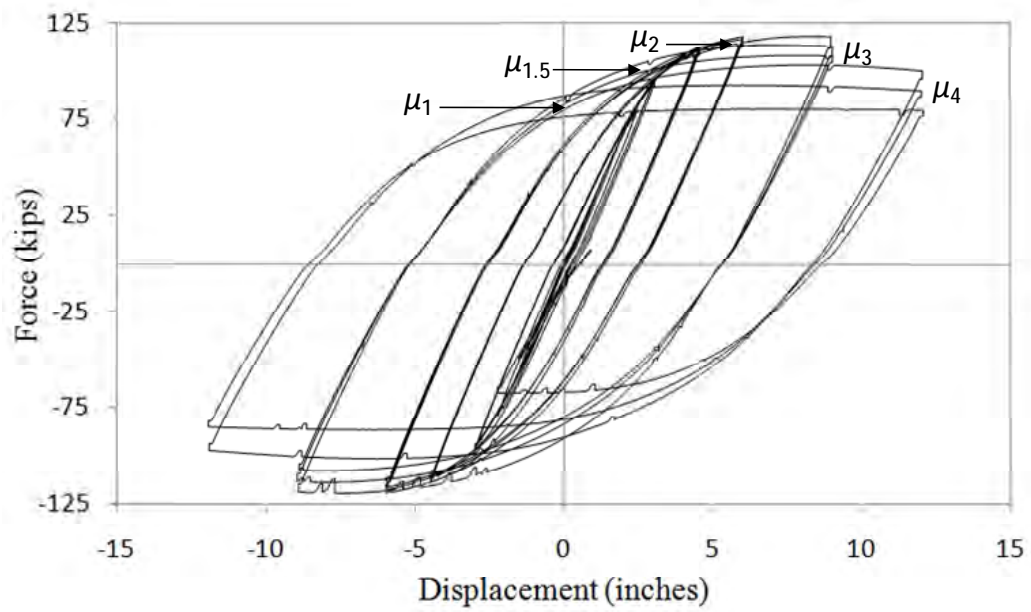


Figure 4.6 Test 6 Force Displacement Hysteresis

Table 4.1 Testing Results Summary

Test	Configuration	F_y (k)	Δ'_y (in)	Failure Ductility	Failure Cycle	Failure Description	Reliable Ductility	Equivalent Reliable Drift
1	3/4" Fillet ³	73.0	2.99 ¹	2	-1	South Column North-Mid Face Crack at Weld Toe in Base Metal	1	0.028
2	45° CJP w/ 3/4" Backer Fillet	73.0	2.49	4	2	South Column North Face Crack at Weld Toe In Base Metal	3	0.070
3	45° CJP	73.0	2.49 ²	3	1	Multiple Cracks in Both Columns at Weld Toe in Base Metal and Through Weld	1.5-2	0.035 - 0.047
4	45° CJP w/ 3/4" Backer Fillet	73.0	2.54	3	3	South Column South Face Crack at Weld Toe in Base Metal	2-3	0.049 - 0.072
5	45° CJP w/ 3/4" Backer Fillet Inside and Out w/ CJP Splice Butt Weld	73.0	2.84	3	3	South Column South Face Crack at Weld Toe in Base Metal	2-3	0.054 - 0.080
6	Flared Column Capital Assembly	79.7	2.33	4	3	South Column North Face Crack at Local Buckling Below Weld in Base Metal	4	0.088
1. Higher yield displacement in test 1 is partially due to support displacement.								
2. Due to loading error no yield displacement was captured for test 3. Test 2 data was used.								
3. Due to construction error the 3/4" fillet weld in test 1 was slightly undersized. The actual weld was approximately 5/8".								

4.2 Force Displacement Response Envelopes

As was mentioned in section 4.1, the connection configuration had very little effect on the force deformation response of the structure. The configuration did however have a significant effect on the ultimate displacement capability of the system. These two issues can be recognized by reviewing the force displacement envelopes provided in this section. These figures represent the envelope to the peak responses at $\frac{1}{4}$ yield, $\frac{1}{2}$ yield, $\frac{3}{4}$ yield, first yield, ductility 1, 1.5, 2, etc. This process has been conducted for each of the three cycles at each ductility level and the various tests have been plotted on the corresponding figures in order to form appropriate conclusions. It should be noted that tests 2 and 3 have been omitted due to the loading errors experienced during testing.

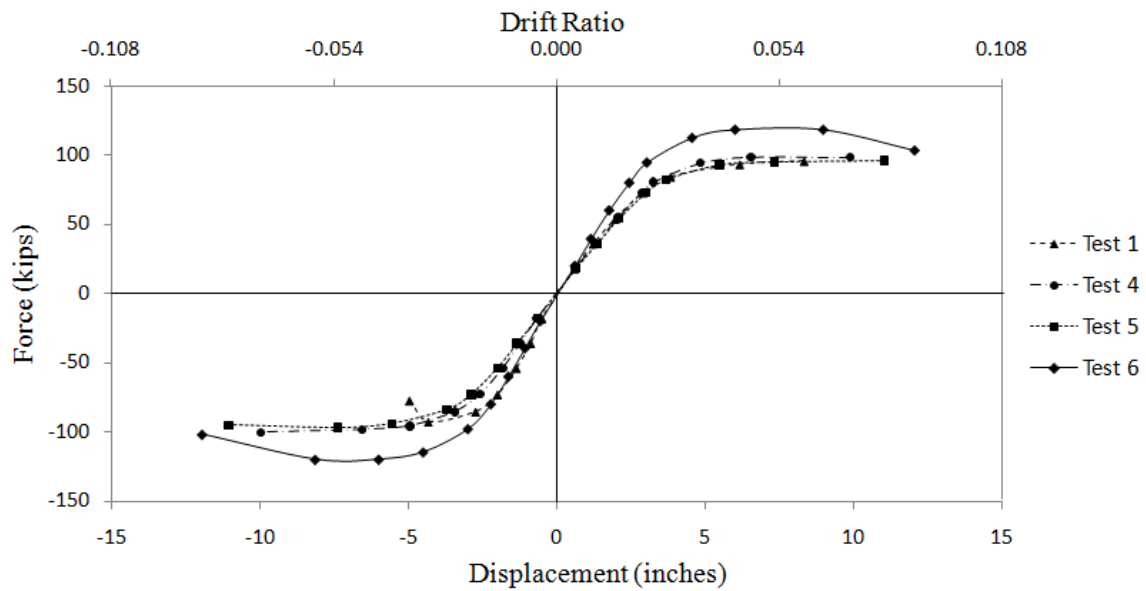


Figure 4.7 Cycle 1 Force Displacement Envelopes

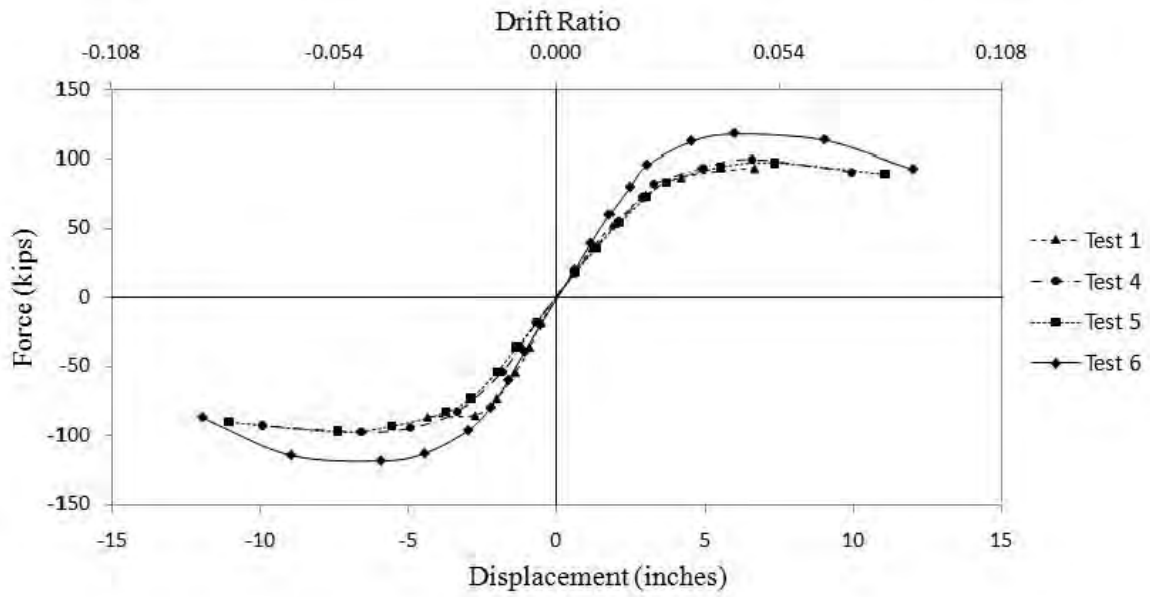


Figure 4.8 Cycle 2 Force Displacement Envelopes

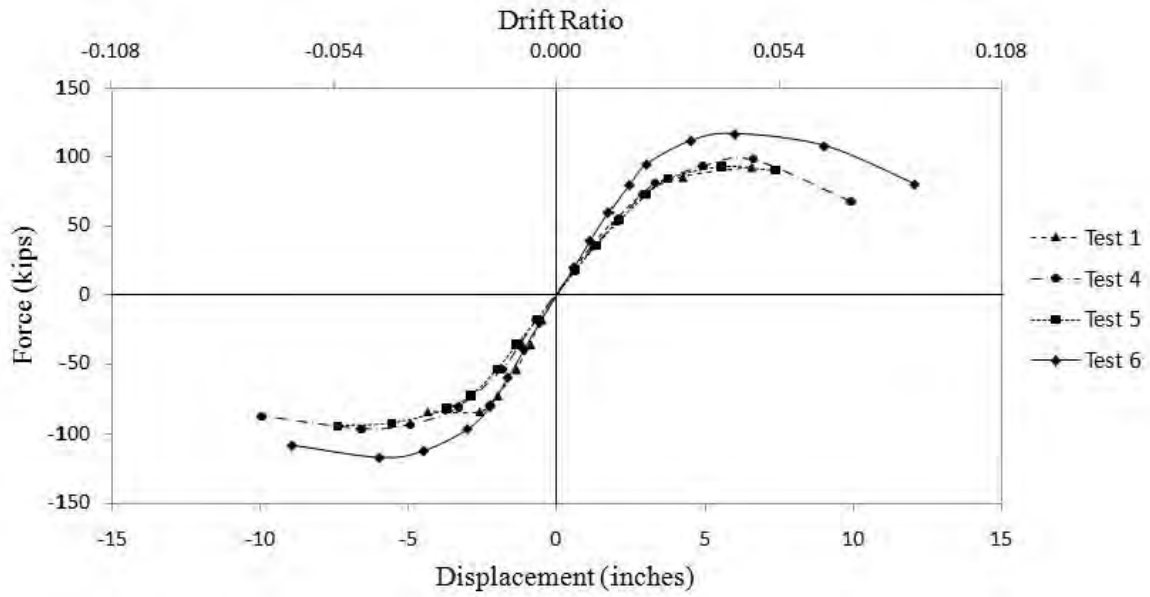


Figure 4.9 Cycle 3 Force Displacement Envelopes

It is not surprising that the envelopes of test 1, 4, and 5 match almost exactly in magnitude prior to their respective failures since the global systems were the same. It should be noted that in all tests prior to test 6, strength degradation occurred between cycles of the same ductility level rather than between cycles of different levels of ductility. Although it is not uncommon to observe some strength loss between cycles of the same ductility level, it is indicative of a rapid failure for significant strength degradation of a system to take place at a given ductility. This behavior can also be observed in the force displacement hysteresis provided in earlier in this Chapter.

4.3 Equivalent Viscous Damping Comparison

The equivalent viscous damping values for each ductility level of testing have been calculated in order to compare the structures inelastic damping capabilities with typical values. The method used to calculate the total equivalent viscous damping is based on a modified Jacobsen's approach (Jacobsen, 1930). Jacobsen's approach is based on an energy balance method which equates the area encompassed within a full force displacement cycle of a rigid perfectly plastic oscillator to the input energy from a sinusoidal forcing function. The outcome of this approach shows the total hysteretic damping ratio to be equal to $2/\pi$. It can also be shown that the total hysteretic damping of a non rigid-perfectly plastic response can be determined by scaling the value of $2/\pi$ by the ratio of the area contained in the realistic hysteric loop divided by the area contained in the rigid-perfectly plastic response as shown in Eq. 4.1 and Figure 4.10 (Priestley et al. 2007).

Since the loading history used to generate the actual response is not based on a sinusoidal forcing function as considered in Jacobsen's derivation, it is necessary to apply a modification factor as shown in Eq. 4.2 to avoid inappropriately large values of hysteretic damping (Montejo, 2008; Priestley et al. 2007). It is also necessary to apply a modification factor to the elastic viscous damping which was assumed to be 2% in these calculations to capture a conservative value for steel structures. This is necessary because typical values of elastic viscous damping are based on tangent stiffness while the hysteretic damping calculated by the Jacobsen approach is based on secant stiffness which is recommended for use with the DDBD approach (Priestley et al. 2007). The modification factor κ is a function of the ductility level and a variable λ which is equal to -

0.617 assuming a Ramberg-Osgood model for the ductile steel structure (Priestley et al. 2007). Both the loading history and tangent stiffness modification factors have been calibrated using non-linear time history analysis to match maximum response displacements with the DDBD approach. The values of total equivalent viscous damping obtained from the combination of corrected elastic viscous damping and corrected hysteretic damping as shown in Eq. 4.3 will be compared with the typical relationship for a steel frame provided in Eq. 4.4.

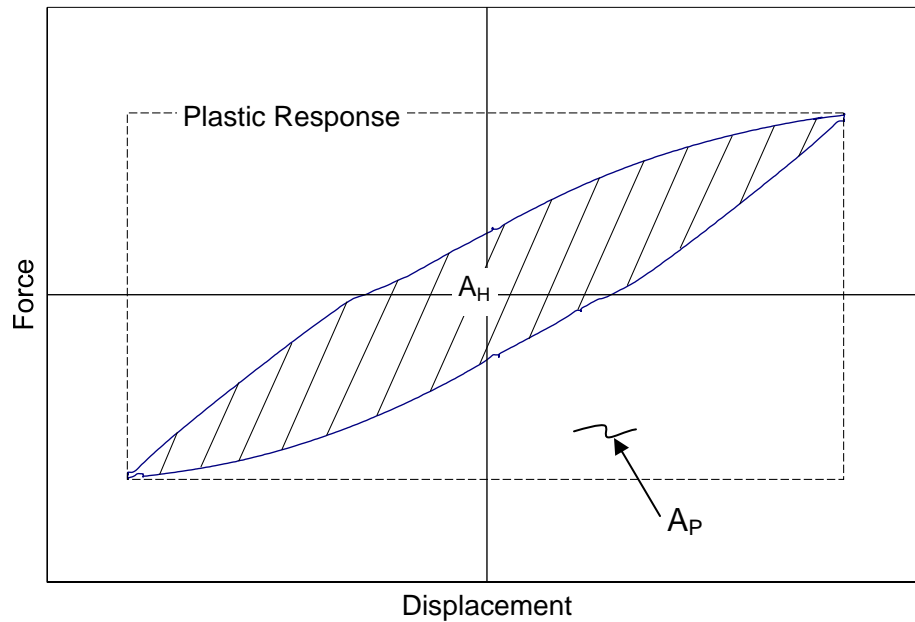


Figure 4.10 Relationship Between Hysteretic and Plastic Response

$$\xi_{\text{Jac}} = \left(\frac{2}{\pi} \right) \cdot \left(\frac{A_{\text{H}}}{A_{\text{P}}} \right) \quad \text{Eq. 4.1}$$

ξ_{Jac} = "Jacobsen's Approach Hysteretic Damping"

A_{H} = "Area of Hysteretic Loop"

A_{P} = "Area of Rigid-Perfectly Plastic Response"

$$\xi_{\text{hyst}} = \xi_{\text{Jac}} \cdot \left[(0.53\mu + 0.8) \left(\frac{\mu}{40} + 0.4 \right) \right] \quad \text{Eq. 4.2}$$

ξ_{hyst} = "Equivalent Hysteretic Damping"

μ = "Ductility Level Under Evaluation"

$$\xi_{\text{eq}} = \kappa \cdot \xi_{\text{eq}} + \xi_{\text{hyst}} \quad \text{Eq. 4.3}$$

ξ_{eq} = "Total Equivalent Viscous Damping"

$\kappa = \mu^\lambda$ = "Tangent Stiffness Elastic Damping Correction Factor"

λ = "Prescribed Modification Factor"

$$\xi_{\text{eq_typ}} = 0.05 + 0.577 \cdot \left(\frac{\mu - 1}{\mu \cdot \pi} \right) \quad \text{Eq. 4.4}$$

$\xi_{\text{eq_typ}}$ = "Typical Steel Fram Total Equivalent Viscous Damping"

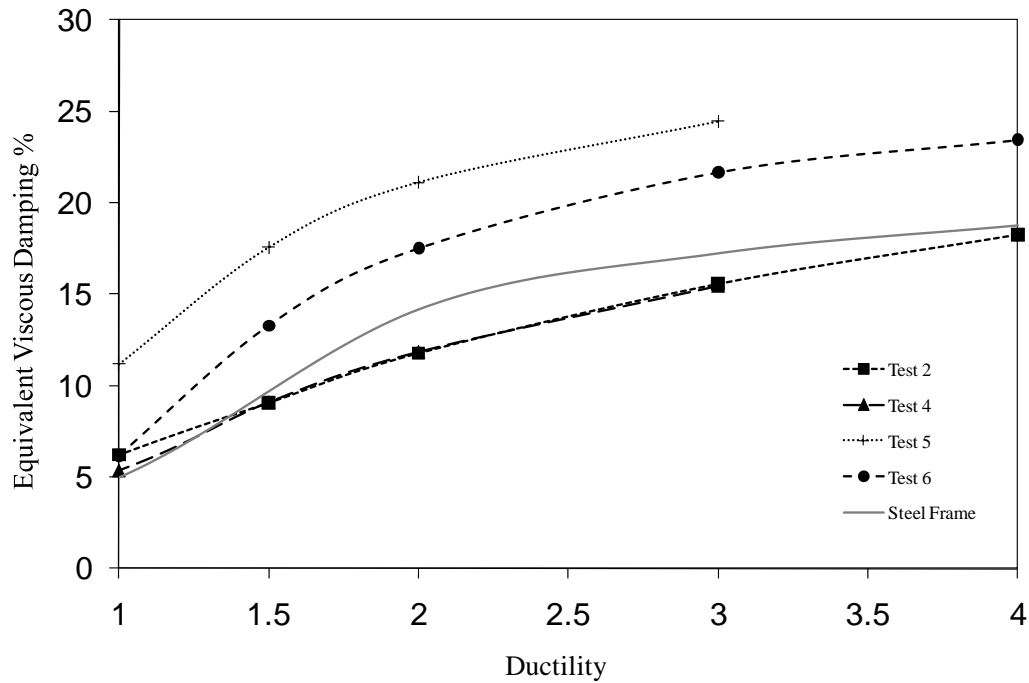


Figure 4.11 Damping Comparison

From Figure 4.11 it is clear that each of the tests follow the general trend of the steel frame recommendation. It is also clear that the test 6 specimen was able to dissipate a considerably larger amount of energy than that of the prior tests. Although it appears that the test 5 specimen was able to dissipate an unreasonably high amount of energy especially at the lower ductility levels the situation is explainable. As can be seen in Figure 4.12, the yield cycle used to establish the ductility level displacements for test 5 experienced a considerable amount of inelastic action compared to the yield cycle of test 6 which is more indicative of all prior tests. It should be noted that this was not due to any loading errors during testing. It is possible that the addition of the splice weld and the additional welding of the inside fillet in test 5 increased the heat zone effects and softened the specimen to some degree. Regardless of the cause, the amount of inelastic action seen during this cycle likely caused the ductility level displacements to be slightly over calculated. As a result, the calculated values of total equivalent viscous damping would also be high. This effect would be even more significant at lower levels of ductility where the modification factor for hysteric damping is much larger (0.886 for ductility 1) as compared to higher levels of ductility (0.661 for ductility 3). Taking this into account, should the damping curve for test 5 be shifted to the right by a value of approximately $\frac{1}{2}$

of a ductility level, the calculated values of damping would be much more reasonable. It is important to note that this possible over calculation of ductility level displacements in test 5 has no significant effects on the general conclusions about the specimen's response. It is only important in the case of damping due to the fact that the modified Jacobsen's approach is very sensitive to hysteretic energy dissipation.

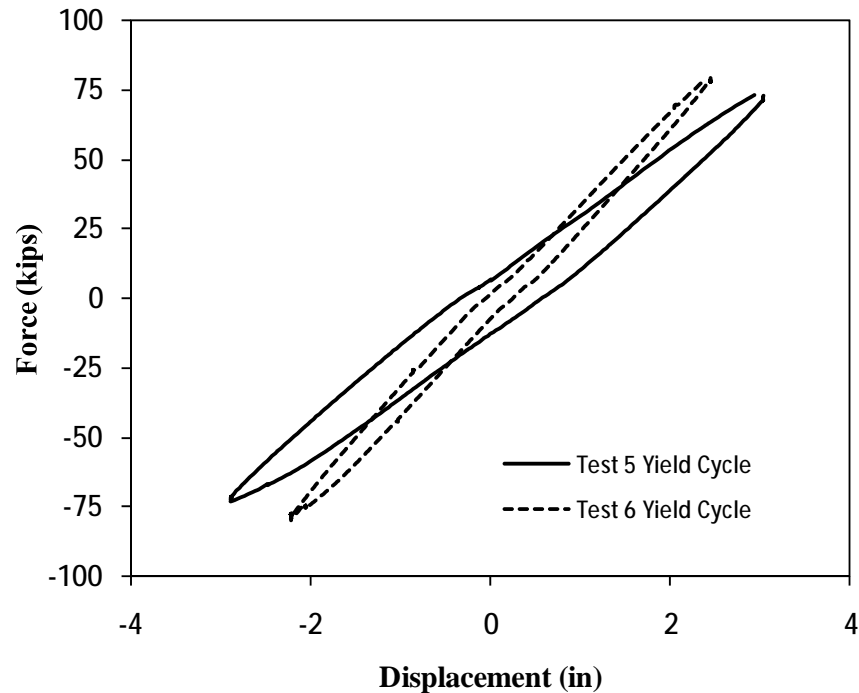


Figure 4.12 Yield Cycle Comparison

4.4 Selected Strain Topics

4.4.1 General Introduction to Strain Considerations

As was discussed in earlier sections, two main strain measurement devices were used during testing for all six specimens. These two methods consisted of traditional strain gauges and the Optotrak system. In each test, multiple strain gauges were placed in the longitudinal direction on the extreme fibers of both columns. These gauges will

generally be referred to by the face of the column they were applied to and their distance below the cap beam. For example, N-N-3 would reference a strain gauge on the north face of the north column three inches below the cap beam. A small number of gauges were also placed in other locations throughout the testing series to monitor local deformation such as the elastic actions of the cap beam flanges. These will similarly be referred to by their respective location when necessary.

Optotrak markers or LEDs were placed in the critical region of the south column and varied in number between tests but not in general layout. Post processing of the data provided from the marker locations throughout the tests allowed for the calculation of average strain between any two markers. The calculations were of course conducted between successive markers to minimize gauge length and maximize the accuracy of the average strain value. Optotrak markers were not only placed on the extreme fibers of the pile but also on the radial quarter points and the centerline, as can be seen in Figure 4.13. This layout allowed for strain cross section profiles to be generated at various heights along the columns as well vertical strain profiles to be plotted for either extreme fiber.

4.4.2 Validation of Optotrak Capabilities

Given that the Optotrak system was relatively new technology to our research group during this testing series, it was necessary to validate the reliability of the system. To achieve this objective, traditional strain gauges were placed within many of the LED gauge lengths and the resulting strain histories were compared. As can be seen in Figure 4.14, Figure 4.15, and Figure 4.16 the Optotrak data proved to be very reliable by matching the traditional strain gauge readings well.

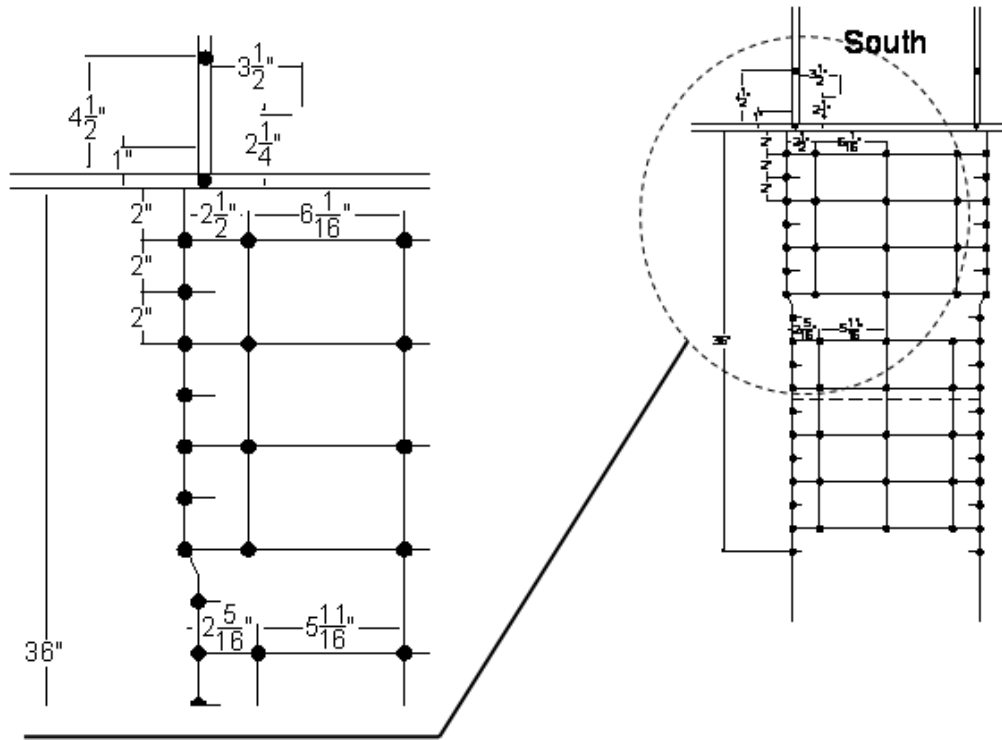


Figure 4.13 Example Optotrak Marker Grid

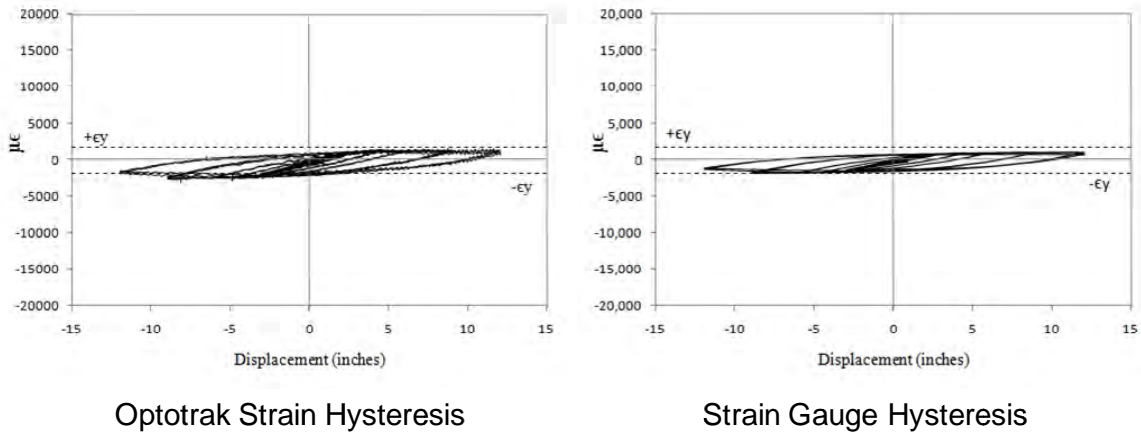


Figure 4.14 Strain Comparison (S-S-3'', Test 6)

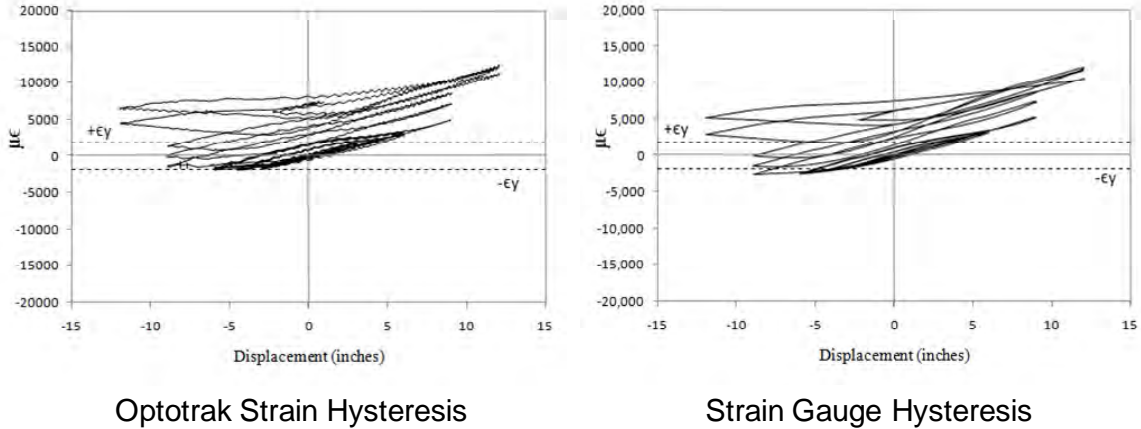


Figure 4.15 Strain Comparison (S-S-19", Test 6)

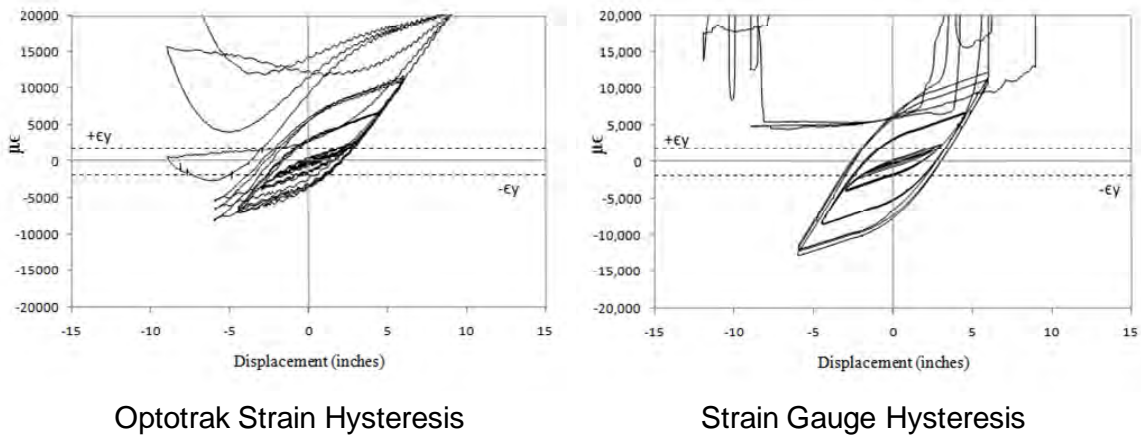


Figure 4.16 Strain Comparison (S-S-25", Test 6)

It should be noted these comparisons have been provided as examples of typical behavior not as the best relationships. This type of similarity was seen throughout the analysis of the test data and has led to confidence in the system. Similarity between the two systems can also be noted throughout various figures provided in support of other conclusions throughout the remainder of this report.

It is also worth noting from Figure 4.13 that the Optotrak system is adept at recording strains beyond the point where conventional electrical resistance strain gages

fail. As can be seen the strains at a location 25 inches down the south column reached a value of approximately 20000 $\mu\epsilon$ prior to buckling, which was accurately captured by the Optotrak while the conventional strain gauge failed at approximately 10000 $\mu\epsilon$. This is an important attribute for the system in that it allows for the measure of very large strains that would not otherwise be assessed with traditional techniques. This in turn allows identification of the occurrence of key performance limit states.

4.4.3 Strain Issues Relating to Local Buckling

The primary method for evaluation of local buckling, a possible limit state for these structures, utilizes Optotrak produced strain measurements to plot horizontal strain cross sections. The grid system used for the layout of Optotrak markers allows for strain measurements to be calculated at both extreme fibers, the radial quarter points, and the centerline of the pile at the same vertical location. Plotting the calculated strains versus their respective horizontal position on the pile produces a cross sectional strain profile.

During data analysis it was noticed by the research team that the strain diagrams at locations of known local buckling did not remain linear after the buckling had taken place and therefore the common bending theory assumption that plane sections remain plane was no longer true as is shown in Figure 4.17 and Figure 4.18. It was further noticed that the non-linearity of the strain diagrams began before visual signs of local buckling indicating that the onset of local buckling takes place before visual signs develop. This information was in turn used to qualitatively evaluate the relationship between buckling and strength degradation as is shown in Chapter 6. Conversely, at lower levels of response, the Optotrak data supports the assumptions of plane sections remaining plan after bending, first sketched by Robert Hooke in 1678.

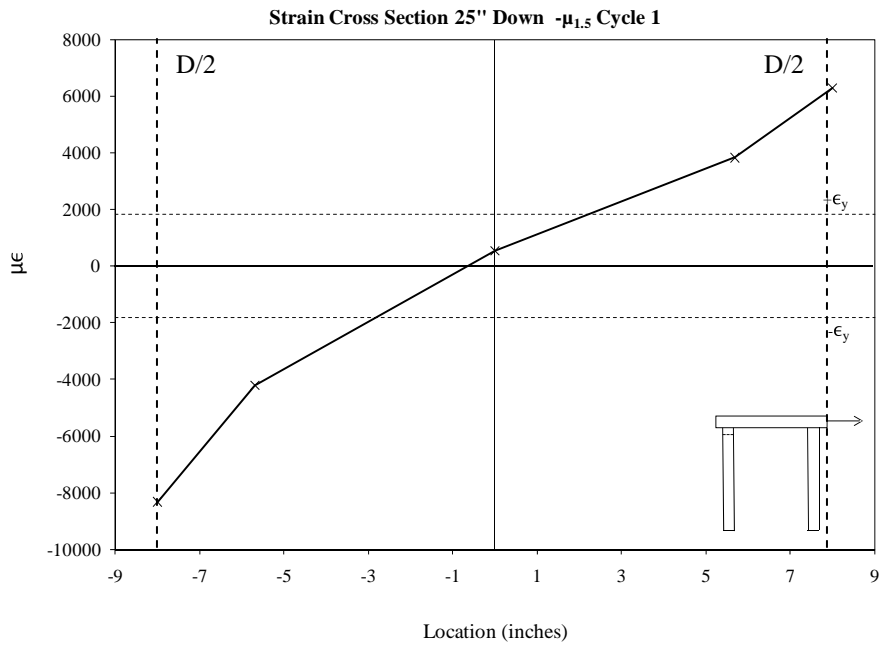


Figure 4.17 Example Strain Cross Section Prior to Local Buckling

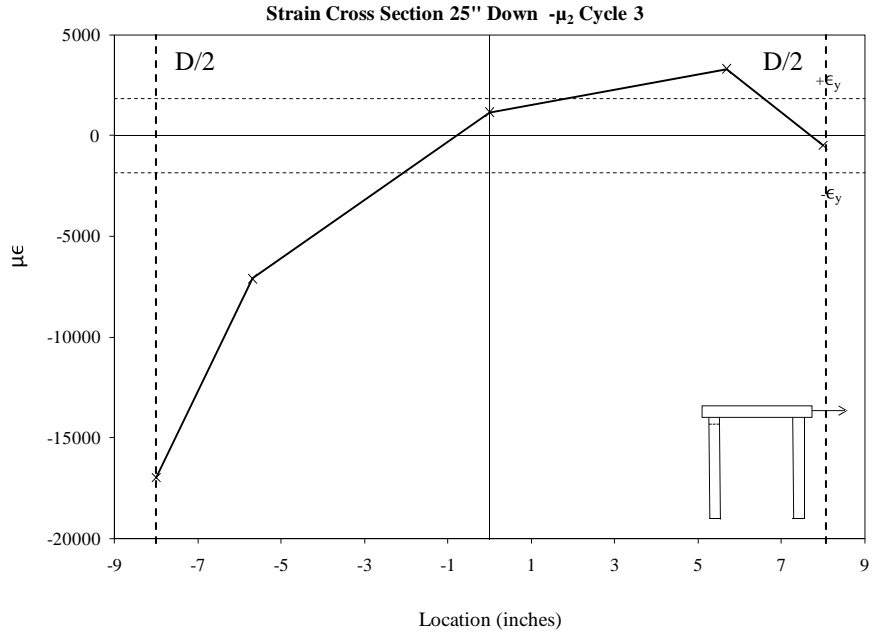


Figure 4.18 Example Strain Cross Section Following Local Buckling

As can be seen in Figure 4.19 the ability of Optotrak to function at significantly higher strains than can be handled by traditional strain gauges allowed for this data to be captured. It should be noted though, after significant propagation of local buckling the strains calculated are no longer indicative of flexural engineering strains. As shown in Figure 4.19, the compressive strains near the location of local buckling in test 6 reached values as large as 200000 $\mu\epsilon$. This is absurdly large and simply indicates that buckling has occurred and plane sections no longer remain plane. However, the data is still valuable to describe the transformed shape of the cross section allowing for the linearity of the strain diagram to describe the propagation of local buckling. It should also be noted that at the early stages of local buckling (prior to visual signs) the calculated strains are likely still indicative of flexural engineering strains.

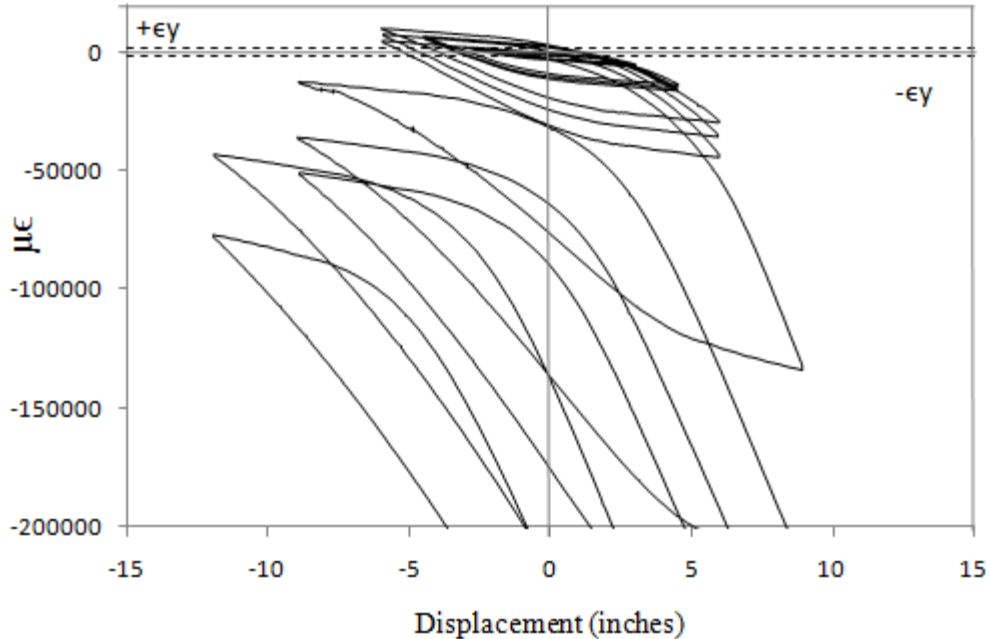


Figure 4.19 Strain Hysteresis Test 6 at S-S-29

Attempts have been made to produce a more quantitative evaluation of local buckling. These attempts include methods related to the rapid change in lateral movement of the LED markers as well evaluation of radial hoop strain or ovalization changes. Although these methods are theoretically correct, they require a set of LED markers to be directly located at the location of local buckling for the necessary data to be captured.

Coincidentally, buckling observed in this testing series (generally only the buckling in test 6 was considered since it was the only test with a buckling related failure) occurred between LED markers. In future tests, it would likely be beneficial to include LED markers at the closest interval possible in order to capture the data necessary for these alternate methods of buckling analysis. It should be noted that the original intent of the Optotrak system was primarily for strain calculations and the ability to evaluate local buckling with the data by any method should be considered complimentary to the original intent. However, this unintended ability depicts very well the versatility of the system.

4.4.4 Curvature and Plastic Hinge Length

As was mentioned earlier in this report, it is possible to calculate cross section curvature utilizing the Optotrak grid by simply dividing the total difference between extreme fiber strains by the diameter of the cross section. It was attempted to utilize the testing data to calibrate a plastic hinge length for the specimens tested. This data could then be utilized in the basic plastic hinge method of calculating structural displacement in the inelastic range. This method essentially simplifies a non-linear curvature profile, which is experienced in the inelastic range, by representing the actual profile with a linear elastic component and a rectangular plastic component with a length equal to the plastic hinge length as can be seen in Figure 4.20. This simplified diagram can then be utilized to calculate structural deformation by the second moment area method.

In design, a plastic hinge length is assumed or calculated using an appropriate relationship allowing total structural deformation to then be calculated using Eq. 4.5. For this research project, structural deformation is known along with all other parameters of the relationship with exception of the plastic hinge length (L_p). The relationship can simply be rearranged to solve for L_p using testing data. The results of this analysis which are presented in Table 4.2 and Table 4.3 indicate that the calculated plastic hinge length follows no particular pattern. This is largely due to the numerous modes of deformation taking place during testing. This method of calculating plastic hinge length is essentially attempting to capture all modes of deformation and represent the effect within an artificial pile plastic hinge length. Unfortunately, the results indicate that this attempt was not successful and it is the view of the research team that the use of the plastic hinge method is not recommended for calculating displacements in regards to this type of structure.

Although this attempt to calibrate the plastic hinge method was not successful, it may be possible to appropriately calibrate the method for response prior to local buckling

if single column tests were conducted for analysis. However, this presents two key problems. First, in actual design all modes of deformation should be accounted for such as the cap beam flexibility. Secondly, designers will likely utilize this type of structures capabilities past the onset of local buckling when designing for the maximum considered earthquake. These items again support that the plastic hinge method is likely not the best option for design of steel bridge bents.

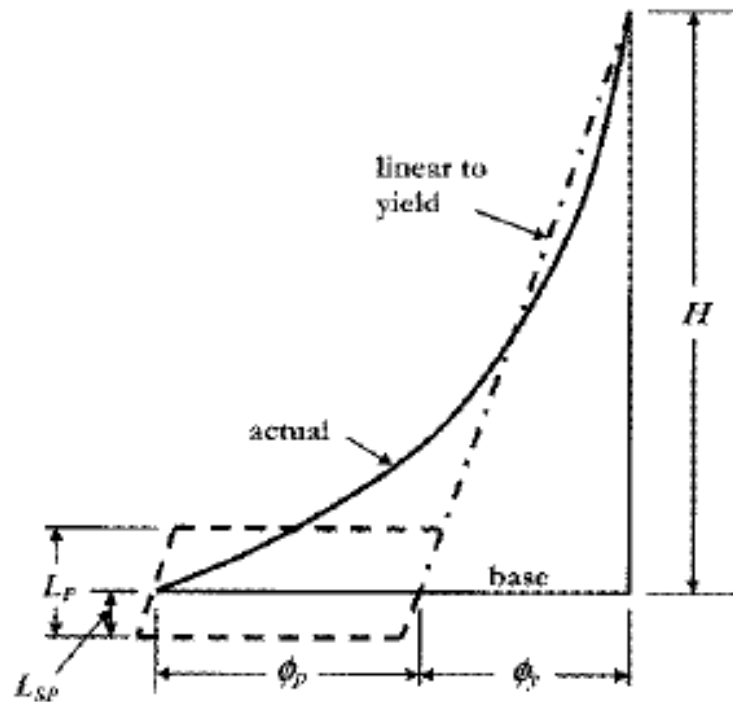


Figure 4.20 Plastic Hinge Idealization of Non-Linear Curvature Distribution
(Priestley, et. al. 2007)

$$\Delta_u = \Delta_y + (\phi_u - \phi_y) \cdot L_p \cdot H \quad \text{Eq. 4.5}$$

Table 4.2 Detailed Test 6 Lp Calculations

Test Six Lp Calculations					
Ductility	1.5	-1.5	2	-2	L (in) = 131.16
Δ'_y (in)	2.2	2.2	2.2	2.2	Measured
Δ_y (in)	3	-3	3	-3	Measured - Extrapolated
Φ'_y (1/in)	0.000310	-0.000327	0.000310	-0.000327	Measured
Φ_y (1/in)	0.000515	-0.000563	0.000515	-0.000563	Measured
Φ_{max} (1/in)	0.001423	-0.001090	0.003555	-0.003770	Measured
Φ_p (1/in)	0.000908	-0.000527	0.003040	-0.003208	$\Phi_{max} - \Phi_y$
Δ_p (in)	1.5	-1.5	3	-3	$\Delta_y * (\mu - 1)$
Lp (in)	12.60	21.69	7.52	7.13	$\Delta_p / (\Phi_p * L)$

Table 4.3 Selected Lp Results

Test	Ductility Level			
	1.5	-1.5	2	-2
1	13.0 in	37.3 in	N/A	N/A
2	12.5 in	11.8 in	11.1 in	13.0 in
4	19.5 in	14.4 in	16.2 in	15.4 in

DDBD Analysis and Drift Considerations

5.1 Introduction to DDBD Analysis of Hollow Steel Pile Bents

It has been the goal of this research study to determine (and improve) the reliable displacement ductility of the steel bent structures under consideration. Using the information found from testing it is possible to conduct a simple Direct Displacement Based Design (DDBD) analysis of the structure to determine the minimum seismic hazard to either require explicit design of the lateral force resisting system or more practically to develop the full strength of the system. It is envisioned by the research team that these tools may be of particular use to AKDOT as a quick assessment tool of existing structures or even as a design aid for new structures

The development of these analysis tools is based on first principles and remains fairly generalized. As a result, the application of these relationships is valid for any circular HSS pile bent regardless of number of piles, height, aspect ratio, D/t ratio, and material type. The relationships also allow for user specified levels of total equivalent viscous damping and ductility capacity. This allows for issues such as radiant soil damping to be taken into account should the user care to do so. Although much of the formulation is based on recommendations provided in “Displacement-Based Seismic Design of Structures” (Priestley, et. al., 2007), parameters such as damping reduction factors could easily be altered to match applicable codes or other recommendations as necessary. Similar relationships could be developed for any steel pile section bent about a symmetric axis with only slight modification to the relationship provided for circular sections.

However, it should be noted that multiple assumptions have been made in regards to the system response. First, the displacement is based solely on pile flexural displacement. Secondly, the calculation of target displacement is based on reliable ductility where the yield displacement is calculated in regards to a simplified moment distribution. As is shown in Figure 5.1 the moment distribution assumed within these calculations is that of a double bending moment frame with a total pile length extending to

the in ground hinge where the moment is assumed equal to the moment that exists at the top of pile. This is a simplification of the actual moment distribution that would become non-linear below grade due to the non-linear spring characteristics of the resisting soil. In addition, the maximum in ground moment is likely less than that of the top moment as has been shown in prior research (Suarez, Kowalsky, 2007). Regardless of these assumptions, the purpose of this chapter is to illustrate how simple direct displacement-based design procedures can be used to develop a rapid assessment tool and to obtain general estimates of the seismic hazard necessary to exhaust the capabilities of the systems tested in this research. Should more accurate results be desired, the relationships can be revised to directly consider a reliable drift or displacement (determined by the engineer's method of choice) as is discussed later in this chapter.

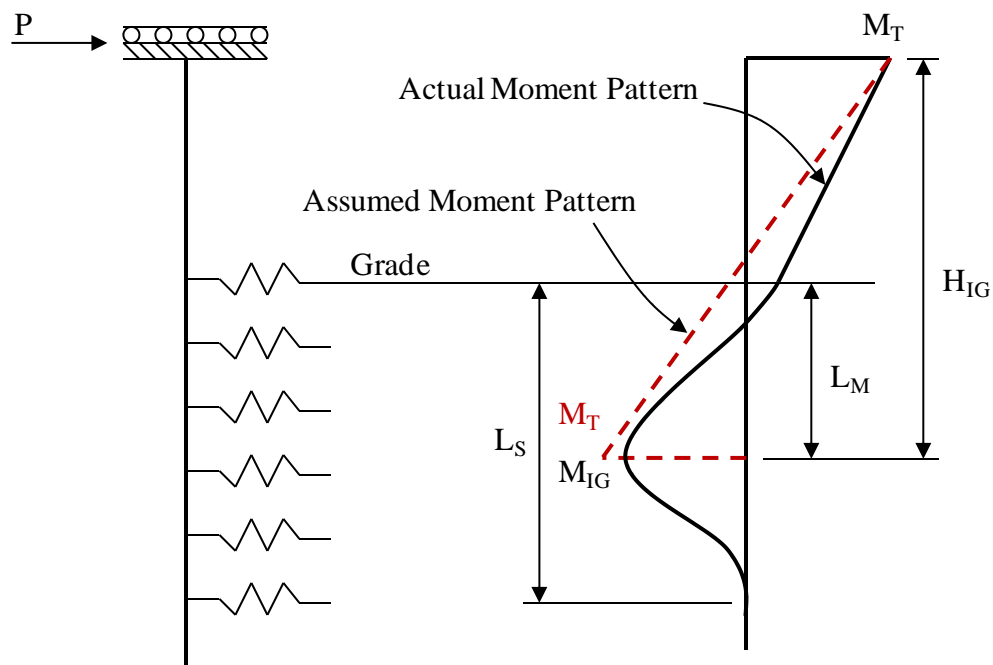


Figure 5.1 Actual vs. Assumed Pile Moment Pattern

5.2 Development of DDBD Analysis Tools

5.2.1 Minimum Hazard to Require Explicit Lateral Strength Design

It may be of interest to the AKDOT to determine the minimum seismic hazard, based on the mapped 1 second design spectral acceleration value (S_{D1}), to require explicit lateral strength consideration for a given steel bent bridge. Included in this section is the development of a simple relationship (Eqs 5.1-5.6) between target displacement (Δ_T), structural characteristics, mapped corner point period (T_C), and the minimum S_{D1} value desired. As noted earlier, the relationship provided is based on first principles but also utilizes the design response acceleration spectrum provided by ASCE7-05 and damping reduction factors provided by EuroCode 2003. The general approach used to develop the relationship equates target displacement to the corner point spectral displacement (Δ_C) and back solves for the minimum S_{D1} value to require explicit lateral strength design. Simply stated, a S_{D1} value less than that generated by the relationship provided will create a maximum spectral displacement less than that of the structural yield displacement.

$$\phi_y = \frac{2(SF) \cdot \epsilon_y}{D} \quad \text{Eq. 5.1}$$

SF = "Section Shape Factor"

$$\Delta_y = \frac{\phi_y \cdot L^2}{6} = \frac{(SF) \cdot \epsilon_y \cdot L^2}{D \cdot 3} \quad \text{Eq. 5.2}$$

$$\Delta_T = \mu \cdot \Delta_y = \frac{\mu \cdot (SF) \cdot \epsilon_y \cdot L^2}{D \cdot 3} \quad \text{Eq. 5.3}$$

$$\Delta_c = \frac{S_{ac}}{\omega^2} \cdot \left(\frac{7}{2 + \xi} \right)^\alpha = \frac{S_{D1}}{T_c} \cdot \left(\frac{T_c^2}{4 \cdot \pi^2} \right) \cdot \left(\frac{7}{2 + \xi} \right)^\alpha = \frac{S_{D1} \cdot T_c}{4 \cdot \pi^2} \cdot \left(\frac{7}{2 + \xi} \right)^\alpha \quad \text{Eq. 5.4}$$

α = "0.5 for Farfield Event or 0.25 for Nearfield Event"

$$\Delta_T = \Delta_c \quad \text{Eq. 5.5}$$

$$S_{D1} = \frac{\mu \cdot (SF) \cdot \epsilon_y \cdot L^2 \cdot 4 \cdot \pi^2}{3 \cdot D \cdot T_c} \cdot \left(\frac{7}{2 + \xi} \right)^{-\alpha} \quad \text{Eq. 5.6}$$

As an example, this analysis tool has been used to evaluate the capabilities of the bents tested in this research project. For this example the reliable ductility levels and corresponding equivalent viscous damping ratios determined from the results of testing of each individual specimen have been used. In the case of test 2 and 4 which consisted of the same connection detail, different results have been provided since the actual specimens performed in different manners likely due to the natural variability that exists within construction tolerances. From a design standpoint it would be advantageous to consider test 4 as a lower bound response from the results of the two tests of a CJP weld with a reinforcing fillet. Similarly from a design standpoint it may be advantageous to conservatively consider test 6 as reliable ductility of 3 or 3.5. Although these results have not been provided, Eq. 5.6 is directly proportional to change in ductility. Results can therefore be linearly extrapolated in regards to ductility.

Pile length (L) was assumed to be 20 feet as the point of inflection was modeled at 10 feet during testing. Table 5.1 provides the results of the analysis for a far field event. Thus $\alpha = 0.5$. It is also possible to use the relationship to produce a graphical solution with regards to a given corner point period, event type, and aspect ratio. However as can be seen in Figure 5.2, which provides the graphical solution for a 12 second corner point period far field event, this type of solution is somewhat restrictive and would require a large number of graphs to cover a likely range of structural configurations.

Table 5.1 Minimum S_{D1} to Require Explicit Lateral Strength Design

Test	Configuration	Reliable Ductility	ξ_{eq} (%)	Minimum S_{D1} to Require Explicit Lateral Strength Design (g)		
				$T_c=6\text{sec}$	$T_c=12\text{sec}$	$T_c=16\text{sec}$
1	3/4" Fillet	1	5.0*	0.050	0.025	0.019
2	45° CJP w/ 3/4" Backer Fillet	3	15.6	0.237	0.119	0.089
3	45° CJP	1.5	11.5*	0.104	0.052	0.039
4	45° CJP w/ 3/4" Backer Fillet	2	11.8	0.140	0.070	0.052
5	45° CJP w/ 3/4" Backer Fillet Inside and Out w/ CJP Splice Butt Weld	2	14.2**	0.152	0.076	0.057
6	Flared Column Capital Assembly	4	23.5	0.381	0.190	0.143

* Recommended Steel Frame Value Used Due to Lack of Data

** Recommended Steel Frame Value Used Due to Unreasonably High Calculated Value

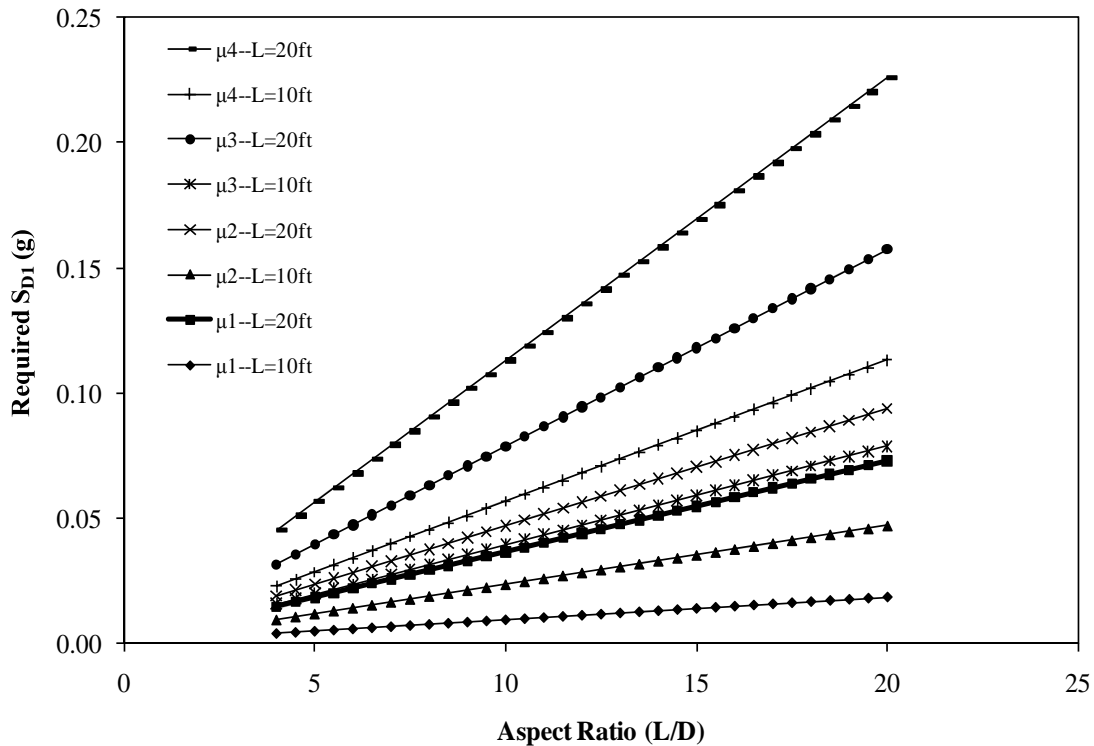


Figure 5.2 Minimum S_{D1} to Require Explicit Lateral Strength Design ($T_c=12\text{s}$)

It can be seen from Figure 5.2 that a linear relationship exists between the aspect ratio and minimum seismic hazard for a given ductility level, length of pile, and corner point period. As may seem logical for the purpose of Displacement Based Design, the minimum hazard to require explicit lateral strength design increases proportionally to aspect ratio and is relatively sensitive to the magnitude of corner point period. This can be seen by comparing Figure 5.2 and Figure 5.3 Minimum S_{D1} to Require Explicit Lateral Strength Design ($T_c=6s$) which display the results for 12 and 6 second corner points, respectively. It should be noted that a typical steel frame damping ductility relationship ($\xi_{eq}=0.05+0.577[[\mu-1]/[\mu\pi]]$) as recommended in “Displacement-Based Seismic Design of Structures” (Priestly, et. al.) was used in the generation of the graphs.

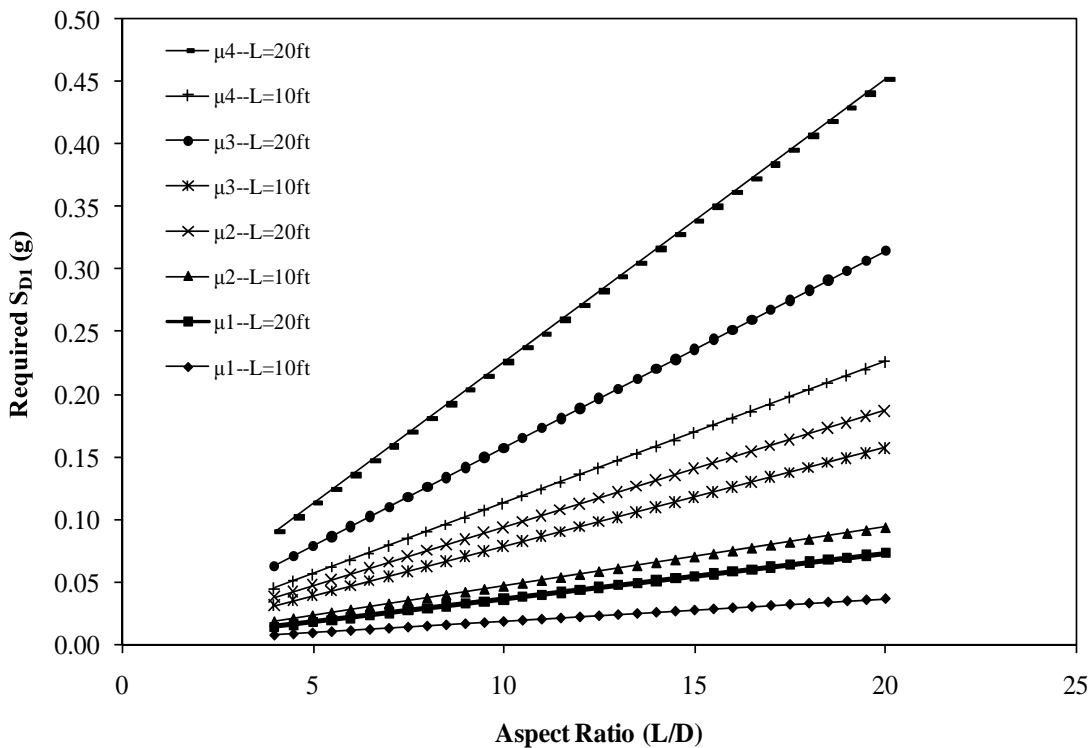


Figure 5.3 Minimum S_{D1} to Require Explicit Lateral Strength Design ($T_c=6s$)

In general, the minimum seismic hazard as discussed in this section is relatively low for normal structures. As can be seen in Table 5.1 the best response (test 6) still requires only a 0.381g S_{D1} value for the shortest considered corner point period (6

seconds). This is a fairly low value and generally indicates that explicit seismic design for lateral strength is going to be necessary. Nonetheless, it is felt that the relationship provided is still valuable to determine areas in which explicit seismic design is not necessary for a given structures regardless of the inherently low values of seismicity that will be present.

5.2.2 Required Hazard to Develop the Full Lateral Strength of the System

Although the minimum hazard to require explicit lateral strength consideration may be pertinent information, it will likely be far more useful to determine the required hazard (mapped S_{D1} value) to develop the full strength of the column sections. As in the prior section, this relationship can be developed utilizing first principles, a design response spectrum provided by ASCE7-05, and damping reduction factors provided in EuroCode 2003. In general the approach calculates a required moment of inertia (which is actually already known from the given dimensions) and back solves for the required S_{D1} value. The relationship is dependent on several parameters including structural configuration, material type, and anticipated performance. Again emphasis was placed on maintaining generality within the approach. However, the relationship provided has been specialized for circular HSS piles. As can be seen in Eq. 5.7-5.14, which provide the development of the analysis tool, minor changes would allow the relationship to be valid for any steel pile section bent about a symmetrical axis.

$$V_b = \frac{4 \cdot \pi^2 \cdot m}{T_c^2} \cdot \frac{\Delta_c^2}{\Delta_T} \cdot \left(\frac{7}{2 + \xi} \right)^{2 \cdot \alpha} = \frac{4 \cdot \pi^2 \cdot m}{\Delta_T} \cdot \frac{1}{T_c^2} \cdot \left(\frac{S_{D1} \cdot T_c}{4 \cdot \pi^2} \right)^2 \cdot \left(\frac{7}{2 + \xi} \right)^{2 \cdot \alpha} \quad \text{Eq. 5.7}$$

$$V_b = \frac{4 \cdot \pi^2 \cdot m}{\Delta_T} \cdot \left(\frac{S_{D1}}{4 \cdot \pi^2} \right)^2 \cdot \left(\frac{7}{2 + \xi} \right)^{2 \cdot \alpha} = \frac{S_{D1}^2 \cdot m}{\Delta_T \cdot 4 \cdot \pi^2} \cdot \left(\frac{7}{2 + \xi} \right)^{2 \cdot \alpha} \quad \text{Eq. 5.8}$$

$$V_b = \left[\frac{D \cdot 3}{\mu \cdot (SF) \cdot \epsilon_y \cdot L^2} \right] \cdot \frac{S_{D1}^2 \cdot m}{4 \cdot \pi^2} \cdot \left(\frac{7}{2 + \xi} \right)^{2 \cdot \alpha} = \frac{3 \cdot D \cdot S_{D1}^2 \cdot m}{\mu \cdot (SF) \cdot \epsilon_y \cdot L^2 \cdot \pi^2} \cdot \left(\frac{7}{2 + \xi} \right)^{2 \cdot \alpha} \quad \text{Eq. 5.9}$$

$$M = \frac{V_b}{P} \cdot \left(\frac{L}{2}\right) = \frac{3 \cdot D \cdot S_{D1}^2 \cdot m}{2\mu \cdot (SF) \cdot \epsilon_y \cdot L \cdot \pi^2 \cdot P} \cdot \left(\frac{7}{2 + \xi}\right)^{2 \cdot \alpha} \quad \text{Eq. 5.10}$$

P = "Total Number of Piles"

$$I = \frac{M \cdot D}{(SF) \cdot f_y \cdot 2} = \frac{3 \cdot D^2 \cdot S_{D1}^2 \cdot m}{4\mu \cdot (SF)^2 \cdot \epsilon_y \cdot L \cdot \pi^2 \cdot P} \cdot \left(\frac{7}{2 + \xi}\right)^{2 \cdot \alpha} \quad \text{Eq. 5.11}$$

$$S_{D1}^2 = \frac{4\mu \cdot (SF)^2 \cdot \epsilon_y \cdot L \cdot \pi^2 \cdot P \cdot I}{3 \cdot D^2 \cdot m} \cdot \left(\frac{7}{2 + \xi}\right)^{-2 \cdot \alpha} \quad \text{Eq. 5.12}$$

$$I = \frac{\pi}{64} \cdot [D^4 - (D - 2 \cdot t)^4] \quad \text{Eq. 5.13}$$

$$S_{D1} = \sqrt{\frac{\mu \cdot (SF)^2 \cdot \epsilon_y \cdot L \cdot \pi^3 \cdot P \cdot [D^4 - (D - 2 \cdot t)^4]}{48 \cdot D^2 \cdot m}} \cdot \left(\frac{7}{2 + \xi}\right)^{-2 \cdot \alpha} \quad \text{Eq. 5.14}$$

As was done for the minimum hazard to require explicit lateral design, the test structures from this series have been analyzed using the relationship provided in Eq. 5.13. Again a total pile length of 20 feet was assumed and in this case a random inertial weight of 150 kips was considered. The results of the analysis for a far field event have been provided in Table 5.2 Required SD1 to Develop Column Flexural Strength. It should be noted that the relationship for required SD1 is independent of corner point period due to the configuration of the design response spectrum utilized. The results of the analysis indicate that for this moderate level of inertial weight, the capabilities of the various systems may be adequate for some seismic regions. As would be expected, the results of the analysis are concurrent with the general conclusions for the testing series with respect to structural configuration. The capabilities of the plane fillet weld (test 1) are clearly low and would only be reliable in significantly low seismic regions. Although test 2 shows a reasonable level of capabilities subsequent tests (3, 4 and 5) were not able to replicate this

with weld configurations alone. Alternatively, test 6 is capable of producing adequate response in a moderately high seismic region. Although a reliable ductility of 4 may seem low, this is a parameter that has been normalized to yield displacement and ultimately the capabilities of the system are related to overall deformation capacity. This issue is discussed in further detail in subsequent sections. It should be noted that these results can be extrapolated for other inertial weights by a factor inversely proportional to the square root of the difference (i.e. $(0.5)^{-1/2}$) for and inertial weight of 75 kips). Further interpretation of the relationship between various parameters and required hazard is discussed in the remainder of this section.

Table 5.2 Required SD1 to Develop Column Flexural Strength

Test	Configuration	Reliable Ductility	ξ_{eq} (%)	Minimum SD1 to Develop Full Flexural Strength of the Bent (g)
1	3/4" Fillet	1	5.0*	0.449
2	45° CJP w/ 3/4" Backer Fillet	3	15.6	1.232
3	45° CJP	1.5	11.5*	0.763
4	45° CJP w/ 3/4" Backer Fillet	2	11.8	0.891
5	45° CJP w/ 3/4" Backer Fillet Inside and Out w/ CJP Splice Butt Weld	2	14.2**	0.965
6	Flared Column Capital Assembly	4	23.5	1.712

* Recommended Steel Frame Value Used Due to Lack of Data

** Recommended Steel Frame Value Used Due to Unreasonably High Calculated Value

It is possible to create graphical solutions for the relationship as was done in the prior section by controlling D/t , inertial weight and number of piles. However, it can again be seen in Figure 5.4 and Figure 5.5 that the graphical solutions are very restrictive and would require a large number of graphs to cover a reasonable range of structural configurations. Regardless of this, the graphical solution can be helpful to identify trends between the required seismic hazard and various parameters such as inertial weight. It can be seen from Eq. 5.13 and the provided figures that the relationship between required

hazard (S_{D1}) and structural parameters is generally either proportional or inversely proportional to the square root of the change in variable. This is clear from the non-linearity between required hazard and aspect ratio as well as the non-linear increases between ductility levels. Although from comparison of Figure 5.4 and Figure 5.5 it may appear that a linear relationship exists between required hazard and either number of piles or inertial weight this is not a correct assumption. These relationships are also not linear but proportional (or inversely proportional) to the square root of the change. The comparison of double inertial weight and one half numbers of piles creates a seemingly linear relationship. Should only one variable had been changed, the change would not have been linear.

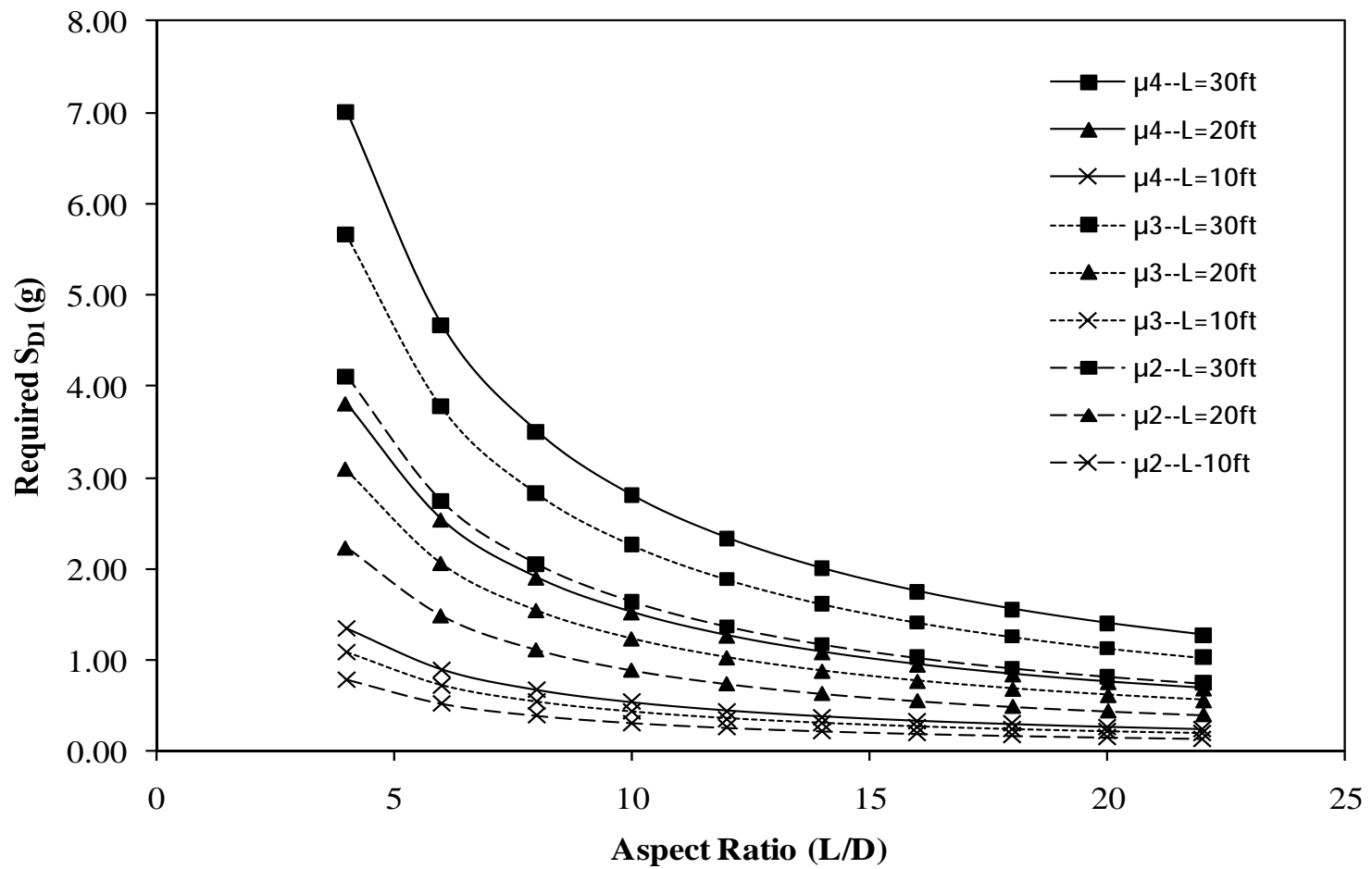


Figure 5.4 Required S_{D1} to Develop Pile Flexural Strength (W=360k, 2 Piles, D/t =32)

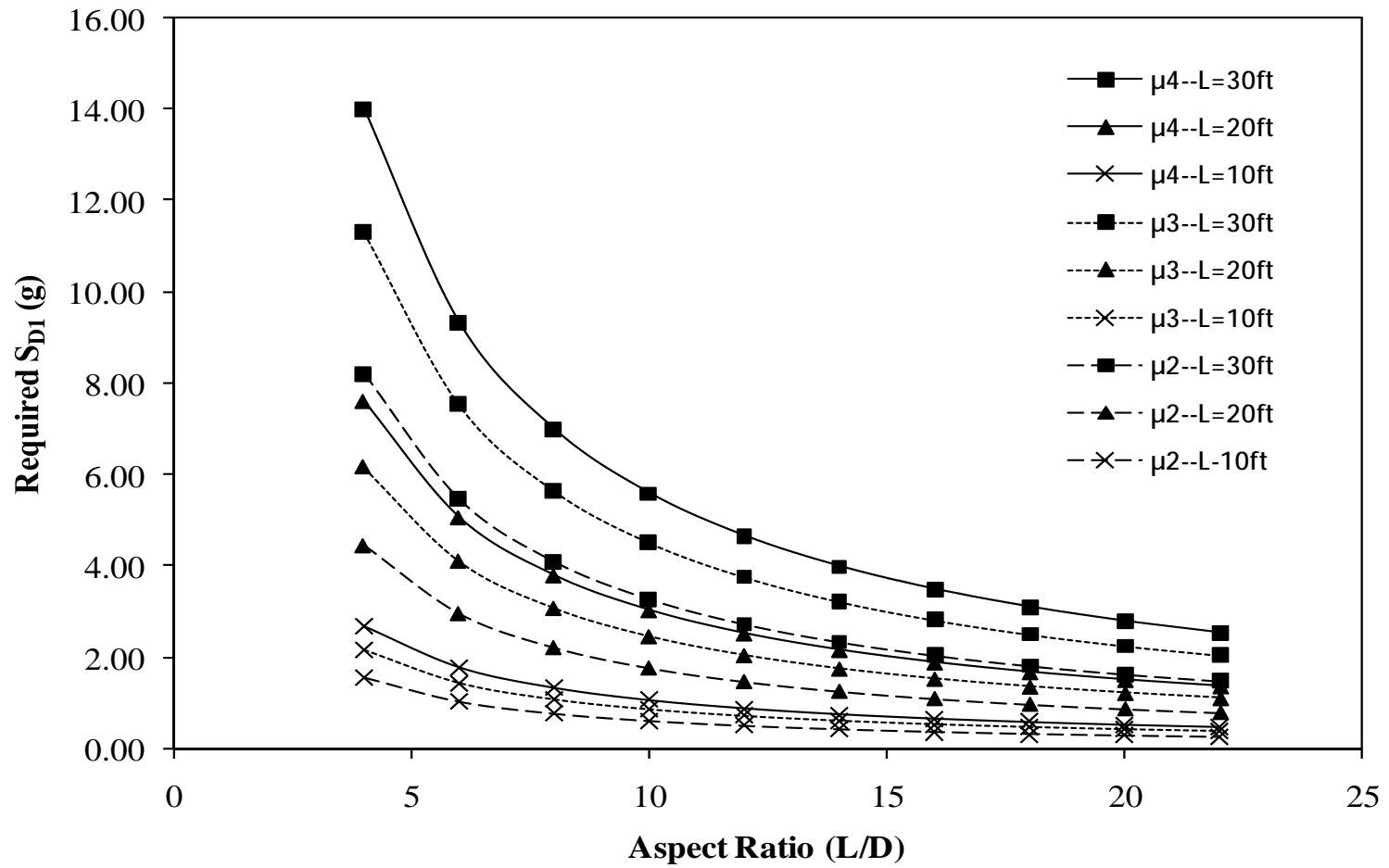


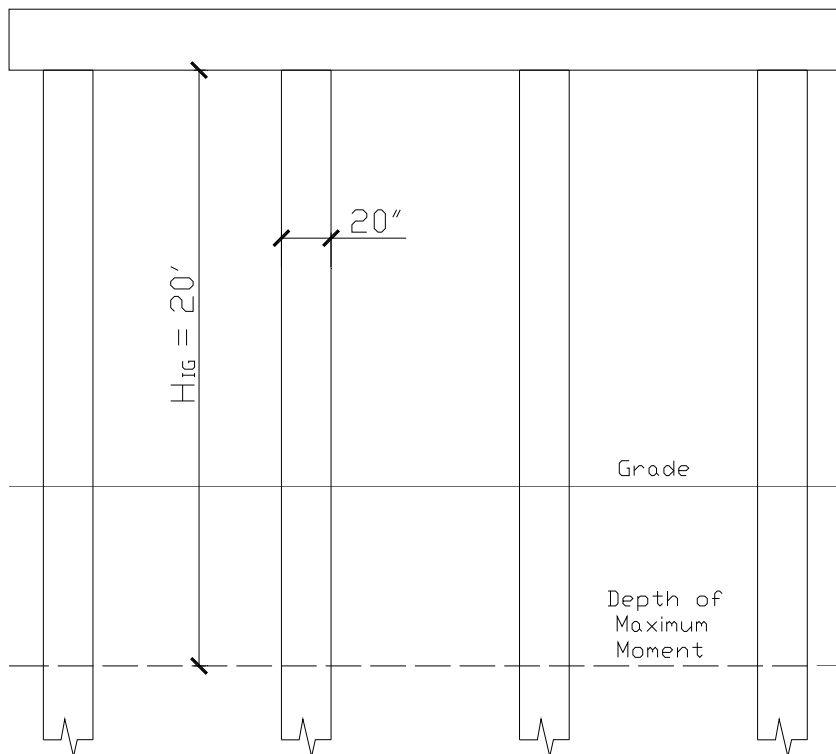
Figure 5.5 Required S_{D1} to Develop Pile Flexural Strength (W=180k, 4 Piles, D/t=32)

The general trends illustrated by Figure 5.4 and Figure 5.5 are not overly surprising. As ductility capacity and pile length is increased, a higher required hazard is necessary to develop the flexural strength of the piles. Both length and ductility capacity will increase deformation capacity as well as effective period which will in turn increase the necessary demand to exhaust the structure. Equally as clear is the effect of aspect ratio. For a given pile length and ductility (and constant D/t) as the diameter increases, so will the necessary demand to develop the flexural strength of the system. Although a wide range of ductility, length, and diameter parameters have been provided in these figures, significant consideration should be given to the appropriate selection of realistic bounds. For example, ductility capacity is typically related to the length of a column. When considering the effect of length it is obvious that that a taller column will have a higher yield displacement but approximately the same amount of plastic curvature as a shorter column with the same dimensions. Taking this into account the taller column will actually have a lower ductility capacity which may seem counter intuitive. This does not indicate that the taller column as a lower displacement capacity, only a lower ductility capacity. In short, consideration must be given the capabilities of the system. Equally detailed systems of different pile lengths may have significantly different ductility capacities. This sort of effect is evident in the ductility 4, 30ft pile length curve. For an aspect ratio of 4, 4 piles, and an inertial weight of 180 kips the required hazard would theoretically be 14g which is obviously unreasonable. Consideration of the differences between ductility capacity and structural deformation capacity is discussed further in the following sections.

5.3 Application of DDBD Analysis Tools

This section is provided to illustrate a simple example of how the DDBD analysis tools developed in prior sections can be used to provide a quick evaluation of a given structure. It is important to note that this analysis does not necessarily fulfill any code requirements and should be used only as a secondary analysis and/or to satisfy engineering judgment. The example bridge bent to be analyzed can be defined by the following parameters:

- Height = 20ft (point of fixity to bottom of cap beam)
- Pile Diameter = 20in
- Thickness = 0.625in
- P=4 (total number of piles)
- Inertial Weight = 180kips (total on pier)
- Target Ductility = 3
- Equivalent Viscous Damping = 15.6% (from Δ_T and $\xi_{eq}=0.05+0.577[[\mu-1]/[\mu\pi]]$)
- Soil Type = E
- Event Type = Farfield
- $F_{ye} = 54\text{ksi}$
- Shape Factor = 1.309 (typical for circular HSS)

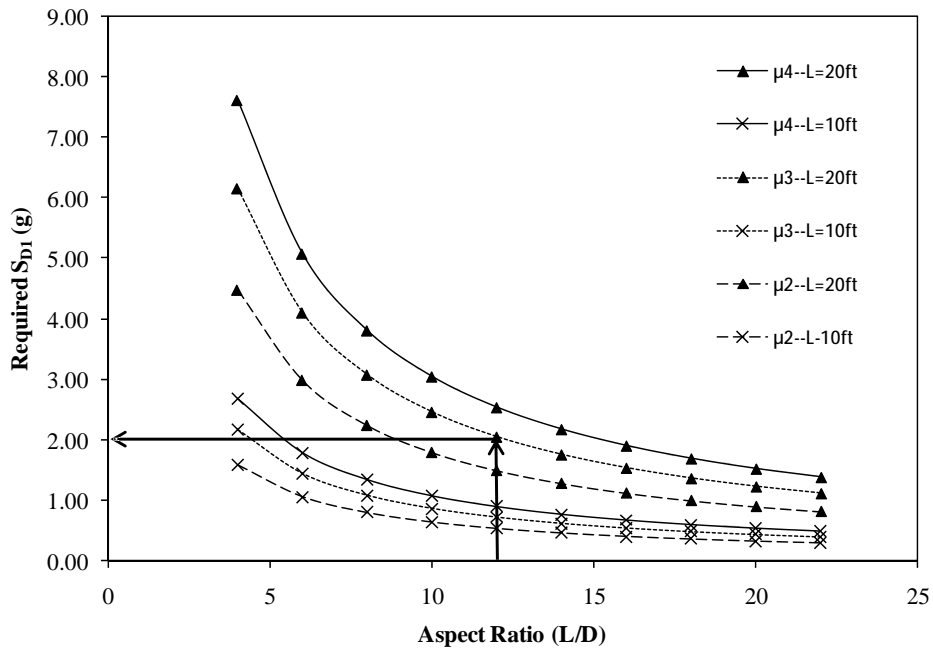


These parameters can now be used in Eq. 5.13:

$$S_{D1} = \sqrt{\frac{(1.309)^2 \cdot 3 \cdot \left(\frac{54\text{ksi}}{29000\text{ksi}}\right) \cdot (54\text{ksi}) \cdot (20\text{ft}) \cdot 4 \cdot \pi^3 \cdot \left[(20\text{in})^4 - [(20\text{in}) - 2 \cdot (0.625\text{in})]^4\right] \cdot 4}{48(20\text{in})^2 \cdot \left(\frac{200\text{kip}}{\text{g}}\right)}} \cdot \left(\frac{7}{2 + 15.6}\right)^{-2 \cdot 0.5}$$

$$S_{D1} = 1.949g$$

Alternatively, the value could also be estimated from the graphical solution:



$$S_{D1} \approx 2.00g$$

The resulting design spectral acceleration must now be adjusted for the given soil conditions. Utilizing the recommended 2006 AASHTO Seismic Design Provisions provided in Table 3.4.2.3-2 of the document the appropriate F_v value can be determined. Note that as the typical design process is being conducted in reverse it may be necessary to iterate the process of determining F_v since this parameter is dependent on S_1 , which the output of this process, not on S_{D1} which is currently known. In this example it is apparent that S_1 will likely be greater than 0.5g indicating that an F_v value of 2.4 will be appropriate but the relationship will not always be this apparent.

$$F_v = 2.4$$

$$S_1 = \frac{S_{D1}}{F_v} = 0.78g$$

The calculated S_1 value can now be compared to the mapped S_1 values for a given earthquake hazard probability to determine suitable locations for the structure.

5.4 Displacement Considerations: Ductility vs. Drift

5.4.1 Ductility Considerations

It is important to consider the sensitivity of ductility capacity to equivalent yield deformation. More flexible structures with higher first yield displacements and consequently higher equivalent yield displacements will likely have a lower ultimate ductility capacity. This concept is not only applicable to steel structures. A simple example of this effect can be provided by considering two concrete columns of the same cross section with one being considerably taller than the other. These sections will clearly possess the same yield curvature and ultimate curvature ductility which is only based on cross sectional characteristics. Given the same yield curvature, the taller column will have a much higher yield displacement. However, since the length of plastic hinging is “rather weakly related to, and is frequently assumed to be independent of, H” (Priestley, et. al. 2007) where H is the height of the column, the plastic displacement capacity of the taller

column will not be much greater than that of the shorter column. In turn the magnitude of ultimate ductility capacity will be considerably lower for the taller column with a matching cross section.

This clearly does not indicate that the taller column is a poor structure, it simply illustrates that ductility capacity should not be a sole factor used to evaluate the performance of a structure. In the case of the steel bents tested in this research project, each test provided significantly higher than expected first yield displacements for reasons discussed throughout this report. In turn the tested ductility levels were not incorrect but relatively large. For example, test 6 was able to withstand a reliable drift of approximately 8 percent. Although this only corresponded to a ductility of 4 it is a significant level of drift and displacement capacity. It is likely that an appropriate design would not even utilize this high of a drift capacity since $P\Delta$ may become very large.

Although the DDBD calculations developed earlier in this Chapter use the principle of ultimate ductility to calculate required hazards, the basic DDBD method is based on target displacements which could be calculated by any method desired. The equations developed could easily have been based on drift capacity or directly on an input target displacement as opposed to the ductility value used.

5.4.2 Alternate Deformation Modes

Of equal if not greater importance to displacement considerations is the issue of alternate modes of deformation. As was seen throughout this testing series, measured first yield displacements were significantly higher than expected, approximately 40% for each test. In no case was a large magnitude of inelastic action experienced during the first yield cycle. This would indicate that other modes of deformation were contributing to the first yield displacement and these modes were not being captured by centerline modeling of the structure. It should be noted that an elevated level of inelastic action was experienced during the first yield cycle of test 5, but the magnitude although significant to damping calculations was still insignificant to the elevated levels of first yield displacement experienced.

It is felt by the research team that at least a portion of the extra deformation can be attributed to joint panel shear which of course would not be captured in a centerline model. As was mentioned earlier in this report and will be covered in more detail in Chapter 6, large inelastic panel joint shears were experienced in test six as well as the other test. The higher than expected joint shear strain likely caused larger joint rotations

and a generally more flexible structure. However, it should be noted that this is only hypothesis and has not been proven analytically. Regardless of this issue it is clear that accounting for alternate modes of deformation is critical in DDBD to capture an accurate response of a given structure.

5.4.3 Conclusions Regarding Displacement Issues

As the two previous sections have indicated, it is important to account for an accurate displacement capacity of a structure for the structures capabilities to be evaluated. No inherent issues exist within the use of reliable ductility as the definition a structures maximum displacement capacity when conducting a DDBD. The flexibility (or lack of) will by nature be included in the use of a ductility factor. However, the flexibility of a structure must be considered when qualitatively evaluating its capabilities using the parameter of reliable ductility. As has been shown, a steel structure will likely have a lower reliable ductility than an equitable concrete structure even if the two structures possess similar ultimate displacement capacities.

It is important to consider all modes contributing to yield displacement if using ultimate ductility to calculate a structures ultimate displacement capacity. As is shown in Table 5.3 should the DDBD analysis of the test results be revised using reliable drift to determine the displacement capacity, a significant increase in the structures capabilities is experienced. This is due to the fact that the reliable drift determined from testing inherently includes all modes of deformation (column shear, cap beam flexibility, panel shear, etc.) while the use of reliable ductility in the relationship developed in this chapter includes only column flexural displacement and greatly under predicts the actual capabilities of the structure.

Table 5.3 Modified Analyses of Test Structures

Test	Reliable Ductility	ξ_{eq} (%)	Reliable Drift	Minimum SD1 to Develop Full Flexural Strength of the Bent (g)		% Increase
				Basis: Reliable Ductility	Basis: Reliable Drift	
1	1	5.0*	0.028	0.449	0.68	1.514
2	3	15.6	0.070	1.232	1.705	1.384
3	1.5	11.5*	0.035	0.763	1.056	1.384
4	2	11.8	0.049	0.891	1.263	1.418
5	2	14.2**	0.054	0.965	1.436	1.488
6	4	23.5	0.088	1.712	2.301	1.344
					Average Increase:	1.422

* Recommended Steel Frame Value Used Due to Lack of Data

** Recommended Steel Frame Value Used Due to Unreasonably High Calculated Value

Detailed Analysis of Test 6

6.1 Introduction

Test 6 was clearly the most successful test considering the desirable failure mode achieved as well as the significantly improved force displacement performance which can be seen in Figure 6.1. Considering this improved performance, the flared column capital will likely be one of the designs that are explored in further research. For this reason a more in depth analysis of the test 6 data is provided in this chapter. The majority of the discussion provided will focus on three particular issues related to the test. First a qualitative relationship between local buckling and strength degradation will be evaluated. Secondly, issues related to the performance of the flared column capital will be considered. Lastly, the effects of joint panel zone shear will be considered. A brief discussion of issues related to a finite element analysis study (FEA), which is currently in its early developmental stages, will also be provided

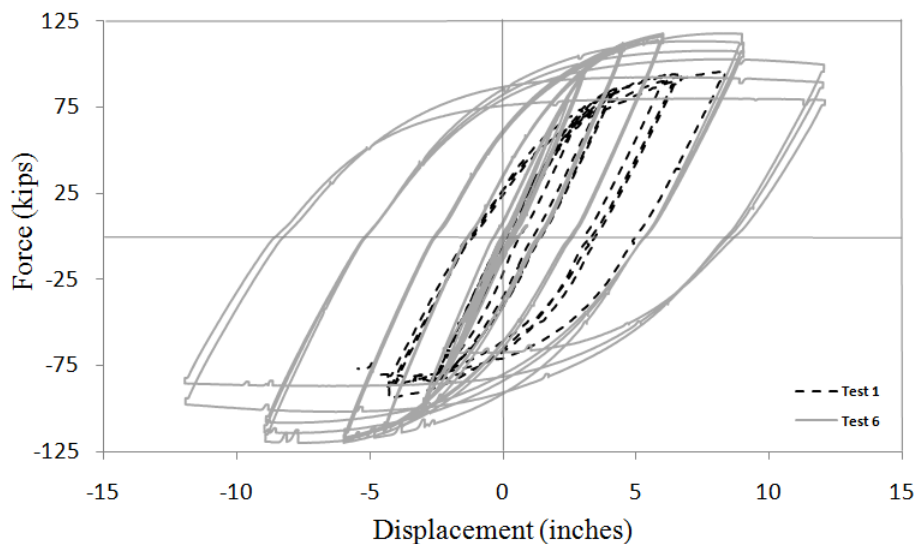


Figure 6.1 Test 1/Test6 Force Displacement Comparison

6.2 Local Buckling Considerations

Throughout the testing series, emphasis was placed on producing a base metal failure by reducing the possibility of brittle connection cracking. Obvious advantages exist in producing a base metal failure as it can be considered utilization of the ultimate capacity of the structure. It was anticipated, and eventually shown in test 6, that a base metal failure would consist of local buckling of the pile wall leading to eventual material rupture at the locally buckled region. Though buckling was also seen on prior tests, the ultimate limit states of all earlier tests were related to connection failure.

It was noted during testing of specimen 6 that visual signs of local buckling developed during the second ductility level. However, as can be seen in Figure 6.2 the maximum strength of the structure was also developed at the second ductility level or possibly even the first cycle of the third ductility level. From this, the reasonable conclusion could be developed that the onset of local buckling and possibly even moderate levels of buckling propagation are not associated with significant strength loss. It was seen during test 6 that severe local buckling, as shown in Figure 6.3, had to develop before significant strength loss occurred which took place during ductility 4.

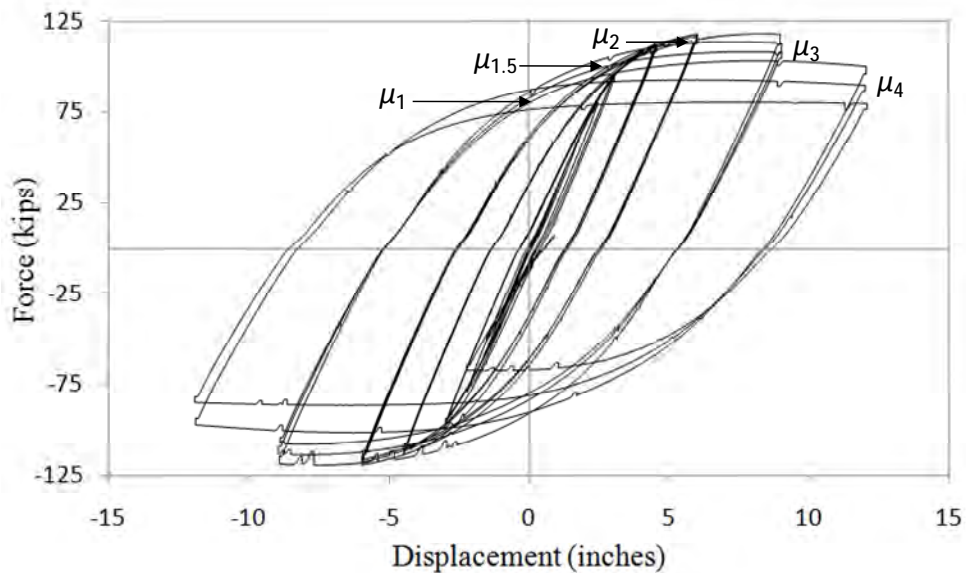


Figure 6.2 Test 6 Force Displacement Hysteresis

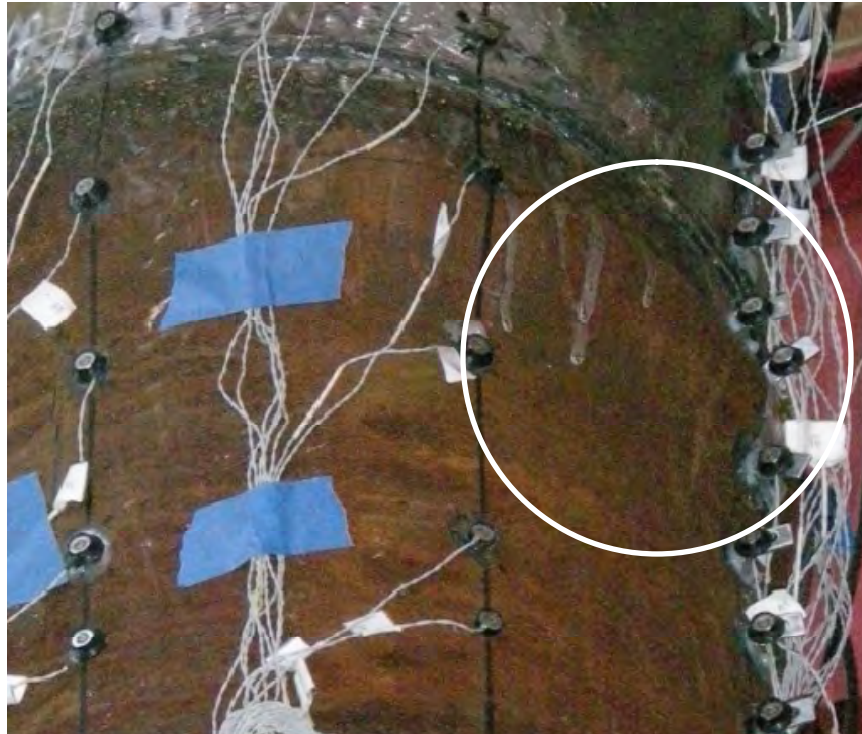


Figure 6.3 Severe Local Buckling in Test 6 – Ductility 4

Although comparison of testing observations and the force displacement hysteresis seem to indicate that initial local buckling did not correlate with strength loss, it was desired to show this in a more analytical manner. As was discussed in Chapter 4, a qualitative relationship between local buckling and strength degradation can be achieved by utilizing horizontal (cross sectional) strain diagrams at a given height along the column. These diagrams can be developed for any position located within the Optotrak grid, only sections of known local buckling will be discussed along with an example of a non-local buckling location for comparison purposes. Although this is still a qualitative analysis, it is valuable support for any conclusions made from testing observations.

As can be seen in Figure 6.4 and Figure 6.5, the strain diagrams of a region that was known to not experience local buckling remain essentially linear throughout the entire test. Contrarily, as can be seen in Figure 6.6 and Figure 6.7, the progression of local buckling at the cross section 25 inches below the cap beam is captured by the non-

linearity of the strain diagrams. Note that these figures provide the diagrams for the first cycle only of each ductility level for clarity. It is also important to note that the figures are not plotted to the same scale and hence the non-linearity seen at the upper ductility levels at a cross section 7 inches below the cap beam is extremely insignificant compared to the non-linearity experienced at 25 inches below the cap beam.

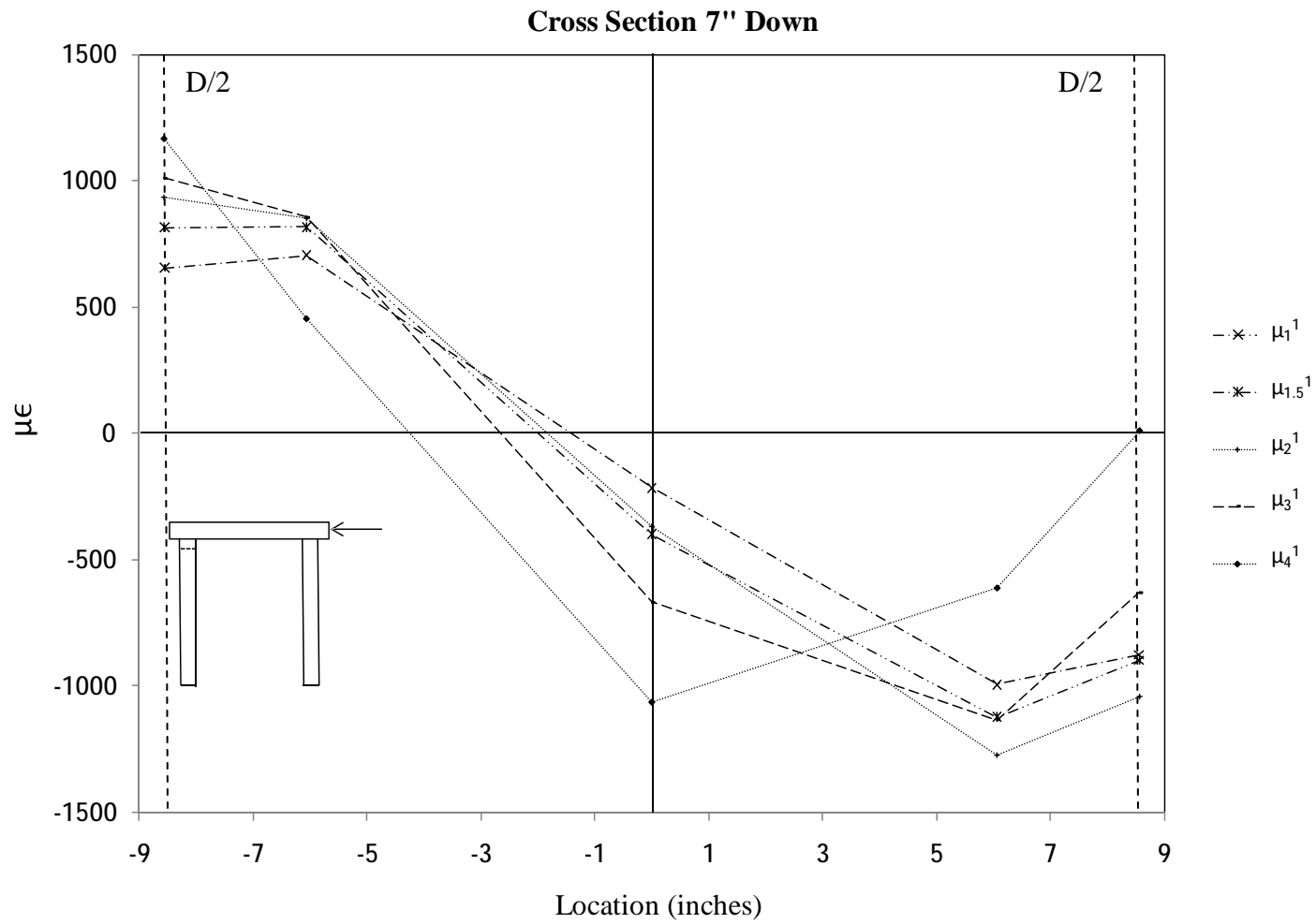


Figure 6.4 Strain Cross Section 7 inches Below the Cap Beam – Push Direction

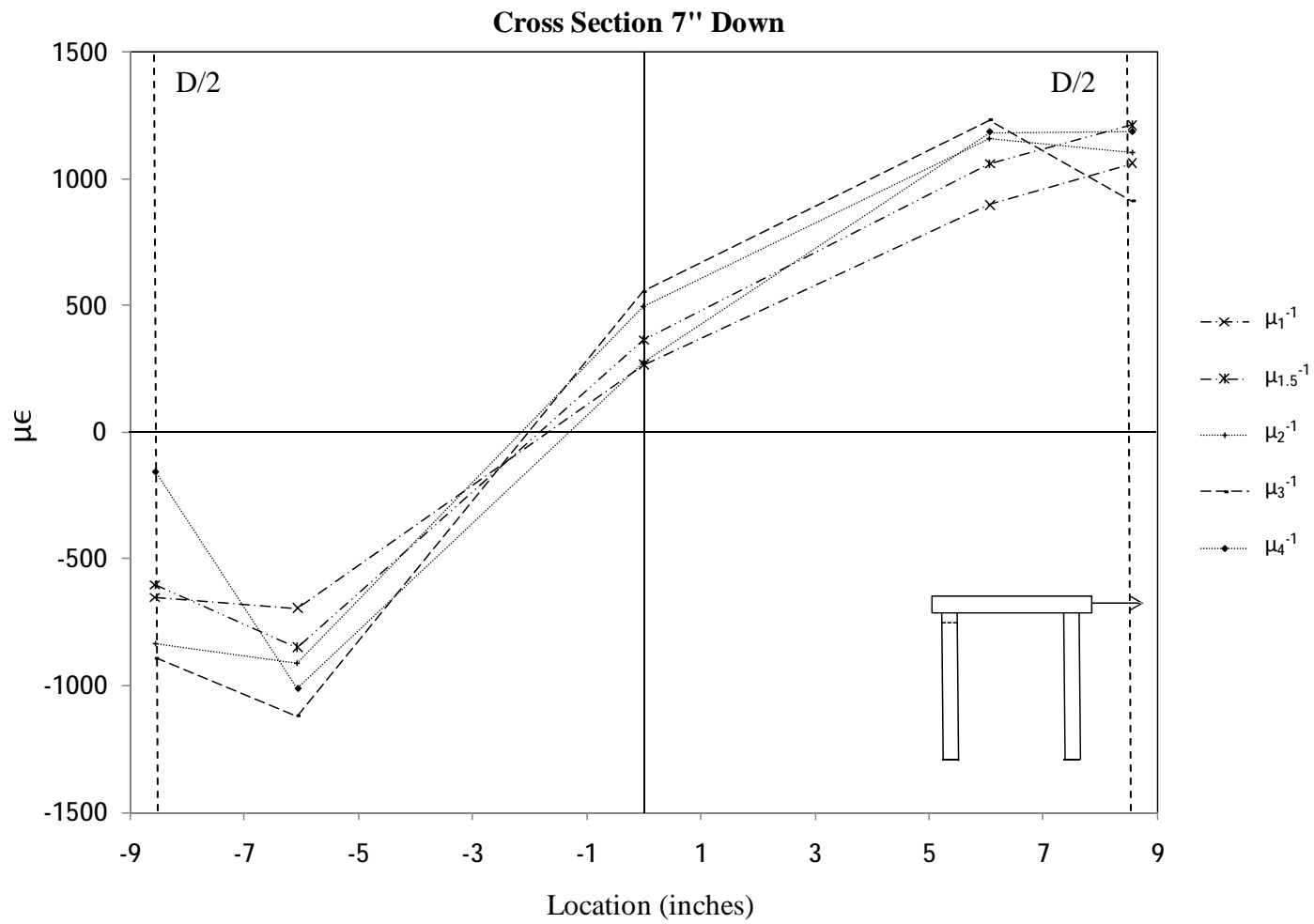


Figure 6.5 Strain Cross Section 7 inches Below the Cap Beam – Pull Direction

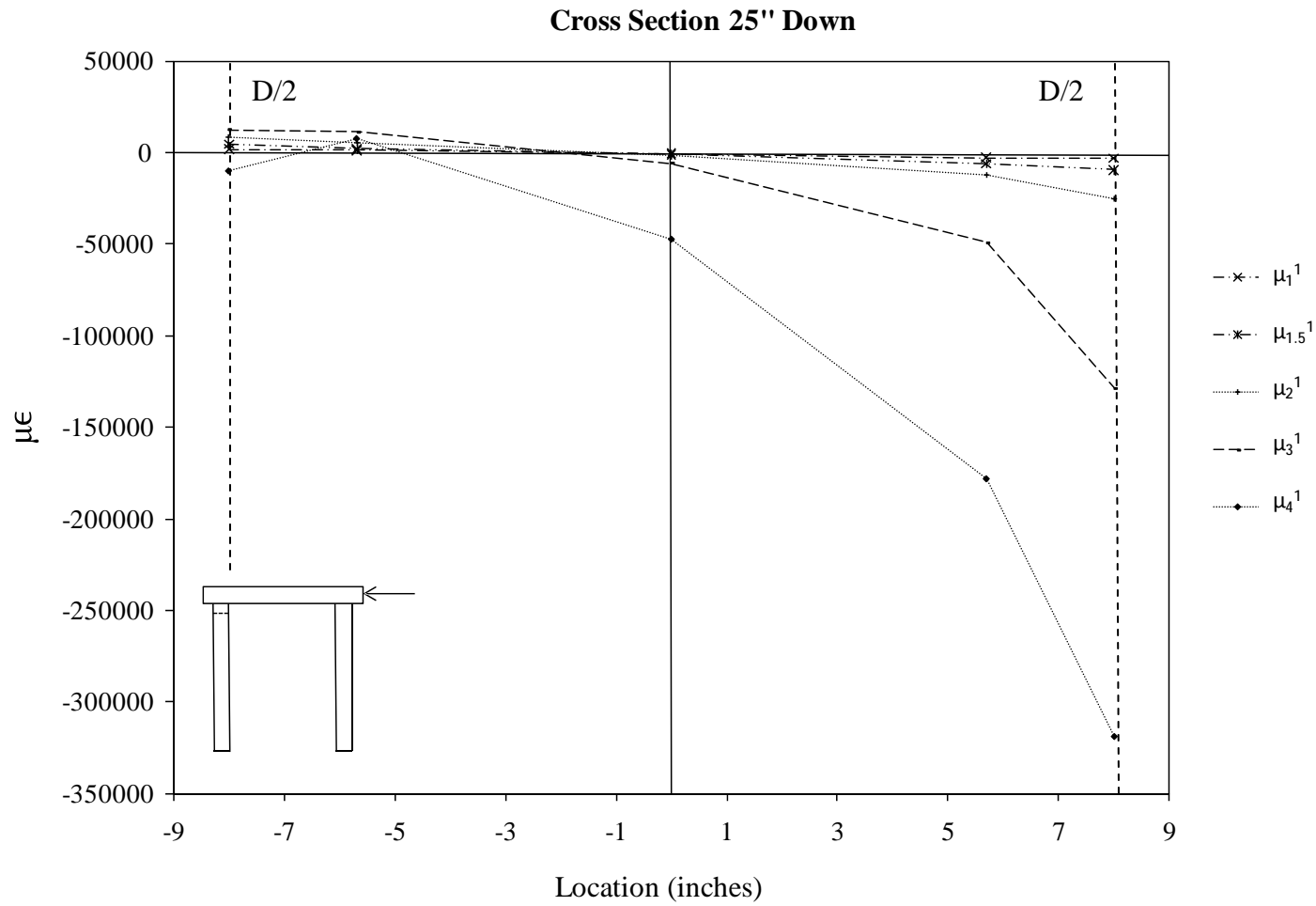


Figure 6.6 Strain Cross Section 25 inches Below the Cap Beam – Push Direction

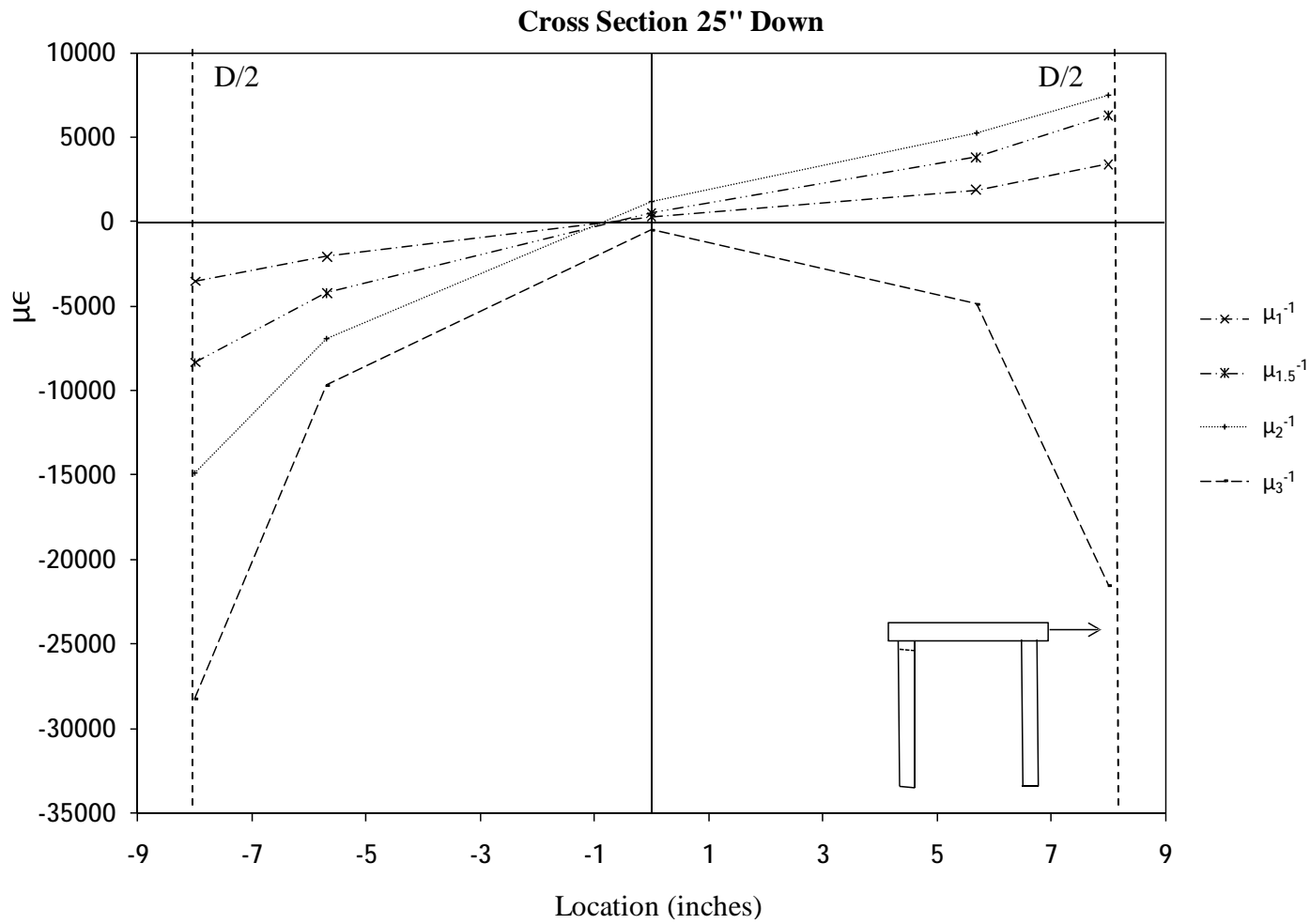


Figure 6.7 Strain Cross Section 25 inches Below the Cap Beam – Pull Direction

As has been shown, severe buckling clearly took place at a location 25 inches below the cap beam. The following figures depict the onset and propagation of local buckling at this location by individually plotting the strain diagrams for each ductility level and cycle. By reviewing Figure 6.20 through Figure 6.25 it is clear that local buckling did begin to develop in the second ductility level and continue to grow in magnitude throughout the remainder of the test. It is also arguable that minor effects of local buckling were experienced during the ductility 1.5 level which clearly produced no adverse effects in load carrying capacity. It should be noted that the specimen was tested through all three cycles of ductility 4 and local buckling was observed to significantly propagate during this level. However, due to erroneously high strain calculations the diagrams for these cycles are skewed and unreliable and there for have not been included in this report.

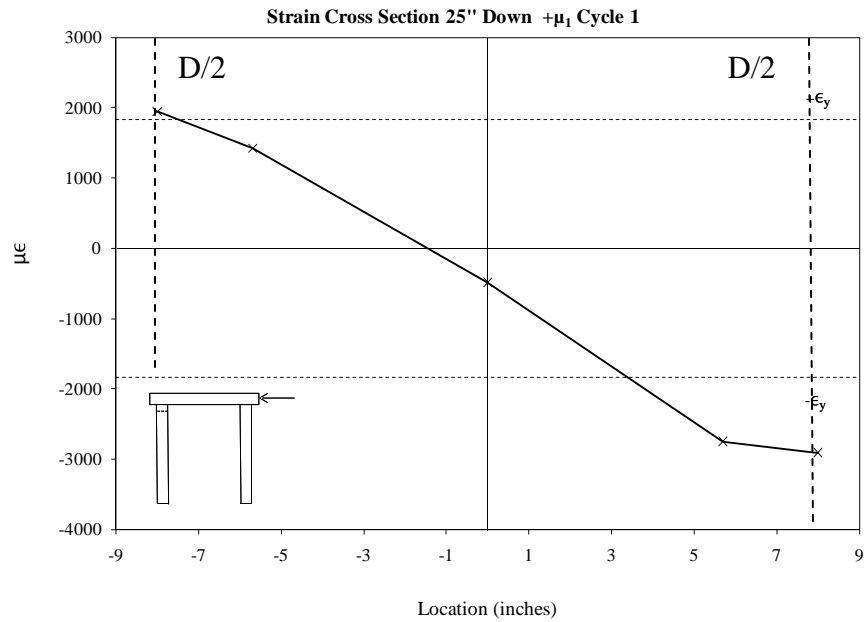


Figure 6.8 Strain Cross Section 25'' Down - Ductility 1 Cycle 1

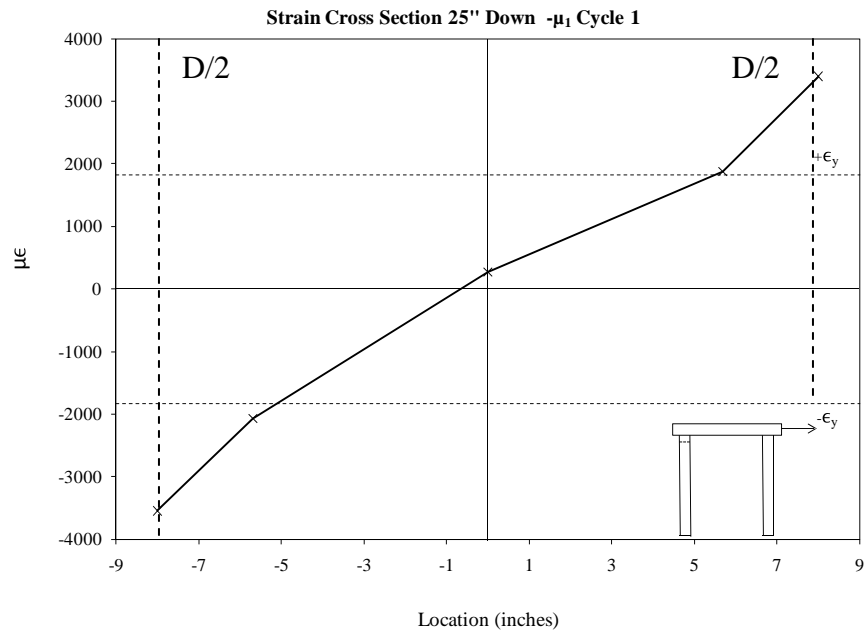


Figure 6.9 Strain Cross Section 25'' Down - Ductility 1 Cycle -1

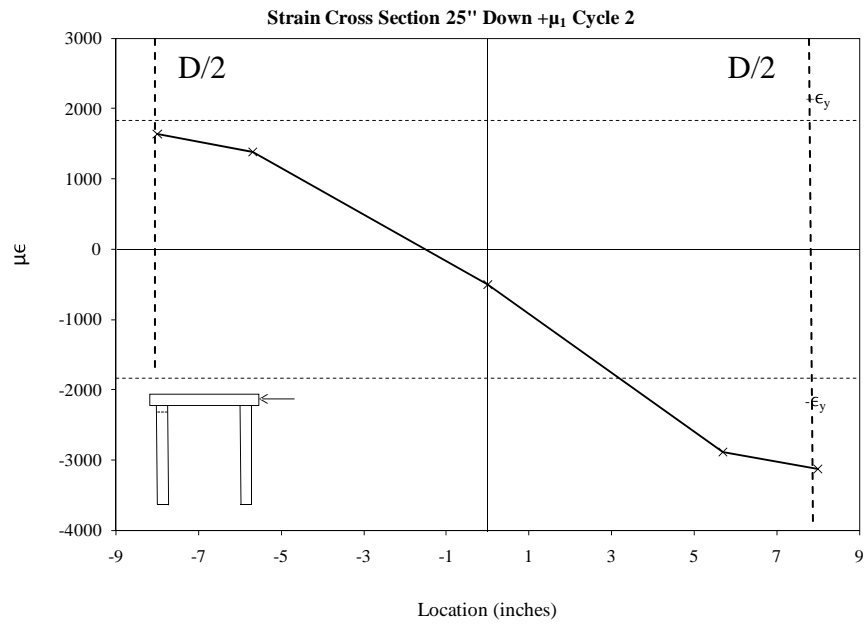


Figure 6.10 Strain Cross Section 25'' Down - Ductility 1 Cycle 2

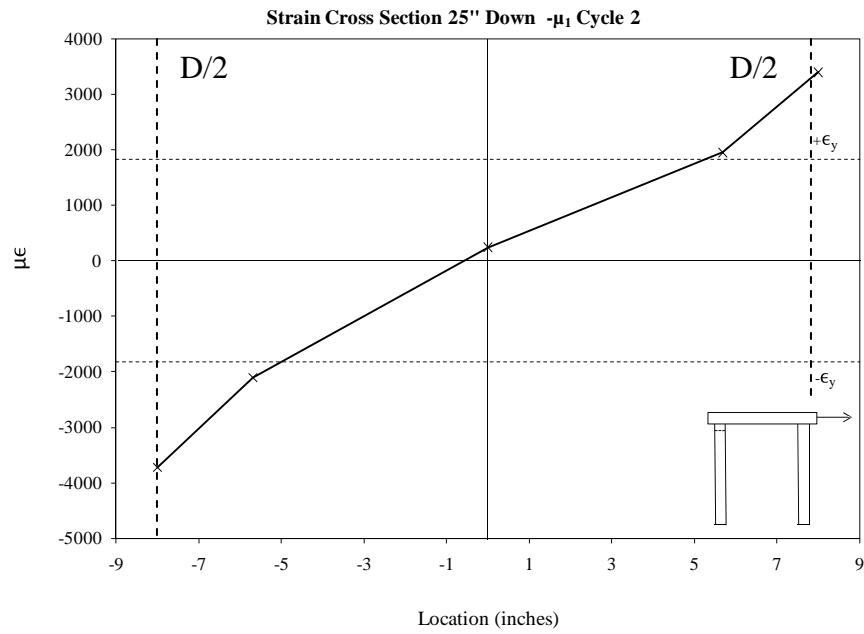


Figure 6.11 Strain Cross Section 25" Down - Ductility 1 Cycle -2

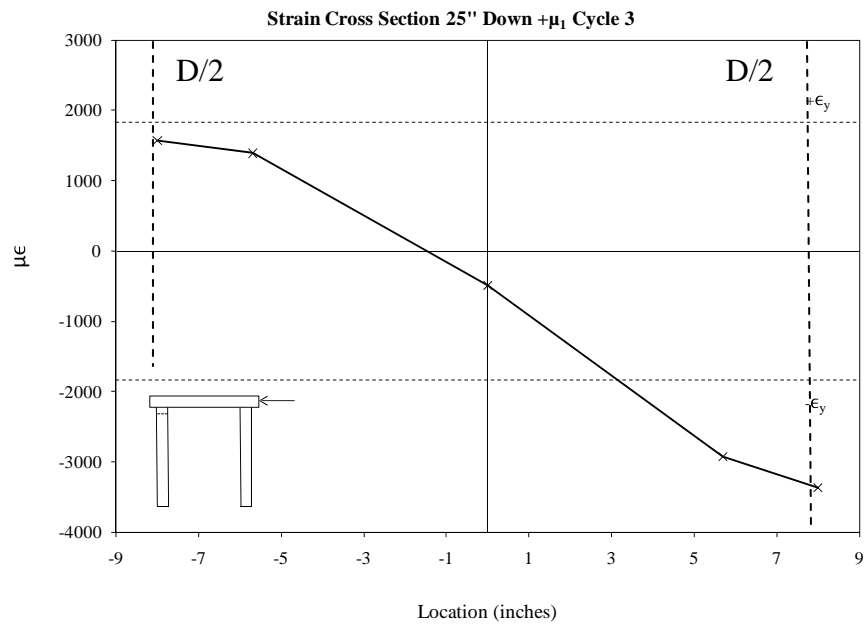


Figure 6.12 Strain Cross Section 25" Down - Ductility 1 Cycle 3

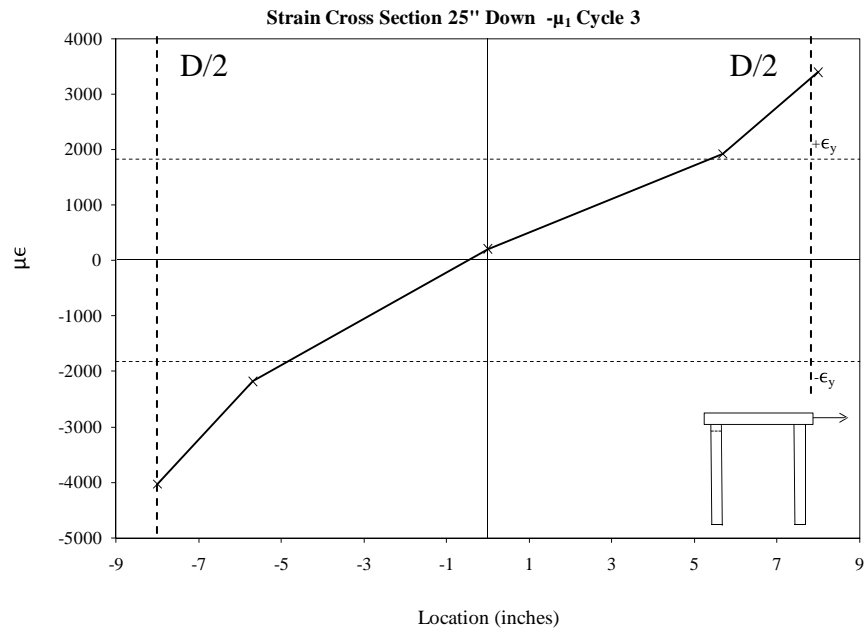


Figure 6.13 Strain Cross Section 25'' Down - Ductility 1 Cycle -3

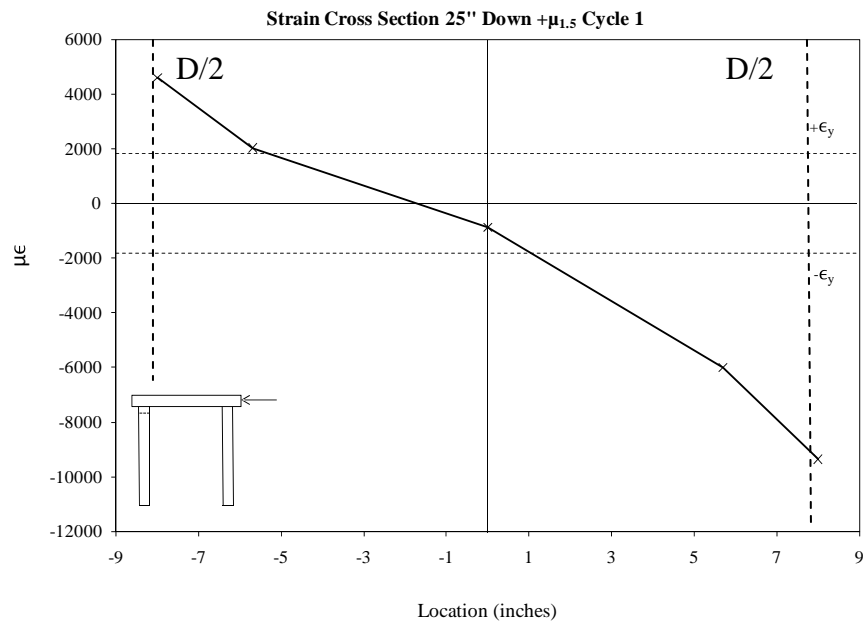


Figure 6.14 Strain Cross Section 25'' Down - Ductility 1.5 Cycle 1

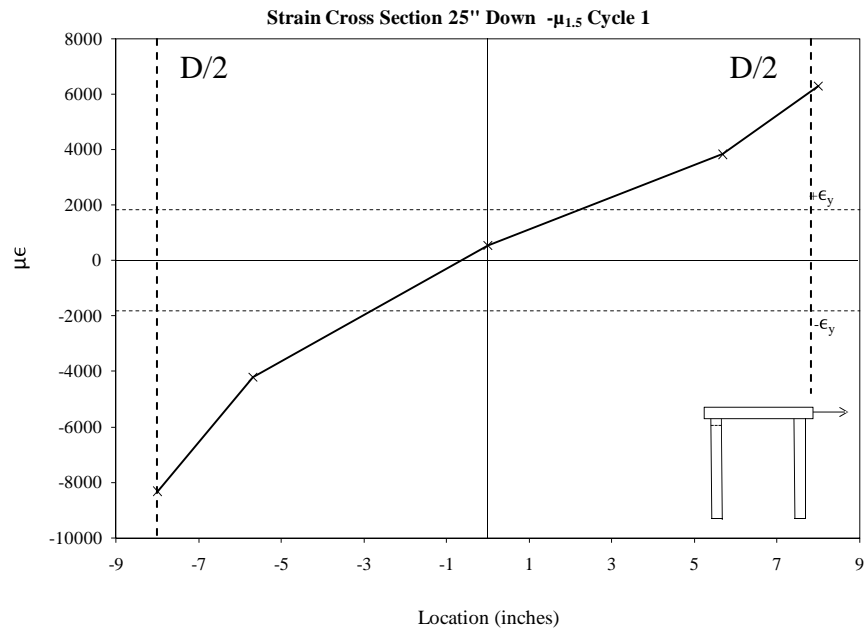


Figure 6.15 Strain Cross Section 25'' Down - Ductility 1.5 Cycle -1

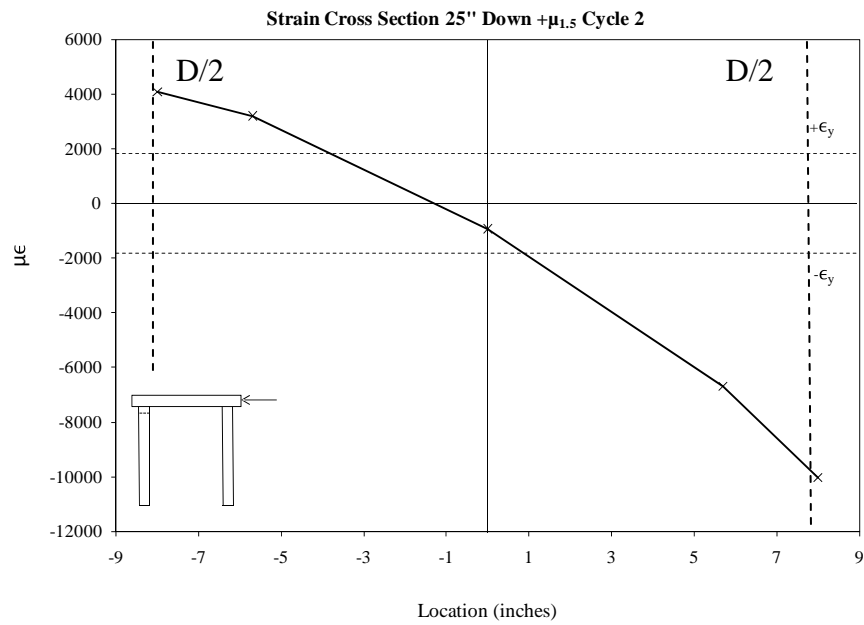


Figure 6.16 Strain Cross Section 25'' Down - Ductility 1.5 Cycle 2

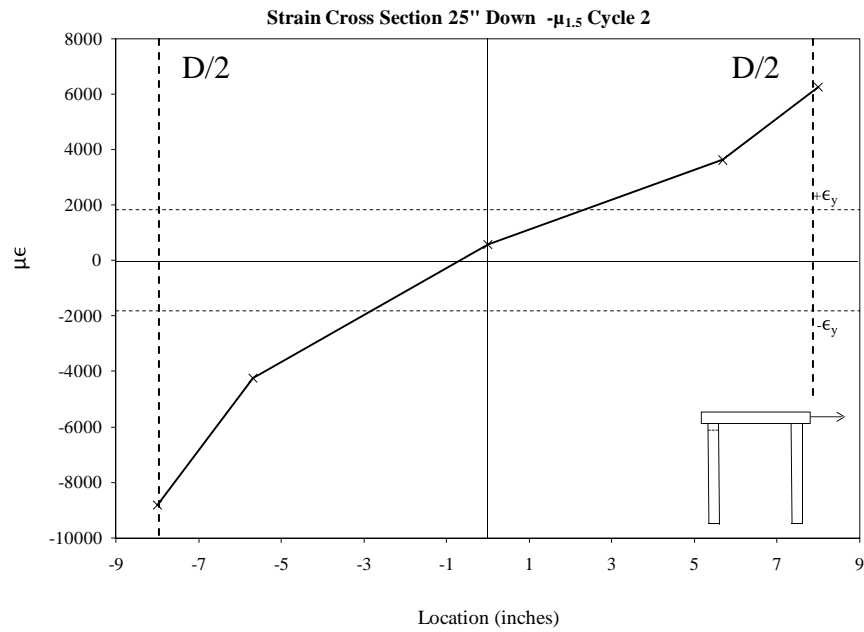


Figure 6.17 Strain Cross Section 25'' Down - Ductility 1.5 Cycle -2

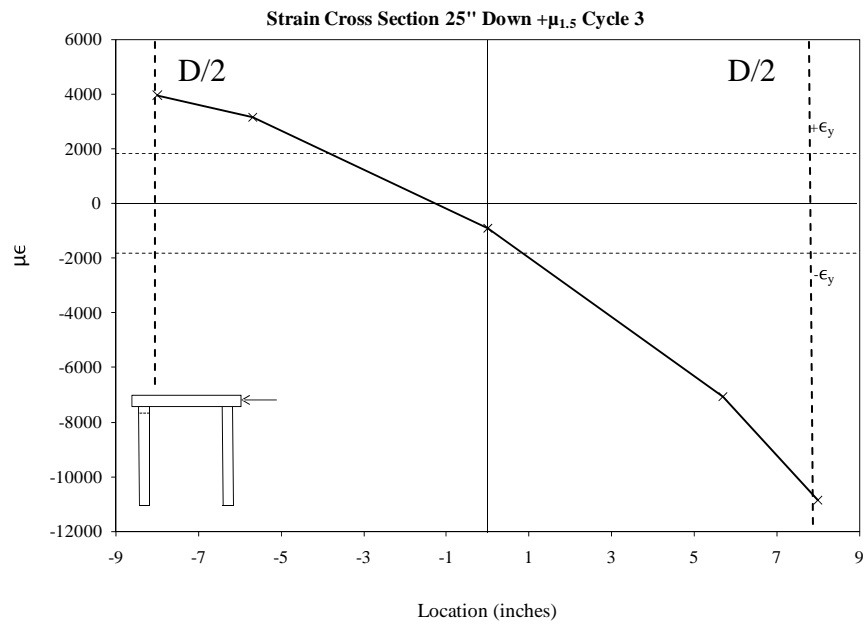


Figure 6.18 Strain Cross Section 25'' Down - Ductility 1.5 Cycle 3

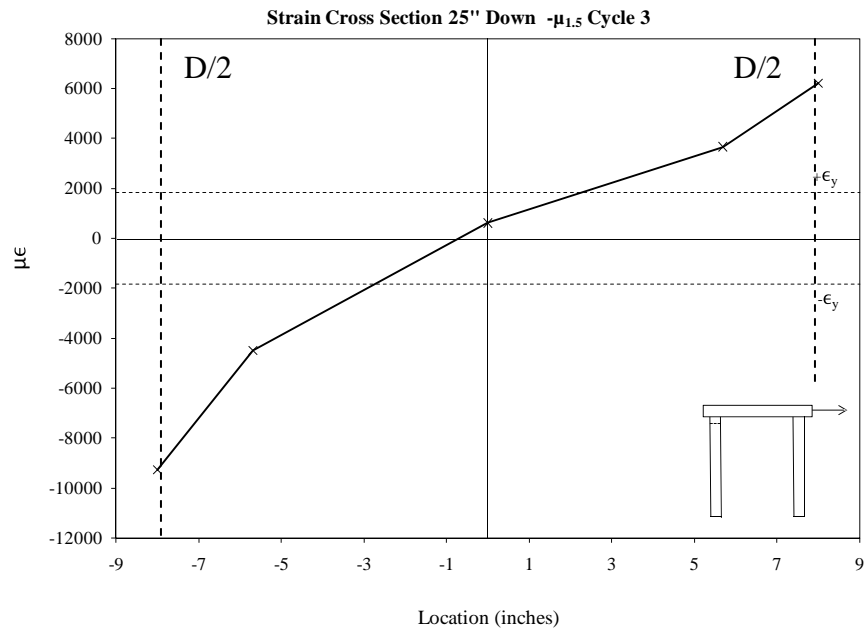


Figure 6.19 Strain Cross Section 25'' Down - Ductility 1.5 Cycle -3

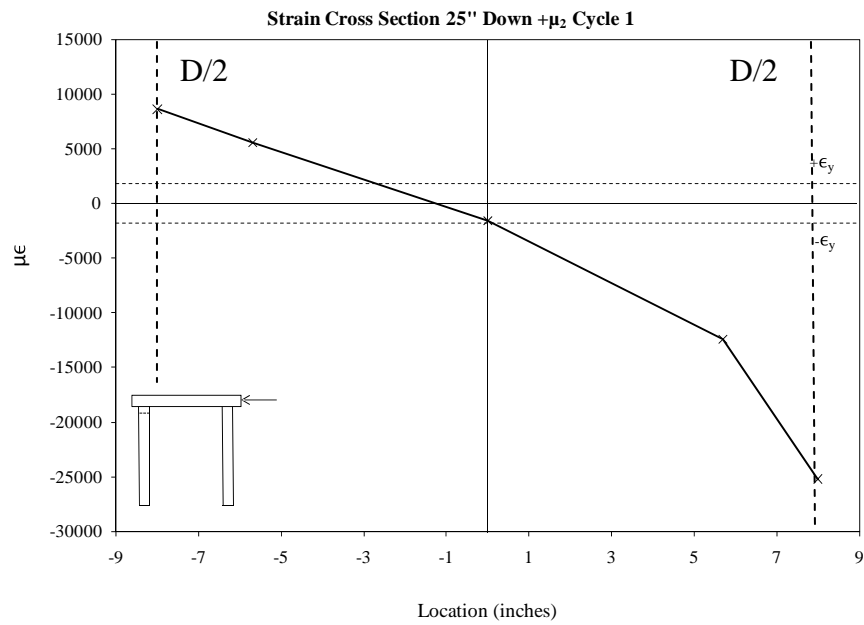


Figure 6.20 Strain Cross Section 25'' Down - Ductility 2 Cycle 1

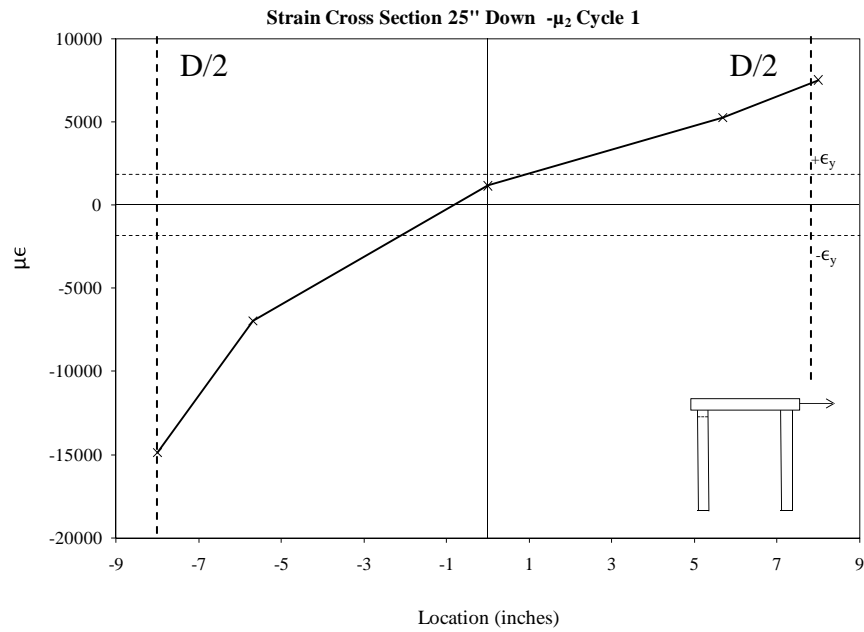


Figure 6.21 Strain Cross Section 25'' Down - Ductility 2 Cycle -1

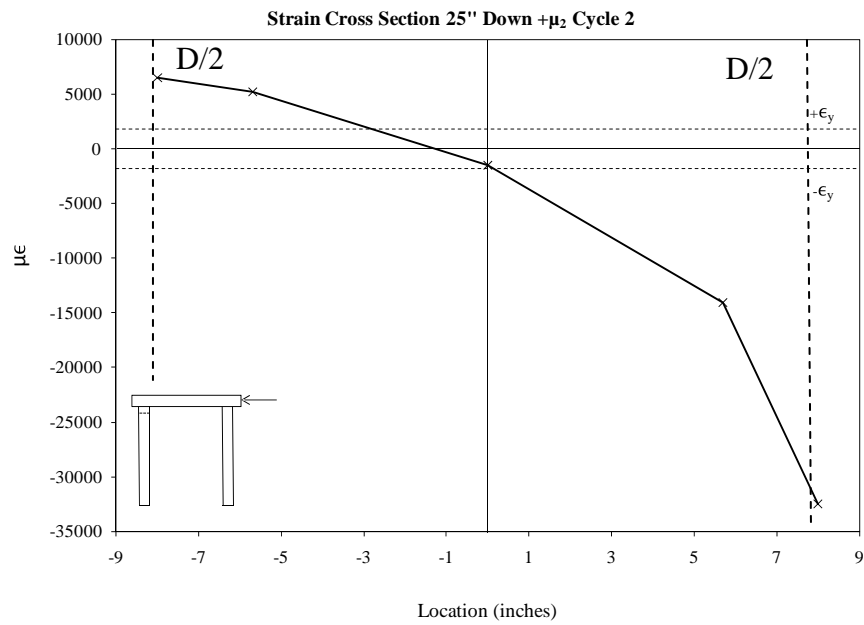


Figure 6.22 Strain Cross Section 25'' Down - Ductility 2 Cycle 2

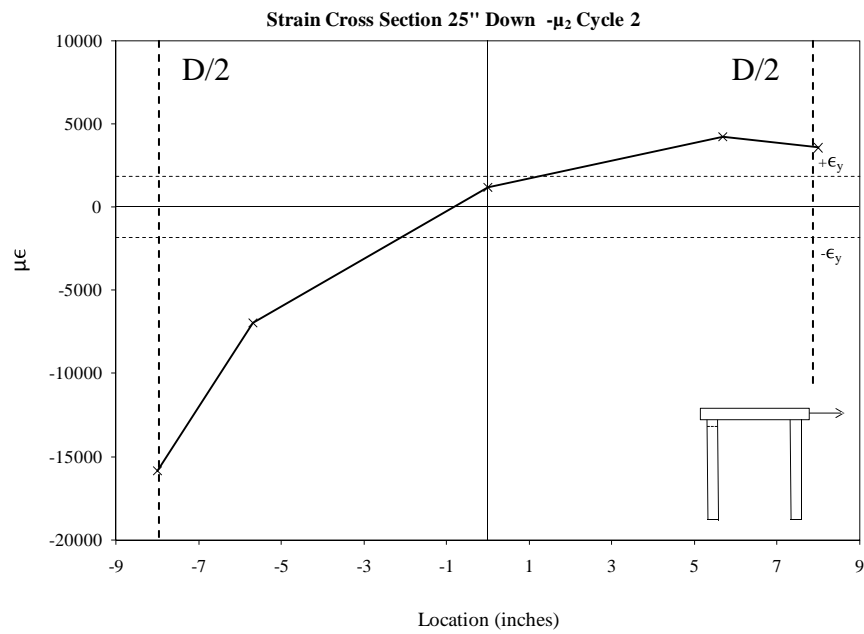


Figure 6.23 Strain Cross Section 25'' Down - Ductility 2 Cycle -2

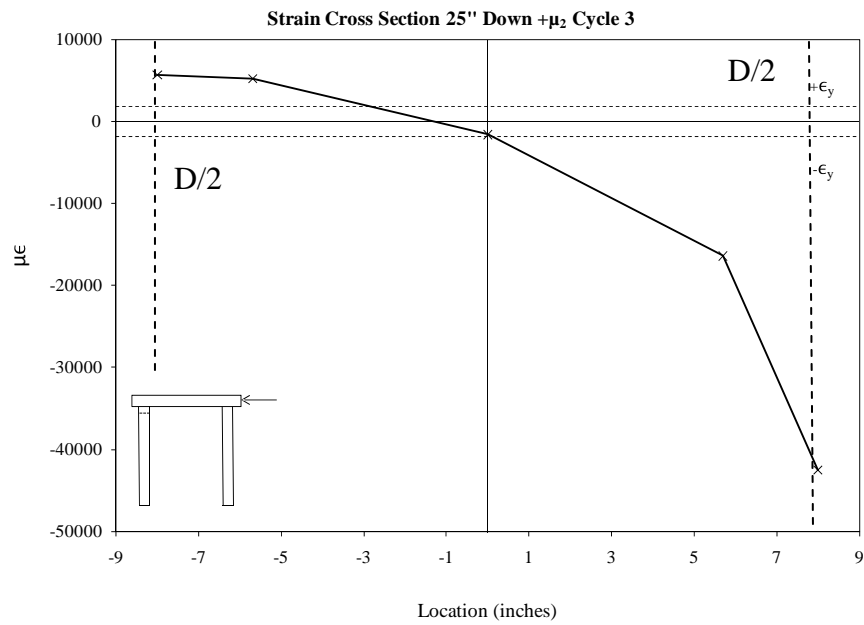


Figure 6.24 Strain Cross Section 25'' Down - Ductility 2 Cycle 3

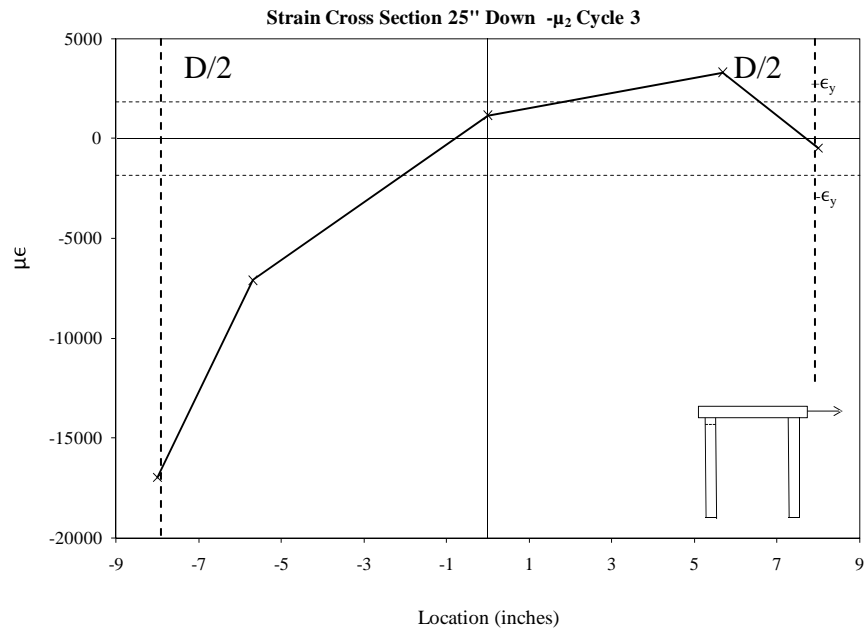


Figure 6.25 Strain Cross Section 25'' Down - Ductility 2 Cycle -3

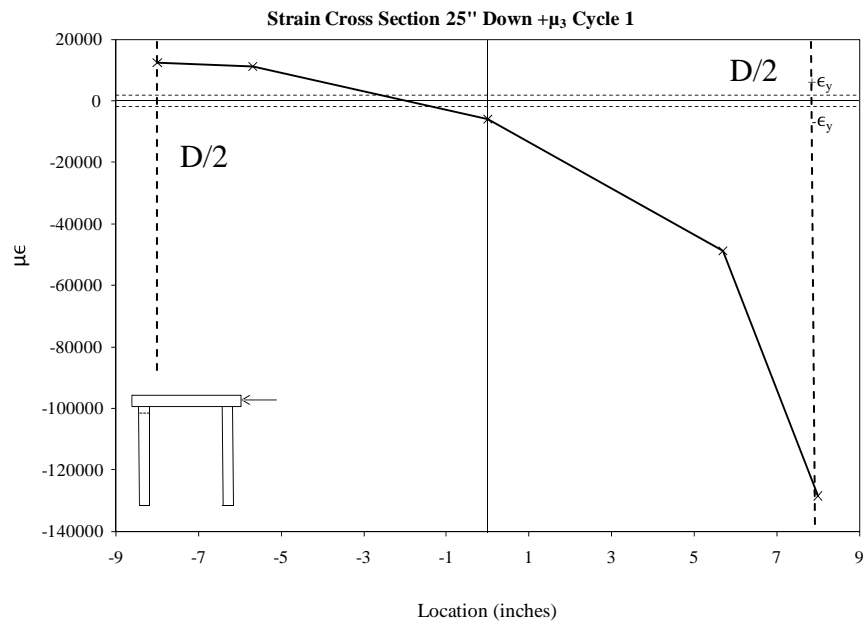


Figure 6.26 Strain Cross Section 25'' Down - Ductility 3 Cycle 1

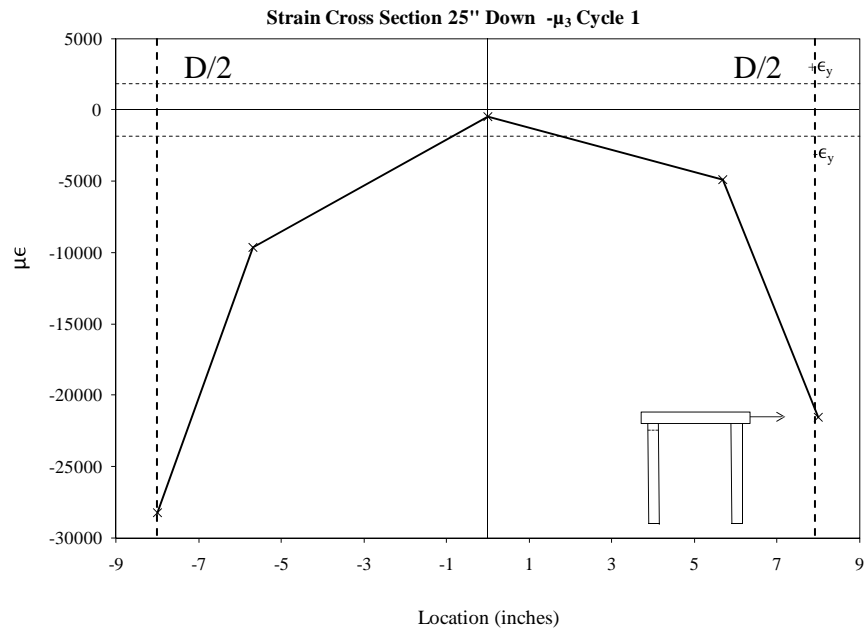


Figure 6.27 Strain Cross Section 25'' Down - Ductility 3 Cycle -1

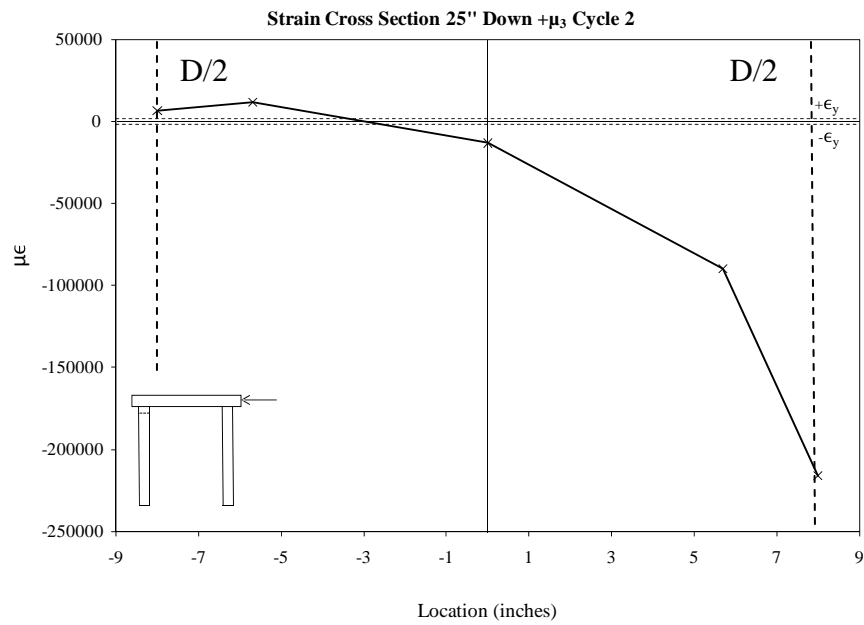


Figure 6.28 Strain Cross Section 25'' Down - Ductility 3 Cycle 2

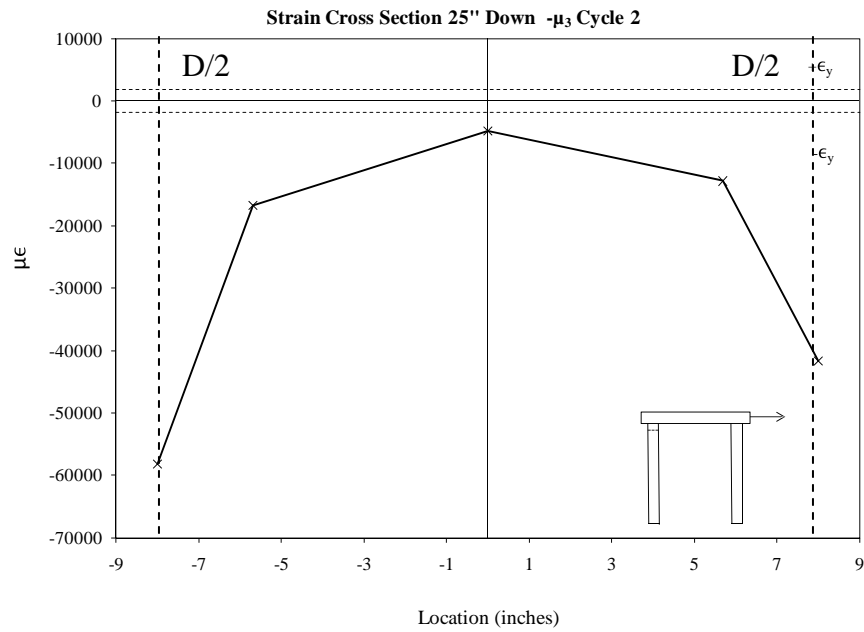


Figure 6.29 Strain Cross Section 25'' Down - Ductility 3 Cycle -2

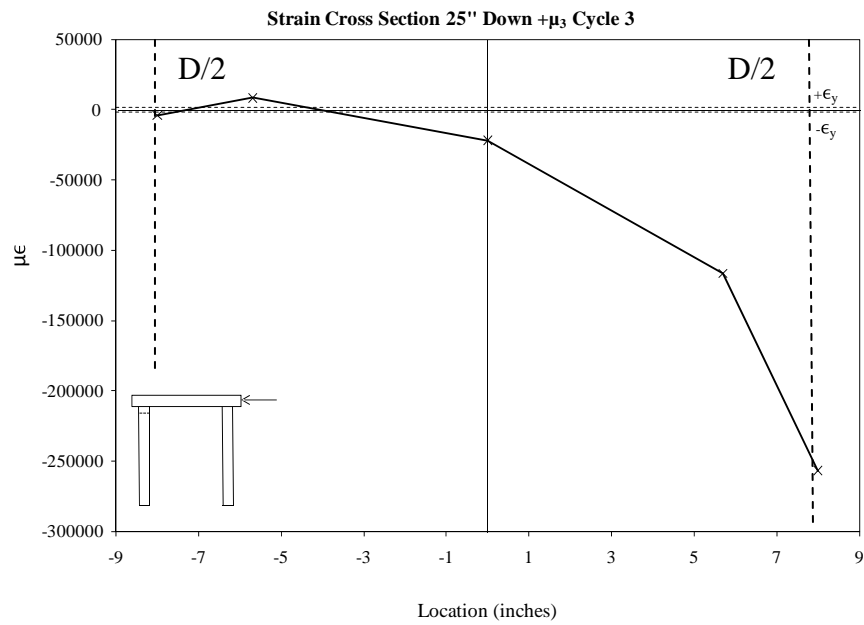


Figure 6.30 Strain Cross Section 25'' Down - Ductility 3 Cycle 3

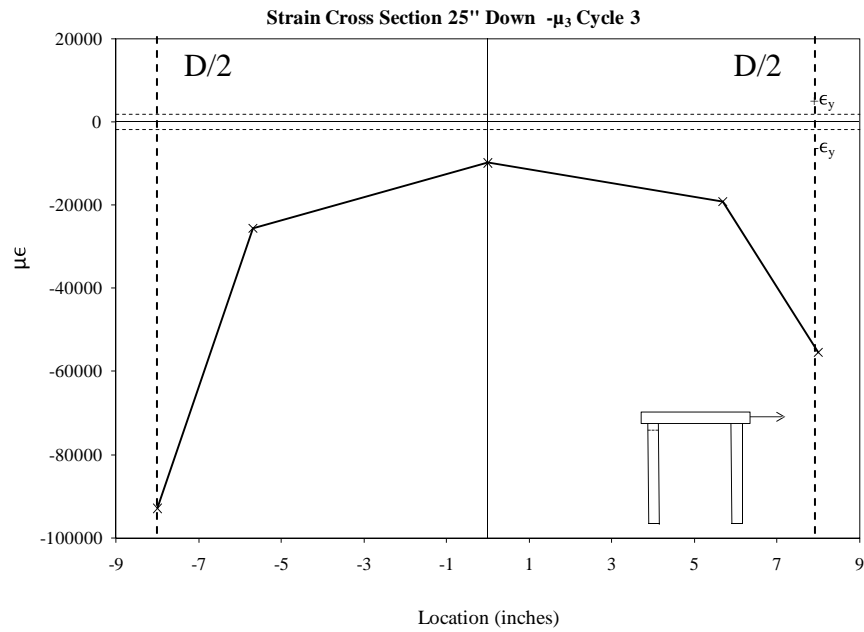


Figure 6.31 Strain Cross Section 25'' Down - Ductility 3 Cycle -3

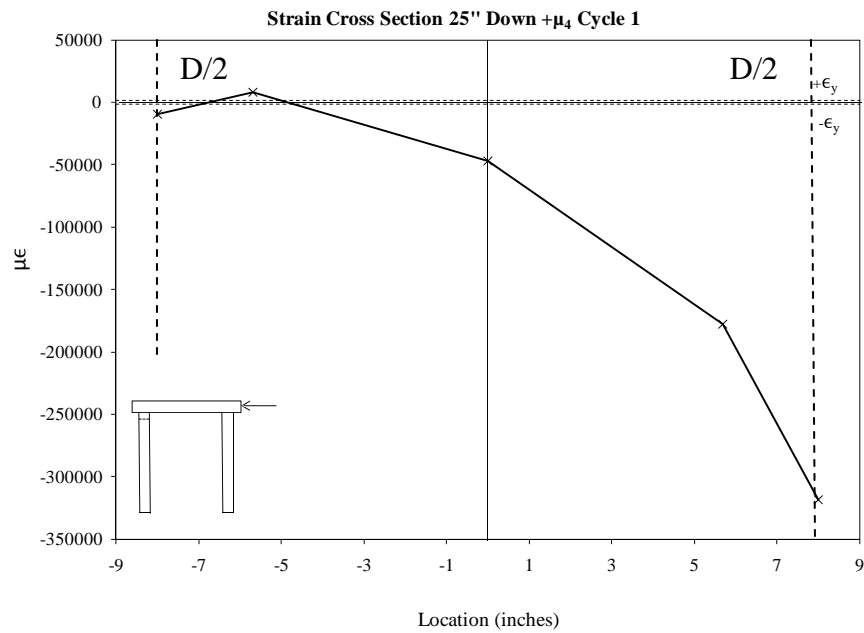


Figure 6.32 Strain Cross Section 25'' Down - Ductility 4 Cycle 1

By superimposing these strain diagrams on their respective force displacement envelope figures, a simple graphical comparison between buckling and strength loss can be made. Reviewing Figure 6.33 through Figure 6.35 it seems to be a reasonable conclusion that the onset of and moderate levels of local buckling do necessarily indicate significant strength loss. This lends to the conclusion that local buckling should not necessarily be taken as an ultimate limit state. It may however be desirable to consider local buckling as a damage control limit state as repair would be difficult following even a moderate level of local buckling. From the results of this testing series, this damage control limit state would approximately correspond to $\mu_{\Delta}=1.5$ for a D/t ratio of 32.

It is important to note that any conclusions about the effects of local buckling developed in this section are in regards to local buckling at the fixed end of a hollow steel circular pile. It should also be noted that very similar modes of local buckling developed in the research discussed in “Retrofitting for seismic upgrading of steel bridge columns” which was also considering a fixed end condition. However, it has been shown in another testing series at North Carolina State University that the effects of local buckling of hollow steel piles away from fixed end conditions produce significantly different effects. In this situation it was observed that local buckling took place very rapidly and in an inward (concave) manner. The buckling was also accompanied with immediate significant strength loss often greater than 30%. The results of that testing series will be discussed in further detail in Chapter 7.

In addition to the fixed end limitation in regards to the response conclusions made here, the results are also limited to members with a D/t ratio of 32. Considering a failure mode of local buckling leading to eventual material rupture, D/t ratio and ultimate ductility capacity are likely inversely proportional. This indicates that the conclusions made here are likely non-conservative for member with D/t ratios greater than 32 since local buckling will likely occur earlier and conservative for members with lower D/t ratios.

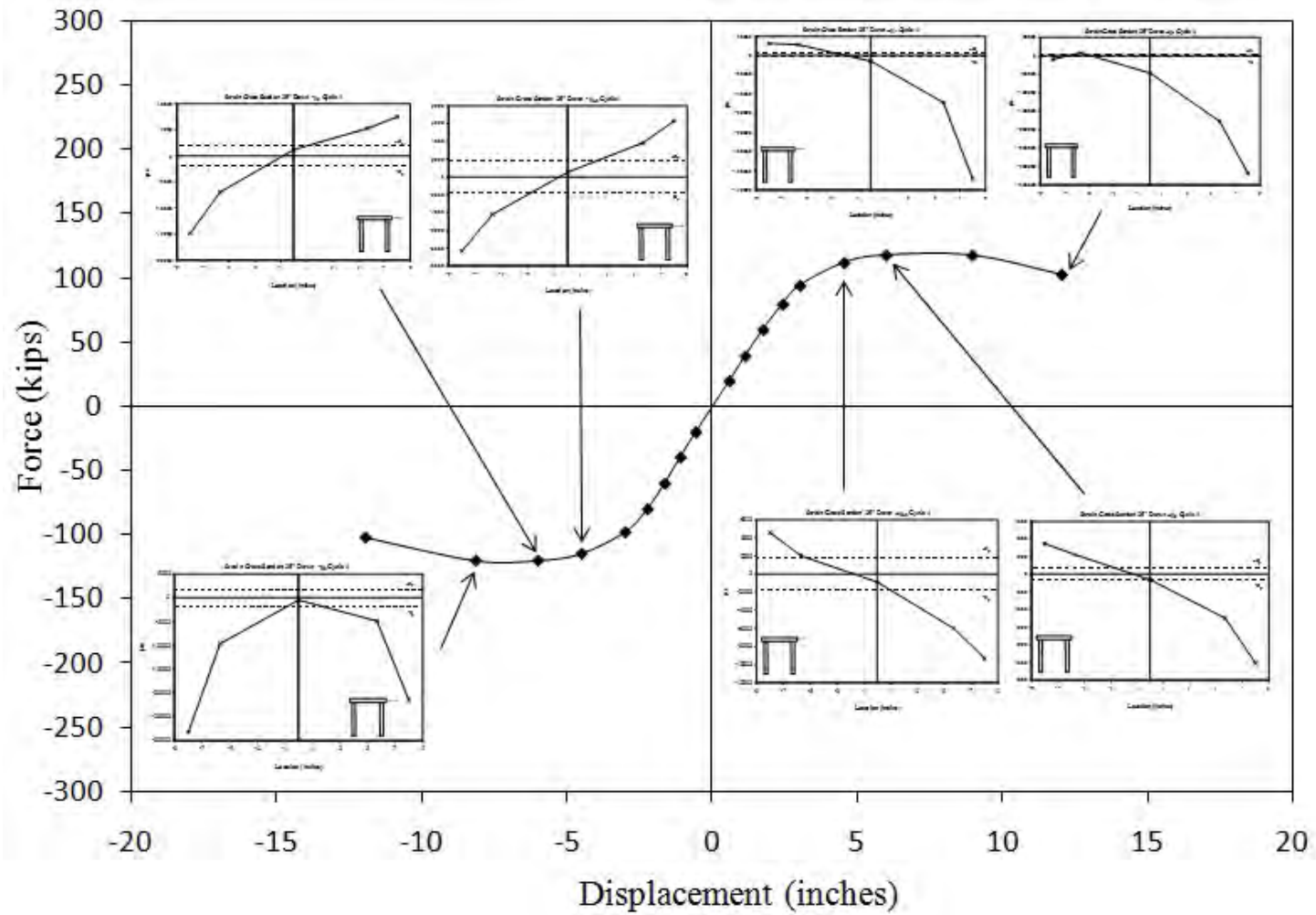


Figure 6.33 Force – Displacement/Buckling Comparison – Cycle 1

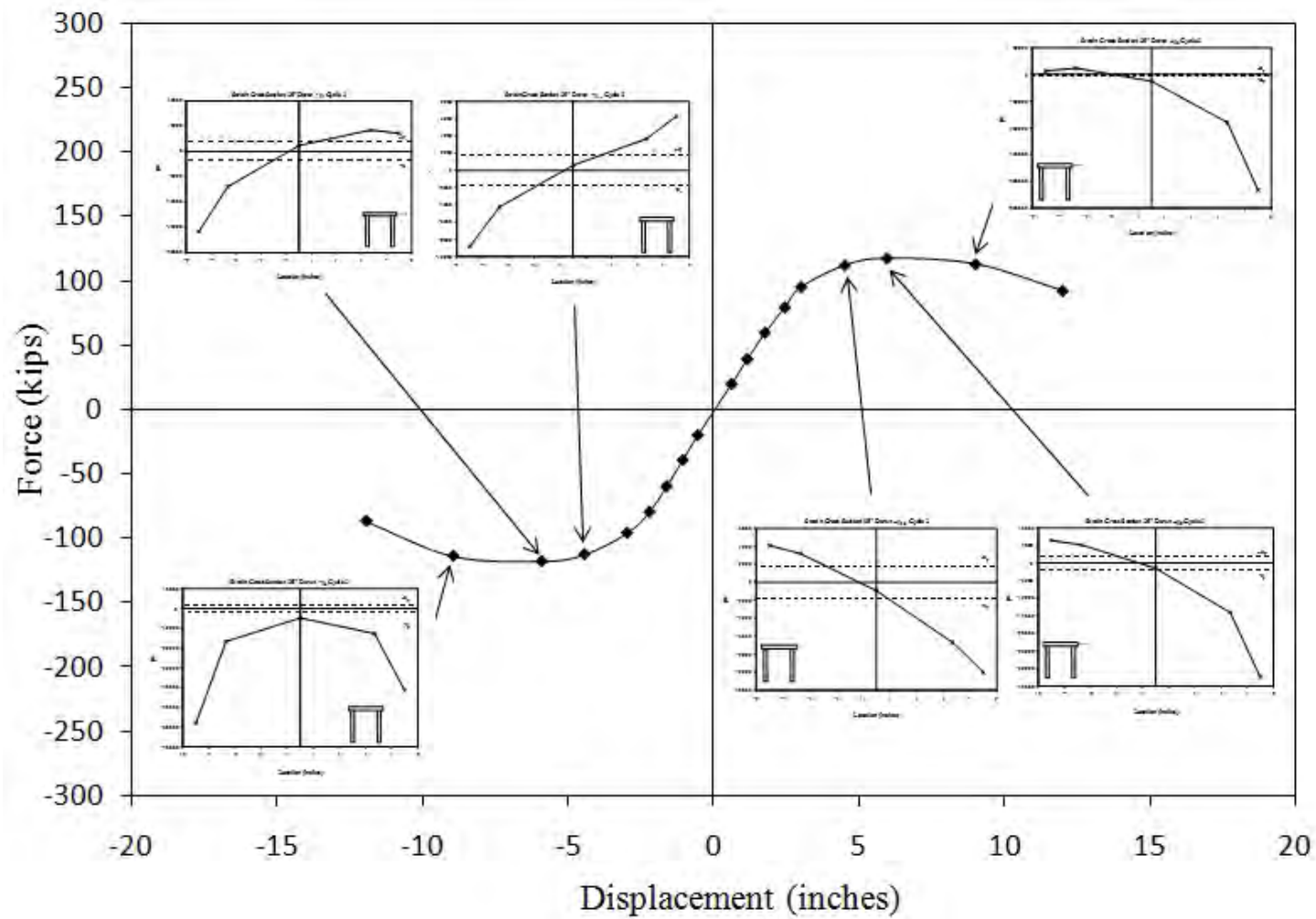


Figure 6.34 Force – Displacement/Buckling Comparison – Cycle 2

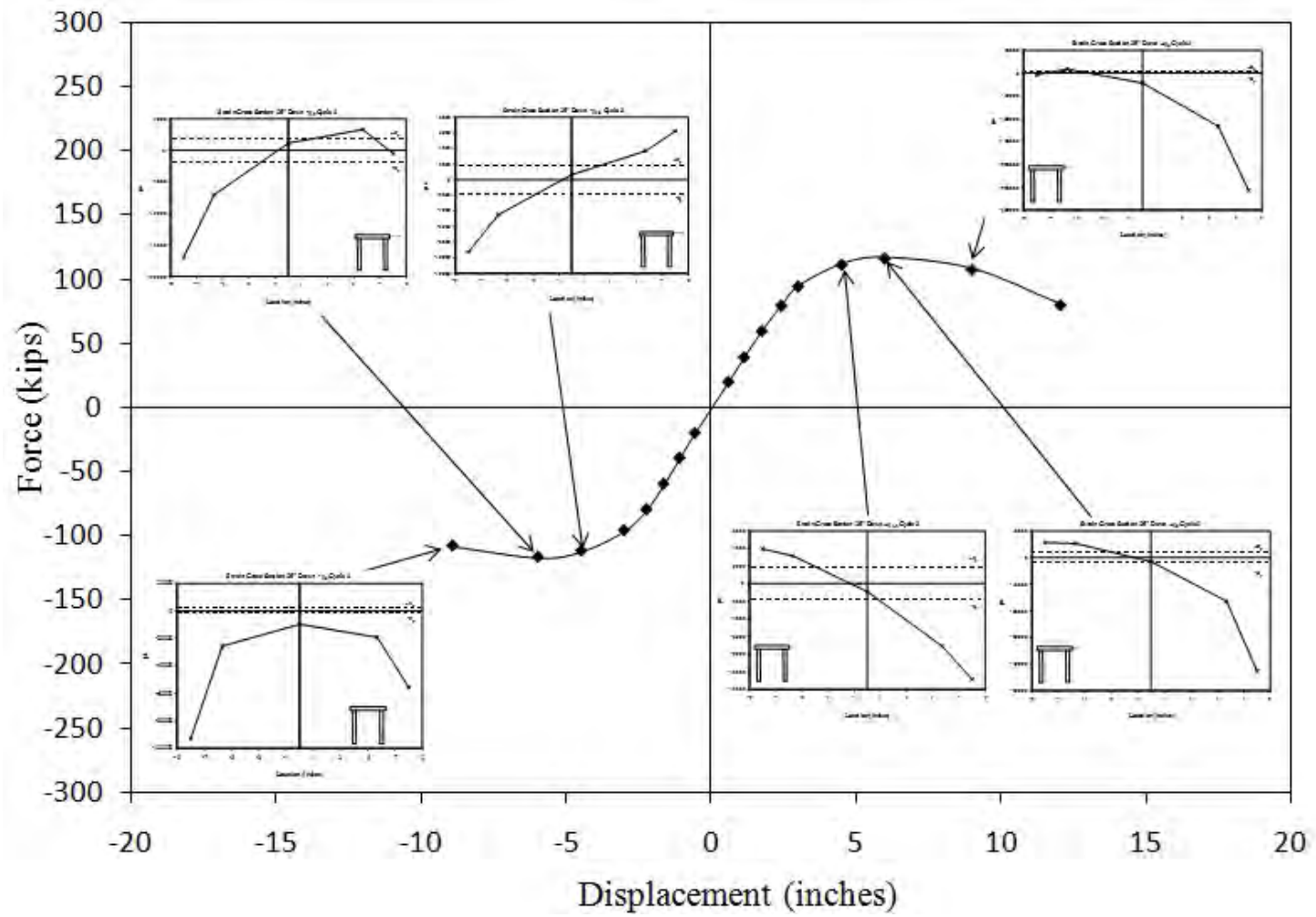


Figure 6.35 Force – Displacement/Buckling Comparison – Cycle 3

6.3 Performance of the Flared Column Capital

As was discussed in Chapter 3, test 6 was successful in relocating the plastic hinge region by forcing local buckling to take place below the column cap beam connection. This was achieved by the use of a flared column capital shown in Figure 6.36. However, as can be seen in Figure 6.37, the local buckling that developed was located below the intended turned down region of the column capital. This effect was seen on both columns. It should be noted that dimensions of the turned down section matched that of the actual pile as did the design strength column capital material. Considering this, along with basic structural analysis that indicates a higher moment demand above the splice weld, buckling theoretically should have taken place in the intended region.



Figure 6.36 Flared Column Capital Prior to Testing



Figure 6.37 Observed Local Buckling in Test 6

An initial hypothesis existed that the entire column capital may have been acting as a rigid stub as opposed to a flexural member for some unknown reason. Although this may not seem logical, it would easily explain the why buckling took place at the observed location. However, from Optotrak data, vertical strain profiles have been developed and indicate the capitals were, in fact, acting as flexural members developing strains similar to what would be anticipated by flexural analysis.

As can be seen in Figure 6.38 through Figure 6.41 the flared column capital remained essentially elastic developing strains near the yield value at the top of the capital. Also as anticipated, the turned down section developed significant inelastic tensile strains. Contrarily, the turned down section developed little compressive inelastic strain while the pile section below the splice weld developed both significant tensile and compressive strains. Taking this into account it is understandable that local buckling, which is of course a compression related failure mode, would take place below the intended hinge region. It is likely that the presence of the splice weld incorporated with the backing ring and the effect of the flared section above, stiffened the intended hinging region in compression. It should be noted though, that from the relationship between non-linear strain diagrams and local buckling developed in the prior section, it does appear that

the intended hinge region was experiencing the onset of local buckling. This can be seen in Figure 6.46 and Figure 6.47.

Figure 6.42 through Figure 6.45 created using traditional strain gauge data, indicate that a similar situation existed on the north pile as would be expected. Unfortunately, these graphs are not as refined since they are based a lower number of data points and may not lead to a clear conclusion on their own, but are use full in support of the conclusions drawn from the Optotrak strain profiles.

From the conclusions made in this section, it is reasonable to assume that by increasing the length of the turned down section, buckling would take place where intended. Alternatively, it is also likely that using weaker material in the turned down section would likewise control the location of buckling. A combination of the two would likely also be effective. It is important to note, that no adverse effects were observed during this test due to the location of local buckling occurring further down the pile than anticipated. The desire to precisely control the location of local buckling is ultimately a function of protecting the splice weld. The splice weld experienced no damage during this test and hence no adverse effects were experienced from the location of buckling. However, it would be difficult to ensure the principles of capacity were fulfilled if the precise location of local buckling was not confidently established.

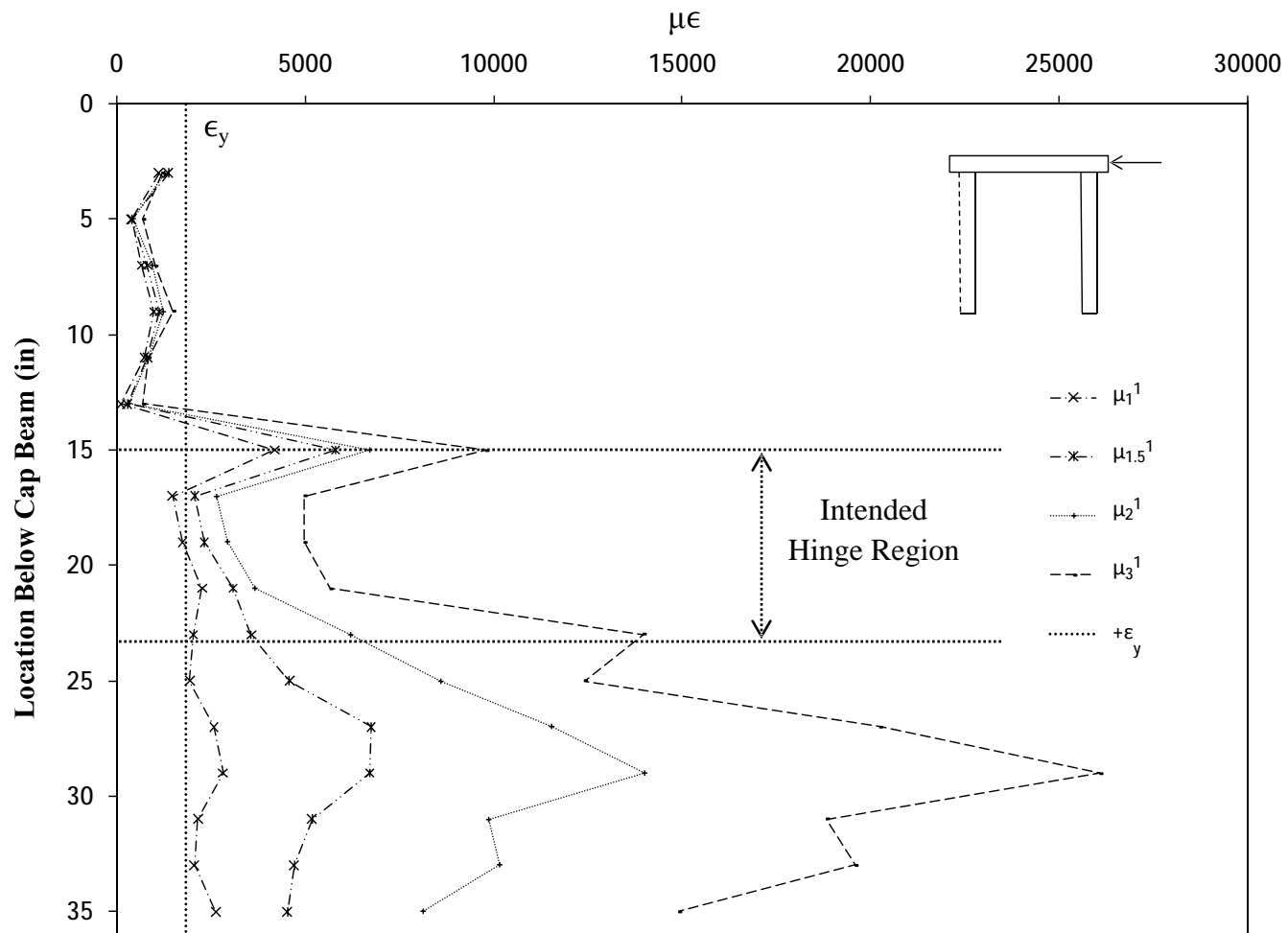


Figure 6.38 Optotrak Vertical Strain Profile – South Column South Face Push Direction

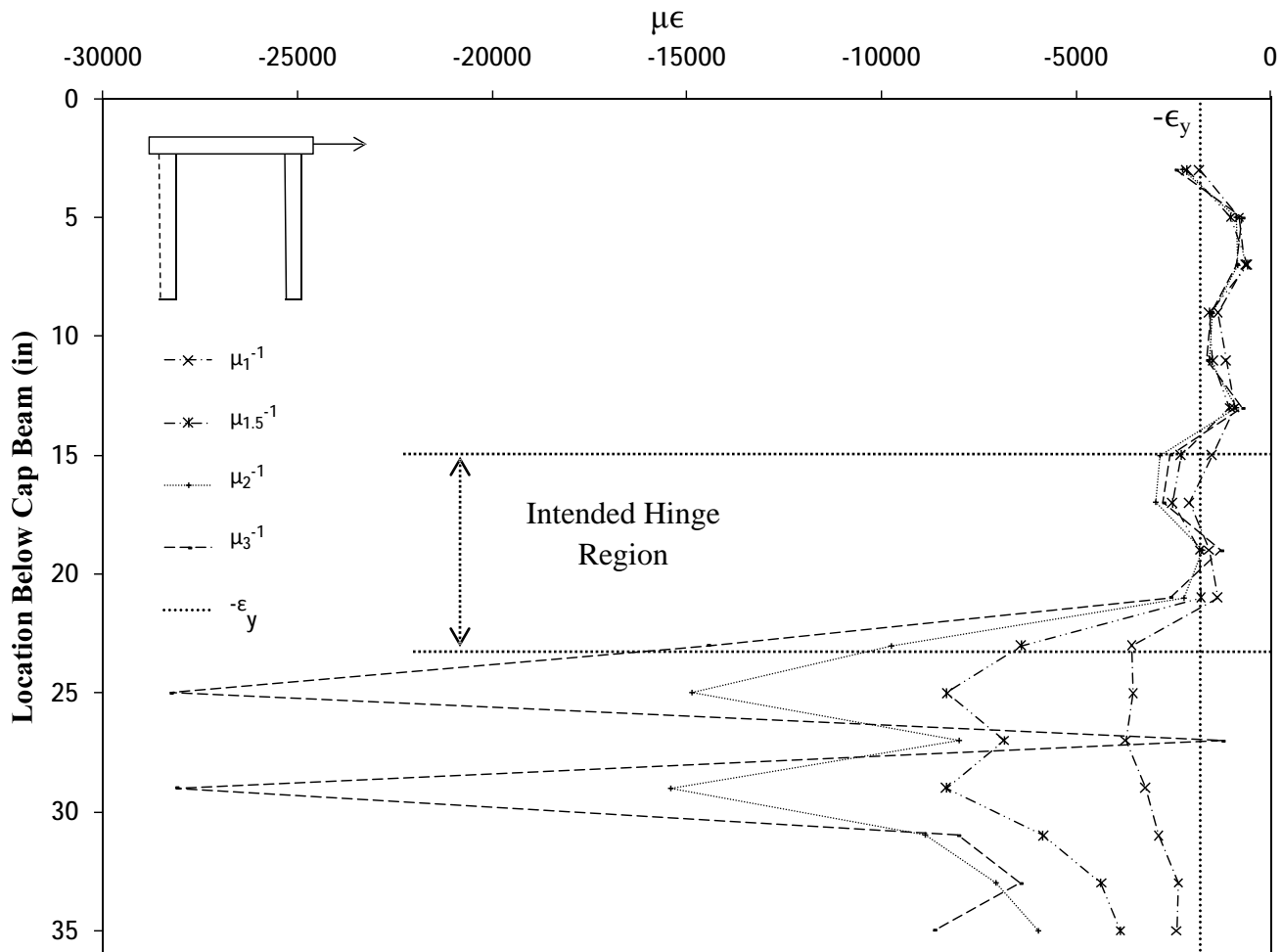


Figure 6.39 Optotrak Vertical Strain Profile – South Column South Face Pull Direction

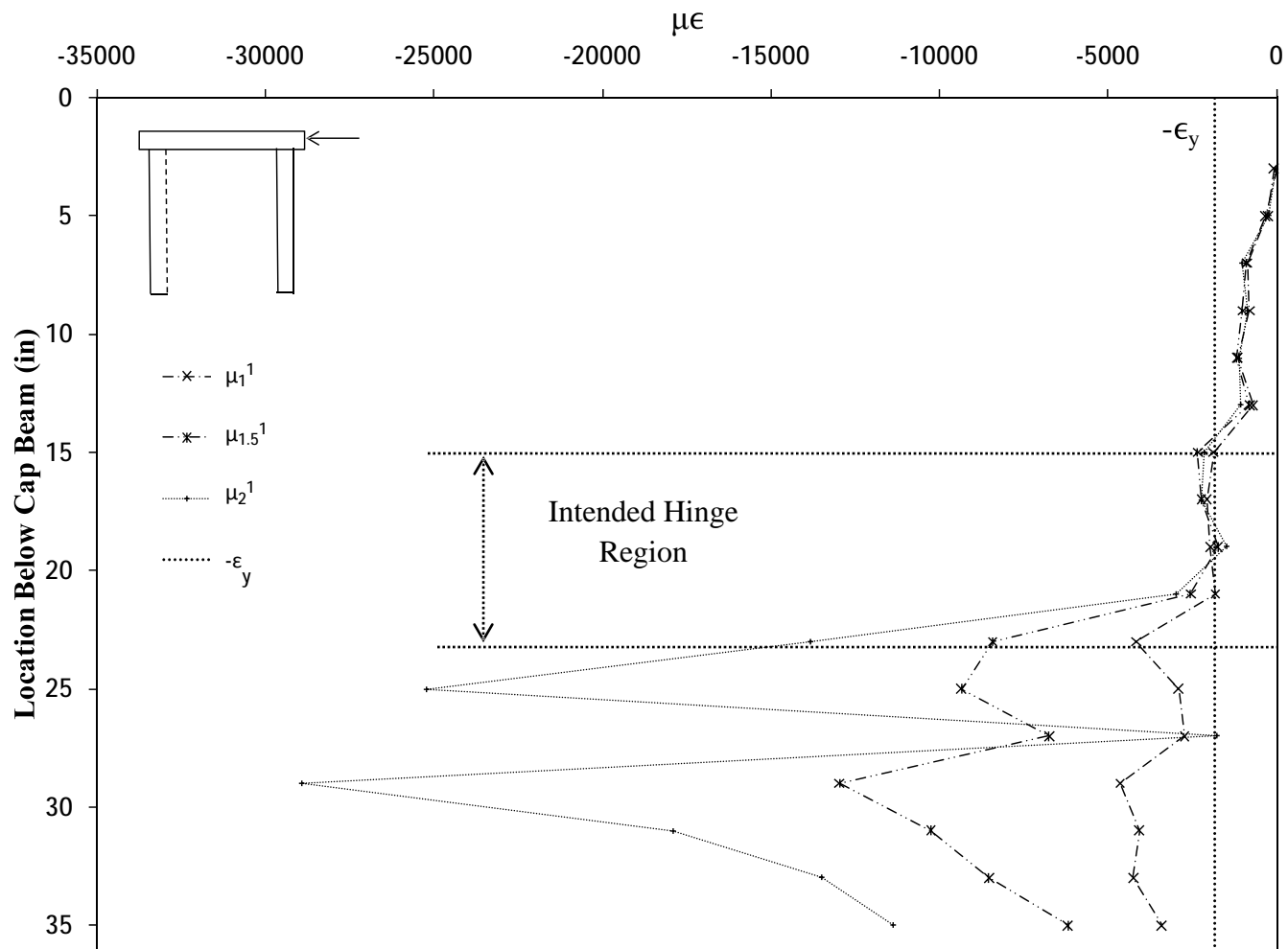


Figure 6.40 Optotrak Vertical Strain Profile – South Column North Face Push Direction

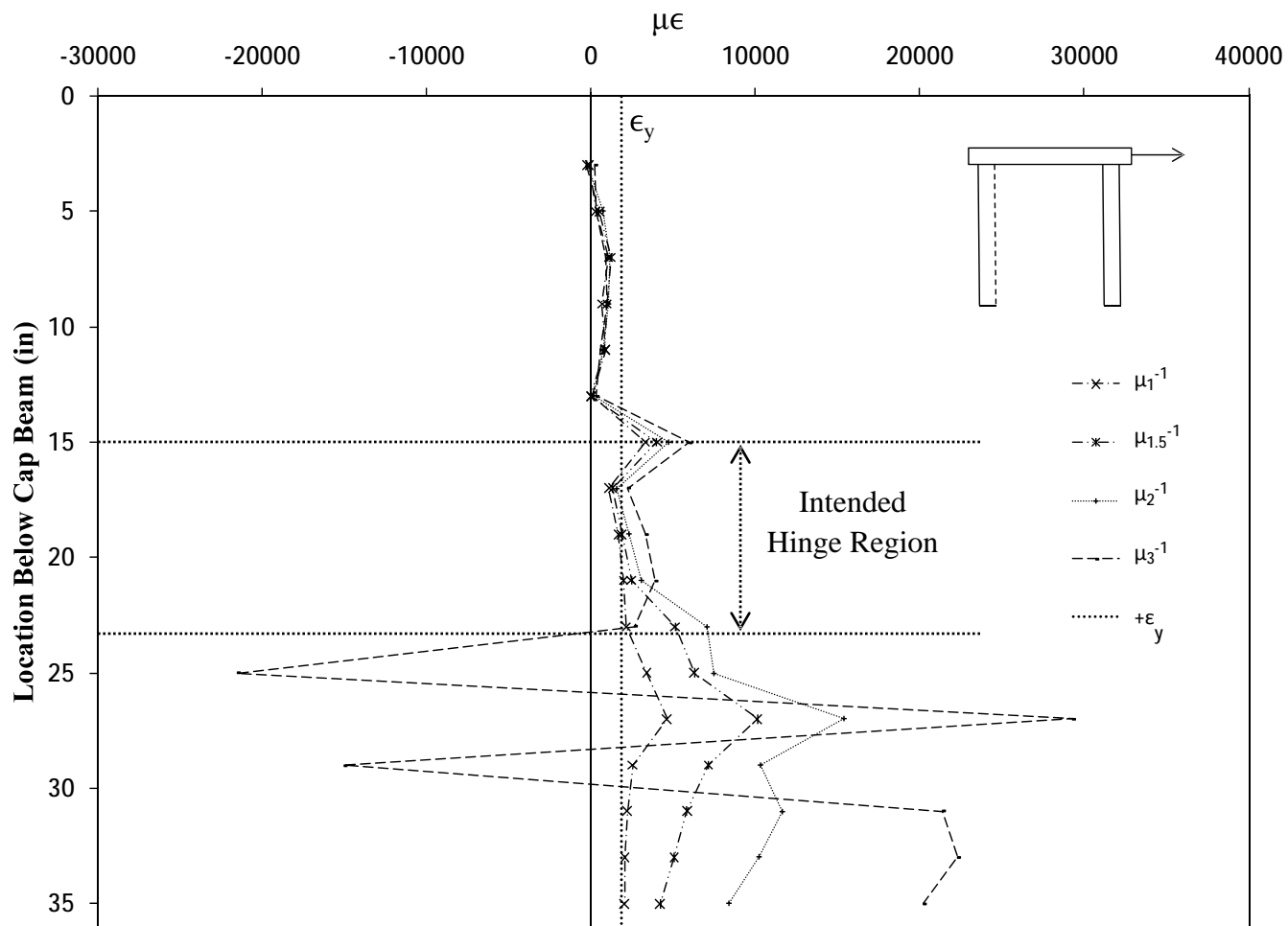


Figure 6.41 Optotrak Vertical Strain Profile – South Column North Face Pull Direction

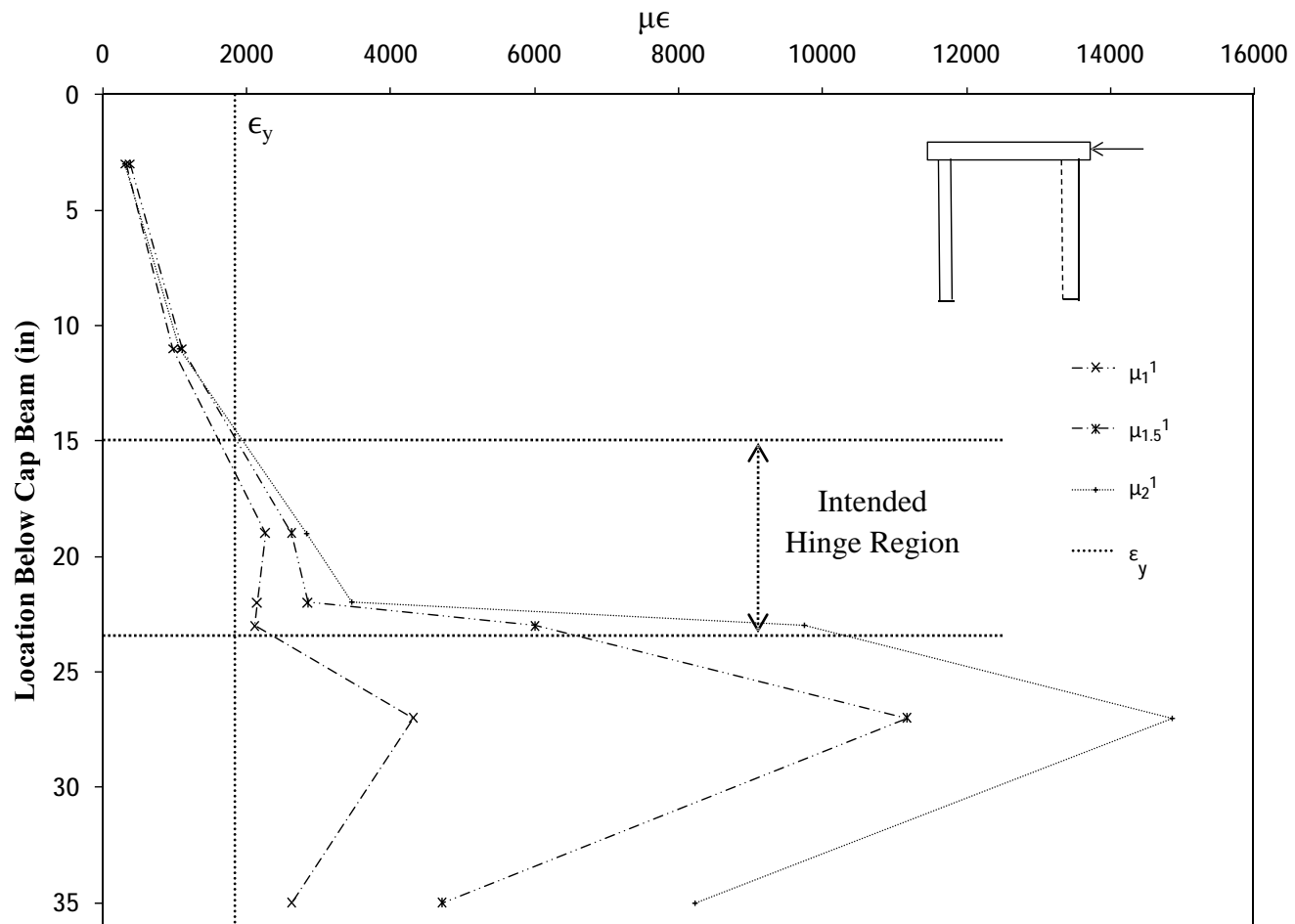


Figure 6.42 Strain Gauge Vertical Strain Profile – North Column South Face Push Direction

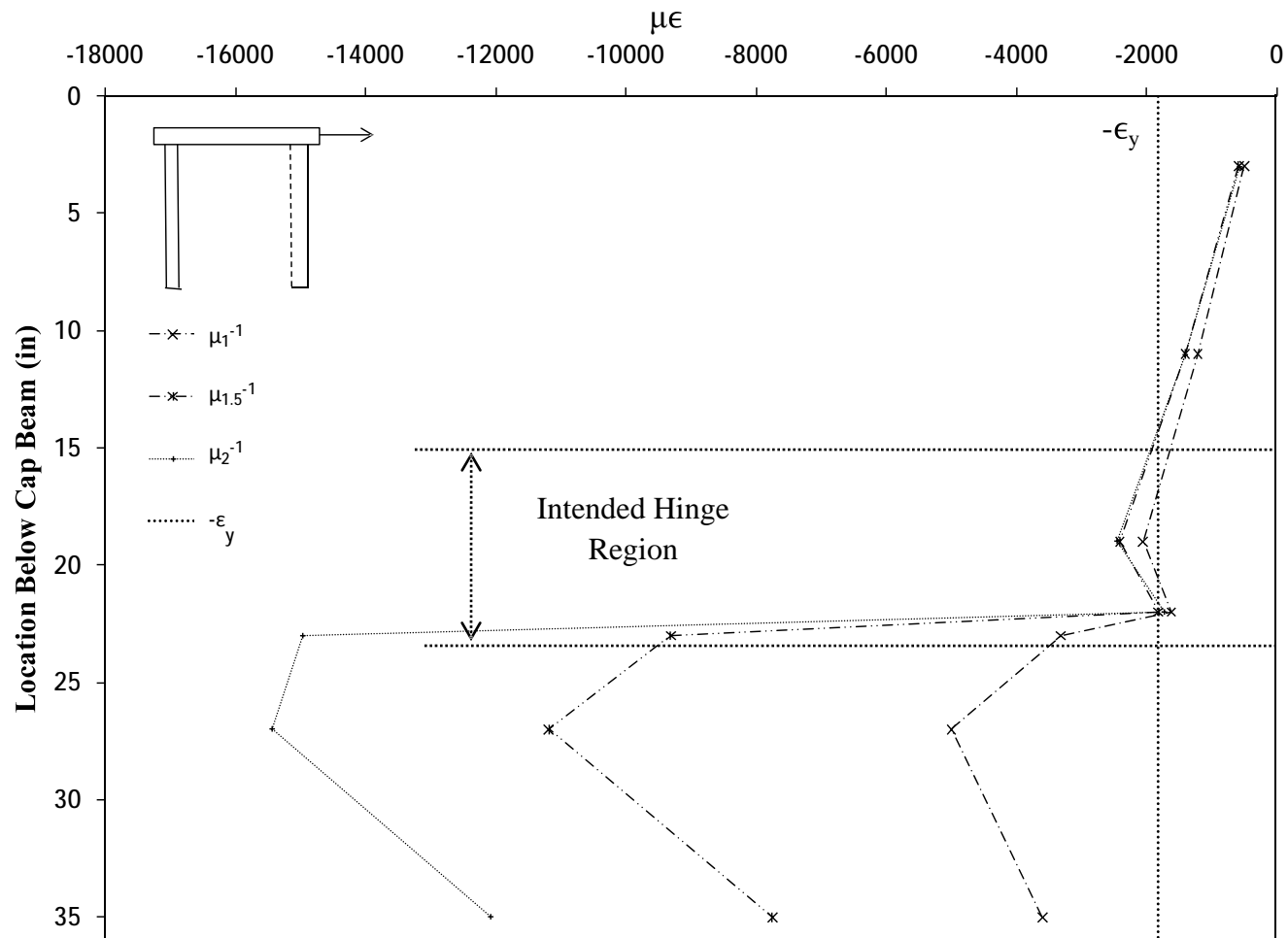


Figure 6.43 Strain Gauge Vertical Strain Profile – South Column South Face Pull Direction

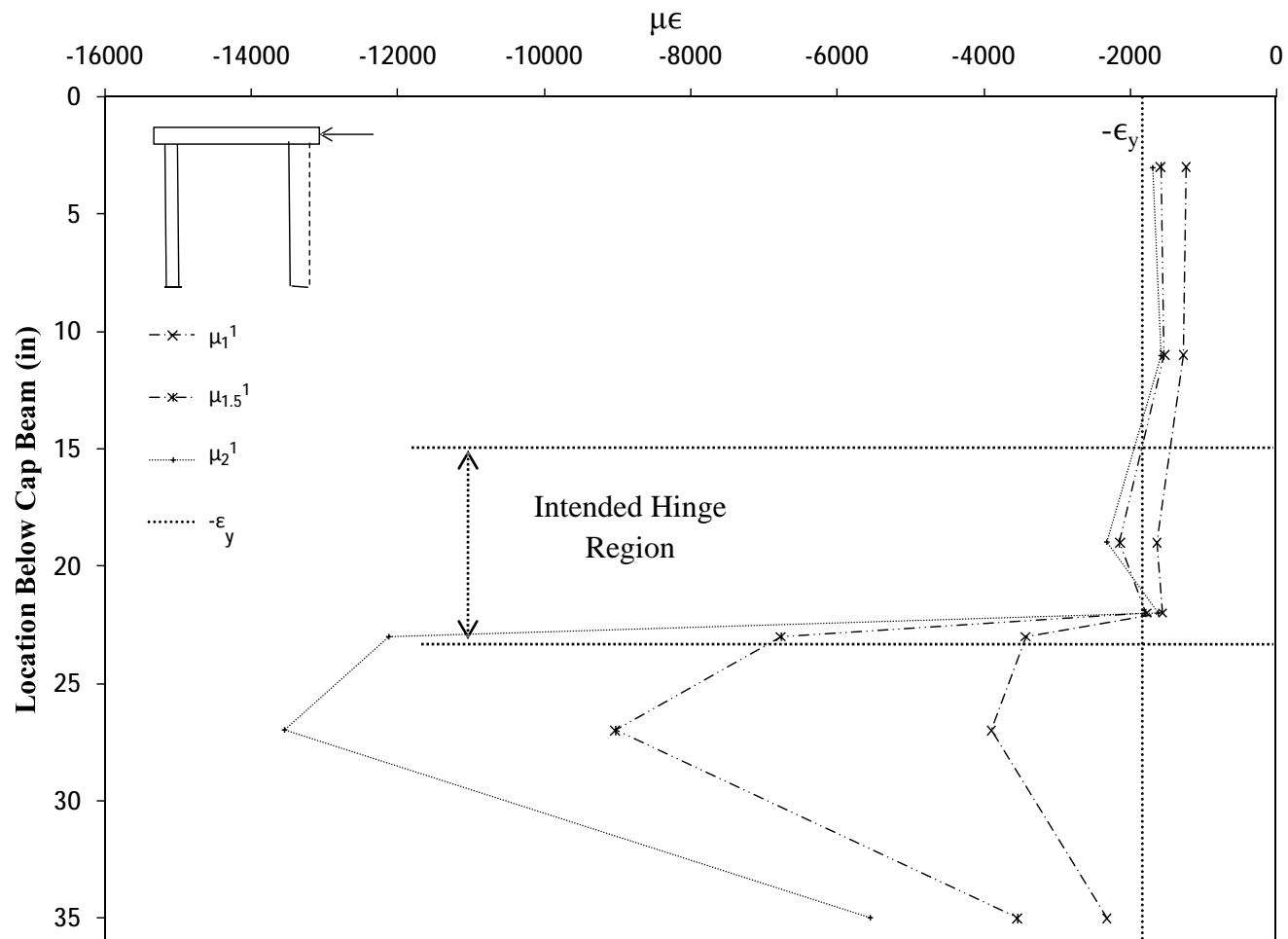


Figure 6.44 Strain Gauge Vertical Strain Profile – North Column North Face Push Direction

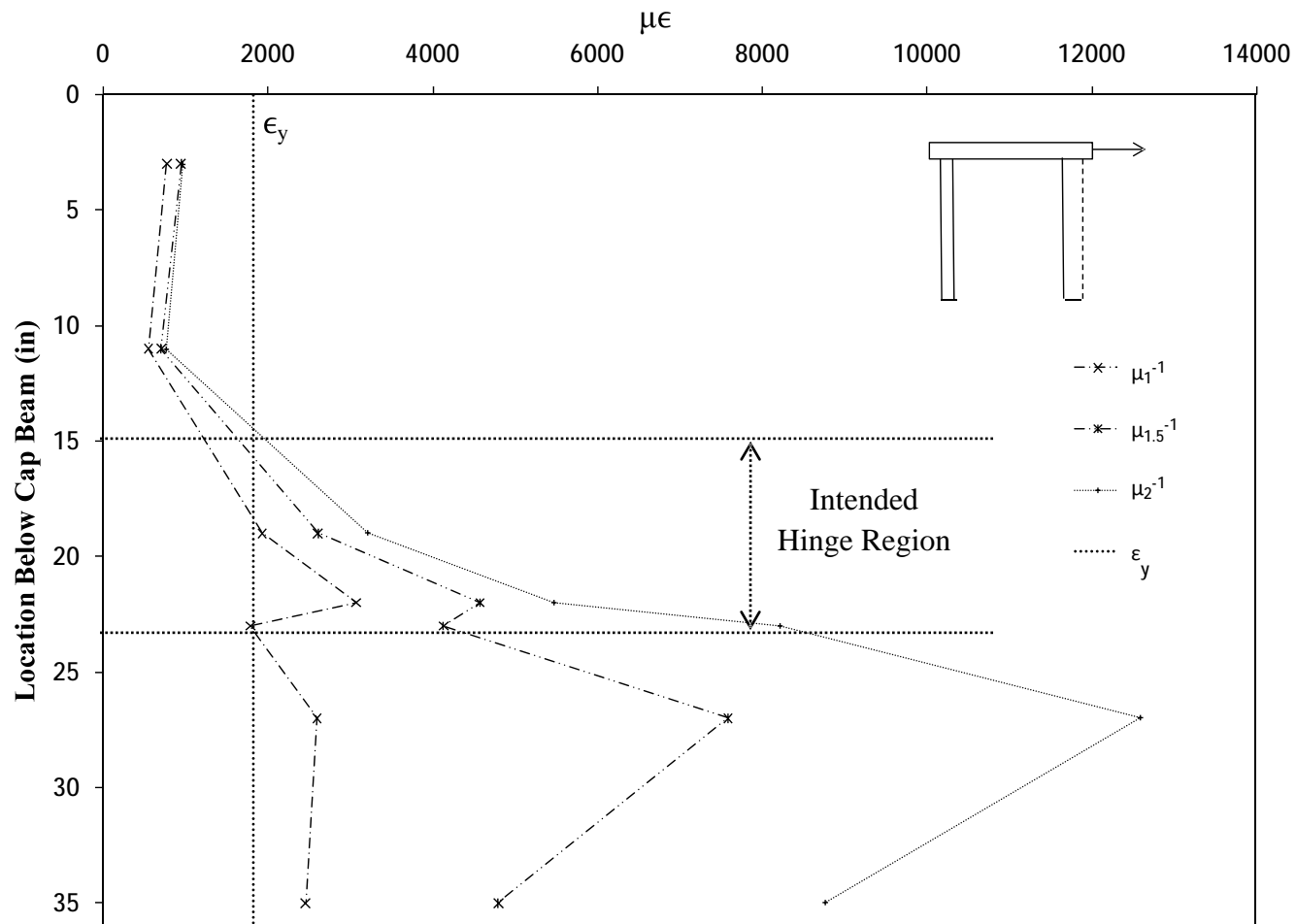


Figure 6.45 Strain Gauge Vertical Strain Profile – North Column North Face Pull Direction

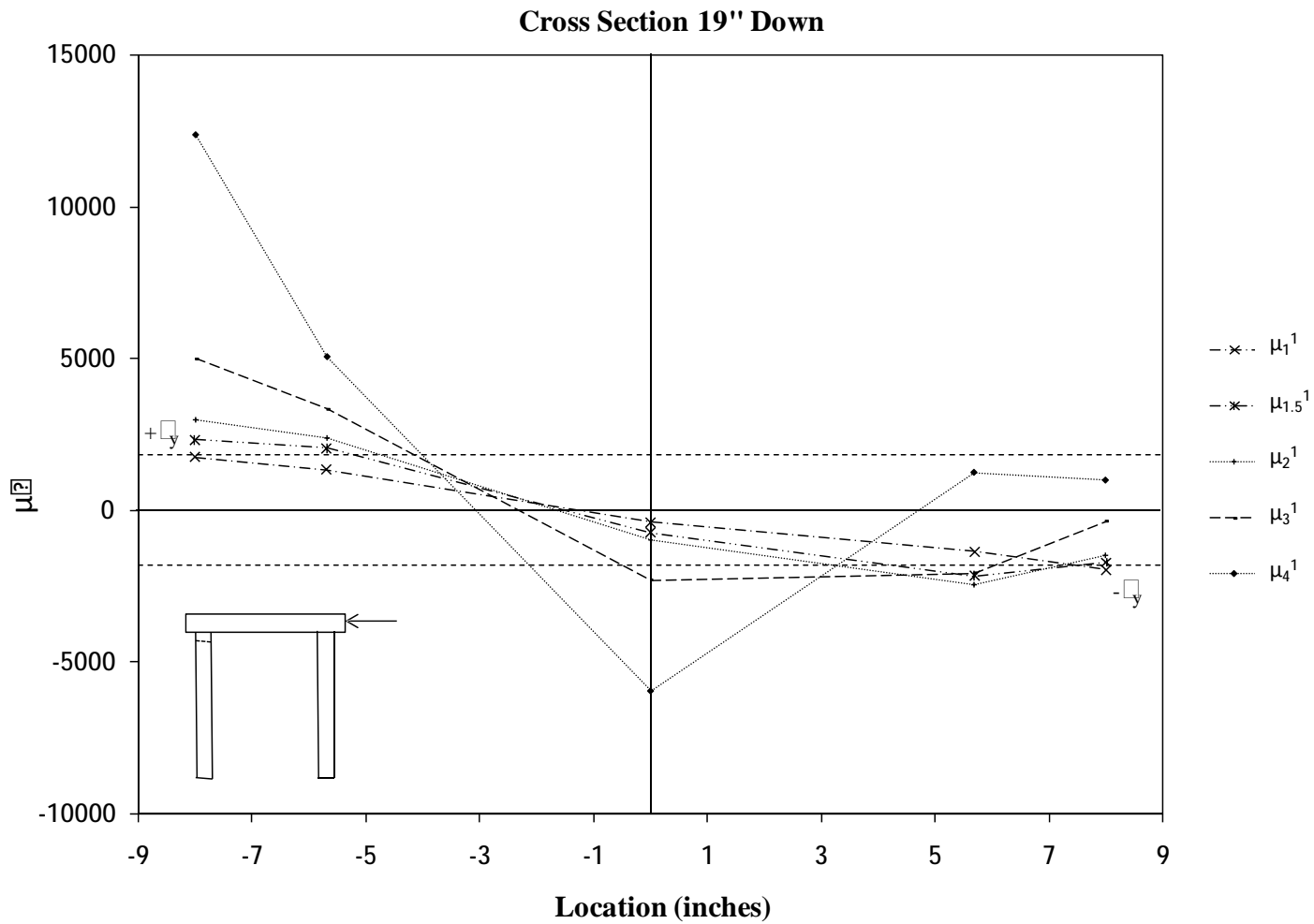


Figure 6.46 Strain Cross Section Diagram—19" Down the South Pile—Push Direction

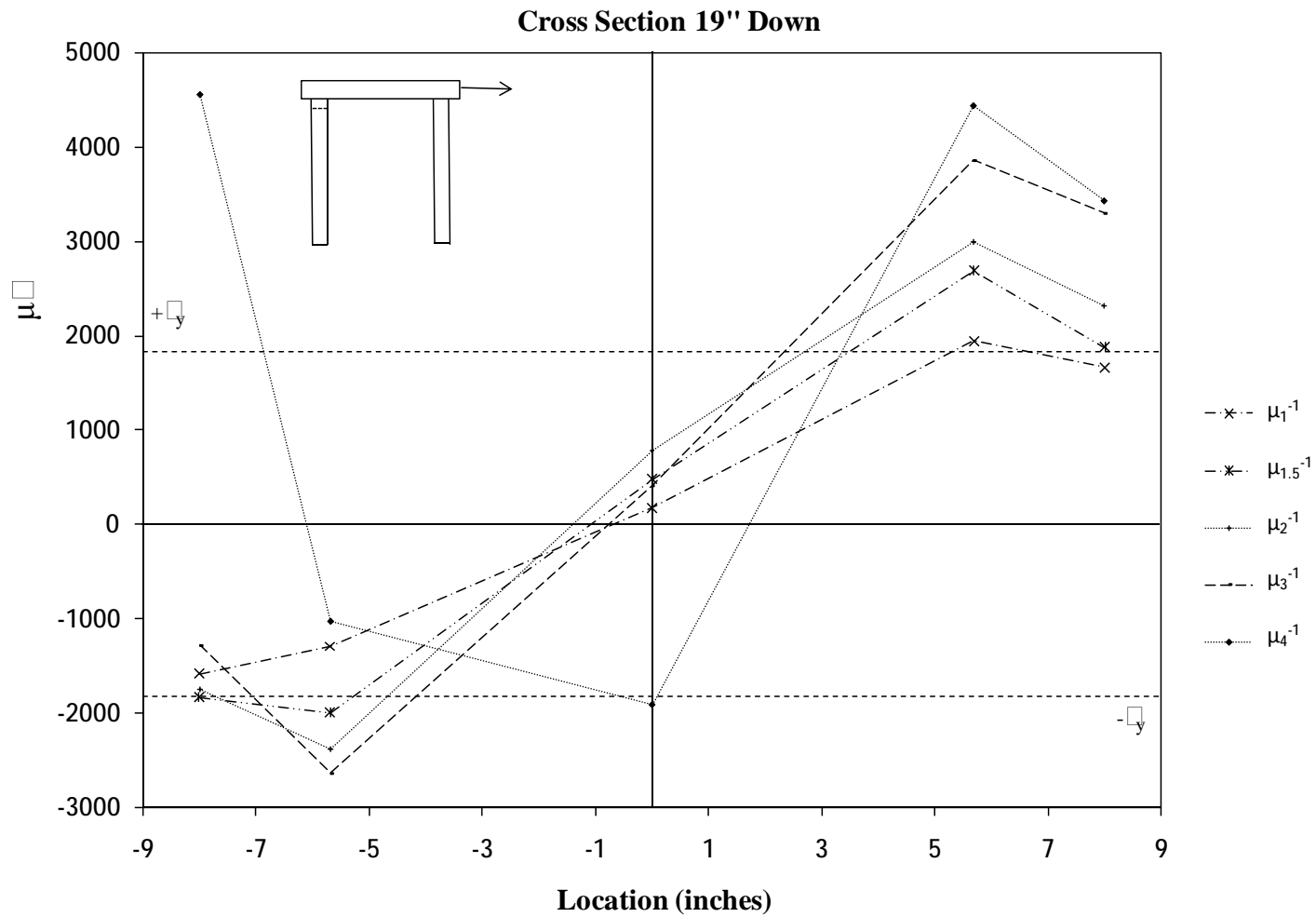


Figure 6.47 Strain Cross Section Diagram—19" Down the South Pile – Pull Direction

6.4 Effects of Joint Panel Zone Shear

During the testing of specimen 6, the inclinometers which were placed on the cap beam/pile centerline intersection as can be seen in Figure 6.48 Location of Inclinometers fell off during the early stages of inelastic loading. Although the loss of valuable data is undesirable, the event did lead the research team to investigate the magnitude of joint rotation that was taking place during testing prior to the loss of these gauges. By plotting the rotation reading of the inclinometer versus structural displacement a joint rotation hysteresis can be generated as shown in Figure 6.49 and Figure 6.50. Appropriate conclusions can then be drawn from these figures.

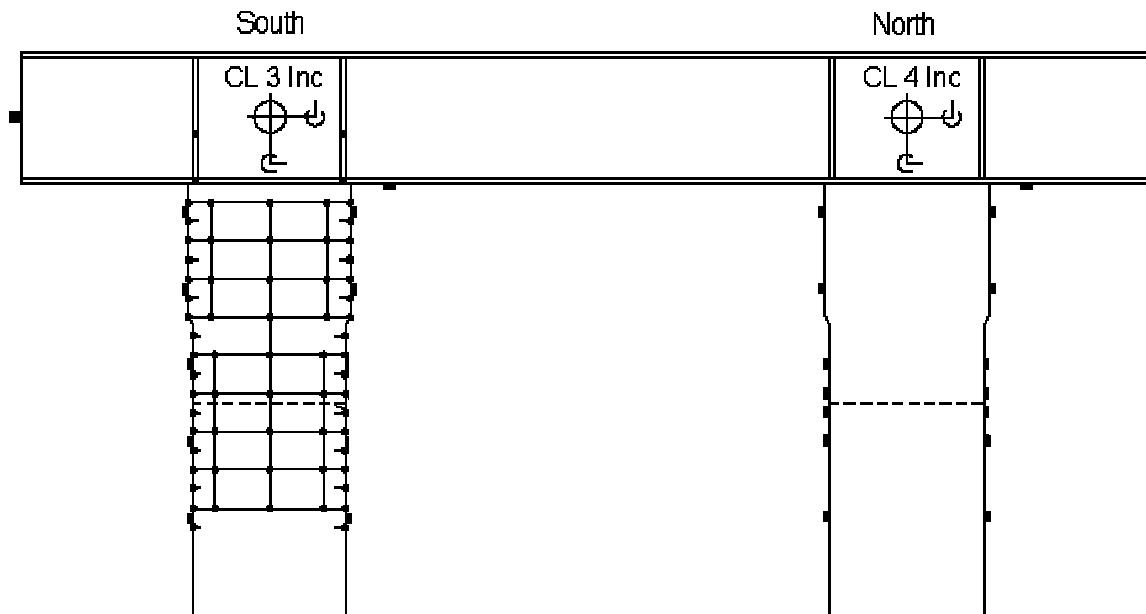


Figure 6.48 Location of Inclinometers

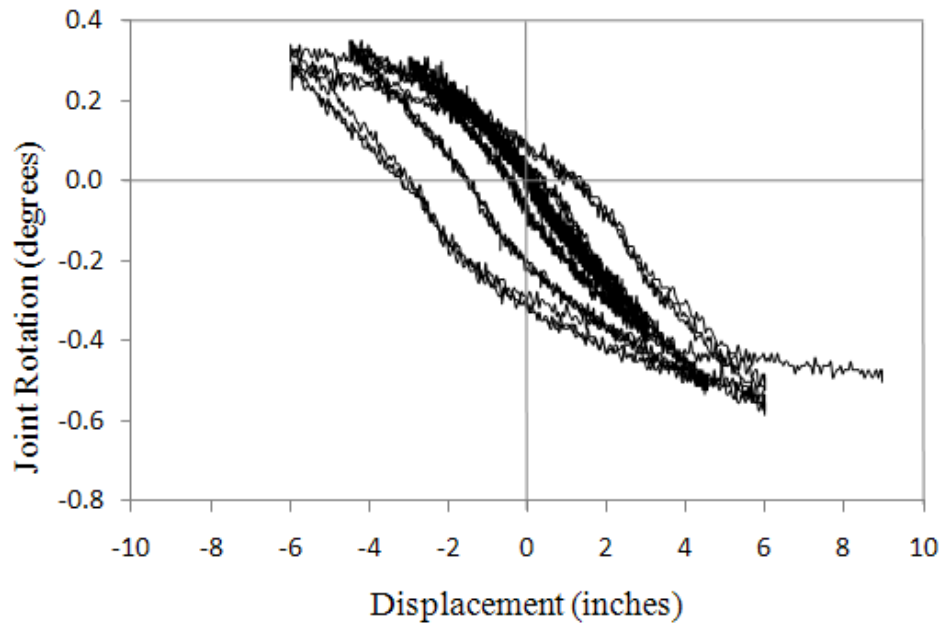


Figure 6.49 Test 6 – North Joint Rotation Hysteresis

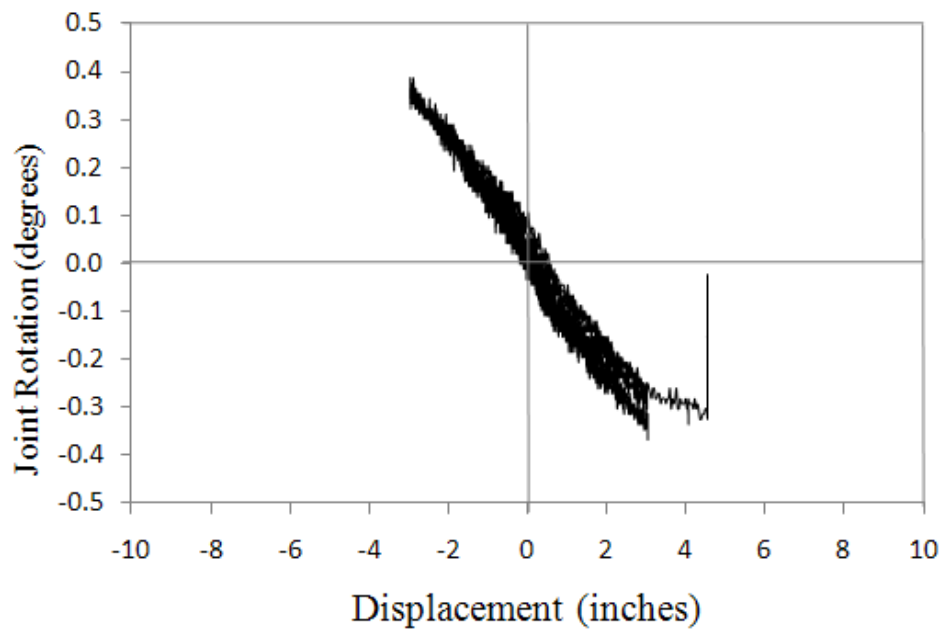


Figure 6.50 Test 6 - South Joint Rotation Hysteresis

As is shown in the joint rotation hysteresis provided for test 6, inelastic rotation at the location of the inclinometers was clearly occurring even during the low ductility cycles. The recorded joint rotations at first yield in the push direction for the north and south column joints were -0.288 degrees and -0.291 degrees respectively. In the pull direction at first yield these values were recorded as 0.247 degrees and 0.280 degrees, clearly in good agreement. However, the predicted joint rotation from centerline modeling (including all applicable typical modes of deformation: flexible cap beam, member shear deformation, etc) was found to be +/- 0.1606 degrees. This indicates that the actual joint rotation experienced at first yield was approximately 75% greater than the predicted value.

Considering that that the cap beam was designed to remain elastic (and did outside the joint as is shown in Figure 6.51) it is possible that the additional joint rotation is a result of large panel zone shear strains within the web of the beam. This would at least explain a portion of the higher than expected yield displacements that were experienced during testing since this mode of deformation would not be captured by a centerline model. It should also be noted that the presence of large/inelastic joint rotations was not limited to test 6. This effect was also experienced in prior test as shown in Figure 6.52.

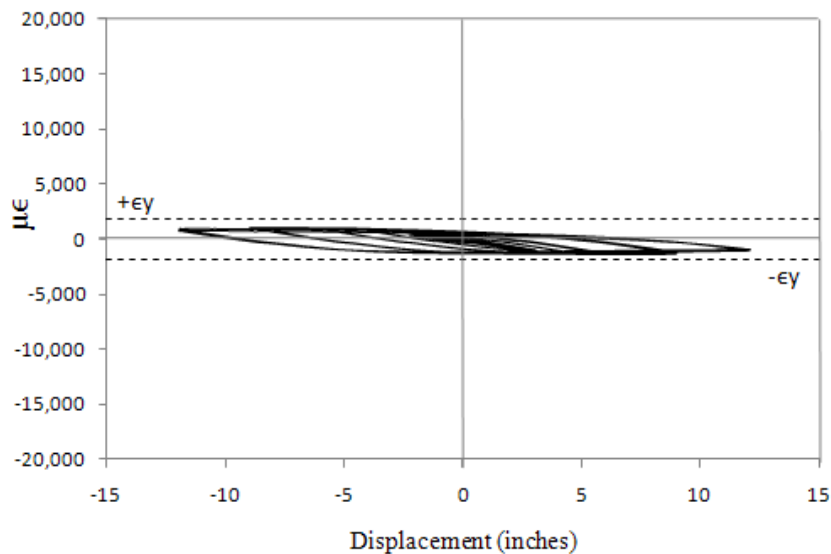


Figure 6.51 Strain Gauge Hysteresis - Bottom Flange of Cap Beam at South Column

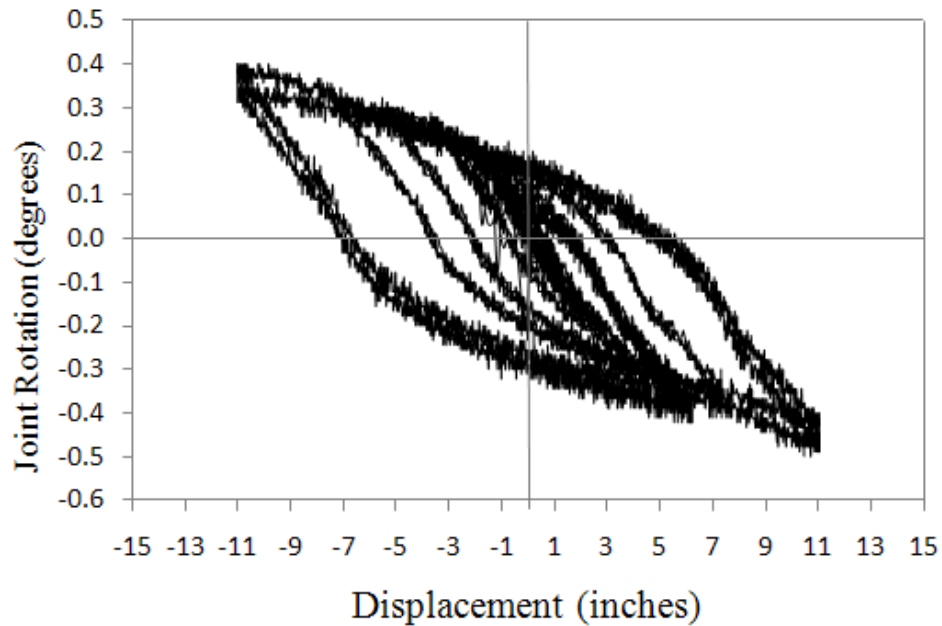


Figure 6.52 Test 5 – South Joint Rotation

Assuming that the hypothesis of panel zone shear is correct, it would be possible to eliminate this mode of deformation by adding web stiffener plates or utilizing some other method of stiffening the region. Although this would allow for a simple model to more accurately predict the displacement of the structure, the additional deflection due to the panel zone shear is not necessarily a negative effect. This displacement will increase the reliable displacement of the system and improve its seismic performance. However, caution should also be taken to consider the capabilities of the system to perform with this inelastic action. In this testing series no adverse effects were noted from the presence of the inelastic panel zone shear but should a designer desire to ensure that every part of the cap beam remain elastic to reduce damage, web doubler plates would be necessary in addition to the stiffener plates used in the test specimen.

6.5 Development of a Finite Element Model

The development of a finite element model (FEM) is planned in particular for the purpose of verifying the results obtained in test 6. The model will likely utilize advanced shell elements and represent the entire bent to capture the highest accuracy possible. It is desired by the research team to verify the effects of panel zone shear as well as the capabilities of the flared column capital to control strains at the cap beam column interface. The use of the model will likely also include verification of failure modes from test 1-5 and more importantly predict the capabilities of other connections systems which will be discussed in further detail in Chapter 7.

General Conclusions and Design

Recommendations

7.1 General Conclusions of the Research Program

As has been discussed throughout this report, the failures observed during testing of the first 5 specimens would generally be considered unsatisfactory. Although test 2 began to develop desirable base material failure modes, the ultimate failure was still related to the welded connection. In addition to this issue, the results of this test were not found to be repeatable in test 4. It may seem that these tests lacked ductility capacity but with the exception of test 1 the specimens were able to endure moderate amounts of displacement or drift. This point is not provided to indicate that the structures tested in tests 1-5 may in fact be satisfactory but rather to highlight the importance of observed failure modes. In all cases for tests 1-5, the failures occurred in a rapid manner (within the cycles of a single ductility level) and were related to weld cracking which is clearly an undesirable failure mode considering the principles of capacity design and the desire to fully utilize a structures capability.

However in the case of test 6, a higher ductility capacity as well as a desirable failure mode were produced by relocating the location of hinging. Although the specimen was only able to reach a reliable ductility capacity of 4, this corresponds to approximately 8% drift which is a considerable displacement as has been discussed in earlier sections of this report. Regardless of this, the more significant achievement of tests 6 was the successful production of a base material failure. Although a more optimal design of the flared column capital should allow for more accurate locating of plastic hinging, the test was successful in showing that relocating the hinge will help prevent brittle connection failure. Ultimately, it is felt by the research team that weld configuration alone will not produce a reliable steel bent structure for a moderate or high seismic region.

7.2 Design Recommendations for Hollow Steel Pipe Pile to Cap Beam Connections

As has been discussed, the results of the six full scale bent tests indicate that brittle connection cracking is likely for any weld configuration without direct consideration of strain control at the pile cap beam interface. As a result of testing observations and data analysis it is the recommendation of the research team that direct consideration for the relocation of hinging away from the welded cap beam/pile joint be made for the design of any steel bent expected to endure inelastic displacements. It is further recommended that a proper design should allow for the strains experienced at the cap beam/pile interface to remain essentially elastic when subjected to the full over strength moment capacity of the intended hinging location as was the case of test 6. However, it should be noted that although sufficient data exist indicating that weld configuration alone will not produce reliable results (test 1-5), the favorable results obtained by the plastic hinge relocation method (test 6) have not yet been verified in subsequent tests. Nonetheless, the research team feels that this method would prove to be reliable in further testing as similar methods have worked well in building design where reduced section W-shapes are used to control locations of hinging.

However, this recommendation only indicates that the relocation of hinging will produce a favorable base material failure not necessarily an adequate response. The ultimate capacity of the section will be dependent upon member parameters such as D/t ratio. Consideration must also be given to the quality of all welds utilized and control of construction tolerances. In this testing series the minimum requirements of the AWS D1.1 code were considered and an emphasis was placed on minimizing construction tolerances while maintaining realistic construction practice. Significant increase in construction tolerance issues and utilization of welds with quality less than that indicated by applicable codes will possibly jeopardize the capabilities of the hinge relocation method.

It should be noted that methods other than the relocation of plastic hinging exist which may also produce adequate response. The relocation of hinging method has been recommended as the most applicable method for retaining the simple nature of the structure utilizing a weld at the pile cap beam interface. Alternate methods which may produce adequate response include, but are not limited to, post tensioning systems,

pocketed type connections, and kerf type connections as will be discussed in subsequent sections of this chapter.

7.3 Consideration of Pipe Buckling Under Pure Bending

Consideration should be given to the general limit states of circular HSS members subjected to pure bending with no boundary condition effects. This situation would somewhat capture the condition of a plastic hinge relocated at a significant distance from the fixed end or a plastic hinge formation occurring at the point of fixity of a driven pile. Similar limit states will exist between this condition and the fixed end condition tested including local buckling, strength loss, and cracking associated only with base metal.

The physical differences between the two conditions are the presence of axial load and boundary condition effects. It is likely that the boundary condition effects will have a greater impact on any variation in member failure mode response considering the nature of the axial load being relatively low. However, it should be noted that this is only a hypothesis and is not supported by any analytical or physical research.

A research project conducted at North Carolina State University shortly after the completion of lab testing of the steel bent project, focused on the pure bending performance of hollow circular HSS sections. In that research, specimens with D/t ratios varying from 36-55 were tested under four point bending. The specimens ranged from 18 – 24 inches in diameter and were all 36 feet long.

Although the ultimate ductility capacity of those members was moderately sensitive to the D/t ratio, as would be expected, the ultimate failure modes were all similar. In each case, very rapid local buckling took place within the constant moment region of the test specimen as is shown in Figure 1.1. This local buckling was also associated with significant immediate strength loss as shown in Figure 7.2. Data analysis utilizing the strain linearity method has not yet been conducted to determine if small magnitudes of local buckling were actually occurring before this rapid onset of large local buckling. However, in no case were any clear visual signs of local buckling noted before this time. In each case eventual material rupture occurred near this location of local buckling although the strength loss was already large.



Figure 7.1 Example of Local Buckling of a Pile Subjected to Pure Bedding

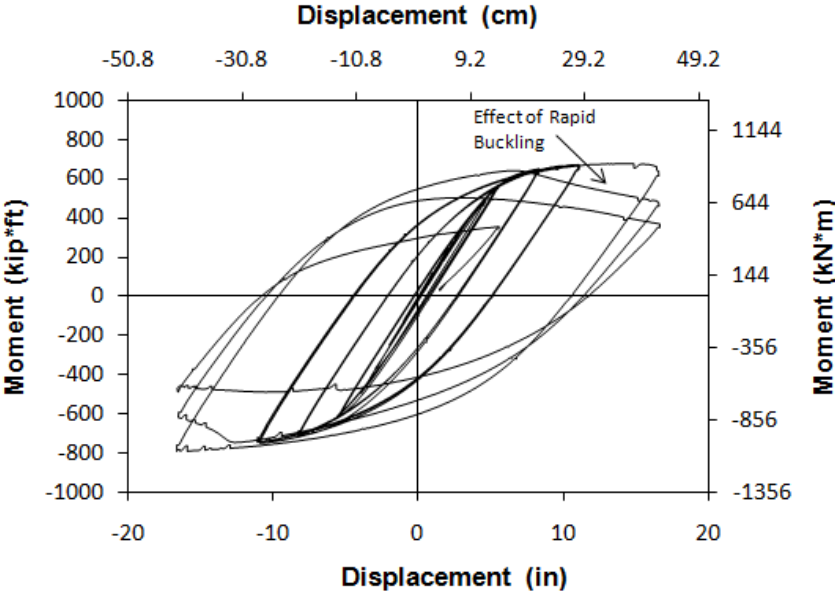


Figure 7.2 Example of Strength Loss Due to Rapid Buckling

The failure modes observed in this test are clearly different from those seen in the steel bent tests. Obviously no correlation exist between the pipe bending tests and the failures observed in tests 1-5 of the steel bent series since those failures were related to connection weld cracking. However, comparison can be made between this series and steel bent test 6 where base metal buckling and rupture occurred. In that case the buckling occurred in an outward circumferential manner over several cycles as was expected and desirable. In the case of pure bending the buckling occurred rapidly in an inward manner and was not circumferential. It is likely that this difference exists due to the fixed end condition of the steel bent test. Regardless of why this difference exist, it may be important to consider locations of pile hinging at significant distances from the cap beam as possessing different failure modes and reliable ductility than at a location near the cap beam.

7.4 Future Considerations

7.4.1 General Issues Related to Future Research

Three possible options exist in regards to future research. First, future considerations could solely focus on new designs by searching for an optimal configuration of the cap beam pile connection. Secondly, future considerations could focus on retrofitting techniques by only considering options that are applicable to existing structures. Lastly, a combination of consideration for both new and existing structures could occur simultaneously.

Benefits may exist in pursuing a retrofit solution since this solution would inherently also be applicable to new designs. However, restrictive limitations that exist in regards to altering an existing structure will likely cause any solution determined in regards to retrofit to be less optimal than that of a connection configuration developed by focusing on new design. For example, the reduction of the existing cross section of the pile may control the location of hinging and produce a more desirable failure mode. However, this will also weaken the structure which may or may not be a problem given the increased deformation capacity. Nonetheless, the same objective can be achieved for a new structure using a system such as the flared column capital which actually

strengthened the structure and increased the deformation capacity. Clearly separate benefits exist for either option.

Regardless of whether focusing on new design or retrofit, future research will likely include five major areas of study. One of the five major areas will of course include full scale testing as has been discussed in this report. Another task would focus on dynamic shake table testing of approximately ½ scale bents which could be conducted at North Carolina State University's Constructed Facilities Laboratory. Thirdly, environmental chamber testing could be conducted at the CFL on full scale single column specimens to evaluate the capabilities of any new connection configurations at extremely low temperatures. Fourth, finite element and global analytical modeling could be used to assist in the process of developing a new connection. Lastly, the methods described in the first four areas of study could be utilized to focus on construction tolerance and weld quality issues. It is envisioned by the research team that any future research projects will focus on a combination of these task utilizing full scale testing and analytical modeling to develop an optimal connection which could then be dynamically tested as well as evaluated at low temperatures.

7.4.2 New Design Options

As has been discussed, one possible option for future research would focus on new designs. Consideration has been given as to what possible connection configurations, out of the many options that are possible, would produce the best results with the least difficulty of construction. Four possible options have been provided that the research team feels have the highest likelihood of producing adequate failure modes. One of these options would utilize a pocketed type connection where the pile is passed through the bottom flange of the cap beam and welded to both the bottom and top flanges of the beam. Note that this is similar to the pocketed type connection used in the research discussed in "Retrofitting for seismic upgrading of steel bridge columns" which produced desirable base material failures. Secondly a kerf connection has been suggested which utilizes a cross plate member that is welded to the cap beam and inserted into a slotted pile. The plate member would then be longitudinally welded to the pile. Thirdly, a truss style connection has been suggested which utilizes a shallow cross bracing system to force hinging lower in the section and reduce strains near the cap beam. Lastly, an improved flared column capital could be tested utilizing a larger, and possibly weaker, intended hinging region. Sketches of these four options have been provided in Figure 7.3.

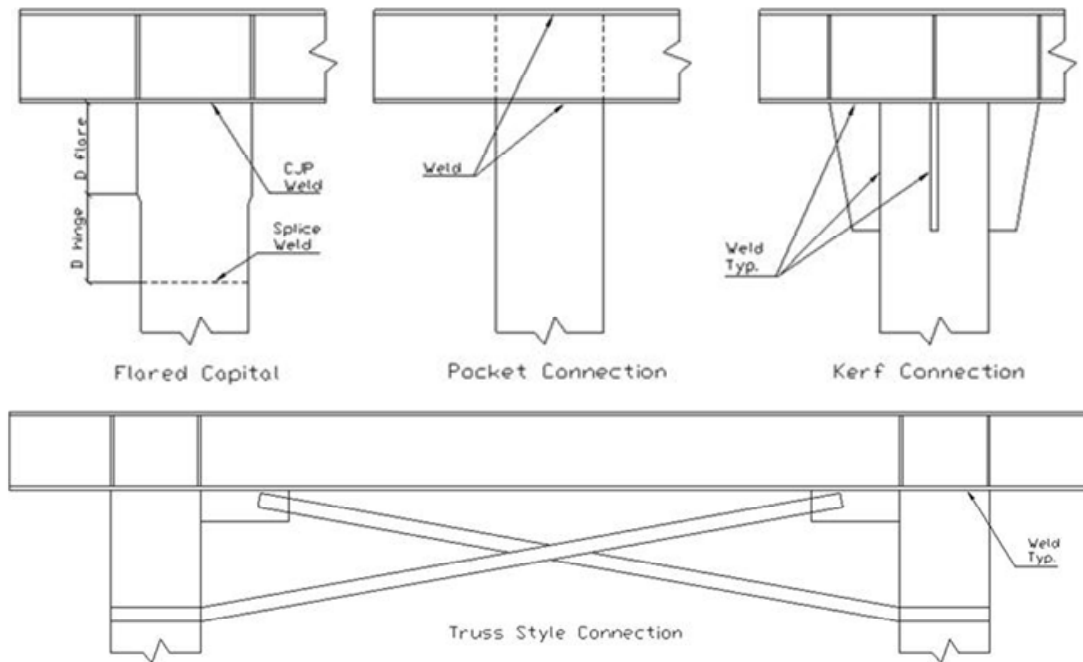


Figure 7.3 Possible New Design Conections

7.4.3 Retrofit Options

In addition to new designs, consideration has also been given to possible retrofit options. These options may be of particular interest to AKDOT since the organization has a considerable amount of these existing structures within their inventory. As has already been noted, these options could clearly be used as new design options but it is generally felt that although they may improve the capabilities of the structure, they will not be as effective as the options presented for new designs. A few of these options have been provided in this section such as the non-welded stiffened collar option and the heat treatment options where a zone of the pile is weakened by heat treatment to control the location of local buckling.

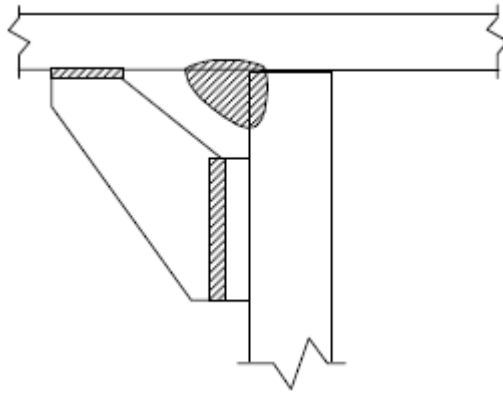


Figure 7.4 Non-Welded Stiffened Collar Option

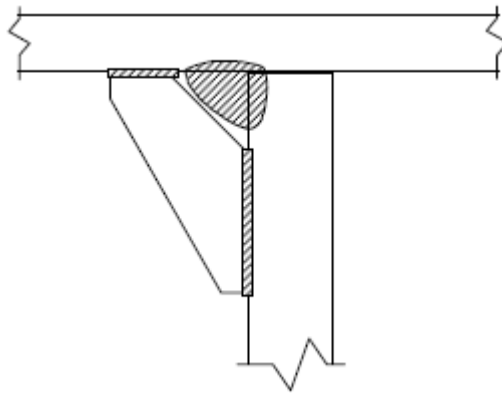


Figure 7.5 Plane Stiffener Option

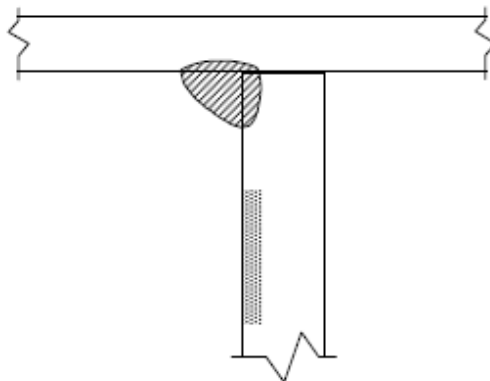


Figure 7.6 Reduced Section Option

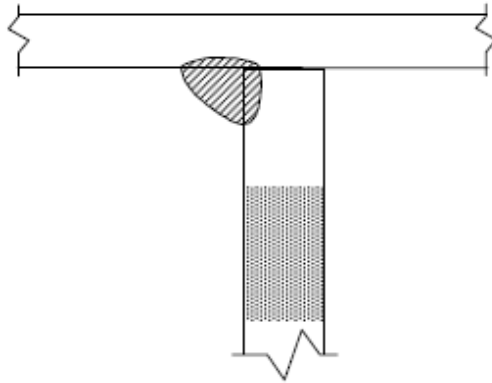


Figure 7.7 Heat Treatment Option

7.4.4 Future Research Conclusions

It is clear from the results of this project that these structures potentially possess considerable capabilities for seismic design purposes. However, it is important that direct consideration be given to the protection of the connection zone. Regardless of whether future research focuses on new design or retrofit, continued study of methods to protect the connection will be undoubtedly produce useful results.

7.5 Final Conclusions

The following list of items is provided as an encompassing list of conclusions developed throughout this research project.

- Modifying weld geometry alone will not produce an adequate ductility capacity or desirable failure mode as seen in tests 1-5. This would indicate that structures with modified weld geometry only should not be used in high seismic areas should the designer intend for the structure to experience even moderate levels of inelastic action as is typical in seismic design.

- Relocating the plastic hinge will likely produce both a higher ductility capacity and more desirable failure mode as was seen in test 6.
- The success of the relocating the plastic hinge is likely due to the ability to limit strains at the cap beam/pile joint to the elastic range.
- Attempts to calibrate an accurate plastic hinge length were not successful due to multiple sources of deformation and local pipe buckling. As a result the use of the plastic hinge method to calculate displacement in the inelastic range is not recommended for this type of system.
- Consideration should be given to ductility capacity as well as drift and failure mode. Displacement ductility is normalized to yield displacement and will inherently be lower for structures with higher elastic flexibility.
- Although a structure similar to test 6 may not be suitable for areas with extremely high seismic demands, the structure could perform well under considerable seismic attack if proper considerations are provided in regards to protection of the connection zone.
- Future research will likely focus on determining the most optimal connection system for new designs. However, retrofit investigations would also be beneficial.

REFERENCES

"Alaska." U.S. Geological Survey Earthquake Hazards Program.

<<http://earthquake.usgs.gov/regional/states/alaska/history.php>>.

Hooke, R (1678) "Explaining the Power of Springing Bodies" Royal Society of London.

Jacobsen, L.S. Steady forced vibrations as influenced by damping, ASME Transactione
52(1), 1930. Pgs.169–181.

Montejo, L. A., M. J. Kowalsky, and T. Hassan. Seismic Behavior of Reinforced Concrete
Bridge Columns at Sub-Freezing Temperatures. Rep. no. RD-08-01. Constructed
Facilities Laboratory, Department of Civil, Construction and Environmental
Engineering, North Carolina State University, 2008.

Nishikawa, K., Yamamoto, S., Natori, T., Terao, K., Yasunami, H., and Terada, M.
"Retrofitting for seismic upgrading of steel bridge columns," Engineering
Structures, Vol. 20, Nos 4-6 pp. 540-551, 1998.

Priestley, M. J. N., G. M. Calvi, and M. J. Kowalsky. Displacement Based Seismic Design
of Structures. New York: IUSS P, 2007.

Steunenbergh, M., R. G. Sexsmith, and S. F. Stiemer. "Seismic Behavior of Steel Pile to
Precast Concrete Cap Beam Connections." Journal of Bridge Engineering Vol.3,
No. 4 (1998): 177-85.

Suarez, V., and Kowalsky, M. J. "Direct Displacement-Based Design of Drilled Shaft
Bents with Soil-Structure Interaction." Journal of Earthquake Engineering" 2007.

Appendix 1: Specimen and Set Up Design Drawings

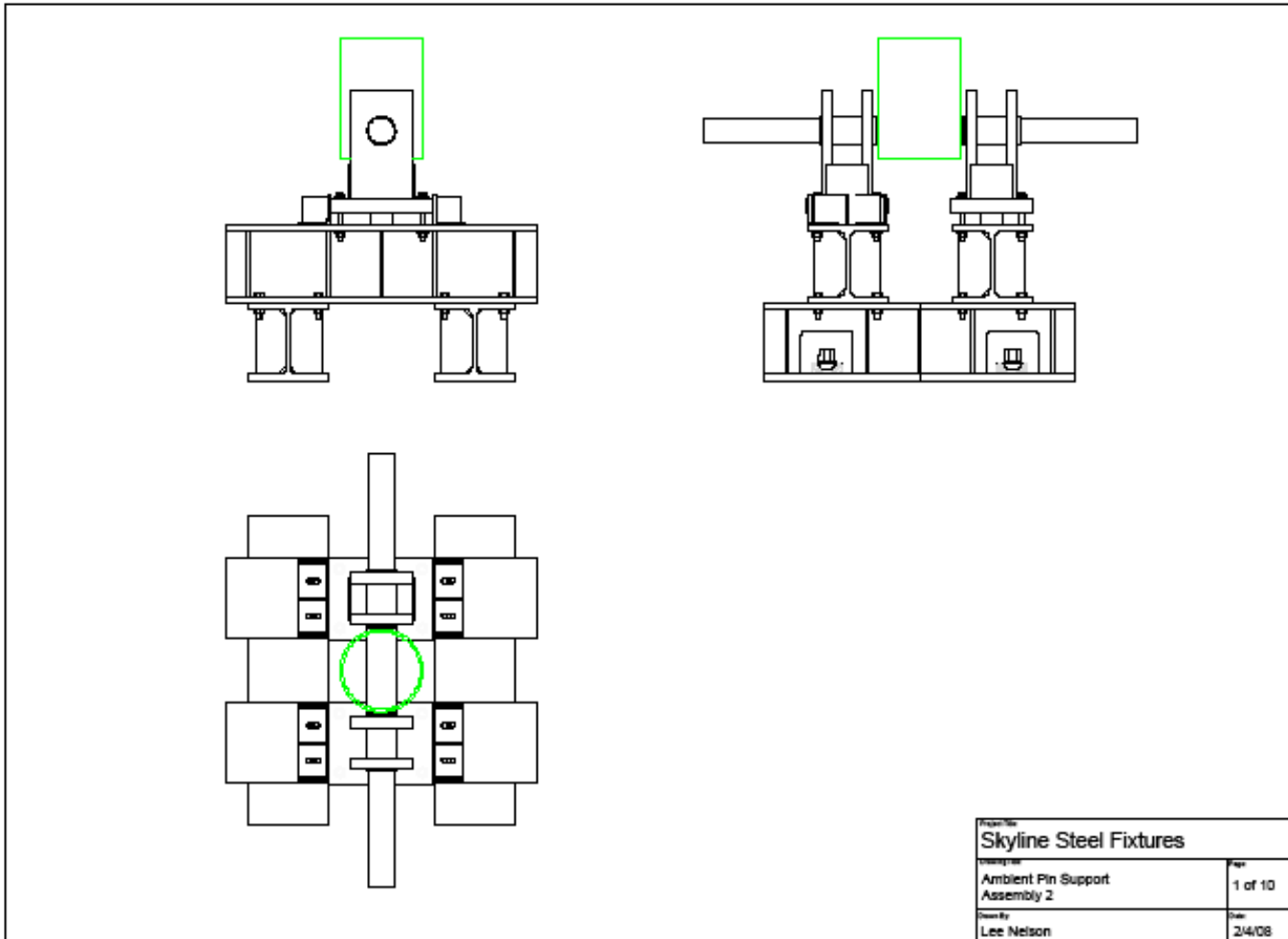


Figure A 1.1 Pin Base Construction

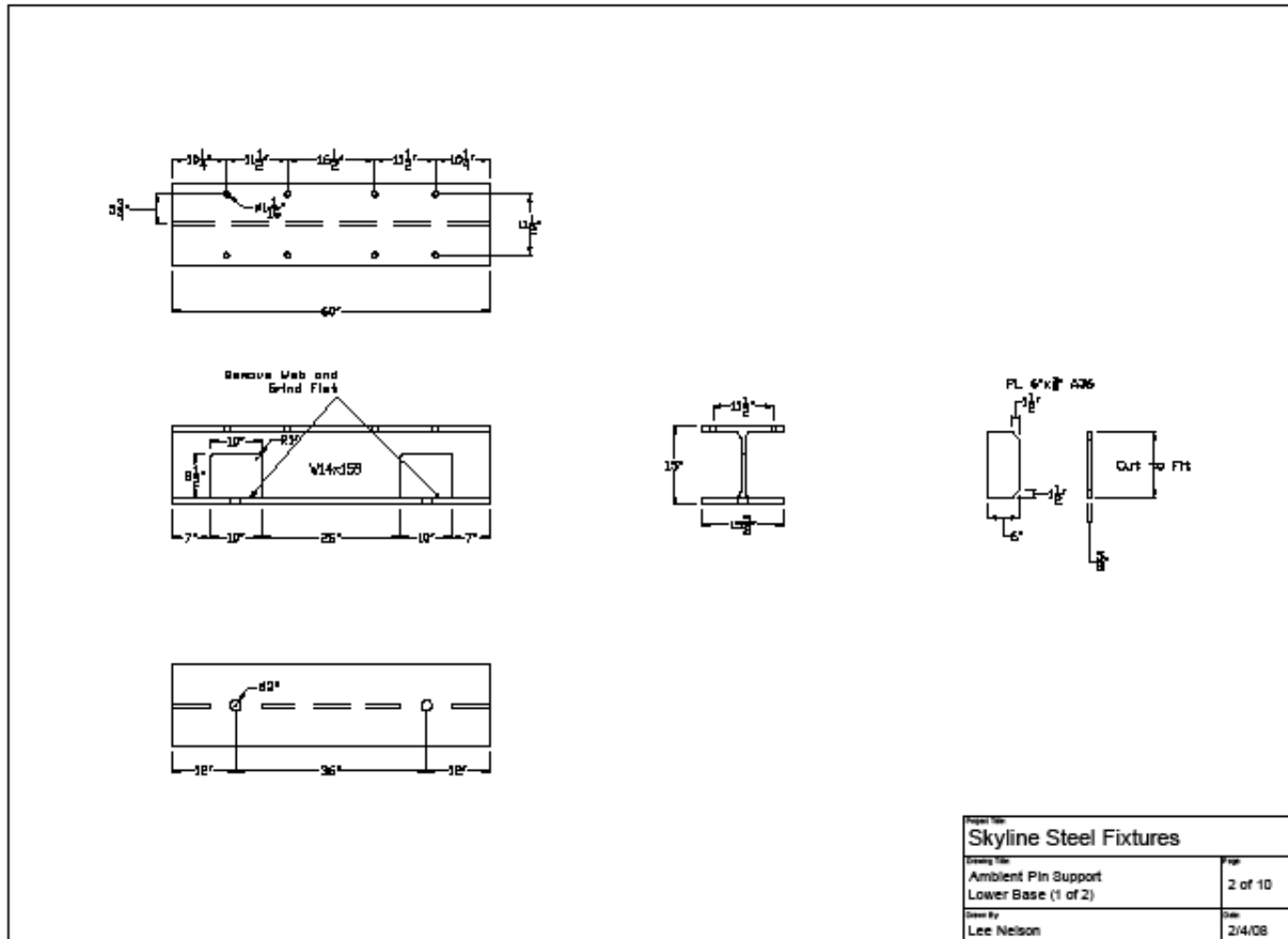


Figure A 1.2 Lower Base Support Detail

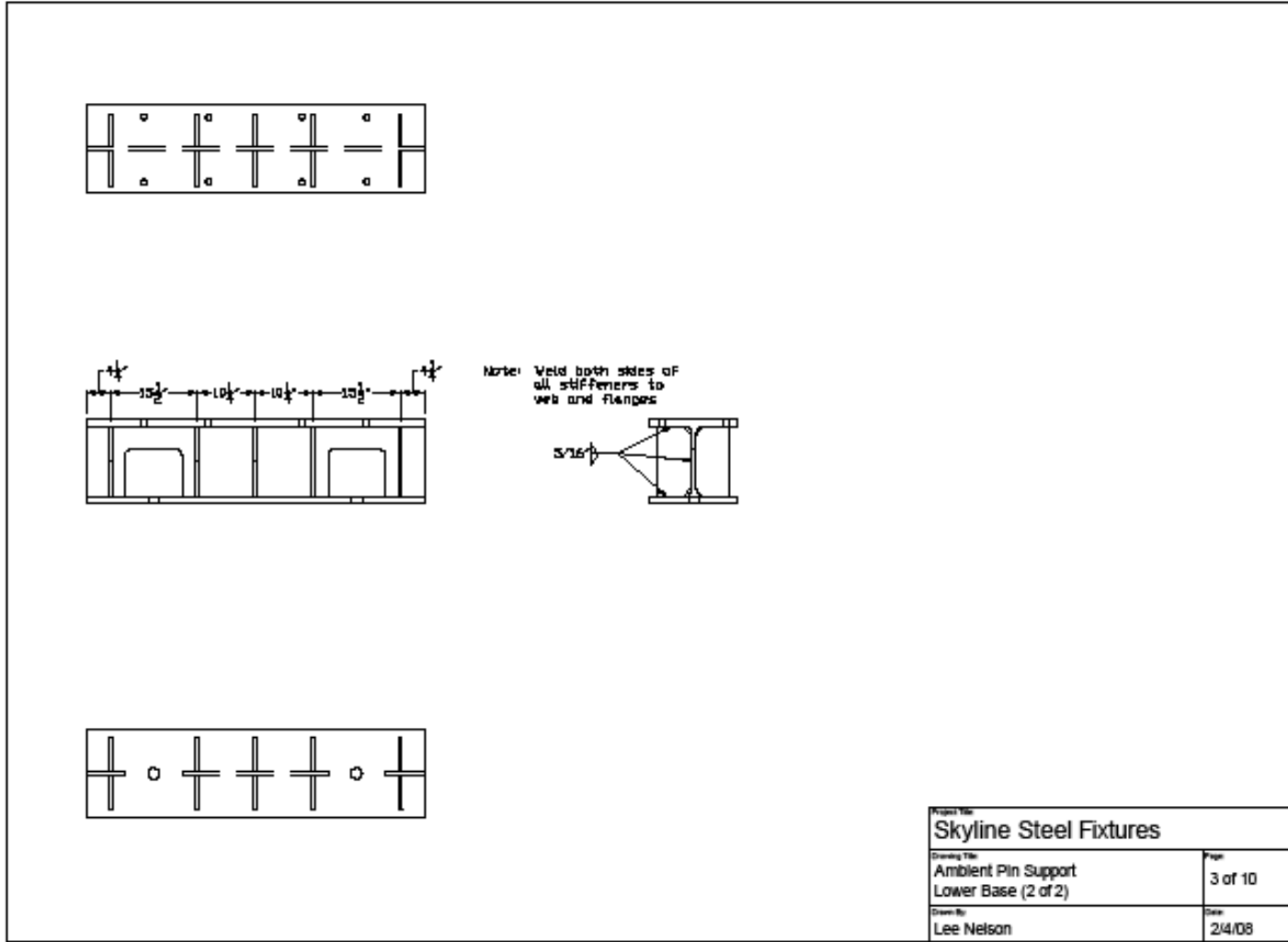


Figure A 1.3 Lower Base Support Detail Continued

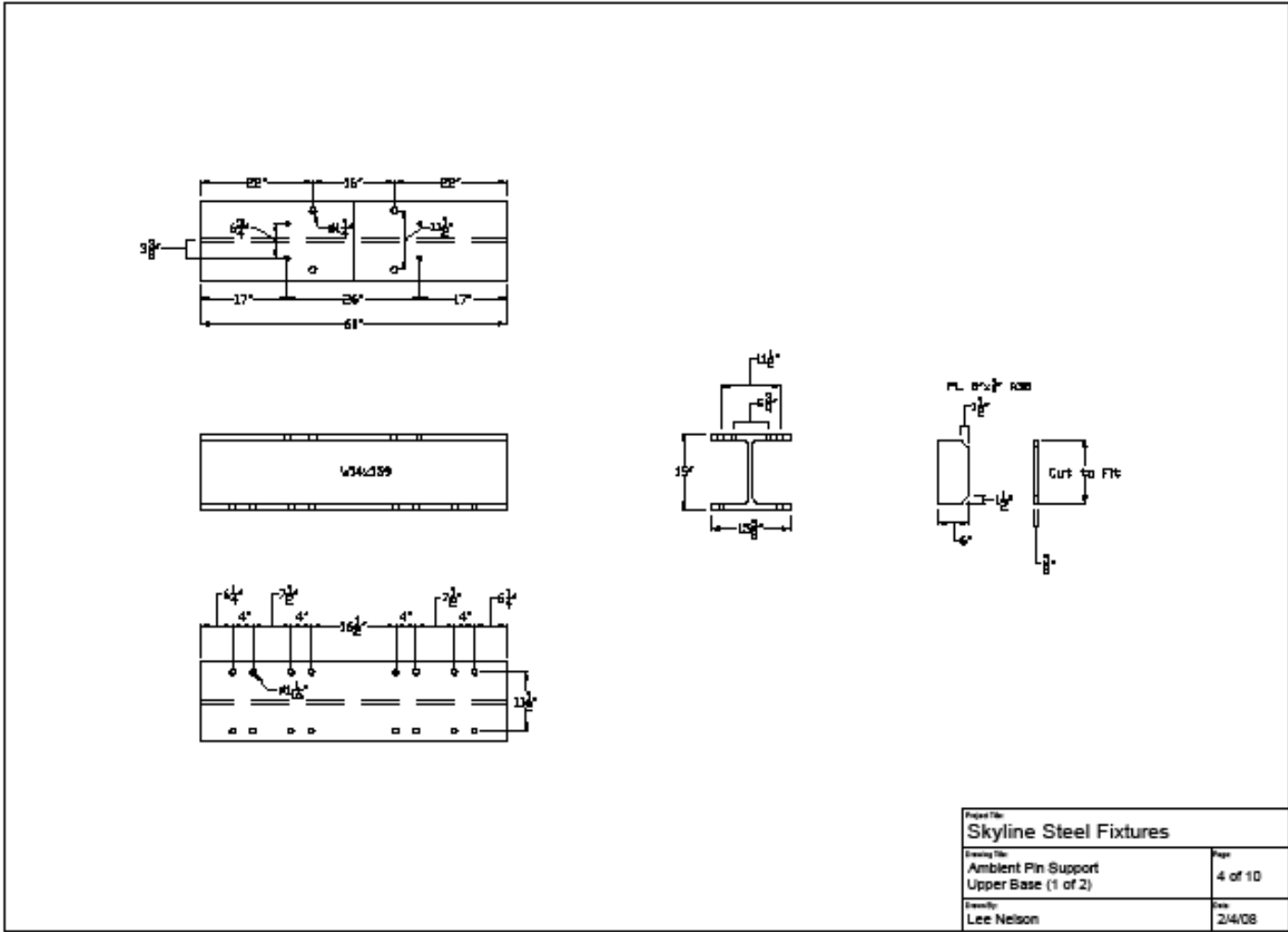


Figure A 1.4 Upper Base Support Detail

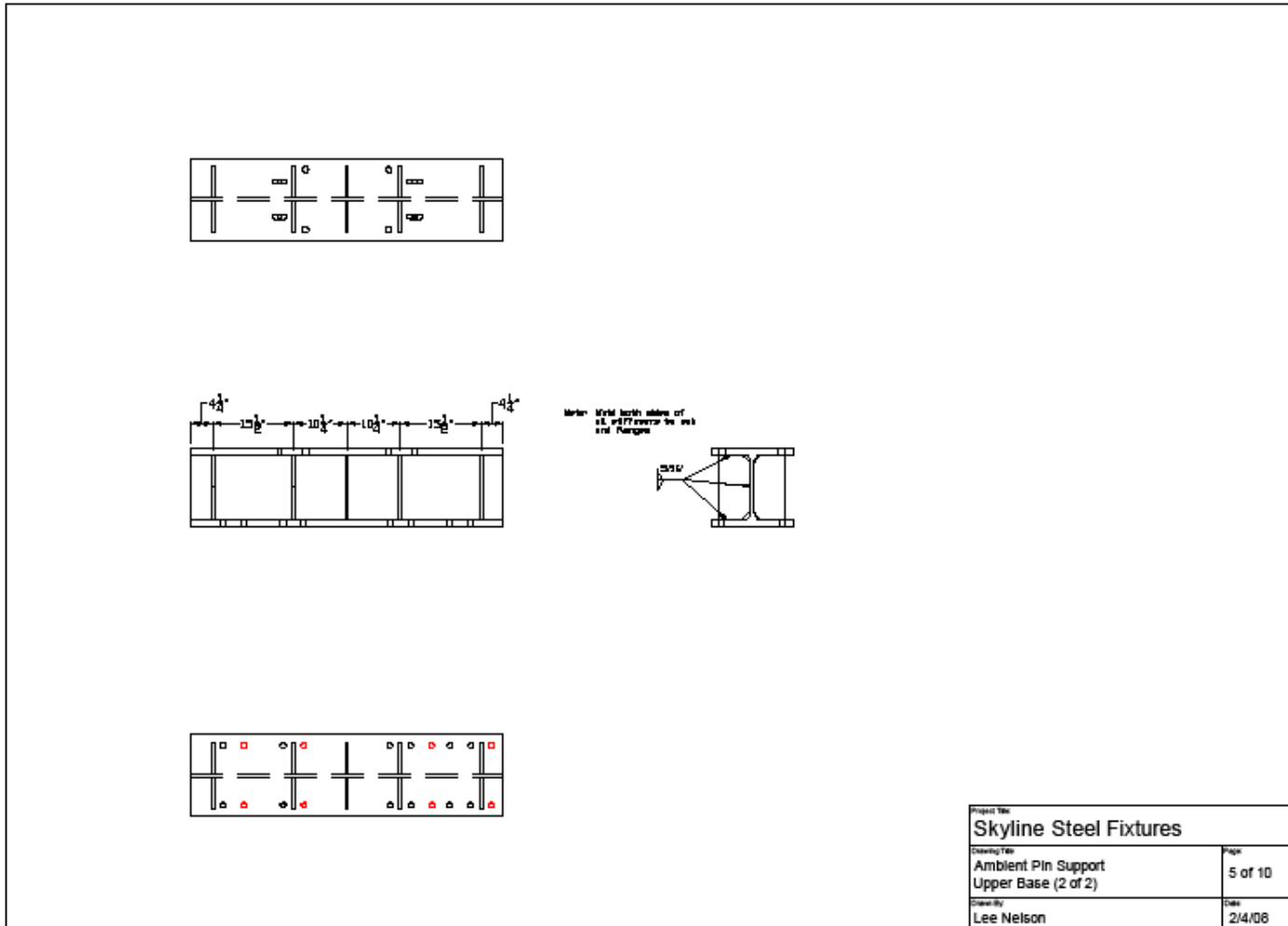


Figure A 1.5 Upper Base Support Detail Continued

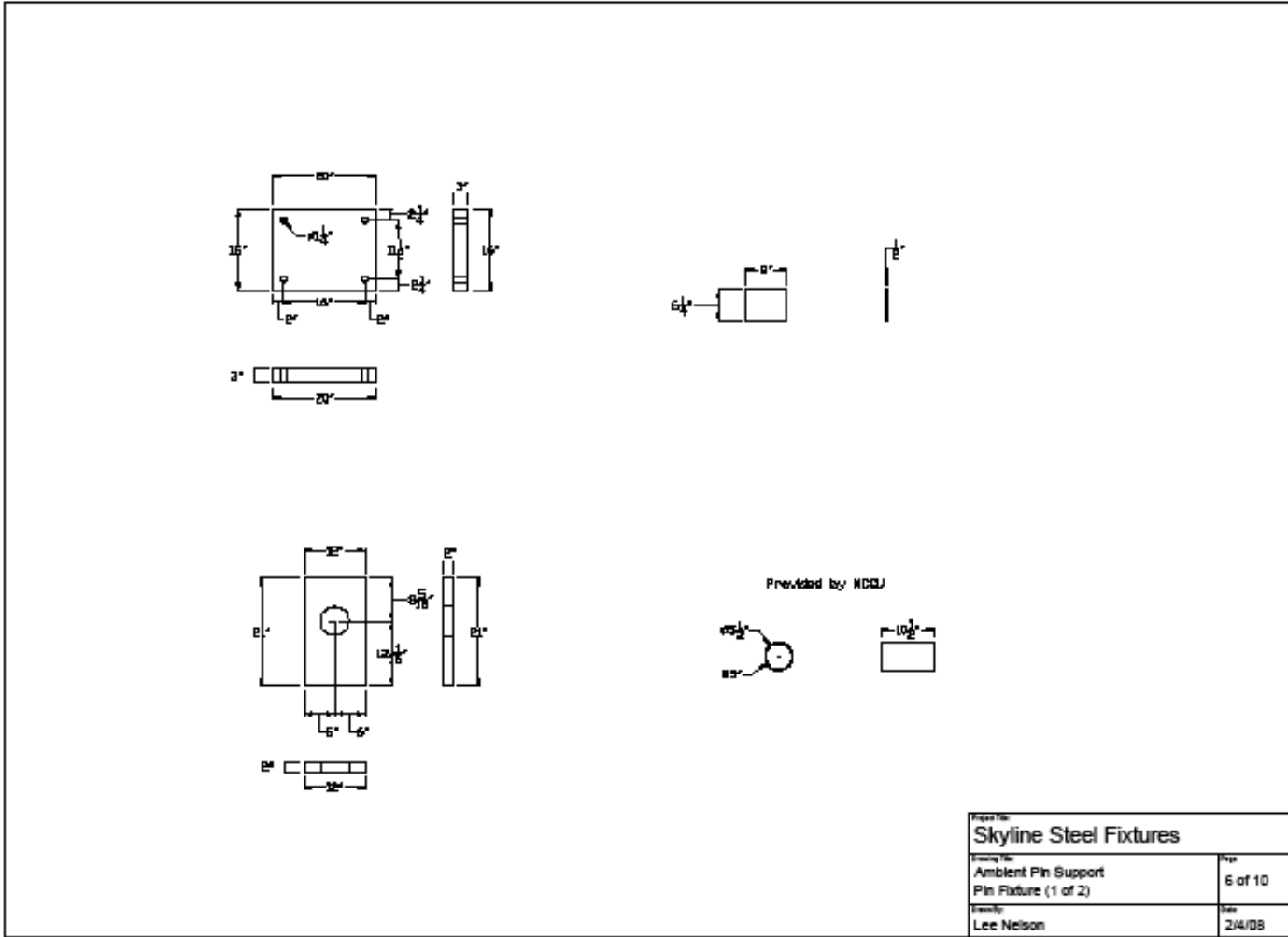


Figure A 1.6 Pin Sleeve Support Details

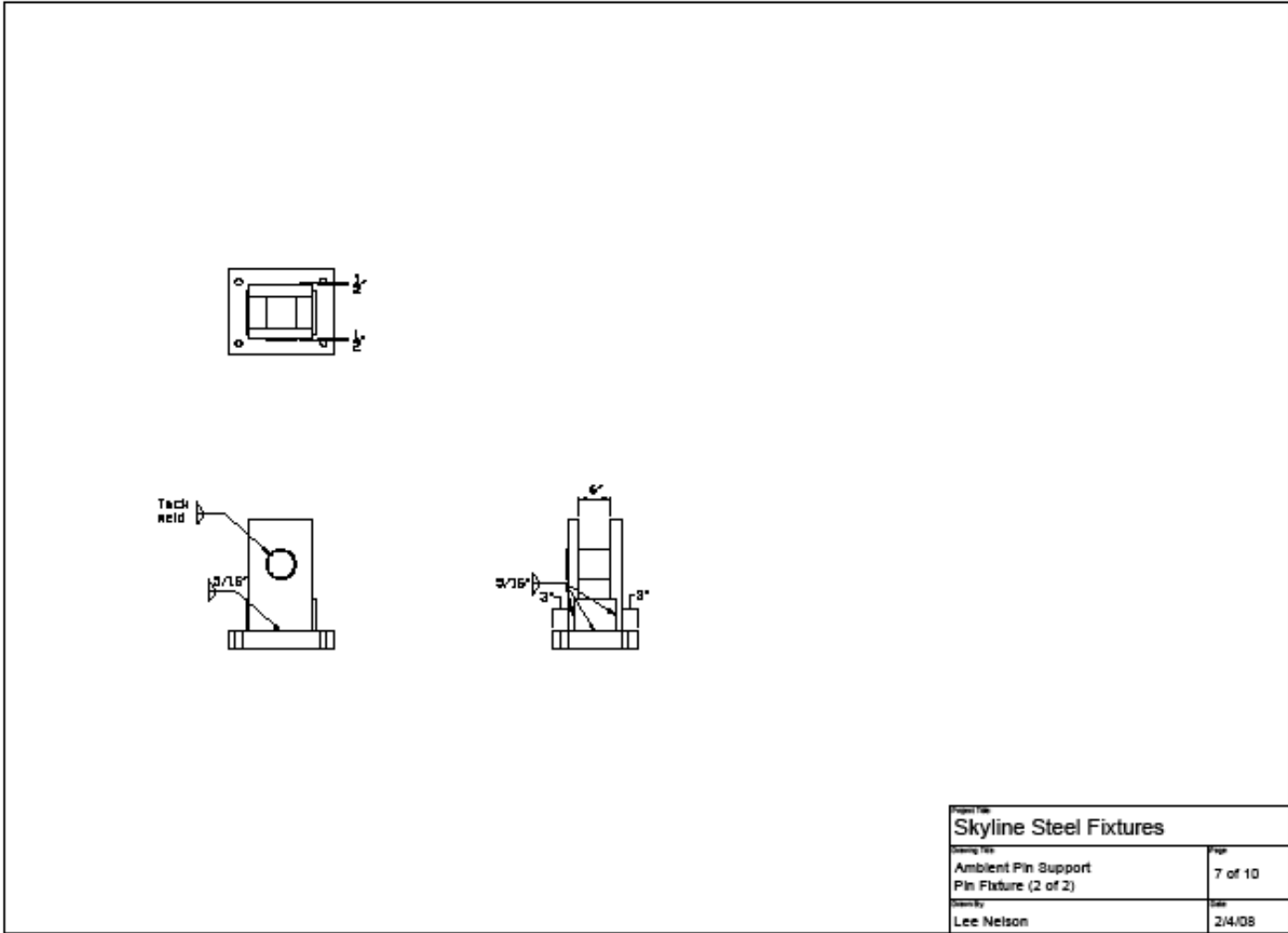


Figure A 1.7 Pin Sleeve Construction Details

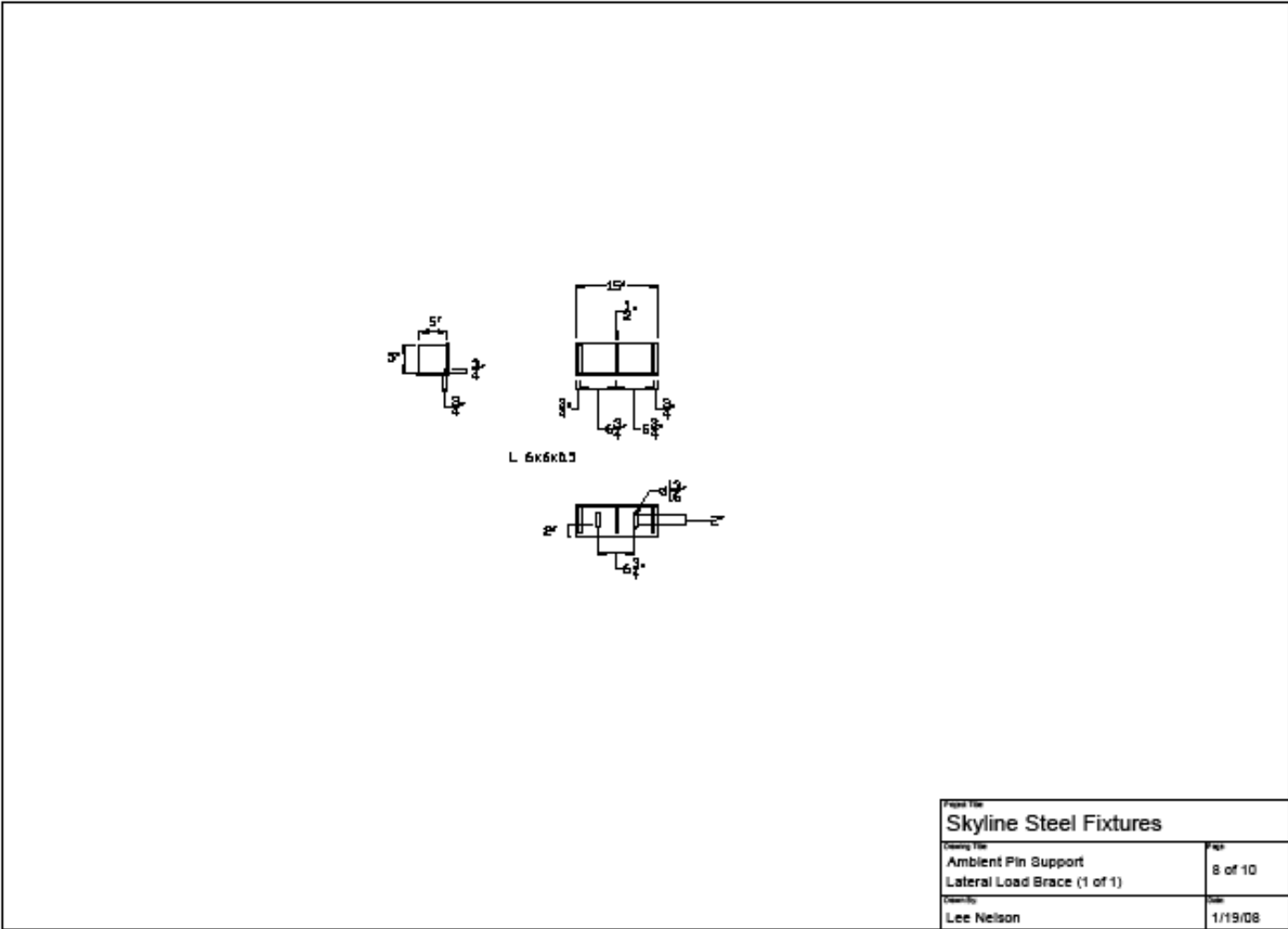


Figure A 1.8 Restraining Angle Detail

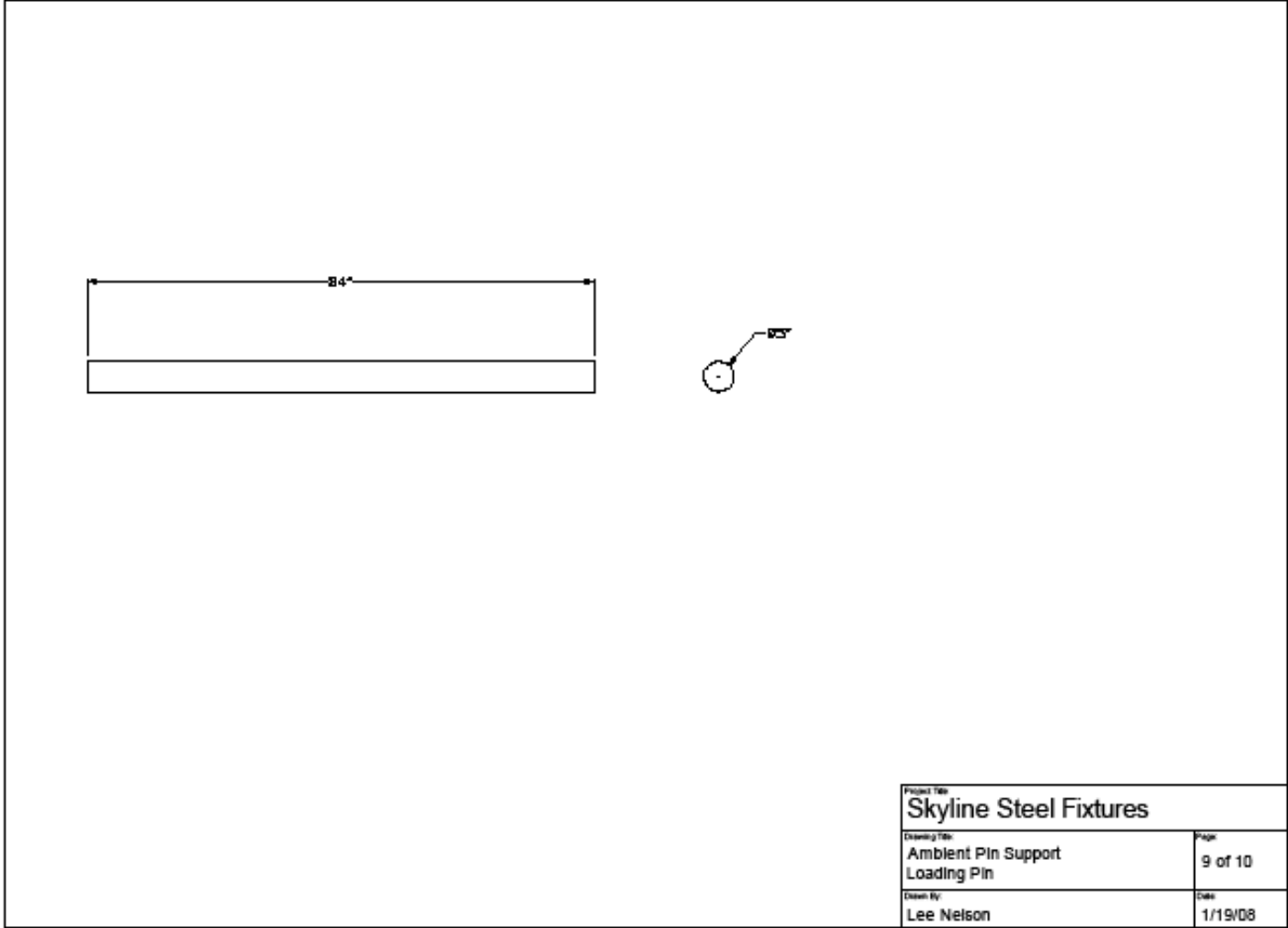
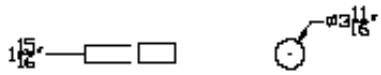


Figure A 1.9 Steel Pin Detail

Enerpac CATG-200
degree tilt saddle
200 ton capacity



Project Title: Skyline Steel Fixtures	
Drawing Title: Ambient Link Support Assembly	Page: 1 of 10
Drawn By: Lee Nelson	Date: 1/19/08

Figure A 1.10 Pin Sleeve Detail

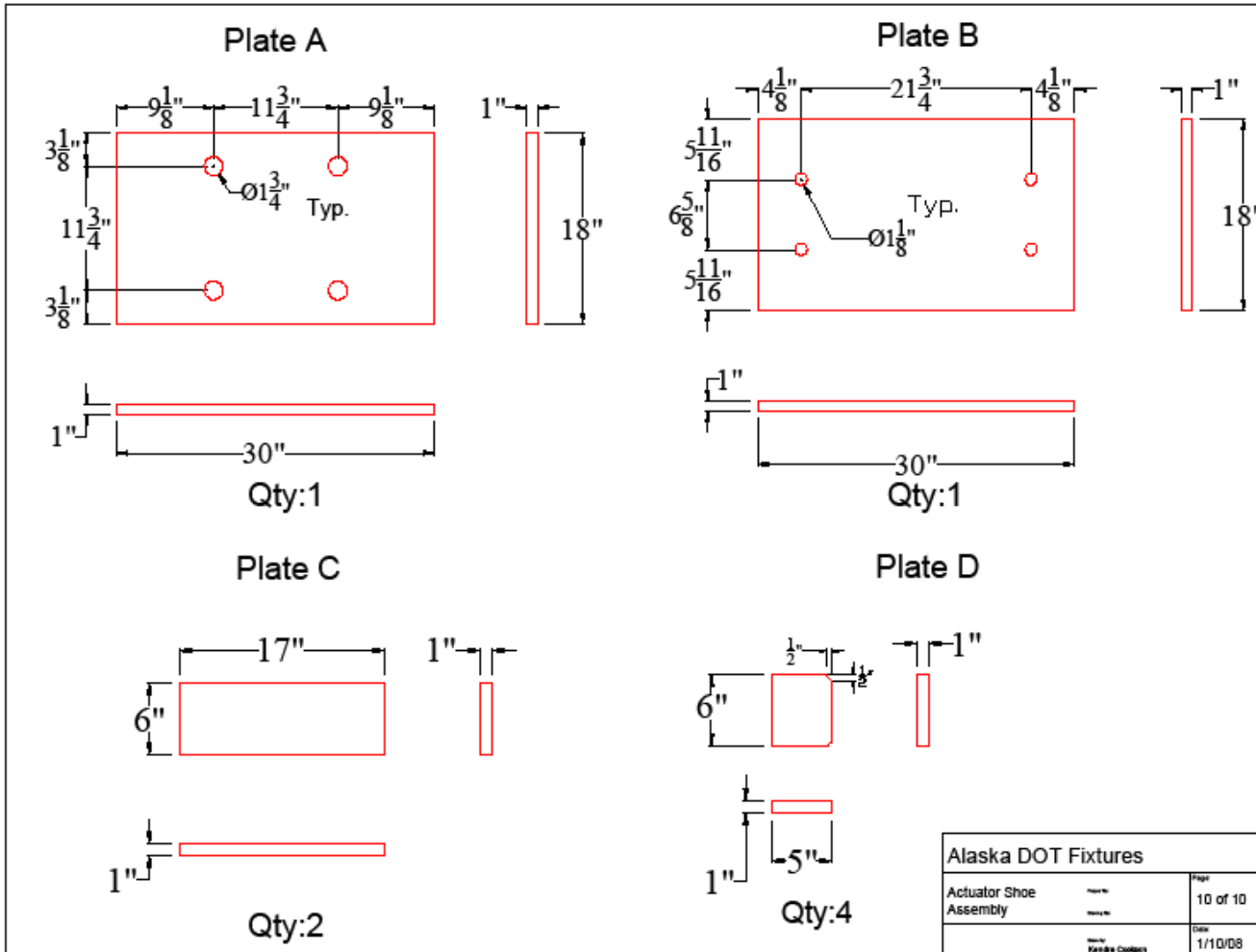
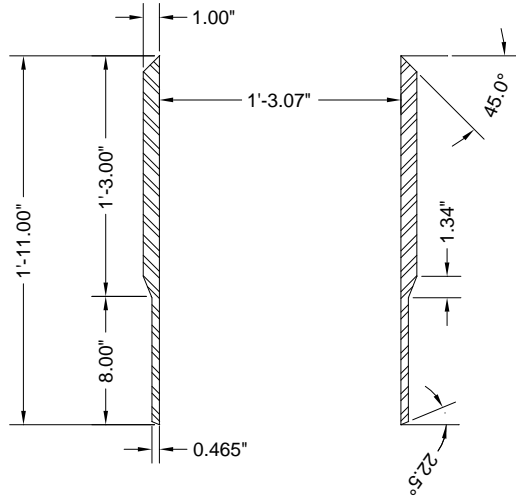


Figure A 1.11 Actuator Connection Details

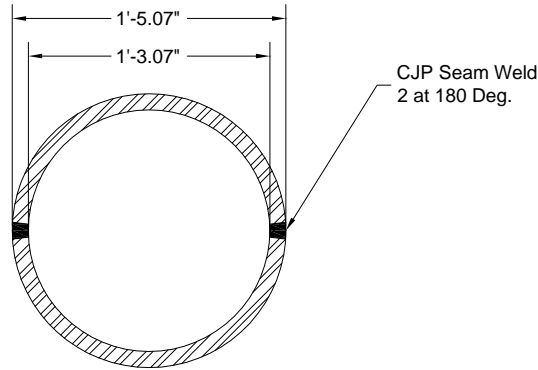
Appendix 2: Flared Column Capital Details



- Sheet Notes:
1. $F_y=50\text{ksi}$
 2. ID Critical
 3. Provide CJP Seam Welds Per AWS D1.5 Spec

Stub Column Detail Elevation Section

Scale: 1" = 0.75'



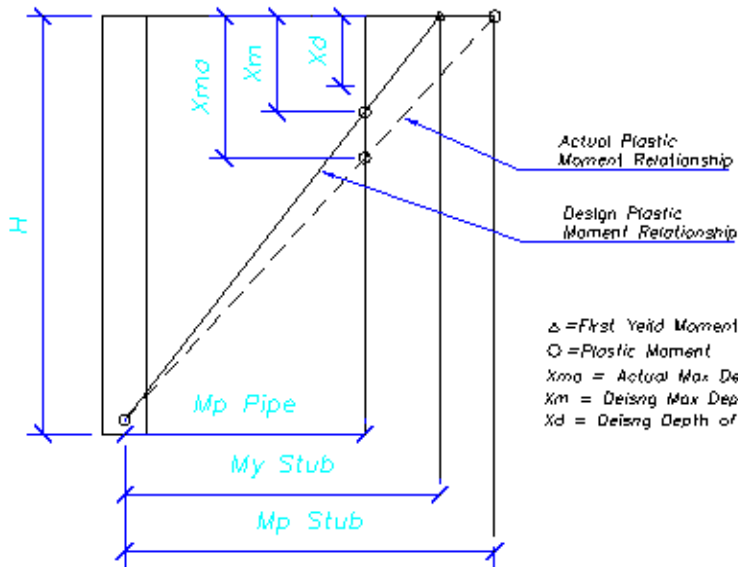
Stub Column Detail Plan Section

Scale: 1" = 0.75'

NCSU STUB COLUMN SECTION

Drawn By: SJF
Date: 16 Jan 09

Figure A 2.1 Column Capital Design Drawing



The Design Plastic Moment Relationship will be used to ensure hinging in the pipe occurs simultaneously with first yield of the stub.

Δ = First Yield Moment
 O = Plastic Moment
 X_{mo} = Actual Max Depth of Stub
 X_m = Design Max Depth of Stub
 X_d = Design Depth of Stub

From Similar Triangles:

$$\frac{H}{M_{y_Stub}} = \frac{H - X_m}{O \cdot M_{p_Pipe}} \quad X_m = H - H \cdot \left(\frac{O \cdot M_{p_Pipe}}{M_{y_Stub}} \right) \quad \text{for: } M_{p_Pipe} < M_{y_Stub}$$

and: $O = \text{"over strength factor"}$

For HSS16x0.5 Pipe:

$$OD_{16x0.5} := 16 \text{ in} \quad t_{16x0.5} := 0.465 \text{ in} \quad Z_{16x0.5} := 112 \text{ in}^3 \quad S_{16x0.5} := 85.7 \text{ in}^3 \quad F_{y_pipe} := 54 \text{ ksi}$$

$$ID_{16x0.5} := OD_{16x0.5} - 2 \cdot t_{16x0.5} \quad ID_{16x0.5} = 15.07 \text{ in} \quad O := 1.25$$

For Stub Column:

$$F_{y_stub} := 50 \text{ ksi} \quad ID_{stub} := 15.07 \text{ in} \quad t := 1 \text{ in}$$

$$S_{stub}(t_i) := \frac{\pi \cdot \left[(2 \cdot t_i + ID_{stub})^4 - (ID_{stub})^4 \right]}{32 \cdot (2 \cdot t_i + ID_{stub})}$$

$$X_m(t_i) := \left[\begin{array}{l} 10.93t - 10.93t \cdot \left(\frac{Z_{16x0.5} \cdot F_{y_pipe} \cdot O}{S_{stub}(t_i) \cdot F_{y_stub}} \right) \\ \text{"My Stub < Mp Column -- Not Valid" otherwise} \end{array} \right] \quad \text{if } Z_{16x0.5} \cdot F_{y_pipe} < S_{stub}(t) \cdot F_{y_stub}$$

$$X_m(t) = 2.308 \text{ ft} \quad S_{stub}(t) = 191.682 \text{ in}^3$$

Figure A 2.2 Column Capital Design Calculations

Appendix 3: Material Certification

SteelFab

PO Box 19289, 28219 Charlotte NC 28214
704-394-5376 Fax: 704-393-1400

Purchase Order 24725ABM-1		This number must appear on all invoices and shipping papers
ISSUED TO: TUBULAR STEEL, INC. 1031 Executive Parkway Dr. ST. LOUIS,, MO 63141-6351 TEL (800)388-7203 FAX 314-851-9336 Attn: Diane Jones		DELIVER TO: SteelFab 8623 Old Dowd Road Charlotte, NC 28214
Ship via FOB Point:	Issued 01-21-08 Deliver by: 02-04-08 A.M. Terms	[x] Material Test Reports Required Please provide prices and delivery schedule before shipping. Notify us immediately if shipping schedule cannot be met.

No.	Qty	Type	Size	Grade	Length	Weight	Unit Cost	Extended Cost
/	12	HSS	16x 500	A500-B	11' 7-3/8"	11,536#	\$61.2200 /LF	\$8,532.54
		Mark: T	Square Cut 2 Ends allocate 12 to 24725-1-1 RCVD.12.01/29@Y-1					
						11,536#	Mat'l Cost	\$8,532.54
							Freight	
							Sales Tax	
							Cut Charges	
							Total	\$8,532.54

Signature: _____
 Issued by: Dwane Burkhardt

Figure A 3.1 HSS Pile Material Certification

Atlas Tube Canada ULC
 200 Clark St.
 Farrow, Ontario, Canada
 N0R 1G0
 Tel: 519-738-3541
 Fax: 519-739-3537



Ref.B/L: 80255184
 Date: 09.04.2007
 Customer: 193

Sold to

Tubular Steel
 1031 Executive Parkway
 ST. LOUIS MO 63141
 USA

MATERIAL TEST REPORT

Shipped to

Tubular Steel
 950 Bunker Hill Rd.
 STAUNTON IL 62068
 USA

Material: 10.750x280x50*1*0(2x1)NMH Material No: R10750250 Made in: Canada
 Sales order: 323849 Purchase Order: 3050

Heat No	Pcs	C	Mn	P	S	Si	Al	Cu	Cb	Mo	Ni	Cr	V
894321	2	0.200	0.790	0.007	0.006	0.020	0.038	0.020	0.004	0.002	0.008	0.019	0.000
Bundle No	Yield		Tensile		Eln.2in		Certification						
M200469358	055891 Psi		066500 Psi		30.8 %		ASTM A500-03A GRADE B&C						

Material Note:
 Sales Or.Note:

Material: 16.000x500x42*0*0(2x1)NMH Material No: R16000500 Made in: Canada
 Sales order: 321369 Purchase Order: 2895

Heat No	Pcs	C	Mn	P	S	Si	Al	Cu	Cb	Mo	Ni	Cr	V
480876	2	0.180	0.790	0.010	0.002	0.150	0.039	0.056	0.006	0.005	0.018	0.040	0.000
Bundle No	Yield		Tensile		Eln.2in		Certification						
M200469737	054353 Psi		069010 Psi		39.0 %		ASTM A500-03A GRADE B&C						

Material Note:
 Sales Or.Note:

Material: 16.000x500x42*0*0(2x1)NMH Material No: R16000500 Made in: Canada
 Sales order: 321369 Purchase Order: 2895

Heat No	Pcs	C	Mn	P	S	Si	Al	Cu	Cb	Mo	Ni	Cr	V
480876	2	0.180	0.790	0.010	0.002	0.150	0.039	0.056	0.006	0.005	0.018	0.040	0.000
Bundle No	Yield		Tensile		Eln.2in		Certification						
M200469738	054363 Psi		068010 Psi		39.0 %		ASTM A500-03A GRADE B&C						

Material Note:
 Sales Or.Note:

ALL INCLUDED ROUNDS MEET A500 GRADE B/C AND A53 NON-HYDRO-TESTED

Authorized by Quality Assurance: *M. Weber*

The results reported on this report represent the actual attributes of the material furnished and indicate full compliance with all applicable specification and contract requirements.



Certs Received by *[Signature]*

Figure A 3.2 HSS Pile Certification Continued

Atlas Tube Canada ULC
 200 Clark St.
 Harrow, Ontario, Canada
 NOR 1G0
 Tel: 519-738-3541
 Fax: 519-738-3537



Ref.B/L: 80278234
 Date: 01.19.2008
 Customer: 193

MATERIAL TEST REPORT

Sold to

Tubular Steel
 1031 Executive Parkway
 ST. LOUIS MO 63141
 USA

Shipped to

Tubular Steel
 950 Bunker Hill Rd.
 STAUNTON IL 62088
 USA

Material: 7.000x260x210*0(7x1)		Material No: R07000250		Made in: Canada									
Sales order: 362488		Purchase Order: 1319-cut order											
Heat No	Pcs	C	Mn	P	S	Si	Al	Cu	Cb	Mo	Ni	Cr	V
482380		0.160	0.810	0.012	0.008	0.015	0.051	0.057	0.006	0.002	0.011	0.029	0.000
Bundle No	Yield	Tensile	Eln.Zin		Certification								
M100704317	053017 Psi	066370 Psi	35.7 %		ASTM A500-03A GRADE B&C								

Material Note:
 Sales Or.Note:

Material: 16.000x500x50*0*0(2x1)NMH		Material No: R16000600		Made in: Canada									
Sales order: 360283		Purchase Order: 1072		Cust Material #: 1072-103									
Heat No	Pcs	C	Mn	P	S	Si	Al	Cu	Cb	Mo	Ni	Cr	V
482577	2	0.200	0.800	0.010	0.004	0.150	0.040	0.032	0.005	0.002	0.013	0.039	0.000
Bundle No	Yield	Tensile	Eln.Zin		Certification								
M200508808	053872 Psi	067910 Psi	38.3 %		ASTM A500-03A GRADE B&C								

Material Note:
 Sales Or.Note:

Material: 16.000x500x50*0*0(2x1)NMH		Material No: R16000600		Made in: Canada									
Sales order: 360283		Purchase Order: 1072		Cust Material #: 1072-103									
Heat No	Pcs	C	Mn	P	S	Si	Al	Cu	Cb	Mo	Ni	Cr	V
482577	2	0.200	0.800	0.010	0.004	0.150	0.040	0.032	0.005	0.002	0.013	0.039	0.000
Bundle No	Yield	Tensile	Eln.Zin		Certification								
M200508808	053872 Psi	067910 Psi	38.3 %		ASTM A500-03A GRADE B&C								

Material Note:
 Sales Or.Note:

ALL INCLUDED ROUNDS MEET A500 GRADE B/C AND A53 NON-HYDRO-TESTED

Authorized by Quality Assurance: *M. Weber*

The results reported on this report represent the actual attributes of the material furnished and indicate full compliance with all applicable specification and contract requirements.



Certs Received by

Figure A 3.3 HSS Pile Material Certification Continued

Appendix 4: Construction Inspection and Weld Certification Details

A4.1 Welder Certifications

Green's Welding

Page 1 of 1

Welder Qualification Test Record

Green, Justin

WQTR No. <u>Green, Justin</u>	Welder Name <u>Justin Green</u>	Welder Id _____	
WPS No. <u>Prequalified</u>	Revision _____	Date <u>5/14/2008</u>	
Variables Record Actual Values Used in Qualification		Qualification Range	
Process (Table 4.10, Item (1)) <u>FCAW</u>		<u>FCAW</u>	
Transfer Mode (GMAW): Short-Cir. <input type="checkbox"/> Globular <input type="checkbox"/> Spray <input type="checkbox"/>		Short-Circuiting <input type="checkbox"/> Globular <input type="checkbox"/> Spray <input type="checkbox"/>	
Type Manual <input type="checkbox"/> Machine <input type="checkbox"/> Semi-Auto <input checked="" type="checkbox"/> Auto <input type="checkbox"/>		Manual <input type="checkbox"/> Machine <input type="checkbox"/> Semi-Auto <input checked="" type="checkbox"/> Auto <input type="checkbox"/>	
Number of Electrodes Single <input checked="" type="checkbox"/> Multiple <input type="checkbox"/>		Single <input checked="" type="checkbox"/> Multiple <input type="checkbox"/>	
Current/Polarity AC <input type="checkbox"/> DCEP <input checked="" type="checkbox"/> DCEN <input type="checkbox"/> Pulsed <input type="checkbox"/>		AC <input type="checkbox"/> DCEP <input checked="" type="checkbox"/> DCEN <input type="checkbox"/> Pulsed <input type="checkbox"/>	
Position (Table 4.10, Item (4)) <u>1G</u>		<u>Flat</u>	
Weld Progression: (Table 4.10, Item (6)) Up <input type="checkbox"/> Down <input type="checkbox"/>		Up <input type="checkbox"/> Down <input type="checkbox"/>	
Backing [Table 4.10, Item (7)] Use Backing <input checked="" type="checkbox"/>		With Backing <input checked="" type="checkbox"/> Without Backing <input checked="" type="checkbox"/>	
Consumable Insert (GTAW) Use Insert <input type="checkbox"/>		With Insert <input type="checkbox"/> Without Insert <input type="checkbox"/>	
Material/Spec. <u>A-36</u> to <u>A-36</u>		Group 1 Material	
Thickness (Plate): Groove (in) <u>1.0</u>		<u>0.125</u> - <u>Unlimited</u> in	
Fillet () _____		<u>Unlimited</u> - <u>Unlimited</u> in	
Thickness (Pipe/tube): Groove () _____		- _____	
Fillet () _____		<u>Unlimited</u> - <u>Unlimited</u> in	
Diameter(Pipe): Groove () _____		- _____	
Fillet () _____		<u>Unlimited</u> - <u>Unlimited</u> in	
Notes _____		_____	
Filler Metal (Table 10, Item (2))		<u>5/64" Tri-mark</u>	
Spec. <u>AWS A5.20</u>		_____	
Class. <u>E70T-4</u>		_____	
F-No. <u>6</u>		_____	
Gas/Flux Type (Table 4.10, Item (3)) _____		_____	
Other _____		_____	
VISUAL INSPECTION (4.8.1) Acceptable Yes			
GUIDED BEND TEST RESULTS (4.30.5)			
Type	Result	Type	Result
Fillet Test Results (4.30.2.3 and 4.30.4.1)			
Appearance	_____	Fillet Size	_____
Fracture Test Root Penetration	_____	Macroetch	_____
Inspected By	<u>Leroy Spangler</u>	Test No.	<u>04-162</u>
		Organization	<u>Triad NDT, Inc.</u>
		Date	<u>4/7/2004</u>
RADIOGRAPHIC TEST RESULTS (4.30.3.1)			
Film Identification No.	Result	Remark	
JG-1G	Satisfactory		
			Interpreted By <u>Leroy Spangler</u> Organization <u>Triad NDT, Inc.</u> Test No. <u>04-162</u> Date <u>5/14/2008</u>
We, the undersigned, certify that the statements in this record are correct and that the test welds were prepared, welded, and tested in accordance with the requirements of section 4 of ANSI/AWS D1.1, (2006) Structural Welding Code-Steel.			
Manufacturer	<u>Green's Welding</u>	Authorized By	<u>Justin Green</u>
		Date	<u>5/14/2008</u>

Figure A 4.1 Justin Green Welding Certification (Test 1-6)

WELDER, WELDING OPERATOR OR TACK WELDER QUALIFICATION TEST RECORD

Type of Welder: WELDER
 Name: Moises Sanchez Identification No.: 506-11-8500
 Welding Procedure Specification No.: CPB 2036 Rev.: _____ Date: 6-17-07

Variables	Record Actual Values Used in Qualification	Qualification Range
Process/Type [Table 4.10, Item (2)]	SMAW	FLAT HORIZONTAL VERTICAL OVERHEAD
Electrode (single or multiple) [Table 4.10, Item (9)]	SINGLE	
Current/Polarity	DCEN	
Position [Table 4.10, Item (5)]	4G OVER/HEAD 3G VERTICAL	
Weld Progression [Table 4.10, Item (7)]		
Backing (YES or NO) [Table 4.10, Item (8)]	YES	
Material/Spec. [Table 4.10, Item (1)]	ASTM to A36	UNLIMITED GROOVE & FILLET
Base Metal		
Thickness: (Plate)	1" PLATE	
Groove	N/A	
Fillet	N/A	
Thickness: (Pipe/tube)	N/A	
Groove	N/A	
Fillet	N/A	
Diameter: (Pipe)	N/A	
Groove	N/A	
Fillet	N/A	
Filler Metal [Table 4.10, Item (3)]	AWS A5.1	
Spec No. A	E-7018	
Class E	F-4	
F.No.	N/A	
Gas/Flux Type [Table 4.10, Item (4)]		
Other		

VISUAL INSPECTION (4.6.1)			
Acceptable YES or NO YES			
Guided Bend Test Results (4.30.5)			
Type	Result	Type	Result
3G1 SIDE	SATISFACTORY	4G1 SIDE	SATISFACTORY
3G2 SIDE	SATISFACTORY	4G2 SIDE	SATISFACTORY
Fillet Test Results (4.30.2.3 and 4.30.4.1)			
Appearance	_____	Fillet Size	_____
Fracture Test Root Penetration	_____	Macroetch	_____
(Describe the location, nature, and size of any crack or tearing of the specimen.)			
Inspected by	JERRY CAGLE	Test Number	CPB 2036
Organization	AWS D1.1	Date	6-17-07

RADIOGRAPHIC TEST RESULTS (4.30.3.1)					
Film Identification Number	Results	Remarks	Film Identification Number	Results	Remarks

Interpreted by _____ Test Number _____
 Organization _____ Date _____

We, the undersigned, certify that the statements in this record are correct and that the test welds were prepared, welded, and tested in accordance with the requirements of section 4 of ANSI/AWS D11, (2004) Structural Welding Code-Steel (year)

Manufacturer or Contractor C.P.BUCKNER STEEL Authorized by _____
 Form E-4 Date 6-17-07



Figure A 4.2 Moises Sanchez Welding Certification (Test 2)

WELDER, WELDING OPERATOR OR TACK WELDER QUALIFICATION TEST RECORD

Type of Welder: WELDER
 Name: Ralph Quick Identification No.: 244-88-2558
 Welding Procedure Specification No.: CPB 1023 Rev.: _____ Date: 6-27-08

Variables	Record Actual Values Used in Qualification	Qualification Range
Process/Type [Table 4.10, Item (2)]	fcaw	FCAW
Electrode (single or multiple) [Table 4.10, Item (9)]	SINGLE	
Current/Polarity	DCEp	
Position [Table 4.10, Item (5)]	2G HORIZONTAL	FLAT HORIZONTAL
Weld Progression [Table 4.10, Item (7)]	N/A	
Backing (YES or NO) [Table 4.10, Item (8)]	YES	WITH BACKING ONLY
Material/Spec. [Table 4.10, Item (1)]	ASTM to A36	
Base Metal		
Thickness: (Plate)	1" PLATE	1/8" UNLIMITED GROOVE & UNLIMITED FILLET
Groove		
Fillet	N/A	
Thickness: (Pipe/tube)		
Groove	N/A	
Fillet	N/A	
Diameter: (Pipe)	N/A	
Groove	N/A	
Fillet	N/A	
Filler Metal [Table 4.10, Item (3)]		
Spec No. A	AWS A5.20	
Class E	AWS E70T-4	
F.No.		
Gas/Flux Type [Table 4.10, Item (4)]	NR-311	
Other		

VISUAL INSPECTION (4.8.1)					
Acceptable YES or NO <u>YES</u>					
Guided Bend Test Results (4.30.5)					
Type	Result	Type	Result		
2G1 SIDE	SATISFACTORY				
2G2 SIDE	SATISFACTORY				
Fillet Test Results (4.30.2.3 and 4.30.4.1)					
Appearance _____		Fillet Size _____			
Fracture Test Root Penetration _____		Macroetch _____			
(Describe the location, nature, and size of any crack or tearing of the specimen.)					
Inspected by <u>JERRY CAGLE</u>		Test Number <u>CPB 1023</u>			
Organization <u>AWS</u>		Date <u>6-27-08</u>			
RADIOGRAPHIC TEST RESULTS (4.30.3.1)					
Film Identification Number	Results	Remarks	Film Identification Number	Results	Remarks

Interpreted by _____ Test Number _____
 Organization _____ Date _____

We, the undersigned, certify that the statements in this record are correct and that the test welds were prepared, welded, and tested in accordance with the requirements of section 4 of ANSI/AWS D11.1 (2006) Structural Welding Code-Steel
 (year)

Manufacturer or Contractor C.P.BUCKNER STEEL Authorized by _____
 Form E-4 Date 6-27-08

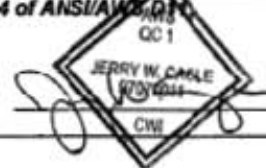


Figure A 4.3 Ralph Quick Weld Certification (Test 5)

WELDER, WELDING OPERATOR OR TACK WELDER QUALIFICATION TEST RECORD

Type of Welder: WELDER
 Name: RALPH QUICK Identification No.: 244-98-2556
 Welding Procedure Specification No.: CPB 1022 Rev.: _____ Date: 6-7-08

Variables	Record Actual Values Used in Qualification	Qualification Range
Process/Type [Table 4.10, Item (2)]	SMAW	FLAT HORIZONTAL VERTICAL OVERHEAD
Electrode (single or multiple) [Table 4.10, Item (9)]	SINGLE	
Current/Polarity	DCEN	
Position [Table 4.10, Item (5)]	4G OVERHEAD	FLAT HORIZONTAL VERTICAL OVERHEAD
Weld Progression [Table 4.10, Item (7)]	3G VERTICAL	
Backing (YES or NO) [Table 4.10, Item (8)]	YES	
Material/Spec. [Table 4.10, Item (1)]	ASTM to A36	
Base Metal		UNLIMITED GROOVE & FILLET
Thickness: (Plate)	1" PLATE	
Groove	N/A	
Fillet	N/A	
Thickness: (Pipe/tube)	N/A	
Groove	N/A	
Fillet	N/A	
Diameter: (Pipe)	N/A	
Groove	N/A	
Fillet	N/A	
Filler Metal [Table 4.10, Item (3)]	AWS A5.1	
Spec No. A	E-7018	
Class E	F-4	
F-No.	N/A	
Gas/Flux Type [Table 4.10, Item (4)]	N/A	
Other		

VISUAL INSPECTION (4.8.1)			
Acceptable YES or NO <u>YES</u>			
Guided Bend Test Results (4.30.5)			
Type	Result	Type	Result
3G1 SIDE	SATISFACTORY	4G1 SIDE	SATISFACTORY
3G2 SIDE	SATISFACTORY	4G2 SIDE	SATISFACTORY
Fillet Test Results (4.30.2.3 and 4.30.4.1)			
Appearance	_____	Fillet Size	_____
Fracture Test Root Penetration	_____	Macroetch	_____
(Describe the location, nature, and size of any crack or tearing of the specimen.)			
Inspected by	<u>JERRY CAGLE</u>	Test Number	<u>CPB 1022</u>
Organization	<u>AWS D1.1</u>	Date	<u>6-7-08</u>

RADIOGRAPHIC TEST RESULTS (4.30.3.1)					
Film Identification Number	Results	Remarks	Film Identification Number	Results	Remarks

Interpreted by _____ Test Number _____
 Organization _____ Date _____

We, the undersigned, certify that the statements in this record are correct and that the test welds were prepared, welded, and tested in accordance with the requirements of section 4 of ANSI/AWS D1.1 (2006) Structural Welding Code-Steel (year)

Manufacturer or Contractor
 Form E-4

C.P. BUCKNER STEEL

Authorized by _____
 Date 6-7-08

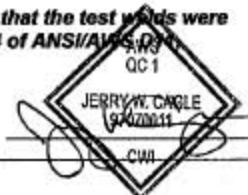


Figure A 4.4 Ralph Quick Weld Certification Continued (Test 5)

A4.2 Inspector Certifications

JUN-18-2008 07:14 FROM

TO:19195155301

P.8-8

State of West Virginia
DEPARTMENT OF LABOR

CERTIFICATE
of
TEST AND APPROVAL OF WELDING PROCESS
and
**QUALIFICATION OF OPERATOR OF
WELDING EQUIPMENT**

The State Department of Labor, Boiler Division, has witnessed the welding and testing of test specimens welded by an employee of

Randy David Dempsey

in accordance with

Code American Society of Mechanical Engineers Boiler Construction Code, Section IX, and American Welding Society Standard Qualification Procedure.

Welding Operator Randy David Dempsey No. _____ Symbol p
Welding Process Shielded Metal Arc - E8018

This is to certify that the Welding Technic used in this test and described in SPECIFICATIONS for WELDING PROCESS No. See above and the results of the test given in PHYSICAL TEST REPORT NO. 1620 complied with the requirements of the above code within the following limitations:

Maximum Pressure See Code
Maximum Temperature See Code
Maximum Plate or Wall Thickness 3/4"
Minimum Plate or Wall Thickness 1/16"
Welding Positions Horizontal, Vertical, Over-
Other Limitations See Code head.

Operator Tested

Remarks Plate Test

No. _____
Order No. _____
File No. 7820
Approved 2/23/76

Randy Dempsey

Commissioner of Labor

Figure A 4.5 Randy Dempsey Certification (Test 1-4)

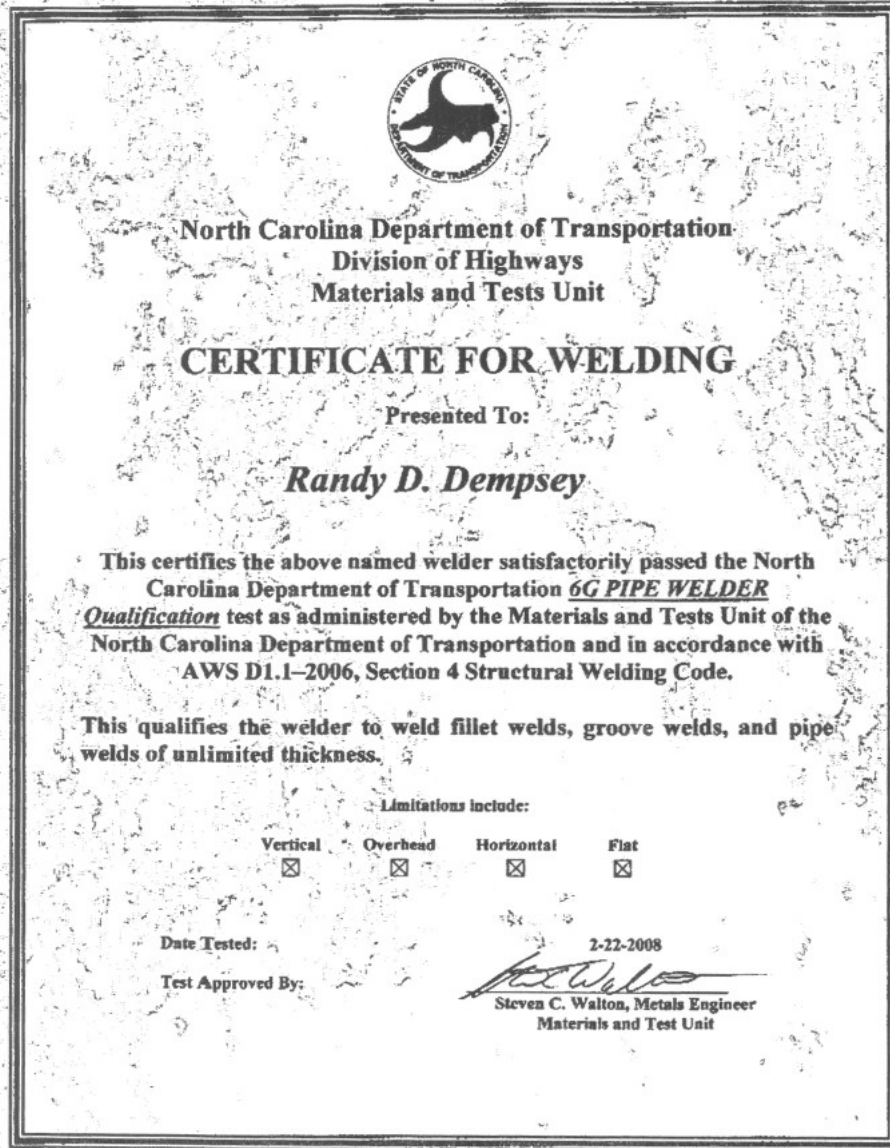


Figure A 4.6 Randy Dempsey Certification (Test 1-4)

P. 2/8

TO: 19195155301

JUN-10-2008 07:09 FROM:



American Welding Society



Certifies that Welding Inspector
Randy D Dempsey

*has complied with the requirements of AWS QCI,
Standard for AWS Certification of Welding Inspectors*

08051811
CERTIFICATE NUMBER

May 1 2011
EXPIRATION DATE



Gene Larson
PRESIDENT AWS

Paul R. Evans
CHAIR, QUALIFICATION COMMITTEE

Ros H. Whelan
CHAIR, CERTIFICATION COMMITTEE

Figure A 4.7 Randy Dempsey Certification (Test 1-4)

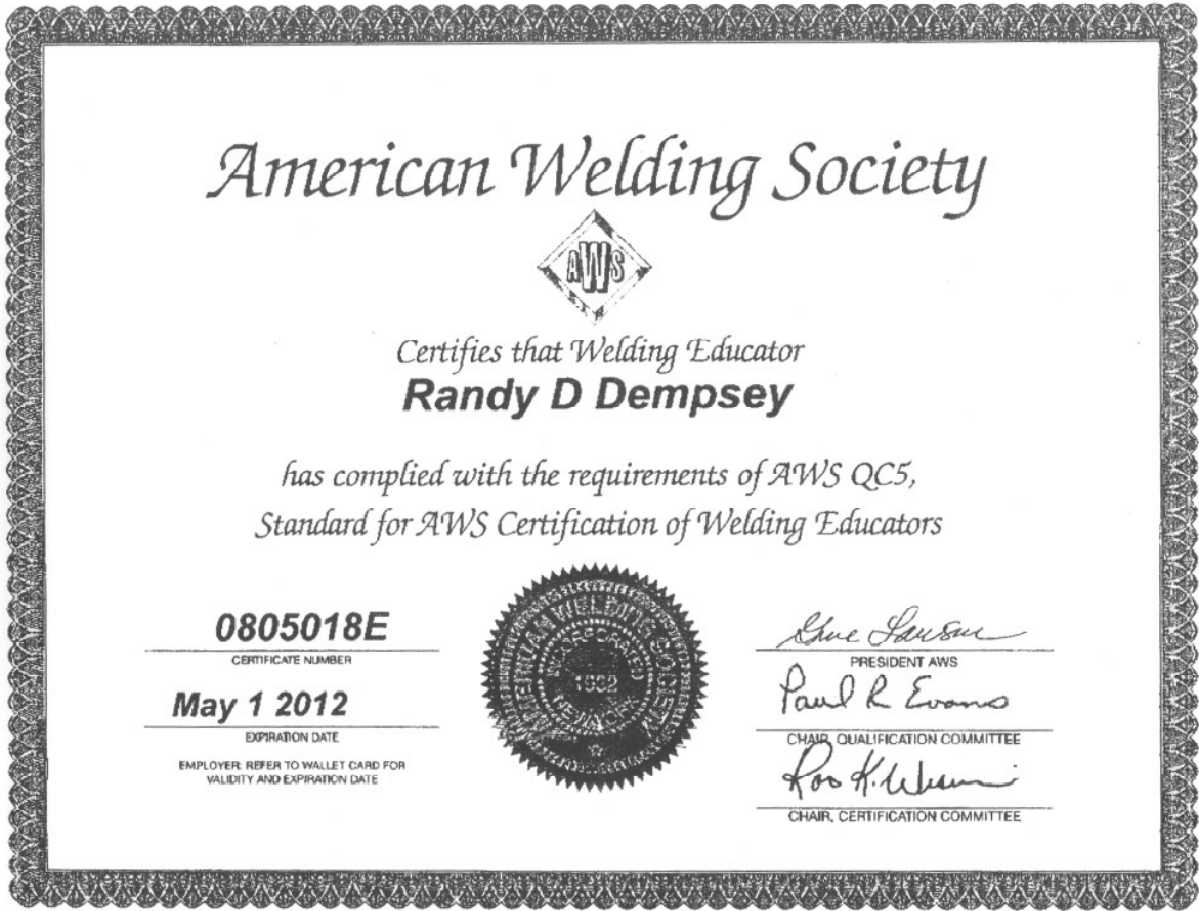


Figure A 4.8 Randy Dempsey Certification (Test 1-4)

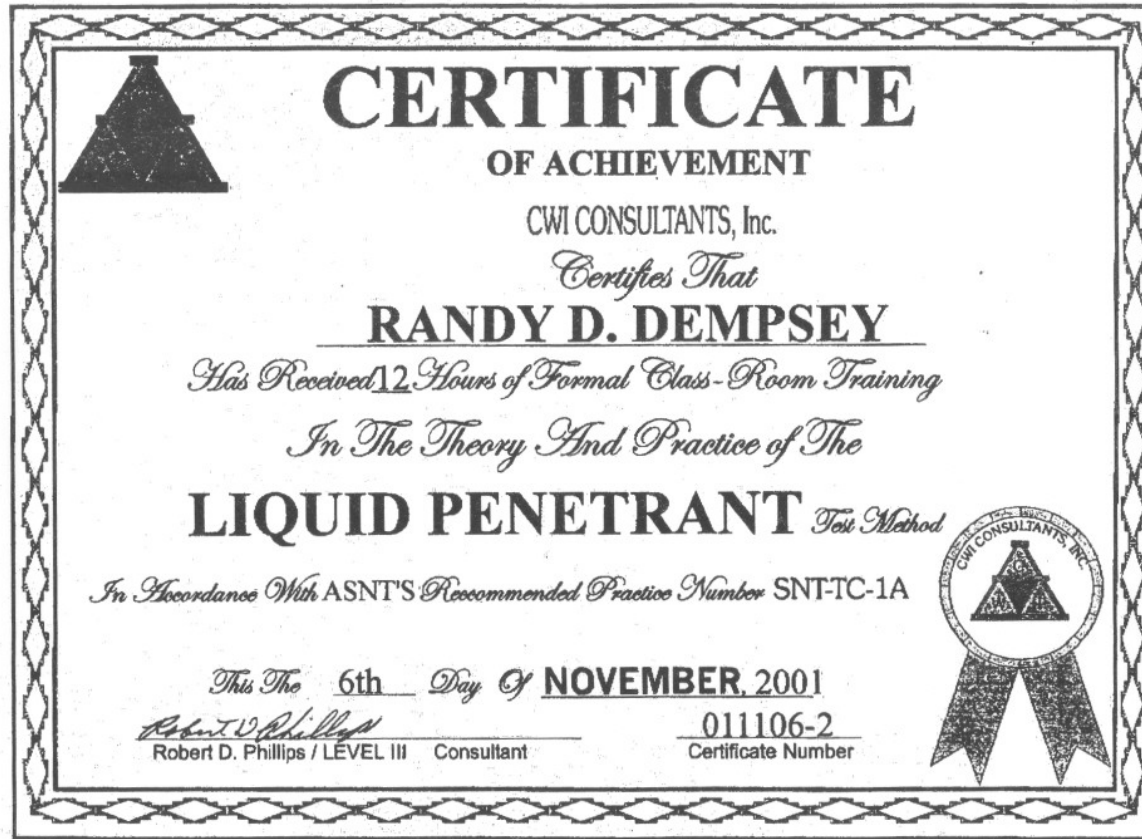


Figure A 4.9 Randy Dempsey Certification (Test 1-4)



Figure A 4.10 Randy Dempsey Certification (Test 1-4)



American Welding Society

Certifies That
WELDING INSPECTOR
Russell W Ogden

Has complied with the requirements of AWS QC1,
Standard for AWS Certification of Welding Inspectors.

with _____, without **X** eye correction, _____ color blind

Gerald Utracki

AWS President

Ron H. Weisman

AWS Certification Chair



07091571

Certificate Number

September 01 2010

Expiration Date

Figure A 4.11 Russell Ogden Certification (Test 5)



American Welding Society

Certifies That
WELDING INSPECTOR

Rhonda G Rogers

Has complied with the requirements of AWS QC1,
Standard for AWS Certification of Welding Inspectors.

with _____ without X eye correction, _____ color blind

Steve Larson

AWS President

Don H. Williams

AWS Certification Chair



08091551

Certificate Number

September 1 2011

Expiration Date

Figure A 4.12 Rhonda Rogers Certification (Test 5)

A4.3 Test 1 Details

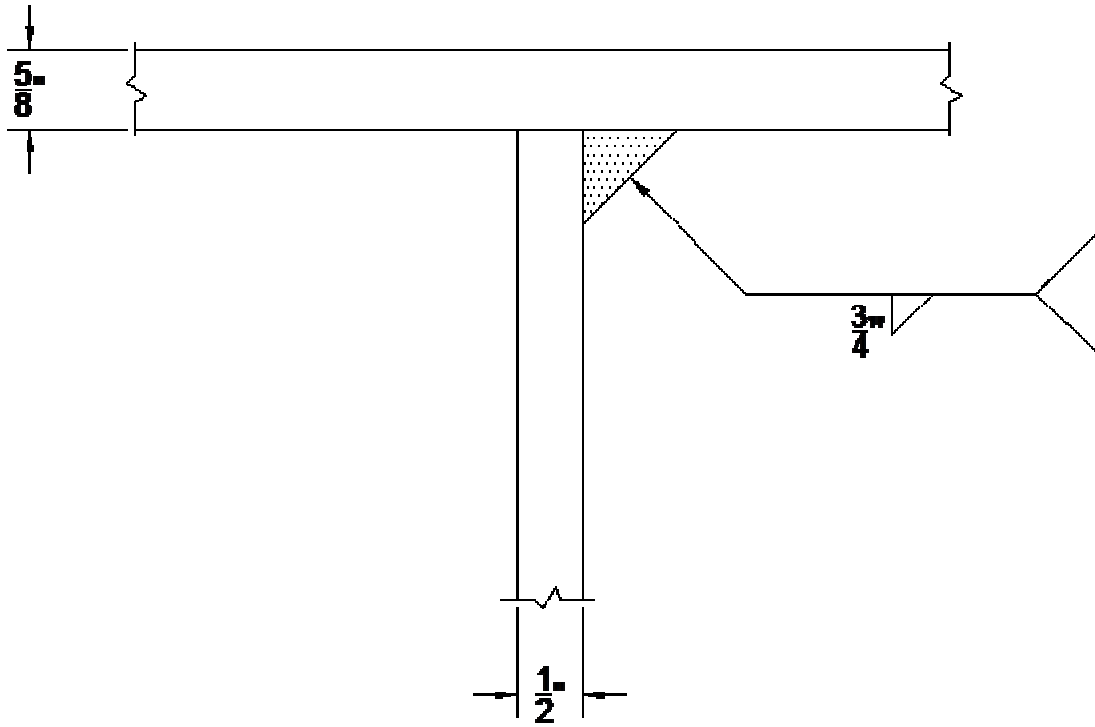


Figure A 4.13 Test 1 Connection Detail

A4.4 Test 2 Details

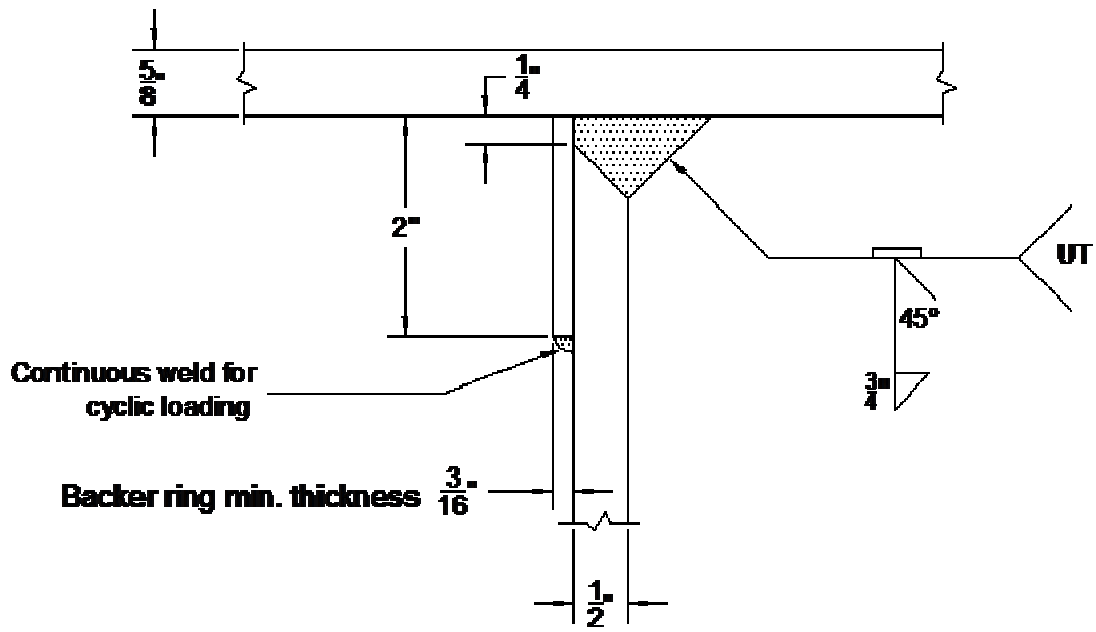


Figure A 4.14 Test 2 Connection Detail

WELDING PROCEDURE SPECIFICATION (WPS) Yes
PREQUALIFIED X QUALIFIED BY TESTING _____
Or PROCEDURE QUALIFICATION RECORDS (PQR) Yes

Company Name Buckner Steel
 Welding Process(es) SMAW
 Supporting PQR No.(s) _____

Identification # CPB1015
 Revision _____ Date _____ By _____
 Authorized by Jerry Cagle Date 6-12-08
 Type: Manual Semi-Automatic
 Machine Automatic

JOINT DESIGN USED
 Type: TC-U4A
 Single Double Weld
 Backing: Yes No
 Backing Material: Steel A36 grade B
 Root Opening 0.25 Root Face Dimension _____
 Groove Angle: 45 Radius (J-U) _____
 Backing Gouging: Yes No Method _____

POSITION
 Position of groove Horizontal/Overhead Fillet Overhead
 Vertical Position: Up Down

BASE METALS
 Material Spec. ASTM A53/ A572 Grade 50 for HP section
 Type of Grade B
 Thickness: Groove 1/2" Fillet _____
 Diameter (Pipe) 16"

ELECTRICAL CHARACTERISTICS
 Transfer Mode (GMAW) _____ Short-circuiting _____
 Globular _____ spray _____
 Current: AC DCEP DCEN Pulsed
 Other _____
 Tungsten Electrode (GTAW)
 Size _____
 Type _____

FILLER METALS
 AWS Specification A 5.1
 AWS Classification E7018

TECHNIQUE
 Stringer or Weave Bead: Stringer
 Multi-pass or Single pass (per side) Multipass
 Number of Electrodes: 1
 Electrode Spacing _____
 Longitudinal N/A
 Lateral N/A
 Angle N/A

SHIELDING
 Flux N/A Gas N/A
 Composition _____
 Electrode-Flux (Class) _____ Flow rate _____
 Gas Cup Size _____

Contact Tube to Work Distance _____
 Peening No
 Interpass Cleaning: Wire brush, grinding or chipping

PREHEAT
 Preheat temp., Min 70 (table 3.2 note A)
 Inter pass Temp., Min 70F Max 500F

POSTWELD HEAT TREATMENT
 Temp: N/A
 Time: N/A

WELDING PROCEDURES

Pass or weld Layer(s)	Process	Filler Metals		Current		Volts	Travel Speed	Joint Details
		Class	Diam.	Type & Polarity	Amps or Wire Feed Speed			
12	SMAW	E7018	1/8"	DC+	100 - 130	20 - 24	5 to 7 in/min	Please see attached

Form N-1 (Front)

Figure A 4.15 Test 2 WPS

Table A 4.1 Test 2 QC Report

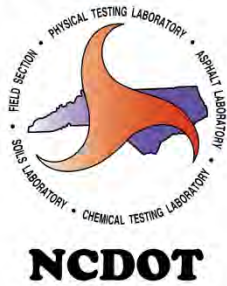
North Carolina Department of Transportation

QA Inspection Check List

Project Description

Alaska DOT

Materials & Tests Unit



Part Description

Owner Representative: **Kendra Cookson**

NCSU Constructed

Project Location: **Facilities Lab**

Bridge Bent

Fabricator Name: **Buckner Companies**

Welder's Name: **Justin Green**

Weld Location

QA Inspector: **Randy Dempsey,
CWI/CWE**

**North & South
Pipe Pile**

Date

Comments

Consumable Storage/Control - - - - -

6/13/08

see note 1

Base Metal Preparation - - - - -

6/13/08

see note 2

Joint Fit-Up - - - - -	6/13/08	see note 3
Pre-Heat & Interpass Temperature Control - - - - -		
Interpass Cleaning - - - - -		
Visual Inspection of Groove Weld - - - - -		
Witness UT Testing of Groove Weld - - - - -		
Groove Weld Repair - - - - -		
Follow-Up UT of Groove Weld - - - - -		
Pre-Heat & Interpass Temp. fillet weld - - - - -		
Interpass Cleaning, fillet weld - - - - -		
Visual Inspection of Fillet Weld - - - - -		

note 1: An electrode oven was delivered to the site. The E7018HR (9 hour exposure limit rods) electrodes were delivered in a hermetically sealed container and placed in the oven immediately after breaking the seal.

note 2: The North and South pipe piles were beveled using a grinder and all mill scale and rust within 1" of the area to be welded was removed.

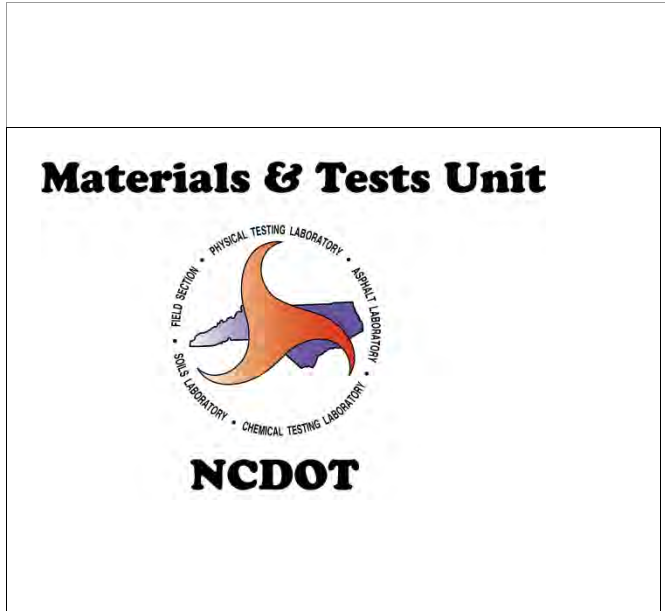


note 3: A 2"x 3/16" flat bar (w/ MTR) was formed and installed in each pipe pile with a CJP weld aligned to the neutral axis and

welded continuous to the pipe with a 1/4" extension for the root opening + 1/16" to 1/8" fit-up tolerance.



North Carolina Department of Transportation



Part Description

Bridge Bent

Weld Location

**North & South
Pipe Pile**

QA Inspection Check List

Project Description

Alaska DOT

Owner Representative: **Kendra Cookson**

NCSU Constructed

Project Location: **Facilities Lab**

Fabricator Name: **Buckner Companies**

Justin Green, Moises

Welder's Name: **Sanchez**

Randy Dempsey,

QA Inspector: **CW/CWE**

Date

Comments

Consumable Storage/Control - - - - -

Base Metal Preparation - - - - -

Joint Fit-Up - - - - -

6/19/08	see note 1
6/19/08	see note 2

Pre-Heat & Interpass Temperature Control - - - - -	6/19/08	see note 3 and 4
Interpass Cleaning - - - - -	6/19/08	see note 5
Visual Inspection of Groove Weld - - - - -	6/19/08	acceptable, see note 6
Witness UT Testing of Groove Weld - - - - -		
Groove Weld Repair - - - - -		
Follow-Up UT of Groove Weld - - - - -		
Pre-Heat & Interpass Temp. fillet weld - - - - -		
Interpass Cleaning, fillet weld - - - - -		
Visual Inspection of Fillet Weld - - - - -		

note 1: The power to the electrode oven was interrupted. The electrodes from the oven were returned to the Buckner facility for re-drying and a new box of E7018HR electrodes were opened.

note 2: Due to flange tilt mill tolerance issues on the cap beam, 1/16" to 1/8" was removed (using a grinder) from the extension of the backing bar as needed to improve the joint fit-up.



note 3: Although preheat was not required due to the 70° lab temperature, a Makita Thermocouple Heat Gun (model HG 1100) was used to raise the base metal temperature to approximately 100° F to reduce the cooling rate of the weld metal.



note 4: Interpass temperature was monitored using an EDL Pocket-Probe (model NMP) Pyrometer, which indicated temperatures from 280° F to 320° F.



note 5: All slag was removed with a chipping hammer. The start of some welds was contoured to a concave finish prior to covering with additional weld metal. Any anomalous material or weld discontinuity that might be detrimental to the integrity of the completed weld was removed using a wire brush or grinder.

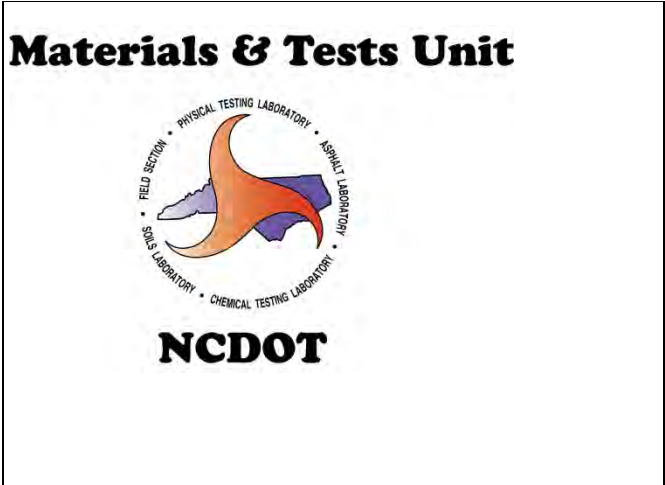
note 6: The North Pile was welded by Justin Green and the South Pile was welded by Moises Sanchez. Both grooves were filled to the full cross section of the pipe member and found to be visually acceptable in accordance with AWS D1.1 2006 Table 6.1.

North Carolina Department of Transportation

QA Inspection Check List

Project Description

Alaska DOT



Part Description

Owner Representative: **Kendra Cookson**

Bridge Bent

NCSU Constructed

Project Location: **Facilities Lab**

Fabricator Name: **Buckner Companies**

Justin Green, Moises

Welder's Name: **Sanchez**

Weld Location

Randy Dempsey,
QA Inspector: **CWI/CWE**

**North & South
Pipe Pile**

Date

Comments

Consumable Storage/Control - - - - -

Base Metal Preparation - - - - -

Joint Fit-Up - - - - -

6/20/08	see note 1

Pre-Heat & Interpass Temperature Control - - - - -		
Interpass Cleaning - - - - -		
Visual Inspection of Groove Weld - - - - -		
Witness UT Testing of Groove Weld - - - - -	6/20/08	refer to the UT Inspection Report
Groove Weld Repair - - - - -	6/20/08	no repair required
Follow-Up UT of Groove Weld - - - - -	N/A	
Pre-Heat & Interpass Temp. fillet weld - - - - -	6/20/08	see note 2 and 3
Interpass Cleaning, fillet weld - - - - -	6/20/08	see note 4
Visual Inspection of Fillet Weld - - - - -	6/20/08	acceptable; see note 5

note 1: The electrode oven is working correctly.

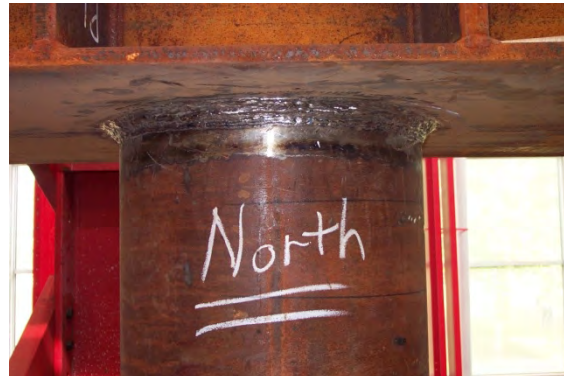
note 2: Although preheat was not required due to the 70° lab temperature, a Makita Thermocouple Heat Gun (model HG 1100)

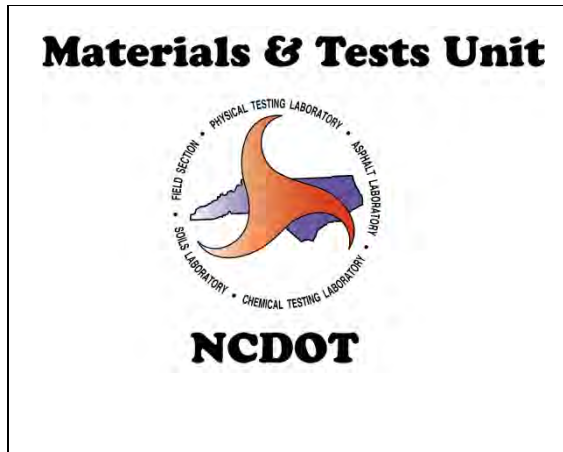
was used to raise the base metal temperature to approximately 100° F to reduce the cooling rate of the weld metal.

note 3: Interpass temperature was monitored using an EDL Pocket-Probe (model NMP) Pyrometer, which indicated temperatures from 260° F to 300° F.

note 4: All slag was removed using a chipping hammer. Any anomalous material or weld discontinuity that might be detrimental to the integrity of the completed weld was removed using a wire brush or grinder.

note 5: The leg and the throat was inspected using a 3/4" G.A.L. weld gage with a flash light as a luminous aid. The profile of the completed weld was improved using a grinder. The completed weld was found to be visually acceptable in accordance with AWS D1.1 2006 Figure 5.4 and Table 6.1.





Part Description

Bridge Bent

Weld Location

North & South
Pipe Pile

Owner Representative: **Kendra Cookson**

NCSU Constructed

Project Location: **Facilities Lab**

Fabricator Name: **Buckner Companies**

Justin Green, Moises

Welder's Name: **Sanchez**

QA Inspector: **Randy Dempsey, CWI/CWE**

C1. If the cap beam was assembled with the stipulation that the bottom side needs to be flat by pushing the mill tolerance to the top, the fit-up and weld quality at the root could be improved.

C2. Purchasing the backing rings (<http://www.robvon.com/html/backing.html>) may prove to be a more practical and efficient method for actual production conditions.

C3. Due to the low interpass temperatures that were recorded, a WPS that stipulates 1/8" electrodes for passes 1, 2, and 3, but permits 5/32" electrodes for all subsequent passes could improve efficiency of production conditions.

C4. The approximate labor that was recorded (excluding QA and NCSU involvement) included 16 man hours for beveling the pipe and attaching the backing ring, 22 man hours for the groove weld, 2 hours for the UT (excluding travel time) with no flaws detected and 20 man hours for the 3/4" fillet weld.

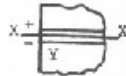
N
TRIAD
T

Triad
Nondestructive
Testing, Inc.
P.O. Box 2342
Kannapolis, NC 27295-2342
(336) 996-2676

REPORT OF ULTRASONIC TESTING OF WELDS

Project ALASKA DOT

Job No. Bridge Permit



Weld Identification SEE BELOW
 Material Thickness 1/2"
 Weld Joint AWS IC-MAA
 Welding Process SMAW
 Quality requirements - section no. TAB 6.3 (AWS D1.1 2006)
 Remarks FULL PENETRATION WELDS

Line Number	Pierce Number	Transducer Angle	From Face	Legs	Indication Level	Decibels			Discontinuity				Discontinuity Elevation	Remarks	
						Reference Level	Attenuation Factor	Indication Rating	Length	Angular distance (sound path)	Depth from PA* surface	Distance			
												From X			From Y
a	b	c	d												
1	1	70°	A	1 1/2	SI									ACCEPT	NORTH
2	2	70°	A	1 1/2	SI									ACCEPT	SOUTH
3															
4															
5															
6					NOTE:	NORTH END WELD HAD SURFACE INDICATIONS WHICH WERE									
7						REMOVED BY GRINDING									
8															
9															

We, the undersigned, certify that the statements in this report are correct and that the welds were prepared and tested in accordance with the requirements of 6C of AWS D1.1, (2006) Structural Welding Code.

Test date 6/20/08 year
 Manufacturer or Contractor NCSC

Inspected by [Signature]
 Authorized by [Signature] Date 6/20/08

Figure A 4.16 Test 2 UT Report

A4.5 Test 3 Details

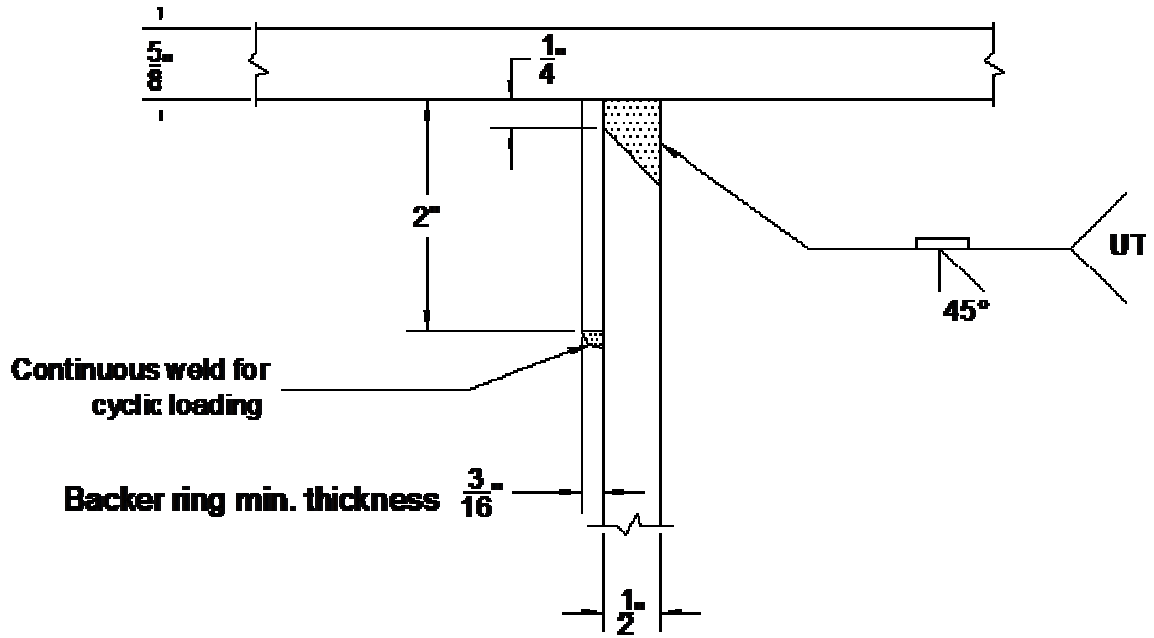


Figure A 4.17 Test 3 Connection Detail

WELDING PROCEDURE SPECIFICATION (WPS) Yes
 PREQUALIFIED X QUALIFIED BY TESTING _____
 Or PROCEDURE QUALIFICATION RECORDS (PQR) Yes

Company Name <u>Buckner Steel</u> Welding Process(es) <u>SMAW</u> Supporting PQR No.(s) _____ <hr/> JOINT DESIGN USED Type: TC-U4A Single <input type="checkbox"/> Double Weld <input type="checkbox"/> Backing: Yes <input checked="" type="checkbox"/> No <input type="checkbox"/> Backing Material: Steel A36 grade B Root Opening <u>0.25</u> Root Face Dimension _____ Groove Angle: <u>45</u> Radius (J-U) _____ Backing Gouging: Yes <input type="checkbox"/> No <input checked="" type="checkbox"/> Method _____ <hr/> BASE METALS Material Spec. <u>ASTM A53/ A572 Grade 50 for HP section</u> Type of Grade <u>B</u> Thickness: Groove <u>1/2"</u> Fillet _____ Diameter (Pipe) <u>16"</u> <hr/> FILLER METALS AWS Specification <u>A 5.1</u> AWS Classification <u>E7018</u> <hr/> SHIELDING Flux <u>N/A</u> Gas <u>N/A</u> Composition _____ Electrode-Flux (Class) _____ Flow rate _____ Gas Cup Size _____ <hr/> PREHEAT Preheat temp., Min <u>70</u> (table 3.2 note A) Interpass Temp., Min <u>70F</u> Max <u>500F</u>	Identification # <u>CPB1015</u> Revision _____ Date _____ By _____ Authorized by <u>Jerry Cagle</u> Date <u>10/20/08</u> Type: Manual <input checked="" type="checkbox"/> Semi-Automatic <input type="checkbox"/> Machine <input type="checkbox"/> Automatic <input type="checkbox"/> <hr/> POSITION Position of groove <u>Horizontal/Overhead</u> Fillet <u>Overhead</u> Vertical Position: Up <input type="checkbox"/> Down <input type="checkbox"/> <hr/> ELECTRICAL CHARACTERISTICS Transfer Mode (GMAW) _____ Short-circuiting _____ Globular <input type="checkbox"/> spray <input type="checkbox"/> Current: AC <input type="checkbox"/> DCEP <input checked="" type="checkbox"/> DCEN <input type="checkbox"/> Pulsed <input type="checkbox"/> Other _____ Tungsten Electrode (GTAW) Size _____ Type _____ <hr/> TECHNIQUE Stringer or Weave Bead: <u>Stringer</u> Multi-pass or Single pass (per side) <u>Multipass</u> Number of Electrodes: <u>1</u> Electrode Spacing _____ Longitudinal <u>N/A</u> Lateral <u>N/A</u> Angle <u>N/A</u> Contact Tube to Work Distance _____ Peening <u>No</u> Interpass Cleaning: <u>Wire brush, grinding or chipping</u> <hr/> POSTWELD HEAT TREATMENT Temp: <u>N/A</u> Time: <u>N/A</u>
--	---

WELDING PROCEDURES

Pass or weld Layer(s)	Process	Filler Metals		Current		Volts	Travel Speed	Joint Details
		Class	Diam.	Type & Polarity	Amps or Wire Feed Speed			
12	SMAW	E7018	1/8"	DC+	100 - 130	20 - 24	5 to 7 in/min	Please see attached

Form N-1 (Front)

Figure A 4.18 Test 3 WPS

Table A 4.2 Test 3 QC Report

North Carolina Department of Transportation

QA Inspection Check List

Project Description

Materials & Tests Unit



Part Description

Owner Representative:

NCSU Constructed

Project Location: Facilities Lab

Bridge Bent Test 3

Fabricator Name: Buckner Companies

Welder's Name: Justin Green

Weld Location

Randy Dempsey,
QA Inspector: CWI/CWE

**North & South
Pipe Pile**

Date

Consumable Storage/Control - - - - -

8/5/08

Base Metal Preparation - - - - -

8/5/08

Joint Fit-Up - - - - -	8/5/08
Pre-Heat & Interpass Temperature Control - -	8/5/08
Interpass Cleaning - - - - -	
Visual Inspection of Groove Weld - -	
Witness UT Testing of Groove Weld - - - - -	
Groove Weld Repair - - - - -	
Follow-Up UT of Groove Weld - - - - - -	
Pre-Heat & Interpass Temp. fillet weld - - - - -	
Interpass Cleaning, fillet weld - - - - -	
Visual Inspection of Fillet Weld - - - - -	

note 1: An electrode oven was delivered to the site. The E7018 (4 hour exposure limit rods) electrodes were delivered in a hermetically sealed container and placed in the oven within one hour after breaking the seal. The oven was plugged into an outlet on the inside of the lab to ensure an uninterrupted power source.



note 2: The North and South pipe piles were beveled to a 45° angle using a grinder and all mill scale and rust within 1" of the area to be welded was removed. The bevel angle was inspected using a mechanical protractor. One area on the North Pile was found to be less than the specified angle and was corrected prior to fit-up of the backing bar.





note 3: A 2"x 3/16" flat bar was formed and installed in each pipe pile with the CJP weld that is transverse to the length of the material aligned to the neutral axis of the pipe. The full length of the flat bar was welded continuous to the pipe with a 1/4" extension for the root opening + 1/16" fit-up tolerance. Tack welds placed in the area to be groove welded were removed by grinding.



note 4: The 50° F preheat was not necessary due to the thickness of the material and the atmospheric conditions at the work site being recorded at 98° F using an air thermometer that was placed in the shade at the same elevation and location as the material to be welded.



Alaska DOT

Materials & Tests Unit



Part Description

Owner Representative: **Kendra Cookson**

NCSU Constructed

Project Location: **Facilities Lab**

Bridge Bent Test 3

Fabricator Name: **Buckner Companies**

Welder's Name: **Justin Green**

Randy Dempsey,

QA Inspector: **CWI/CWE**

Weld Location

**North & South Pipe
Pile**

Date

Comments

Consumable Storage/Control - - - - -

8/11/08

see note 1

Base Metal Preparation - - - - -

Joint Fit-Up - - - - -

8/11/08

see note 2

Pre-Heat & Interpass Temperature Control - - - - -

8/11/08

see note 3 and 4

Interpass Cleaning - - - - -	8/11/08	see note 5
Visual Inspection of Groove Weld - - - - -	8/12/08	acceptable, see note 6
Witness UT Testing of Groove Weld - - - - -		
Groove Weld Repair - - - - -		
Follow-Up UT of Groove Weld - - - - -		
Pre-Heat & Interpass Temp. fillet weld - - - - -		
Interpass Cleaning, fillet weld - - - - -		
Visual Inspection of Fillet Weld - - - - -		

note 1: The electrodes and electrode oven were inspected and found to be hot and undisturbed from the previous activity.



note 2: The nt fit-up was acceptable without making adjustments to the backing bar.

note 3: Although preheat was not required due to the 70° lab temperature, an oxygen/acetylene torch was used to drive away



moisture and raise the base metal temperature to approximately 125° to reduce the cooling rate of the weld metal.

note 4: Interpass temperature was monitored using 248° and 302° Nissen® Temperature Sticks. Due to one welder alternating between pipe piles, interpass temperatures did not exceed 302°.



note 5: All slag was removed with a chipping hammer. The start of some welds was contoured to a concave finish prior to covering with additional weld metal. Any anomalous material or weld discontinuity that could have been detrimental to the

integrity of the completed weld was removed using a wire brush or grinder.



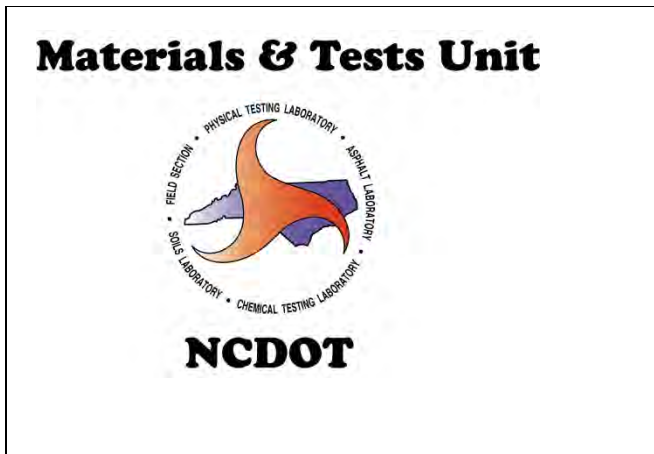
note 6: The North and South Pipe Piles were welded by Justin Green. Both grooves were filled to the full cross section of the pipe member and found to be visually acceptable in accordance with AWS D1.1 2006 Table 6.1.

North Carolina Department of Transportation

QA Inspection Check List

Project Description

Alaska DOT



Part Description

**Bridge Bent
Test 3**

Weld Location

**North & South
Pipe Pile**

Owner Representative: **Kendra Cookson**

NCSU Constructed

Project Location: **Facilities Lab**

Fabricator Name: **Buckner Companies**

Welder's Name: **Justin Green**

Randy Dempsey,

QA Inspector: **CWI/CWE**

Date

Comments

Consumable Storage/Control - - - - -

8/12/08

see note 1

Base Metal Preparation - - - - -

Joint Fit-Up - - - - -

Pre-Heat & Interpass Temperature Control - - - - -	8/12/08	see note 2 and 3
Interpass Cleaning - - - - -	8/12/08	see note 4
Visual Inspection of Groove Weld - - - - -	8/12/08	acceptable, see note 5
Witness UT Testing of Groove Weld - - - - -		
Groove Weld Repair - - - - -		
Follow-Up UT of Groove Weld - - - - -		
Pre-Heat & Interpass Temp. fillet weld - - - - -		
Interpass Cleaning, fillet weld - - - - -		
Visual Inspection of Fillet Weld - - - - -		

note 1: The electrodes and electrode oven were inspected and found to be hot and undisturbed from the previous activity.

note 2: Although preheat was not required due to the 70° lab temperature, an oxygen/acetylene torch was used to drive away moisture and raise the base metal temperature to approximately 125° to reduce the cooling rate of the weld metal.

note 3: Interpass temperature was monitored using a 248° and 302° Nissen® Temperature Sticks. Due to one welder alternating between pipe piles, interpass temperatures did not exceed 248°.

note 4: All slag was removed with a chipping hammer. Any anomalous material or weld discontinuity that might be detrimental to the integrity of the completed weld was removed using a wire brush or grinder.

note 5: The North and South Pipe Piles were welded by Justin Green. Both grooves were filled to the full cross section of the pipe member and after repairing several small deficiencies, found to be visually acceptable in accordance with AWS D1.1 2006 Table 6.1. A grinder was used to improve the profile of the completed weld.

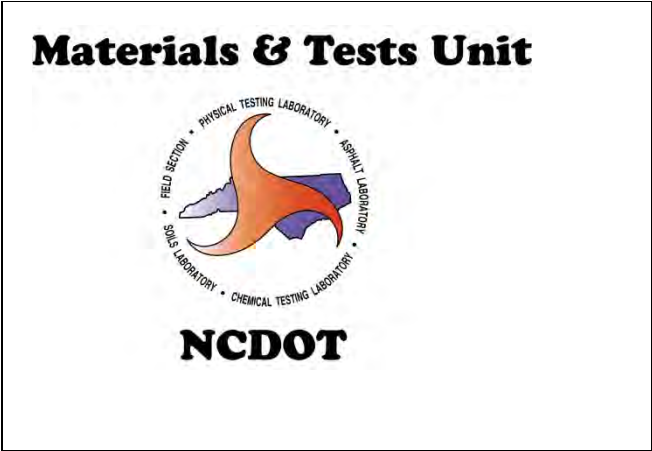


North Carolina Department of Transportation

QA Inspection Check List

Project Description

Alaska DOT



Part Description

Bridge Bent
Test 3

Weld Location

North & South
Pipe Pile

Owner Representative: Kendra Cookson

NCSU Constructed

Project Location: Facilities Lab

Fabricator Name: Buckner Companies

Welder's Name: Justin Green

Randy Dempsey,

QA Inspector: CWI/CWE

Date

Comments

Consumable Storage/Control - - - - -

Base Metal Preparation - - - - -

Joint Fit-Up - - - - -

8/13/08

see note 1

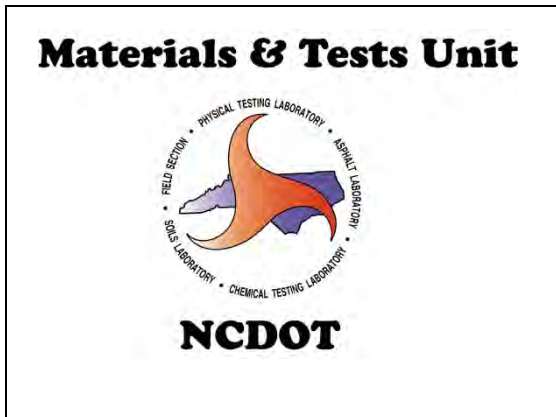
Pre-Heat & Interpass Temperature Control - - - - -		
Interpass Cleaning - - - - -		
Visual Inspection of Groove Weld - - - - -		
Witness UT Testing of Groove Weld - - - - -	8/13/08	see UT report
Groove Weld Repair - - - - -	8/13/08	see note 2
Follow-Up UT of Groove Weld - - - - -	8/13/08	see UT report
Pre-Heat & Interpass Temp. fillet weld - - - - -		
Interpass Cleaning, fillet weld - - - - -		
Visual Inspection of Fillet Weld - - - - -		

note 1: The electrodes and electrode oven were inspected and found to be hot and undisturbed from the previous activity.

note 2: Although preheat was not required due to the 70° lab temperature, an oxygen/acetylene torch was used to drive away moisture and raise the base metal temperature to approximately 125° to reduce the cooling rate of the weld metal



Alaska DOT



Part Description

Bridge Bent
Test 3

Weld Location

North & South
Pipe Pile

Owner Representative: Kendra Cookson

NCSU Constructed Facilities

Project Location: Lab

Fabricator Name: Buckner Companies

Welder's Name: Justin Green

QA Inspector: Randy Dempsey, CWI/CWE

Comments from Test 2

C1. If the cap beam was assembled with the stipulation that the bottom side needs to be flat by pushing the mill tolerance to the top, the fit-up and weld quality at the root could be improved.

C2. Purchasing the backing rings (<http://www.robvon.com/html/backing.html>) may prove to be a more practical and efficient method for actual production conditions.

C3. Due to the low interpass temperatures that were recorded, a WPS that stipulates 1/8" electrodes for passes 1, 2, and 3, but permits 5/32" electrodes for all subsequent passes could improve efficiency of production conditions.

C4. The approximate labor that was recorded (excluding QA and NCSU involvement) included 16 man hours for beveling the pipe and attaching the backing ring, 22 man hours for the groove weld, 2 hours for the UT (excluding travel time) with no flaws detected and 20 man hours for the 3/4" fillet weld.

Additional Comments from Test 3

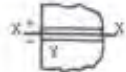
C5. The approximate production man-hours recorded were; 10 hours for beveling the pipe and attaching the backing ring, 18 hours for applying the groove weld, 4 hours for the UT inspection and 4 hours for weld repair.

C6. Due to the deficiency found with the groove bevel, a close inspection prior to backing bar fit-up during actual production is recommended to ensure that the specification of +10°, -0° is maintained.

C7. Close QA verification of the UT Testing and follow-up UT after weld repairs have been made is recommended to ensure that the proper code and section specifications are followed.

**TRIAD
T**

Triad
Nondestructive
Testing, Inc.
P.O. Box 2342
Kannapolis, NC 27285-2342
(336) 996-2570



REPORT OF ULTRASONIC TESTING OF WELDS

Project ALASKA DOT BRIDGE ROAD TEST #3

2000 _____

Weld Identification S&P BELOW
 Material Thickness 1/2"
 Weld Joint AW
 Welding Process SMAW
 Quality Requirements - section no. _____
 Remarks CLYDE 400000

Line Number	Place Number	Transducer Angle	From face	Leg	Indication Level	Decibels			Discontinuity			Discontinuity Elevation	Remarks		
						Reference Level	Attenuation Factor	Indication Rating	Length	Angular distance (sound path)	Depth from "A" surface			Distance	
						a	b	c						d	From X
1	1	70°	A	1/2	+4	64	+6	1/8"		7/16"		REJECT	NE QUAD		
2	2	70°	A	1/2		64	+5	1/8"		1/8"		REJECT	E QUAD		
3	3	70°	A	1/2		64						ACCEPT	NE QUAD		
4	4	70°	A	1/2		64						ACCEPT	E QUAD		
5	5	70°	A	1/2		64						ACCEPT	NORTH		
6	6	70°	A	1/2		64						ACCEPT	SOUTH		
7															
8															
9															

We, the undersigned, certify that the statements in this record are correct and that the welds were prepared and tested in accordance with the requirements of AC of AWS D1.1, (2004) Structural Welding Code.

Test date 7/7/00
 Manufacturer or Contractor WV STATE

Inspected by _____
 Authorized by _____ Date _____

Figure A 4.19 Test 3 UT Report

A4.6 Test 4 Details

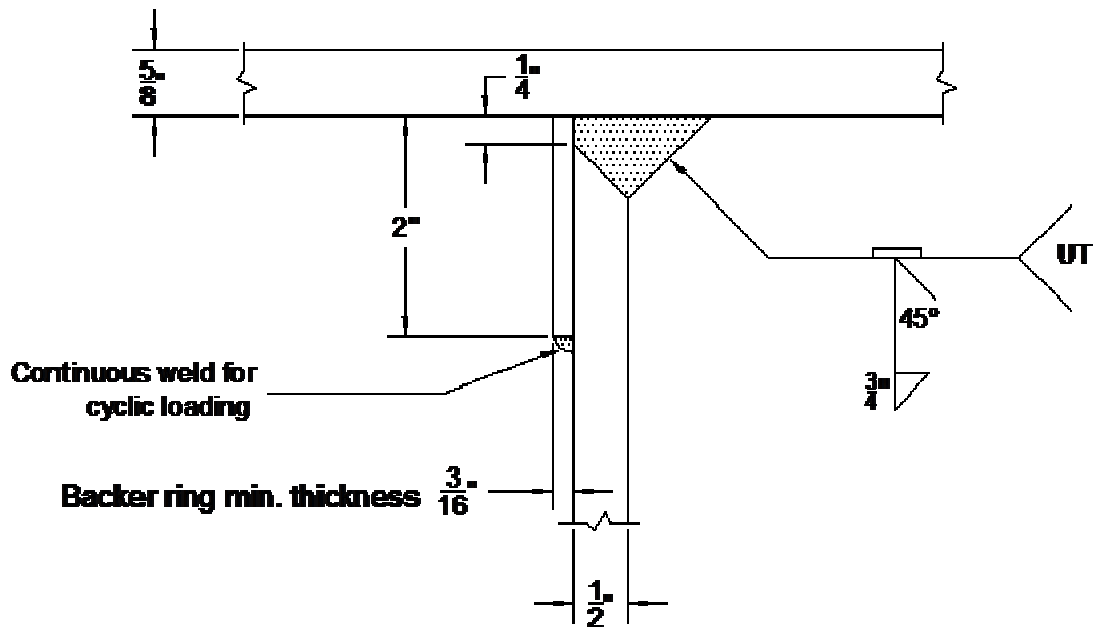


Figure A 4.20 Test 4 Connection Detail

WELDING PROCEDURE SPECIFICATION (WPS) Yes
 PREQUALIFIED X QUALIFIED BY TESTING _____
 Or PROCEDURE QUALIFICATION RECORDS (PQR) Yes

Company Name <u>Buckner Steel</u> Welding Process(es) <u>SMAW</u> Supporting PQR No.(s) _____ <hr/> JOINT DESIGN USED Type: TC-U4A Single <input type="checkbox"/> Double Weld <input type="checkbox"/> Backing: Yes <input checked="" type="checkbox"/> No <input type="checkbox"/> Backing Material: Steel A36 grade B Root Opening <u>0.25</u> Root Face Dimension _____ Groove Angle: <u>45</u> Radius (J-U) _____ Backing Gouging: Yes <input type="checkbox"/> No <input checked="" type="checkbox"/> Method _____ <hr/> BASE METALS Material Spec. <u>ASTM A53/ A572 Grade 50 for HP section</u> Type of Grade <u>B</u> Thickness: Groove <u>1/2"</u> Fillet _____ Diameter (Pipe) <u>16"</u> <hr/> FILLER METALS AWS Specification <u>A 5.1</u> AWS Classification <u>E7018</u> <hr/> SHIELDING Flux <u>N/A</u> Gas <u>N/A</u> Composition _____ Electrode-Flux (Class) _____ Flow rate _____ Gas Cup Size _____ <hr/> PREHEAT Preheat temp., Min <u>70</u> (table 3.2 note A) Interpass Temp., Min <u>70F</u> Max <u>500F</u>	Identification # <u>CPB1015</u> Revision _____ Date _____ By _____ Authorized by <u>Jerry Cagle</u> Date <u>8/5/08</u> Type: Manual <input checked="" type="checkbox"/> Semi-Automatic <input type="checkbox"/> Machine <input type="checkbox"/> Automatic <input type="checkbox"/> <hr/> POSITION Position of groove <u>Horizontal/Overhead</u> Fillet <u>Overhead</u> Vertical Position: Up <input type="checkbox"/> Down <input type="checkbox"/> <hr/> ELECTRICAL CHARACTERISTICS Transfer Mode (GMAW) _____ Short-circuiting _____ Globular _____ spray _____ Current: AC <input type="checkbox"/> DCEP <input checked="" type="checkbox"/> DCEN <input type="checkbox"/> Pulsed <input type="checkbox"/> Other _____ Tungsten Electrode (GTAW) Size _____ Type _____ <hr/> TECHNIQUE Stringer or Weave Bead: <u>Stringer</u> Multi-pass or Single pass (per side) <u>Multipass</u> Number of Electrodes: <u>1</u> Electrode Spacing _____ Longitudinal <u>N/A</u> Lateral <u>N/A</u> Angle <u>N/A</u> Contact Tube to Work Distance _____ Peening <u>No</u> Interpass Cleaning: <u>Wire brush, grinding or chipping</u> <hr/> POSTWELD HEAT TREATMENT Temp: <u>N/A</u> Time: <u>N/A</u>
---	--

WELDING PROCEDURES

Pass or weld Layer(s)	Process	Filler Metals		Current		Volts	Travel Speed	Joint Details
		Class	Diam.	Type & Polarity	Amps or Wire Feed Speed			
12	SMAW	E7018	1/8"	DC+	100 - 130	20 - 24	5 to 7 in/min	Please see attached

Form N-1 (Front)

Figure A 4.21 Test 4 WPS

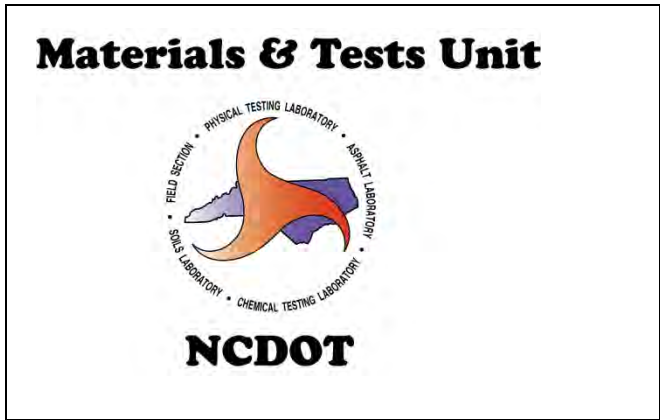
Table A 4.3 Test 4 QC Report

North Carolina Department of Transportation

QA Inspection Check List

Project Description

Alaska DOT



Part Description

Owner Representative: **Kendra Cookson**

**Bridge Bent
Test 4**

Project Location: **NCSU Constructed Facilities
Lab**

Fabricator Name: **Buckner Companies**

Welder's Name: **Justin Green**

Weld Location

QA Inspector: **Randy Dempsey, CWI/CWE**

**North & South
Pipe Pile**

Date

Comments

Consumable Storage/Control - - - - -

9/15/08

see note 1

Base Metal Preparation - - - - -

9/15/08

see note 2

Joint Fit-Up - - - - -

9/15/08

see note 3

Pre-Heat & Interpass Temperature Control - - - - -	9/15/08	see note 4
Interpass Cleaning - - - - -		
Visual Inspection of Groove Weld - - - - -		
Witness UT Testing of Groove Weld - - - - -		
Groove Weld Repair - - - - -		
Follow-Up UT of Groove Weld - - - - -		
Pre-Heat & Interpass Temp. fillet weld - - - - -		
Interpass Cleaning, fillet weld - - - - -		
Visual Inspection of Fillet Weld - - - - -		

note 1: The electrode oven and electrodes (E7018, 4 hour exposure limit rods) from the previous test have remained on site and will be used for today's operations. According to NCSU sources, the oven's power source has been uninterrupted.

note 2: The North and South pipe piles were beveled to a 45° angle using a grinder and all mill scale and rust within 1" of the

area to be welded was removed. The bevel angle was inspected using a tri-square.



note 3: A 2"x 3/16" flat bar was pre-formed to an approximate diameter and installed in each pipe pile with the CJP weld that is transverse to the length of the material aligned to the neutral axis of the pipe. The full length of the flat bar was welded continuous to the pipe with a 1/4" extension for the root opening + 1/16" fit-up tolerance. Tack welds placed in the area to be groove welded were removed by grinding.



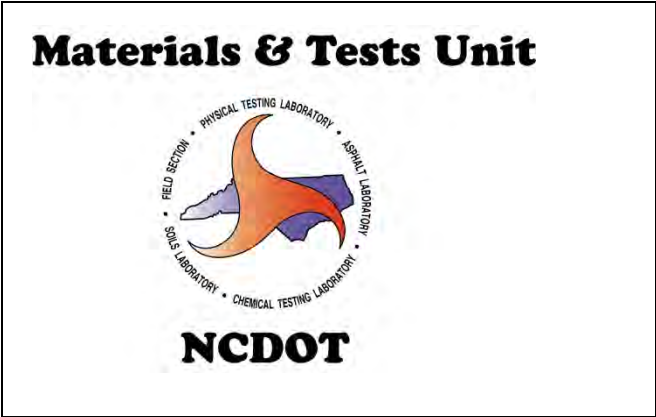
note 4: The 50° F preheat was not necessary due to the thickness of the material and the atmospheric conditions at the work site being 73° F for a low and 85° F for a high, according to weather.com.

North Carolina Department of Transportation

QA Inspection Check List

Project Description

Alaska DOT



Part Description

**Bridge Bent
Test 4**

Weld Location

**North & South
Pipe Pile**

Owner Representative:

Kendra Cookson

Project Location:

**NCSU Constructed
Facilities Lab**

Fabricator Name:

Buckner Companies

Welder's Name:

Justin Green, Chris

QA Inspector:

Randy Dempsey, CWI/CWE

Date

Comments

Consumable Storage/Control - - - - -
 Base Metal Preparation - - - - -
 Joint Fit-Up - - - - -
 Pre-Heat & Interpass Temperature Control - - - - -

9/17/08
9/17/08
9/17/08
9/17/08

see note 1

see note 2

see note 3 and 4

Interpass Cleaning - - - - -	9/17/08	see note 5
Visual Inspection of Groove Weld - - - - -		
Witness UT Testing of Groove Weld - - - - -		
Groove Weld Repair - - - - -		
Follow-Up UT of Groove Weld - - - - -		
Pre-Heat & Interpass Temp. fillet weld - - - - -		
Interpass Cleaning, fillet weld - - - - -		
Visual Inspection of Fillet Weld - - - - -		

note 1: The electrodes and electrode oven were inspected and found to be hot and undisturbed from the previous activity.

note 2: The joint fit-up was acceptable after making adjustments to the backing bar by grinding excess material to close the gap.

note 3: Although preheat was not required due to the 70° lab temperature, an oxygen/acetylene torch was used to drive away moisture and raise the base metal temperature to approximately 125° to reduce the cooling rate of the weld metal.

note 4: Interpass temperature was monitored using 248° and 302° Nissen® Temperature Sticks. Interpass temperatures did not

exceed 302°.

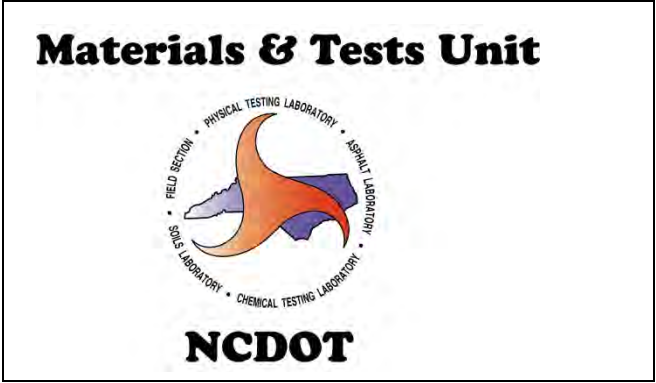
note 5: All slag was removed with a chipping hammer. The start of some welds was contoured to a concave finish prior to covering with additional weld metal. Any anomalous material or weld discontinuity that could have been detrimental to the integrity of the completed weld was removed using a wire brush or grinder.

North Carolina Department of Transportation

QA Inspection Check List

Project Description

Alaska DOT



Part Description

**Bridge Bent
Test 4**

Weld Location

**North & South
Pipe Pile**

Owner Representative:

Kendra Cookson

Project Location:

NCSU Constructed Facilities Lab

Fabricator Name:

Buckner Companies

Welder's Name:

Justin Green, Chris

QA Inspector:

Randy Dempsey, CWI/CWE

Date

Comments

- Consumable Storage/Control - - - - -
- Base Metal Preparation - - - - -
- Joint Fit-Up - - - - -
- Pre-Heat & Interpass Temperature Control - - - - -

9/18/08

see note 1

Interpass Cleaning - - - - -		
Visual Inspection of Groove Weld - - - - -		
Witness UT Testing of Groove Weld - - - - -	9/18/08	refer to the UT Inspection Report
Groove Weld Repair - - - - -	9/18/08	
Follow-Up UT of Groove Weld - - - - -	9/18/08	
Pre-Heat & Interpass Temp. fillet weld - - - - -	9/18/08	see note 2 and 3
Interpass Cleaning, fillet weld - - - - -	9/18/08	see note 4
Visual Inspection of Fillet Weld - - - - -	9/18/08	acceptable; see note 5

note 1: The electrode oven is working correctly.

note 2: Although preheat was not required due to the 70° lab temperature, an oxy/acetylene torch was used to raise the base metal temperature to approximately 100° F to reduce the cooling rate of the weld metal.

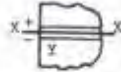
note 4: Interpass temperature was monitored using 248° and 302° Nissen® Temperature Sticks. Interpass temperatures did not exceed 302°.

note 4: All slag was removed using a chipping hammer. Any anomalous material or weld discontinuity that might be detrimental to the integrity of the completed weld was removed using a wire brush or grinder.

note 5: The leg and the throat was inspected using a 3/4" G.A.L. weld gage with a flash light as a luminous aid. The profile of the completed weld was improved using a grinder. The completed weld was found to be visually acceptable in accordance with AWS D1.1 2006 Figure 5.4 and Table 6.1.

N
TRIAD
T

Triad
Nondestructive
Testing, Inc.
P.O. Box 2342
Kannapolis, NC 27285-2342
(336) 994-2576



REPORT OF ULTRASONIC TESTING OF WELDS

Project ALASKA DOT UNIT 44

Job No. _____

Weld Identification SEE BELOW
 Material Thickness 1/2"
 Weld Joint AWS _____
 Welding Process SMALL
 Quality requirements - section no. _____
 Remarks FULL PENETRATION WELD

Line Number	Piece Number	Transducer Angle	From Face	Leg*	Decibels				Discontinuity				Discontinuity Elevation	Remarks	
					Indication Level	Reference Level	Attenuation Factor	Indication Rating	Length	Angular distance (sound path)	Depth from "A" surface	Distance			
												From X			From Y
a	b	c	d												
1	N	70°	A	1/2"		46			1"		1/8"			REJECT	SW QUAD
2	S	70°	A	1/2"					1"		3/16"			REJECT	NW QUAD
3	N	70°	A	1/2"										ACCEPT	
4	S	70°	A	1/2"										ACCEPT	
5															
6															
7															
8															
9															

We, the undersigned, certify that the statements in this record are correct and that the welds were prepared and tested in accordance with the requirements of BC of AWS D1.1, (2006) Structural Welding Code.

Test date 9/18/08
 Manufacturer or Contractor BUCKNOR STEEL

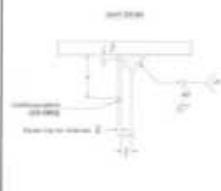
Inspected by [Signature]
 Authorized by _____ Date _____

Figure A 4.22 Test 4 UT Report

WELDING PROCEDURE SPECIFICATION (WPS) Yes
PREQUALIFIED X QUALIFIED BY TESTING _____
Or PROCEDURE QUALIFICATION RECORDS (PQR) Yes _____

<p>Company Name <u>Buckner Steel</u> Welding Process(es) <u>SMAW</u> Supporting PQR No.(s) _____</p> <p>JOINT DESIGN USED Type: TC-U4A Single <input type="checkbox"/> Double Weld <input type="checkbox"/> Backing: Yes <input checked="" type="checkbox"/> No <input type="checkbox"/> Backing Material: Steel A36 grade B Root Opening <u>0.25</u> Root Face Dimension _____ Groove Angle: <u>45</u> Radius (J-U) _____ Backing Gouging: Yes <input type="checkbox"/> No <input checked="" type="checkbox"/> Method _____</p> <p>BASE METALS Material Spec. <u>ASTM A53/ A572 Grade 50 for HP section</u> Type of Grade <u>B</u> Thickness: Groove <u>1/2"</u> Fillet _____ Diameter (Pipe) <u>16"</u></p> <p>FILLER METALS AWS Specification <u>A 5.1</u> AWS Classification <u>E7018</u></p> <p>SHIELDING Flux <u>N/A</u> Gas <u>N/A</u> Composition _____ Electrode-Flux (Class) _____ Flow rate _____ Gas Cup Size _____</p> <p>PREHEAT Preheat temp., Min <u>70 (table 3.2 note A)</u> Interpass Temp., Min <u>70F</u> Max <u>500F</u></p>	<p>Identification # <u>CPB1015</u> Revision _____ Date _____ By _____ Authorized by <u>Jerry Cagle</u> Date <u>6-12-08</u> Type: Manual <input checked="" type="checkbox"/> Semi-Automatic <input type="checkbox"/> Machine <input type="checkbox"/> Automatic <input type="checkbox"/></p> <p>POSITION Position of groove <u>Horizontal/Overhead Fillet Overhead</u> Vertical Position: Up <input type="checkbox"/> Down <input type="checkbox"/></p> <p>ELECTRICAL CHARACTERISTICS Transfer Mode (GMAW) Short-circuiting Globular spray Current: AC <input type="checkbox"/> DCEP <input checked="" type="checkbox"/> DCEN <input type="checkbox"/> Pulsed <input type="checkbox"/> Other _____ Tungsten Electrode (GTAW) Size _____ Type _____</p> <p>TECHNIQUE Stringer or Weave Bead: <u>Stringer</u> Multi-pass or Single pass (per side) <u>Multipass</u> Number of Electrodes: <u>1</u> Electrode Spacing Longitudinal <u>N/A</u> Lateral <u>N/A</u> Angle <u>N/A</u></p> <p>Contact Tube to Work Distance _____ Peening <u>No</u> Interpass Cleaning: <u>Wire brush, grinding or chipping</u></p> <p>POSTWELD HEAT TREATMENT Temp: <u>N/A</u> Time: <u>N/A</u></p>
--	--

WELDING PROCEDURES

Pass or weld Layer(s)	Process	Filler Metals		Current		Volts	Travel Speed	Joint Details
		Class	Diam.	Type & Polarity	Amps or Wire Feed Speed			
12	SMAW	E7018	1/8"	DC+	100 - 130	20 - 24	5 to 7 in/min	

Form N-1 (Front)

Figure A 4.24 Test 5 WPS



3201 Spring Forest Road
 Raleigh, NC 27616
 (919) 872-2660
 (919) 876-3958

Field Report	
Date 12-2-08	Job Number 1057-08-400
Project/Location NC State Constructed Facilities Lab	
Contractor	Weather/Temp Clear/50
Present at Site Russell Ogden	
Time 10	Mileage 30

To:

Services Performed	
<input type="checkbox"/> Concrete Testing	<input type="checkbox"/> Asphalt Core
<input type="checkbox"/> Cylinder Pickup	<input type="checkbox"/> Concrete Core
<input type="checkbox"/> Asphalt Temp	<input type="checkbox"/> Condition Evaluation
<input type="checkbox"/> Soil Testing	<input type="checkbox"/> Foundation Evaluation
	<input type="checkbox"/> Proctoring
	<input type="checkbox"/> In-Place Density
Other (Specify)	

Observations/Remarks:

- I. Examiner arrived on site and met with Steve and Kendra from NC state.
 - II. Examiner reviewed project specs and received copies of welding procedures and welder certification for Justin Green of Green Welding Services.
 - III. Examiner has requested a copy of welder certification for Mr. Quick who is assisting Mr. Green.
 - IV. Examiner observed the beveling of the pipe connections to a 45 degree bevel.
 - V. Examiner observed the welding of the backing bar to the pipe. Weld was examined and was to spec.
 - VI. Examiner observed the root opening and fit up of the connection prior to welding.
 - VII. Examiner observed the preheating of the welded connection and the welding of the inner root pass of both pipe connection 1 and 2. Examiner noted no discrepancies in the root pass welds.
 - VIII. Rhonda Rodgers will return on 12-3-08 to continue the continuous examination of the welded Connections.
 - IX. This examiner will return on 12-4-08 to continue examinations as needed.
- No Further

On-Site Representative/Company

S&ME Personnel

Disclaimer: The presence of S&ME at the project site shall not be construed as an acceptance or approval of activities at the site. S&ME is at the project site to perform specific services and has certain responsibilities which are limited to those specifically authorized in our agreement with our client. In no event shall S&ME be responsible for the safety or the means and methods of other parties at the project site. The information presented in this field report has not been reviewed by an engineer and is to be considered preliminary.

PAGE ___ OF ___

Figure A 4.25 Test 5 QC Report



3201 Spring Forest Road
 Raleigh, NC 27616
 (919) 872-2660
 (919) 876-3958

Field Report	
Date 12-03-08	Job No. 1057-08-400
Project/Location NC State Constructed Facilities Lab	
Contractor Buckner	Weather/Temp SUNNY 50F
Present at Site Rhonda Rogers	
Time	Mileage 30

Services Performed	
<input type="checkbox"/> Concrete Testing	<input type="checkbox"/> Asphalt Curing
<input type="checkbox"/> Cylinders Placed	<input type="checkbox"/> Concrete Curing
<input type="checkbox"/> Asphalt Testing	<input type="checkbox"/> Underlayment Evaluation
<input checked="" type="checkbox"/> Steel Testing	<input type="checkbox"/> Foundation Evaluation
	<input type="checkbox"/> Paving/Sealing
	<input type="checkbox"/> In-Place Density
Other (Explain):	

To:
 Steve, Kendra

Observations:

Subject: **Continuous Examination of CJP welded connections for bridge component testing.**

1) Examiner arrived on site. Met with Justin Green and Mr. Quick of Buckner Steel; Steve Fulmer and Kendra Cookson – NCSU.

2) Welder requested approval to use smaller diameter welding rod for outside root pass.

Due to the specified 1/16" root opening, the 45 degree bevel, and the size of the 1/8" diameter rod, the shortest obtainable distance between the end of the rod and the base metal was excessive enough to cause long-arcing.

NOTE: Welder Certification for Mr. Quick has been faxed to SME Office Raleigh, NC.

3) Examiner observed preheating of welded components at each of the 2 connections.

4) Examiner observed back grinding of inner root pass at each of the 2 connections.

4) Examiner observed welding of inside diameter fillet welds at each of the 2 connections. Acceptable.

5) Kendra Cookson (NCSU) replied back that use of the smaller diameter welding rod for the outside root pass was acceptable.

6) Examiner observed welding and cleaning of the outside root pass at each of the 2 connections.

7) Examined outer root pass at each of the 2 connections.

8) Russ Ogden will return to continue examination 12-4-08.

END REPORT

Rhonda Rogers
 Rhonda Rogers

On-Site Representative/Company

S&ME Personnel

Disclaimer: The presence of S&ME at the project site shall not be construed as an acceptance or approval of activities at the site. S&ME is at the project site to perform specific services and has certain responsibilities which are limited to those specifically authorized in our agreement with our client. In no event shall S&ME be responsible for the safety or the means and methods of other parties at the project site. **The information presented in this field report has not been reviewed by an engineer and is to be considered preliminary.**

PAGE 1 OF 1

Figure A 4.26 Test 5 QC Report Continued



3201 Spring Forest Road
 Raleigh, NC 27616
 (919) 872-2660
 (919) 876-3958

Field Report	
Date 12-4-08	Job Number 1057-08-400
Project/Location NC State Constructed Facilities Lab	
Contractor	Weather/Temp Clear/50
Present at Site Russell Ogden	
Time 5	Mileage 30

To:

Services Performed	
<input type="checkbox"/> Concrete Testing	<input type="checkbox"/> Asphalt Curing
<input type="checkbox"/> Cylinder Pickup	<input type="checkbox"/> Concrete Curing
<input type="checkbox"/> Asphalt Testing	<input type="checkbox"/> Undercut Evaluation
<input type="checkbox"/> Steel Testing	<input type="checkbox"/> Foundation Evaluation
	<input type="checkbox"/> Pave/rolling
	<input type="checkbox"/> In-Place Density
Other (explain)	

Observations/Remarks:

- I. Examiner arrived on site to continue examination of welding
- II. Examiner received copies of Mr. Quick's welding certifications
- III. Examiner observed the completion of the full penetration Groove weld on the pipe to beam Connections.
- IV. Examiner spoke with Perry Vezina of S&ME about conducting the UT examination. He is scheduled To conduct UT testing of the GJP welds on Monday morning.
- V. Rhonda Rodgers will return on Monday to continue examination of multi pass fillet welds after UT Examination of the GJP welds has taken place.
- VI. Examiner will return on Tuesday to continue examination.
- No Further

On-Site Representative/Company

S&ME Personnel

Disclaimer: The presence of S&ME at the project site shall not be construed as an acceptance or approval of activities at the site. S&ME is at the project site to perform specific services and has certain responsibilities which are limited to those specifically authorized in our agreement with our client. In no event shall S&ME be responsible for the safety or the means and methods of other parties at the project site. The information presented in this field report has not been reviewed by an engineer and is to be considered preliminary.

PAGE ____ OF ____

Figure A 4.27 Test 5 QC Report Continued



3201 Spring Forest Road
Raleigh, NC 27616
(919) 872-2660
(919) 876-3958

Field Report	
Date 12-08-08	Job No. 1057-06-400
Project/Location NC State Constructed Facilities Lab	
Contractor Buckner	Weather/Temp SUNNY 27F
Present at Site Rhonda Rogers Perry Vezina	
Time	Mileage 30

Services Performed

- | | |
|---|--|
| <input type="checkbox"/> Concrete Testing | <input type="checkbox"/> Asphalt Coring |
| <input type="checkbox"/> Cylinder Pickup | <input type="checkbox"/> Concrete Coring |
| <input type="checkbox"/> Asphalt Testing | <input type="checkbox"/> Undercut Evaluation |
| <input checked="" type="checkbox"/> Steel Testing | <input type="checkbox"/> Foundation Evaluation |
| | <input type="checkbox"/> Proofrolling |
| | <input type="checkbox"/> In-Place Density |

Other (Explain)

To:
Steve, Kendra

Observations:

Subject: - Continuous Examination of CJP welded connections for bridge component testing.

- UT of same contoured groove welded connections (pipe welded to top of beam).

- 1) Examiner arrived on site. Met with Justin Green, Mr. Quick of Buckner Steel; Steve Fulmer - NCSU.
- 2) Examined welded connections. **Excessive undercut** found on upper edge of inside weld of one connection. Notified welder. (Welder stated that repair will be made after UT of groove welds).
- 3) UT Examiner, Perry Vezina on site for Ultrasonic testing of the 2 connections. Perry pointed out that UT testing of the 2 connections *as they are* may result in "inconclusive" or "invalid" test results due to the following:
 - the construction sequence of the welded connection. (Inner fillet weld interferes with UT reading).
 - the lack of written procedure for UT of this particular set-up.
- 4) Decision was made to repair undercut and to clean up the welds today, and have an alternate Testing agency to come in to perform UT testing on Tuesday a.m. 12-9-08.
- 5) Examined preheating of connections to be welded/repared.
- 6) Re-examined welds – undercut less than 1/32".
- 7) Examiner will return as requested.

END REPORT


 Rhonda Rogers

On-Site Representative/Company

S&ME Personnel

Disclaimer: The presence of S&ME at the project site shall not be construed as an acceptance or approval of activities at the site. S&ME is at the project site to perform specific services and has certain responsibilities which are limited to those specifically authorized in our agreement with our client. In no event shall S&ME be responsible for the safety or the means and methods of other parties at the project site. **The information presented in this field report has not been reviewed by an engineer and is to be considered preliminary.**

PAGE 1 OF 1

Figure A 4.28 Test 5 QC Report Continued



3201 Spring Forest Road
 Raleigh, NC 27616
 (919) 872-2660
 (919) 876-3958

Field Report	
Date 12-09-08	Job No. 1057-08-400
Project/Location NC State Constructed Facilities Lab	
Contractor Buckner	Weather/Temp Partly cloudy 50F
Present at Site Rhonda Rogers	
Time	Mileage 30

To:
 Steve, Kendra

Services Performed	
<input type="checkbox"/> Concrete Testing	<input type="checkbox"/> Asphalt Cutting
<input type="checkbox"/> Cylinder Pick-up	<input type="checkbox"/> Freeze Thaw Testing
<input type="checkbox"/> Asphalt Testing	<input type="checkbox"/> Uniaxial Evaluation
<input checked="" type="checkbox"/> Steel Testing	<input type="checkbox"/> Foundation Evaluation
	<input type="checkbox"/> Overstressing
	<input type="checkbox"/> In-Place Density
Other (Explain)	

Observations:

Subject: - **Continuous Examination of CJP welded connections for bridge component testing.**

- 1) Examiner arrived on site. Met with Justin Green, Mr. Quick of Buckner Steel.
- 2) Monitored welding of 3/4" fillet welds on outside diameter of pipe at both connections of test assembly.
- 3) Examined fillet welds on each of the 2 connections according to AWS D1.5. Acceptable.
- 4) This section of the test assembly was relocated to inside "Constructed Facilities Lab" where J. Green, S. Fulmer, Kendra Cookson, and Mr. Quick made fit-up with 2 sections of 16" vertical pipes.
- 5) Examined fit-up of assembly. Acceptable according to detail and AWS D1.1. 1/4" root opening.
Tacked in place - J. Green.
- 6) Monitored welding of root pass for each of the groove welds on the vertical pipes. Welder J Green.
- 7) Examiner will return tomorrow (12-10-08) to examine root pass after cleanup.

END REPORT

Rhonda Rogers
 Rhonda Rogers

On-Site Representative/Company

S&ME Personnel

Disclaimer: The presence of S&ME at the project site shall not be construed as an acceptance or approval of activities at the site. S&ME is at the project site to perform specific services and has certain responsibilities which are limited to those specifically authorized in our agreement with our client. In no event shall S&ME be responsible for the safety or the means and methods of other parties at the project site. **The information presented in this field report has not been reviewed by an engineer and is to be considered preliminary.**

PAGE 1 OF 1

Figure A 4.29 Test 5 QC Report Continued



3201 Spring Forest Road
 Raleigh, NC 27616
 (919) 872-2660
 (919) 876-3958

To:
 Steve Kendra

Services Performed	
<input type="checkbox"/> Concrete Testing	<input type="checkbox"/> Asphalt Coring
<input type="checkbox"/> Concrete Patching	<input type="checkbox"/> Concrete Fining
<input type="checkbox"/> Asphalt Testing	<input type="checkbox"/> Undercut Evaluation
<input checked="" type="checkbox"/> Steel Testing	<input type="checkbox"/> Foundation Evaluation
	<input type="checkbox"/> Pressure Test
	<input type="checkbox"/> In-Place Density
Other (Specify)	

Field Report	
Date 12-10-08	Job No. 1057-08-400
Project/Location NC State Constructed Facilities Lab	
Contractor Buckner	Weather/Temp Cloudy/misting rain 68F
Present at Site Rhonda Rogers	
Time	Mileage 30

Observations:

Subject: - **Continuous Examination of CJP welded connections for bridge component testing.**
 - (NOTE: Examination - according to AWS D1.5 - Bridge welding code).

- 1) Examiner arrived on site. Met with Justin Green, Mr. Quick of Buckner Steel, S. Fulmer - NCSU.
- 2) Observed welders clean-up root pass on each of the groove welds for inspection.
- 3) Examined 1st root pass. Some slag left in 2 locations. Welder corrected. Acceptable.
- 4) Examined 2nd root pass. Incomplete fusion in 2 locations. Welder corrected. Acceptable.
- 5) Examiner observed welding of groove welds and the preparation of each weld for inspection.
- 6) Examined completed groove weld on each of the 2 connections. Acceptable.
- 7) Examiner will return as requested.

END REPORT

Rhonda Rogers



On-Site Representative/Company

S&ME Personnel

Disclaimer: The presence of S&ME at the project site shall not be construed as an acceptance or approval of activities at the site. S&ME is at the project site to perform specific services and has certain responsibilities which are limited to those specifically authorized in our agreement with our client. In no event shall S&ME be responsible for the safety or the means and methods of other parties at the project site. **The information presented in this field report has not been reviewed by an engineer and is to be considered preliminary.**

PAGE 1 OF 1

Figure A 4.30 Test 5 QC Report Continued

**N
TRIAD
T**

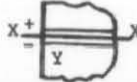
**Triad
Nondestructive
Testing, Inc.**
P.O. Box 2342
Kernersville, NC 27285-2342
(336) 996-2576

REPORT OF ULTRASONIC TESTING OF WELDS

Project ALASKA DOT #5

Job No. _____

Weld Identification SEE BELOW
Material Thickness 1/2"
Weld Joint AMS _____
Welding Process SMAW
Quality requirements - section no. _____
Remarks SPICE WELD IN PIPE COLUMN



Line Number	Piece Number	Transducer Angle	From Face	Leg*	Indication Level	Decibels			Discontinuity				Discontinuity Elevation	Remarks	
						Reference Level	Attenuation Factor	Indication Rating	Length	Angular distance (sound path)	Depth from "A" surface	Distance			
												From X			From Y
a	b	c	d												
1	1A	70°	A	1/2		63								ACCEPT South	
2	2A	70°	A	1/2		63								ACCEPT North	
3															
4															
5															
6															
7															
8															
9															

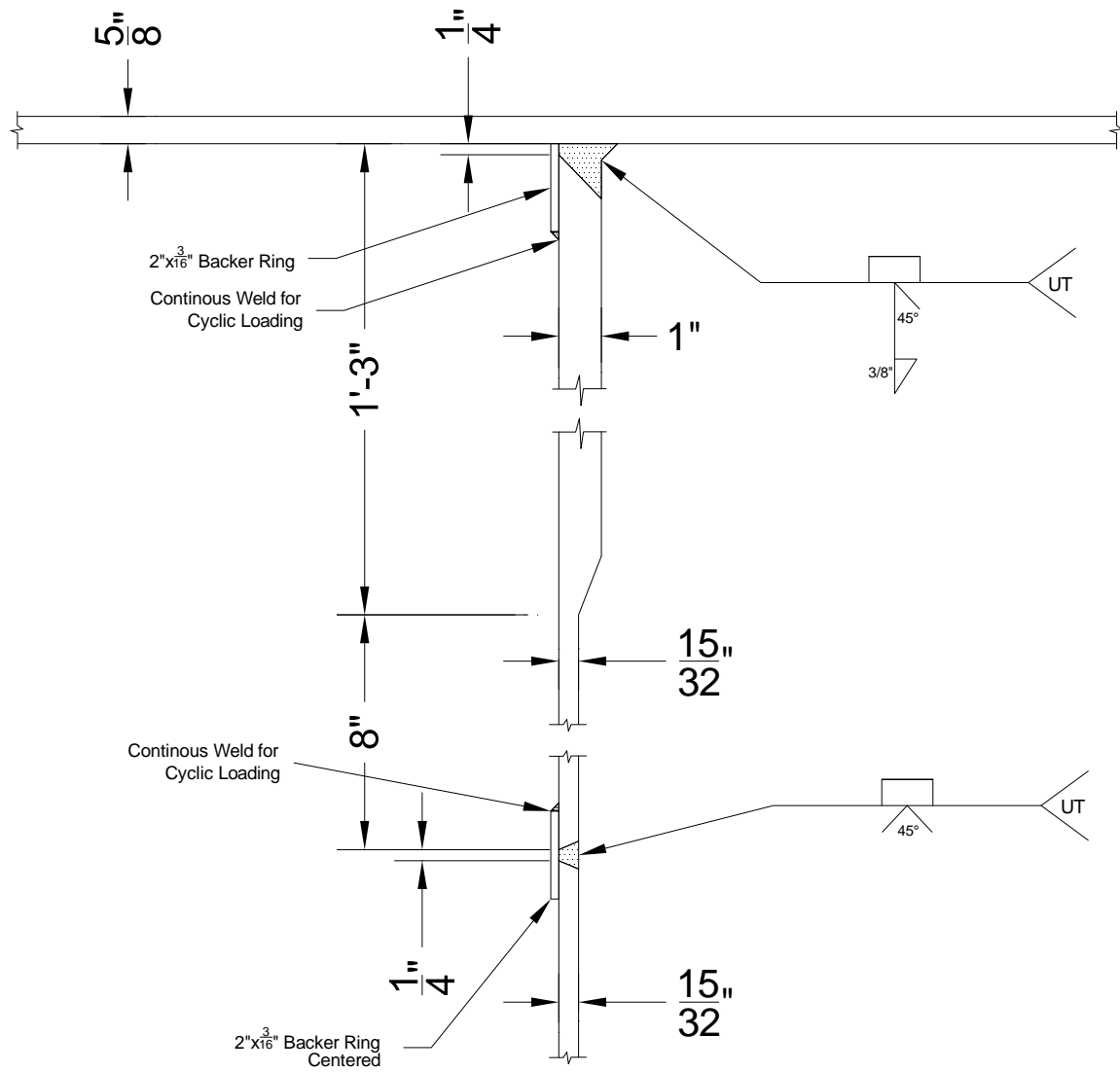
We, the undersigned, certify that the statements in this record are correct and that the welds were prepared and tested in accordance with the requirements of 6C of AWS D1.1, (2006) Structural Welding Code.

Test date 12/10/04 year
Manufacturer or Contractor N.C. STATE

Inspected by L. J. Spagle
Authorized by _____ Date _____

Figure A 4.31 Test 5 UT Report

A4.8 Test 6 Details



Buckner Steel Erectors
Welding Procedure Specification

CPB1015

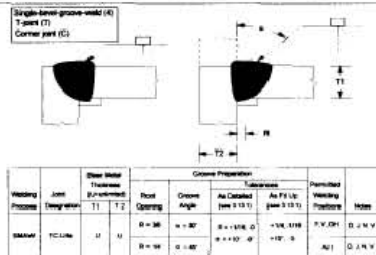
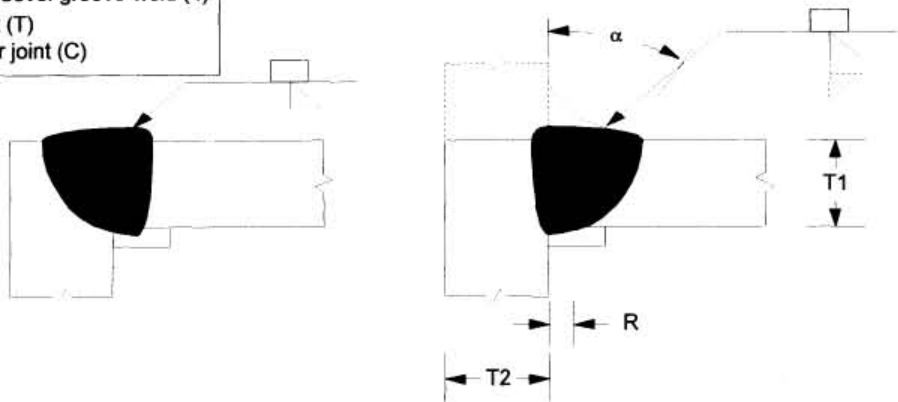
WPS No. CPB1015 Revision _____ Date _____ By L. Leroy Spangler																							
Authorized By Jerry Cagle Date 3/12/2009 Prequalified <input checked="" type="checkbox"/>																							
Welding Process(es) SMAW Type: Manual <input checked="" type="checkbox"/> Machine <input type="checkbox"/> Semi-Auto <input type="checkbox"/> Auto <input type="checkbox"/>																							
Supporting PQR(s) _____																							
<p>JOINT</p> <p>Type T-Joint</p> <p>Backing Yes <input checked="" type="checkbox"/> No <input type="checkbox"/> Single Weld <input checked="" type="checkbox"/> Double Weld <input type="checkbox"/></p> <p>Backing Material A-36</p> <p>Root Opening 1/4" Root Face Dimension 0" to 1/8"</p> <p>Groove Angle 45 deg. Radius (J-U) _____</p> <p>Back Gouge Yes <input type="checkbox"/> No <input checked="" type="checkbox"/></p> <p>Method _____</p>	 <table border="1" style="font-size: small; border-collapse: collapse;"> <thead> <tr> <th rowspan="2">Welding Process</th> <th rowspan="2">Joint Type</th> <th rowspan="2">Shielding Gas</th> <th rowspan="2">Electrode</th> <th rowspan="2">Root Opening</th> <th rowspan="2">Groove Angle</th> <th colspan="2">Subprocess</th> <th rowspan="2">Welding Position</th> <th rowspan="2">Notes</th> </tr> <tr> <th>As Qualified</th> <th>As P. 1.1.1</th> </tr> </thead> <tbody> <tr> <td>SMAW</td> <td>FC-Like</td> <td>Ar</td> <td>E7018</td> <td>R = 3/8"</td> <td>45 - 60°</td> <td>As Qualified</td> <td>As P. 1.1.1</td> <td>P.V. OH</td> <td>D, J, N, V</td> </tr> </tbody> </table>	Welding Process	Joint Type	Shielding Gas	Electrode	Root Opening	Groove Angle	Subprocess		Welding Position	Notes	As Qualified	As P. 1.1.1	SMAW	FC-Like	Ar	E7018	R = 3/8"	45 - 60°	As Qualified	As P. 1.1.1	P.V. OH	D, J, N, V
Welding Process	Joint Type							Shielding Gas	Electrode			Root Opening	Groove Angle	Subprocess		Welding Position	Notes						
		As Qualified	As P. 1.1.1																				
SMAW	FC-Like	Ar	E7018	R = 3/8"	45 - 60°	As Qualified	As P. 1.1.1	P.V. OH	D, J, N, V														
<p>BASE METALS</p> <p>Material Spec. ASTM A-500 to ASTM A-572</p> <p>Type or Grade GR B to Gr 50</p> <p>Thickness: Groove (in) 1.0 - Unlimited</p> <p style="padding-left: 40px;">Fillet (in) All - Unlimited</p> <p>Diameter (Pipe, in) All - All</p>	<p>POSITION</p> <p>Position of Groove All Fillet All</p> <p>Vertical Progression: <input checked="" type="checkbox"/> Up <input type="checkbox"/> Down</p> <p>ELECTRICAL CHARACTERISTICS</p> <p>Transfer Mode (GMAW):</p> <p style="padding-left: 20px;">Short-Circuiting <input type="checkbox"/> Globular <input type="checkbox"/> Spray <input type="checkbox"/></p> <p>Current: AC <input type="checkbox"/> DCEP <input checked="" type="checkbox"/> DCEN <input type="checkbox"/> Pulsed <input type="checkbox"/></p> <p>Other _____</p> <p>Tungsten Electrode (GTAW):</p> <p style="padding-left: 20px;">Size _____ Type _____</p>																						
<p>FILLER METALS</p> <p>AWS Specification AWS A 5.1</p> <p>AWS Classification E7018</p>	<p>TECHNIQUE</p> <p>Stringer or Weave Bead Both</p> <p>Multi-pass or Single Pass (per side) _____</p> <p>Number of Electrodes 1</p> <p>Electrode Spacing: Longitudinal _____</p> <p style="padding-left: 40px;">Lateral _____</p> <p style="padding-left: 40px;">Angle _____</p> <p>Contact Tube to Work Distance _____</p> <p>Peening None</p> <p>Interpass Cleaning Mechanical</p>																						
<p>SHIELDING</p> <p>Flux _____ Gas _____</p> <p style="padding-left: 40px;">Composition _____</p> <p>Electrode-Flux (Class) _____ Flow Rate _____</p> <p style="padding-left: 40px;">Gas Cup Size _____</p>	<p>POSTWELD HEAT TREATMENT PWHT Required <input type="checkbox"/></p> <p>Temp. _____ Time _____</p>																						
<p>PREHEAT</p> <p>Preheat Temp., Min. 32 deg.</p> <p>Thickness Up to 3/4" Temperature 32 deg.</p> <p style="padding-left: 20px;">Over 3/4" to 1-1/2" 150 deg.</p> <p style="padding-left: 20px;">Over 1-1/2" to 2-1/2" 225 deg.</p> <p style="padding-left: 20px;">Over 2-1/2" 300 deg.</p> <p>Interpass Temp., Min. 32 deg. Max. 300 deg.</p>																							
WELDING PROCEDURE																							
Layer/Pass	Process	Filler Metal Class	Diameter	Cur. Type	Amps or WFS	Volts	Travel Speed	Other Notes															
1-15	SMAW	E7018	1/8"	DCEN	90 -130	20-24	5-7IPM																

Figure A 4.32 Test 6 WPS

Single-bevel-groove-weld (4)
T-joint (T)
Corner joint (C)

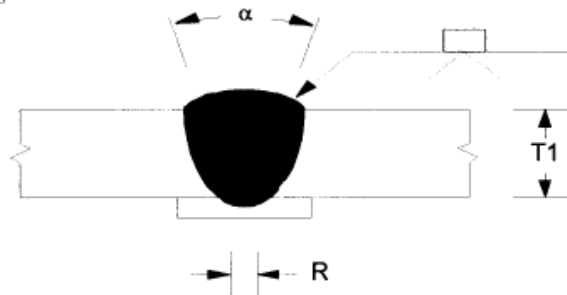


Welding Process	Joint Designation	Base Metal Thickness (U=unlimited)		Groove Preparation				Permitted Welding Positions	Notes
		T1	T2	Root Opening	Groove Angle	Tolerances			
						As Detailed (see 3.13.1)	As Fit Up (see 3.13.1)		
SMAW	TC-U4a	U	U	R = 3/8	$\alpha = 30^\circ$	R = +1/16, -0	+1/4, -1/16	F,V,OH	D, J, N, V
				R = 1/4	$\alpha = 45^\circ$	$\alpha = +10^\circ, -0^\circ$	+10°, -5°	All	D, J, N, V

MEMO

Figure A 4.33 Test 6 WPS Continued

Single-V-groove weld (2)
Butt joint (B)



Welding Process	Joint Designation	Base Metal Thickness (U=unlimited)		Groove Preparation				Permitted Welding Positions	Notes
		T1	T2	Root Opening	Groove Angle	Tolerances			
						As Detailed (see 3.13.1)	As Fit Up (see 3.13.1)		
SMAW	B-U2a	U	-	R=1/4	$\alpha = 45^\circ$	R = +1/16, -0 $\alpha = +10^\circ, -0^\circ$	+1/4, -1/16 +10°, -5°	All	D, N
				R=3/8	$\alpha = 30^\circ$			F,V,OH	D, N
				R=1/2	$\alpha = 20^\circ$			F,V,OH	D, N

Figure A 4.34 Test 6 WPS Continued

TRIAD
N
T

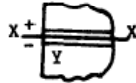
Triad
Nondestructive
Testing, Inc.
P.O. Box 2342
Kannapolis, NC 27285-2342
(336) 996-2576

REPORT OF ULTRASONIC TESTING OF WELDS

Project ALASKA DOT

Job No. 09-114

Weld Identification SEE BELOW
Material Thickness 1"
Weld Joint AWS TC-U FA
Welding Process SAW
Quality requirements - section no. _____
Remarks _____



Line Number	Piece Number	Transducer Angle	From Face	Leg*	Indication Level	Decibels			Discontinuity				Discontinuity Elevation	Remarks	
						Reference Level	Attenuation Factor	Indication Rating	Length	Angular distance (sound path)	Depth from "A" surface	Distance			
												From X			From Y
a	b	c	d												
1	N	70°	A	1/2		60								ACCEPT	
2	S	70°	A	1		6								ACCEPT	
3															
4															
5															
6															
7															
8															
9															

We, the undersigned, certify that the statements in this record are correct and that the welds were prepared and tested in accordance with the requirements of 6C of AWS D1.1, (2008) Structural Welding Code.

Test date 3/18/09^{year}
Manufacturer or Contractor BUCKNER
Copy to Jerry Cagle - 03/23/09

Inspected by L. F. Spangle
Authorized by _____ Date _____

Figure A 4.35 Test 6 UT Report